NIRS
National Institute of Radiological Sciences
Research Promotion Section
4-9-1 Anagawa, Inage-ku, Chiba 263-8555, Japan
E-mail:kokusai@nirs.go.jp
Tel:+81-43-206-3025
Fax:+81-43-206-4061
http://www.nirs.go.jp/ENG/index.html

EBG MedAustron GmbH
Marie Curie-Straße 5, A-2700 Wiener Neustadt, Austria
http://www.medaustron.at

NIRS-M-262 Joint Symposium on Carbon Ion Radiotherapy

NIRS-M-262

NIRS & MedAustron

Joint Symposium on Carbon Ion Radiotherapy

Dec. 5 - 6, 2013
Wiener Neustadt, Austria

Organized by
NIRS
National Institute
of Radiological Sciences, Japan
and
EBG MedAustron GmbH

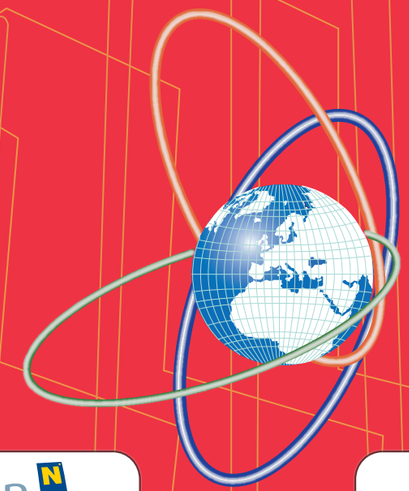

MedAustron

NIRS

NIRS & MedAustron Joint Symposium on Carbon Ion Radiotherapy

December 5-6, 2013

The Technology and Research Center (TFZ)
Wiener Neustadt, Austria

Organized by:
National Institute of Radiological Sciences
and
EBG MedAustron GmbH

Greetings

Dear Ladies and Gentlemen,

We warmly welcome you to the first NIRS & MedAustron Joint Symposium on Carbon Ion Radiotherapy on December 5th and 6th at the "Technologie- und Forschungszentrum" right beside MedAustron in Wiener Neustadt.

The National Institute of Radiological Sciences (NIRS) of Japan has nearly 20 years of experience in the field of carbon ion radiotherapy and can be considered as the pioneer for a number of ion beam projects throughout the world.

MedAustron is not treating patients yet, but we are progressing rapidly towards the beginning of trial operation. The Austrian ion beam center of treatment and research is well on track and will be able to treat patients by the end of 2015.

We do not only want to share the latest findings of NIRS and the latest developments at MedAustron with you, but also invited other centres in order to cover as much expertise on carbon ion therapy as possible.

The first day of the symposium will be dedicated to clinical and radiobiological aspects of ion beam therapy, mainly presented by experts from NIRS. Clinical experiences from other centres, such as HIT, CNAO or Gunma will be outlined in addition to presentations on the current status of the France Hadron and MedAustron project, respectively.

The main topics of the second day of the symposium will be medical physics and ion beam research, focusing on the latest Japanese experiences in these fields. In addition latest developments from the radART institute and the Christian Doppler Laboratory both of them cooperating with MedAustron will be topics of the symposium.

Furthermore you will get the possibility to visit the MedAustron site and see the progress for yourselves first hand.

So once again: Welcome to the beautiful country of Austria, to Wiener Neustadt and MedAustron. We are looking forward to a very productive meeting with all of you!

MedAustron, Austria

Univ.-Doz. Dr. Mock Ulrike
Dr. Thomas Friedrich

NIRS, Japan

Dr. Hirohiko Tsujii, NIRS Fellow
Dr. Tadashi Kamada, Director of Research Center for Charged Particle Therapy

NIRS & MedAustron Joint Symposium on Carbon Ion Radiotherapy & Peer Review of NIRS Research on Carbon Ion Radiotherapy

Wiener Neustadt, Dec. 5-7, 2013

December 5th, 2013	Speakers and Topics
08:45 - 09:00	Welcome and Introductions 1. MedAustron Welcome 2. NIRS Welcome
	Session 1: NIRS Experience, Chair : R. Pötter / R. Mayer
09:00 - 09:30	Over View of Carbon Ion Radiotherapy H. Tsujii
09:30 - 10:10	Carbon Ion Radiotherapy for Patients with H & N, Lung, and Bone & Soft Tissue Tumors T. Kamada, A.Hasegawa, M.Koto, N.Yamamoto, R.Imai
10:10 - 10:50	Carbon Ion Radiotherapy for Patients with Prostate Cancer, HCC, Locally Recurrent Rectal Cancer, and Pancreas Cancer H. Tsuji, S.Yasuda, S.Yamada
10:50 - 11:10	Break
	Session 2: Radiobiology of carbon ion radiotherapy, Chair : M. Durante / E. Blakely
11:10 - 11:30	Modeling of the Biological and Clinical Response of Carbon Ion Radiotherapy N. Matsufuji
11:30 - 11:50	Genetic Variation in Cancer Cells and Effects of Carbon-Ion Irradiation T. Imai
11:50 - 12:10	Oxygen Effect in Carbon Ion Radiotherapy R. Hirayama
12:10 - 14:00	Lunch
	Session 3: Present status at Med-Austron & European Networks, Chair : J. Debus / J. Balosso
14:00 - 14:20	Actual status of MedAustron U. Mock
14:20 - 14:40	Interaction between chemotherapy and Ion Beam Therapy I. Skvortsova
14:40 - 15:00	Ion beam therapy technology developments at MedAustron S. Vatnitsky
15:00 - 15:20	Current status of the European Light Ion Cooperation Projects M. Dosanjh
15:20 – 15:40	Initiation of an European study board on ion beam therapy R. Pötter
15:40 - 16:10	Break
	Session 4: Carbon Ion Therapy in the world, Chair : H. Tsujii / S. Vatnitsky
16:10 - 16:30	Actual and future strategies at HIT J. Debus
16:30 - 16:50	CNAO: Initial results at CNAO R. Orecchia
16:50 - 17:10	Actual status of France Hadron Project J. Balosso
17:10 – 17:30	The current status of carbon ion radiotherapy at Gunma T. Nakano
18:00 - 21:00	Social Event

December, 6th, 2013 Speakers and Topics

Session 5: Medical Physics / Technology, Chair： W. Chu / O. Jäkel

09:00 - 09:30	Development and Promotion of Carbon Ion Radiotherapy Facility K. Noda
09:30 - 10:00	Research Activity in Medical Physics at New Carbon Ion Radiotherapy Facilities T. Shirai
10:00 - 10:20	R & D of Superconducting Rotating Gantry for Carbon Ion Radiotherapy Y. Iwata
10:20 - 10:40	Break

Session 6: Potential fields of research, Chair： R. Orecchia / W. De Neve

10:40 - 11:00	Heavy Ion Research Project at NIRS T. Murakami
11:00 - 11:20	radART ion suite software solution for MedAustron P. Steininger
11:20 - 11:40	Combination of Carbon-ion Irradiation and Immunotherapy in Mouse Models T. Shimokawa
11:40 - 12:00	Ion beam therapy and the Christian Doppler Laboratory D. Georg
12:00 - 13:00	Med-Austron Site Tour
13:00 - 14:00	Lunch

Peer Review of NIRS Research on Carbon Ion Radiotherapy

14:00 - 17:00	Discussion of Peer Review (I) Chair: W. Chu

December, 7th, 2013 **Peer Review of NIRS Research on Carbon Ion Radiotherapy**

09:00 - 11:00	Discussion of Peer Review (II) Chair: W. Chu

Contents

Contents

Session 1: Clinical Presentations – NIRS Experience

Overview of Carbon Ion Radiotherapy at the NIRS

Hirohiko Tsujii

National Institute of Radiological Sciences, Chiba, Japan
email address: tsujii@nirs.go.jp

In June 1994, the National Institute of Radiological Sciences (NIRS) initiated heavy particle radiotherapy using carbon ion beams obtained from the Heavy Ion Medical Accelerator in Chiba (HIMAC), which was built as a part of the nation's "Overall ten-year anti-cancer strategy in Japan," which started in 1984. The construction was completed at the end of 1993, and the facility was opened for carbon ion radiotherapy (C-ion RT) the following year. Since then, the HIMAC has served as a multipurpose, shared facility that is jointly used for cancer therapy and fundamental particle beam studies by Japanese and foreign researchers. In 2010, a new treatment research building with three rooms was built to use beam lines extending from the HIMAC (Fig. 1). The new building was designed to be able to administer adaptive charged particle therapy with pencil beam scanning, as well as to allow a compact rotating gantry to be developed. Treatment with the scanning method started in 2011, and its indications have since been expanded to many types of tumors. [1)]

C-ion RT has been applied for various types of malignancies at the NIRS.[2),3),4)] It was approved by the Ministry of Health, Welfare and Labor as a "Highly Advanced Medical Technology" in 2003. This means that C-ion RT has achieved a solid place in general practice based on the clinical experiences with C-ion RT at the NIRS.

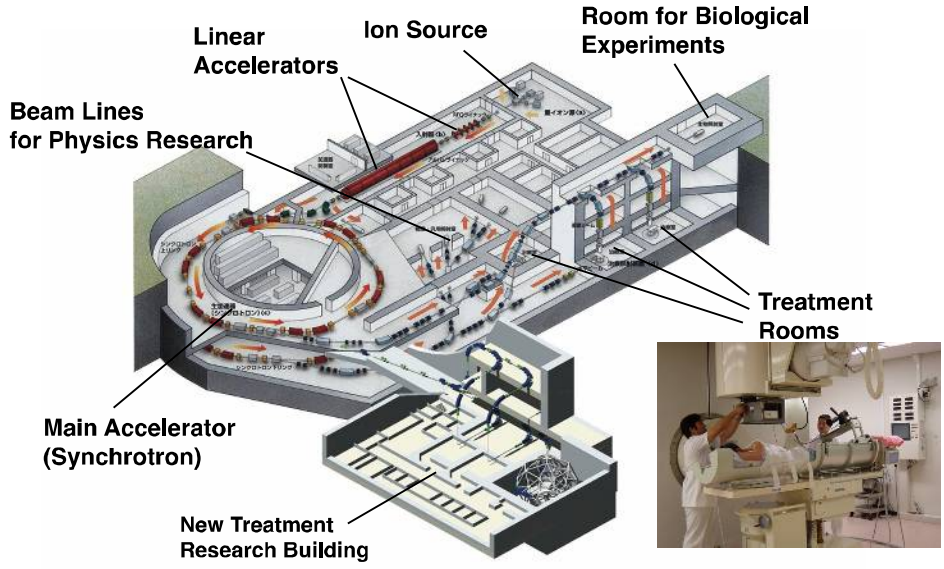

Fig. 1. A bird's-eye view of the HIMAC (Heavy Ion Medical Accelerator in Chiba).

1. Expected benefits of carbon ion radiotherapy

At the NIRS, carbon ions have been chosen for cancer therapy among the various ion species (Fig. 2) because they have two unique features. First, in marked contrast to photon beams, which show an exponential attenuation in the body, carbon ions form a high-dose peak, a so-called Bragg peak (Fig. 3). As a result of such dose concentrating behavior, the carbon ion beams can be focused selectively on the tumor. This property is extremely useful for radiotherapy, because even when there are critical organs in the vicinity of the lesion, it is possible to safely concentrate a high dose in the lesion. Second, the ionization density along the trajectory of the carbon ion beams in the body, in other words, the energy given off per unit length (called LET), is higher for carbon ions than in the case of protons or photons. For this reason, carbon ion beams have a high relative

biological effectiveness (RBE) within the Bragg peak that is twice or three times greater than that of photons in clinical situation. [5),6)]

Further advantageous biological features of carbon ions include: 1) radiation damage induced in cancer tissue will not easily recover, 2) the oxygen concentration in the tissue has little effect on the radiosensitivity and 3) there are only small differences in the radiosensitivity for different phases of the cell cycle. Furthermore, as is shown in Table 1, a comparison of the ratio of the RBE in the peak portion to the RBE in the plateau portion shows that carbon ion beams have the highest value for this ratio among all particle beams.[7)] This means that carbon ion beams have the best balance of any particle beams in terms of both the physical and biological dose distribution, leading to a biological background where the treatment period can be significantly shortened compared with that using low LET radiation.[8)]

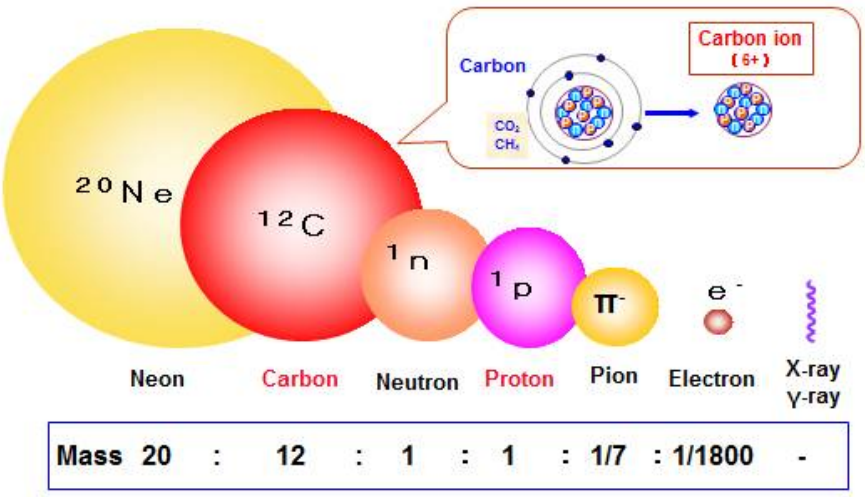

Fig. 2. Carbon ions have the best balanced properties among various types of ion species in terms of both the physical and biological dose distribution.

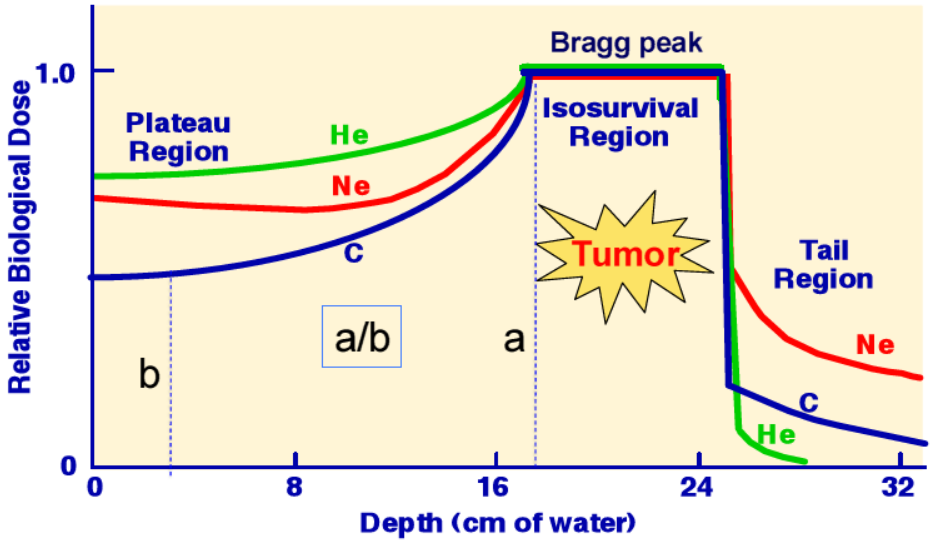

Fig. 3. Carbon ions have the largest ratio of RBE in the peak portion relative to the plateau portion (a/b).

Table 1. The peak-to-plateau ratio of the RBE for jejunal crypt cells is larger for carbon ions than for other ion species (Goldstein et al.: Radiat. Res. 86, 542-558, 1981).

Ion	RBE_{sd}		RBE_2	
	Peak / Plateau	Ratio	Peak / Plateau	Ratio
Proton	1.2/1.1	1.1	1.3/1.2	1.1
Helium	1.2/1.1	1.1	1.5/1.3	1.2
Carbon	1.4~1.5/1.3	1.1~1.2	1.6~2.2/1.3	1.2~1.7
Neon	1.5~1.6/1.4	1.1	2.6~3.0/2.1	1.2~1.4
Argon	1.8~2.0/2.1	0.9	3.6~3.8/4.3	0.8~0.9

RBEsd : single dose, RBE2: fractionated

2. The framework for the administration of carbon ion radiotherapy

Consistent efforts have been made at the NIRS to provide C-ion RT on an ethically and scientifically sound basis under a number of Committees headed by the "Carbon Ion Radiotherapy Network Committee" as the supreme organ responsible for the whole clinical study. All clinical protocols are first prepared by the disease-specific Subcommittees, then are evaluated by Planning Teams and an Ethics Committee, and finally are approved by the Network Committee. An Evaluation Committee is appointed to deliberate on the validity of whether the individual clinical studies should be continued, and the results of all clinical studies are submitted to the Network Committee, whose sessions are invariably held in public. All of the patients' data are submitted to the Tumor Board for an evaluation of the criteria for C-ion RT, as well as to Staff Meetings for evaluations of the treatment planning (Fig. 4).

The total number of patients registered was 7,700 as of August 2013 (Fig. 5). The number of patients continues to rise due not only to the way in which the irradiation techniques have been established and can be executed without problem, but also as a result of the significant reduction in the number of fractions and the treatment time per patient that have been established based on the results of previous clinical trials.

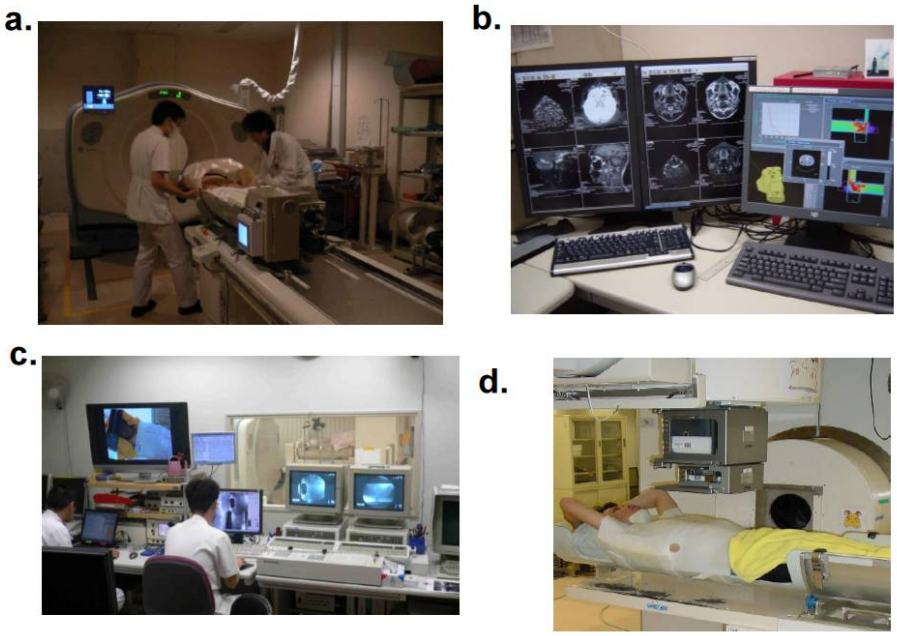

Fig. 4. The step-by-step procedures for C-ion therapy: a. CT scans are performed for treatment planning; b. The dose distribution is calculated and treatment parameters are determined using the treatment planning system; c. The preparations for treatment planning are confirmed in the simulation room; d. The treatment room.

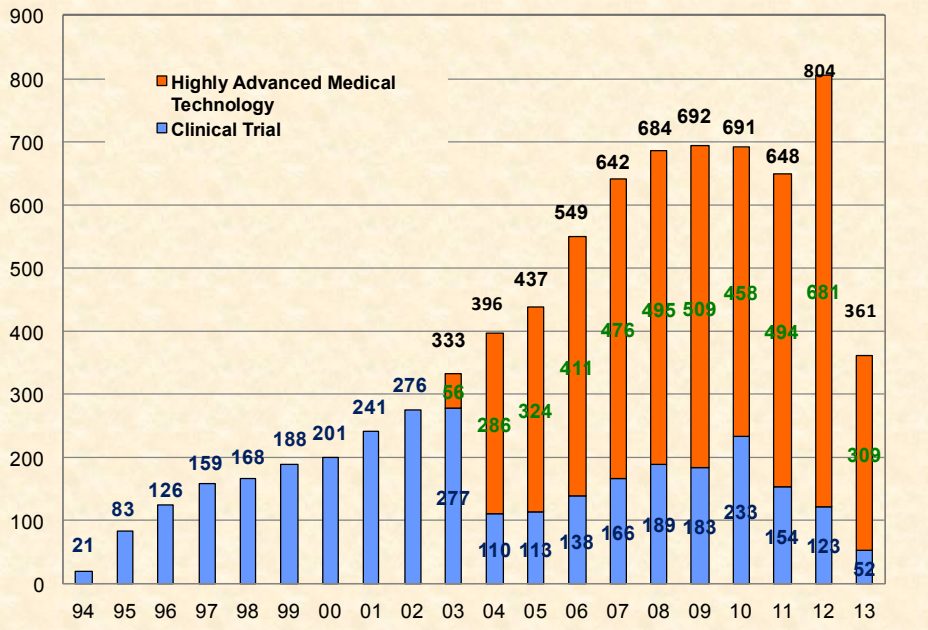

Fig. 5. The annual number of patients treated using C-ion RT at the NIRS (June 1994～August 2013)

3. Clinical results of carbon ion radiotherapy

C-ion RT has been applied for various types of tumors which were considered to be difficult to control with existing modalities. Initially, phase I/II trials were performed in order to confirm the safety and efficacy of this treatment, with the fraction number and treatment time being fixed for each tumor. In this way, the total dose was escalated in successive increments of 5 to 10%.

The experiences to date indicate that carbon ion radiotherapy is advantageous for the following tumors: skull base tumors (chordoma, chondrosarcoma), head and neck cancer (adenocarcinoma, adenoid cystic carcinoma, malignant melanoma), NSCLC (early stage, locally advanced tumors), hepatocellular cancer, pancreatic cancer, prostate cancer, rectal cancer (postoperative pelvic recurrence), bone/soft tissue sarcoma of the pelvis, paraspinal region and head/neck and uterine cervix adenocarcinoma. Tumors located in the vicinity of critical organs such as the eye, spinal cord and digestive tract with a relatively large size and/or irregular shape have also been effectively treated. However, tumors that infiltrate or originate in the digestive tract are difficult to control with C-ion RT.

Regarding dose fractionations, a significant reduction in the overall treatment time has been obtained with acceptable toxicities in most cases. For example, stage I lung cancer and liver cancer can now be treated with only one or two fractions of radiation, respectively. Even for prostate cancers requiring a relatively long course of RT, 12 to16 fractions have been sufficient, less than the half the number of fractions required in the case of photon or proton RT. This means that the facility can be operated more efficiently, permitting treatment for a larger number of patients than is possible with other modalities over the same period of time. Currently, the number of irradiation sessions per patient averages 12 fractions spread over approximately three weeks for C-ion RT at the NIRS.

The current status and anticipated future directions of the role of ion beam therapy in medicine may be a complex subject that involves an intimate interplay among radiobiologists, accelerator physicists and radiation oncologists. In this context, the clinical results, the technical advances as well as the future directions of carbon ion RT are promising.

References

[1] Tsujii H, Minohara S, Noda K: Heavy-particle radiotherapy: System design and application. Reviews of Accelerator Science and Technology Vol 2 (ed. by Chao AW), Imperial College Press, UK, pp1-19, 2009.

[2] Tsujii H, Kamada T, Baba M, et al. Clinical advantages of carbon-ion radiotherapy. *New J Phys.* 2008; 10:1367–2630.

[3] Tsujii H, Kamada T.: A review of update clinical results of carbon-ion radiotherapy. *Jpn J Clin Oncol.* 2012; 42(8): 670–685.

[4] Schulz-Ertner D, Tsujii H: Particle radiation therapy using proton and heavier ion beams. J Clin Oncol. 25(8): 953-964, 2007.

[5] Chen GTY, Castro JR, Quivey JM: Heavy charged particle radiotherapy. Ann.Rev.Biophys.Bioeng. 10: 499-529, 1981.

[6] Kraft G: Tumor therapy with heavy charged particles. Prog Part Nucl Phys. 45: S473-S544, 2000.

[7] Goldstein, et al.: Radiat. Res. 86, 542-558, 1981.

[8] Koike S, Ando K, Uzawa A, et al: Significance of fractionated irradiation for the biological therapeutic gain of carbon ions. Radiat Prot Dos. 99: 405-408, 2002.

Carbon Ion Radiotherapy for Malignant Head-and-Neck Tumors

Azusa Hasegawa, Masashi Koto, Ryo Takagi, Hiroaki Ikawa, Tadashi Kamada, and Hirohiko Tsujii

Research Center for Charged Particle Therapy, National Institute of Radiological Sciences, Chiba, Japan.
E-mail: azusa@nirs.go.jp

Abstract

Carbon ion radiotherapy, with its powerful biological effects, provides excellent therapeutic efficacy for patients with radioresistant tumors. By focusing the irradiation beam on the target lesion, this approach guarantees a low probability of damage to critical organs (e.g., the brain, spinal cord, eyes and optic nerves) in the immediate vicinity of the target tumor. With regard to tumors in the head and neck region, carbon ion radiotherapy is indicated for the treatment of adenoid cystic carcinomas, adenocarcinomas and malignant mucosal melanomas in the oral and maxillofacial area. The safety and efficacy of this therapy have been established. Certain groups of radioresistant tumors are not indicated for surgical resection because of possible surgery-induced injury to critical organs, and these tumors raise a significant clinical concern because of the paucity of effective treatment options. Carbon ion radiotherapy represents a definitive treatment for these malignancies.

1. Phase II Clinical Trial for Malignant Head-and-Neck Tumors (Protocol 9602)

Introduction

A clinical trial of carbon ion radiotherapy for malignant head-and-neck tumors was conducted under the title "Phase I/II Clinical Trial (Protocol 9301) on Heavy Particle Radiotherapy for Malignant Head-and-Neck Tumors", and was initiated in June 1994 by way of a dose escalation study using 18 fractions over six weeks. This trial was followed by another dose escalation study that commenced in April 1996 under the title "The Phase I/II Clinical Trial (Protocol 9504) on Heavy Particle Radiotherapy for Malignant Head-and-Neck Tumors" using 16 fractions over four weeks. Based on the outcomes of these two studies [1], the "Phase II Clinical Trial on Heavy Particle Radiotherapy for Malignant Head-and-Neck Tumors (Protocol 9602)" was initiated using 64.0 GyE in 16 fractions over four weeks (or 57.6 GyE in 16 fractions over four weeks when a wide area of skin was included in the target volume) in April 1997 [2] (Fig. 1).

Patients and Methods

The eligibility criteria for enrollment in this phase II study were the presence of histologically proven malignancy, a measurable tumor in the head-and-neck region, with no co-existent malignant active tumor, no distant metastasis to other parts, an age range from 15 to 80 years and a prospective prognosis of at least six months or longer. The candidates were also required to have a Karnofsky performance status index (KPS) of 60% or more and to give their written informed consent for inclusion in this clinical study.

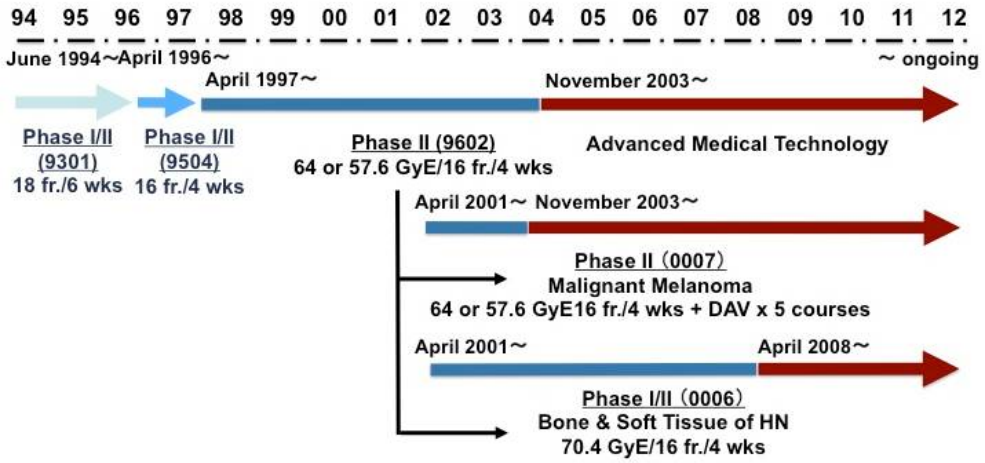

Figure 1. Carbon Ion Radiotherapy for Malignant Head-and-Neck Tumors

A further requirement was the absence of prior radiotherapy for the carbon-ion treated area, the absence of intractable inflammatory lesions and an interval of at least four weeks from completion of the last chemotherapy.

The phase II study commenced in April 1997, and the data for 455 lesions of 452 patients treated until March 2013 were recorded as follows: the patient age range was from 16 to 80 years, with a median of 58 years, with 212 males and 240 females. Histologically, the tumors were classified as 186 adenoid cystic carcinomas, 102 mucosal malignant melanomas, 51 adenocarcinomas, 26 squamous cell carcinomas, 19 mucoepidermoid carcinomas, 13 papillary adenocarcinomas, eight acinic cell carcinomas, seven undifferentiated carcinomas, six osteosarcomas and 37 other histological types. There were six cases of T1, 40 of T2, 68 of T3, 201 of T4, three of TX, 101 of postoperative, 27 of post-chemotherapy, nine of postoperative and post-chemotherapy and one case of post-carbon ion radiotherapy disease. Carbon ion radiotherapy was administered using 16 fractions over four weeks for all cases. The 455 lesions were irradiated with a dose of 57.6 GyE in 280 cases and with 64.0 GyE in 175 cases.

Results

Acute reactions were of a minor nature, as 16 patients (4%) showed a grade 3 skin reaction and 88 patients (20%) showed a grade 3 mucosal reaction. Late toxic reactions comprised a grade 2 skin reaction in eight patients (2%) and mucosal reactions in 13 patients (3%), with no evidence of radiation-induced toxicities worse than these. This therapy can therefore be described as presenting no clinical problems.

The local tumor reactions within six months consisted of a CR for 55 patients, PR for 212 patients, NC for 182 patients and PD for six patients. The response rate was 57%. The five-year LC and OS rates were 75% and 55%, respectively. The five-year LC rate according to histological type was 81% for the 51 adenocarcinomas, 75% for the 186 adenoid cystic carcinomas, 79% for the 102 malignant melanomas, 70% for the 25 squamous cell carcinomas and 24% for the 14 bone and soft tissue sarcomas. The five-year OS rate was 56% for adenocarcinomas, 74% for adenoid cystic carcinomas and 33% for malignant melanomas.

Discussion

The overall LC rate was 75% at five years. The therapeutic effectiveness was particularly outstanding for adenoid cystic carcinoma, a tumor type that is intractable to photon radiotherapy. The treatment results of surgery or radiotherapy in previous studies ranged from 27% to 72% for the five-year LC rate and from 25 to 85% for the five-year survival rate [3, 4] (Table 1). In the present study, the five-year LC rate was 75%, in spite of including 139 cases (74%) of T4 or recurrent tumors after surgery and/or chemotherapy.

Table 1. Clinical characteristics of reported cases of adenoid cystic carcinoma

Institutions	N		5y local control (%)	5y survival (%)
Iowa, 2009 [3]	54	Surgery alone	72	85
Florida, 2004 [4]	101	Radiotherapy alone	56	57
Iowa, 2009 [3]	10	Radiotherapy alone	27	25
NIRS,	186	Carbon ions (all cases)	75	74
(1997~2013)	36	Carbon ions (T1 to T3)	85	94
	149	Carbon ions (T4 or recurrences)	72	69

Although the local control of carbon ion radiotherapy was promising for malignant head-and-neck tumors, excluding sarcoma, the survival rate was not commensurate with the favorable local control rate of the malignant melanoma. Based on the results of the preliminary analysis of this protocol (Protocol 9602), two protocols were derived that went into effect in April 2001: 1) the "Phase I/II Clinical Trial of Carbon Ion Radiotherapy for Bone and Soft Tissue Sarcomas in Head-and-Neck (Protocol 0006)" designed as a dose escalation study for bone and soft tissue tumors, and 2) the "Phase II Clinical Trial of Carbon Ion Radiotherapy Combined with Chemotherapy for Mucosal Malignant Melanoma in Head and Neck (Protocol 0007)" for the treatment of malignant melanoma with concomitant chemotherapy.

2. Phase I/II and II Clinical Trials for Bone and Soft Tissue Sarcomas in the Head-and-Neck Region in Adult (Protocol 0006)

Introduction

A phase I/II protocol was commenced in April 2001 for the purpose of a dose escalation study of carbon ion radiotherapy against bone and soft tissue sarcomas in the head-and-neck regions, since the preliminary analysis of the phase II clinical trial for malignant head-and-neck tumors (Protocol 9602) suggested that the local control and survival of bone and soft tissue sarcomas in the head-and-neck was clearly worse than that of other malignant tumors. We adopted 70.4 GyE in 16 fractions over four weeks as the initial prescribed dose in the present study. It was considered that if the toxicities were acceptable, we might be able to proceed to the next irradiation dose; however, because the local control rate had been approximately 100% with the initial dose for the period of the present study, and because it was clear that more than 70.4 GyE would lead to many unacceptable adverse effects from the results of carbon ion dose escalation study for sarcomas in the trunk in our institution [5], we determined that 70.4 GyE is the recommended dose for unresectable bone and soft tissue sarcomas in the adult head-and-neck region. This phase I/II study was completed in February 2008. In April 2008, a phase II clinical study was started with the same dose fractionation.

Patients and Methods

The 44 patients included in the analysis between April 2001 and March 2013 consisted of 22 males and 22 females. The age range was from 17 to 78 years, with a median of 50 years. There were 15 patients with osteosarcoma, five with MFH, three with chondrosarcoma, three with hemangiopericytoma, three with spindle cell sarcoma, two with myxofibrosarcoma, two with leimyosarcoma, two with small round cell sarcoma and nine with other histological types.

Results

Almost all patients presented less than grade 2 acute reactions; however, seven patients developed a grade 3 mucosal reaction. Although only one patient showed each late grade 2 skin and mucosal reaction, most other late skin and mucosal reactions were grade 1 or less. The five-year LC and OS rates of all patients were 75% and 52%, respectively. The five-year LC rate according to histological type was 55% for the 15 osteosarcomas and 83% for the 29 soft tissue sarcomas.

Discussion

Bone and soft tissue sarcomas in the head-and-neck are rare mesenchymal malignant neoplasms accounting for less than 10% of all bone and soft tissue sarcomas, and approximately 1% of all head-and-neck neoplasms. Willers et al. said that wide resection margins are anatomically difficult to achieve, and the delivery of a high radiation dose can be limited by the proximity of critical normal tissue structures (spinal cord, brain stem, optic chiasm, eyes). Accordingly, the local control rates for head-and-neck sarcomas are lower compared to those of tumor affecting the extremities [6]. The five-year LC rate of combined surgery and radiotherapy is 60-70%. The LC of surgery alone is around 54%, and that of radiotherapy alone is 43- 50% [7]. However, in unresectable sarcomas, the LC and survival prognosis are poor. Conventional radiotherapy with a total dose less than 65 Gy showed no local control [8-10].

The results of carbon ion radiotherapy in our previous study (9602) of bone and soft tissue sarcomas in the head and neck region, in which study patients were treated using 64.0 or 57.6 GyE in 16 fractions, showed a 24% five-year LC rate. On the other hand, the five-year LC rate of this current study (0006) was 75%. This result showed a tendency toward improvement compared with surgery with or without radiotherapy.

3. Phase II Clinical Trial for Mucosal Malignant Melanoma in Head-and-Neck Combined with Chemotherapy (Protocol 0007)

Introduction

Although the phase II clinical study for malignant head-and-neck tumors (Protocol 9602) had achieved a satisfactory local control rate for mucosal malignant melanomas, the survival rate was not commensurate with the favorable local control rate of malignant melanomas. In view of this result, another protocol was started in April 2001 for the purpose of prophylactic therapy against distant metastasis, the major cause of death in patients with malignant melanoma of the head-and-neck region.

Patients and Methods

The carbon ion dose was 57.6 GyE in 16 fractions over four weeks. Concomitant chemotherapy (DAV: Day 1: DTIC 120 mg/m^2 + ACU 70 mg/m^2 + VCR 0.7 mg/m^2; Days 2~5: DTIC 120 mg/m^2, at four week intervals for a total of five courses) was administered as two courses before and three courses after carbon ion radiotherapy. The results for the seven patients treated until February 2002 showed that at the time of completion of the two courses of DAV chemotherapy prior to carbon ion radiotherapy, there was a PR for two patients, NC for two patients and PD for three patients, necessitating the early commencement of carbon ion radiotherapy. From April 2002, carbon ion radiotherapy and DAV chemotherapy were carried out concurrently.

The 116 patients included in the analysis between April 2001 and March 2013 consisted of 53 males and 63 females. Their ages ranged from 26 to 79 years, with a median of 63 years. Their KPS ranged from 70% to 100%, with a median of 90%. For the tumor sites studied, there were 93 nasal cavity and paranasal sinus tumors, 14 oral cavity tumors, six pharyngeal tumors and three orbital tumors.

Results

The acute reactions of 116 patients who were followed-up for more than six months consisted of one patient with a grade 3 skin reaction and 28 patients (24%) with a grade 3 mucosal reaction, while the other toxicities that were observed were grade 2 or less. All late reactions in both the skin and mucosa were grade 1 or less.

The local tumor reactions within six months consisted of a CR for 22 patients, PR for 53 patients, SD for 41 patients and PD for no patients. The effective rate was 68%. The five-year LC and OS rates of all patients were 80% and 50%. In the 109 patients treated with concomitant therapy, the five-year LC and OS rates were 82% and 52%, respectively.

Discussion

The reported local failure of systemic therapy, including surgery, radiotherapy and chemotherapy is very high (45-54%) [11, 12]. The five-year LC rate of carbon ion radiotherapy was 80% in this protocol. These results show the effectiveness of carbon ion radiotherapy for the local control of mucosal malignant melanoma in the head-and-neck region. Previous review articles [13-17] reported that the five-year survival rates ranged from 18-35% (Table 2), which was attributed mainly to the development of distant metastasis. The five-year OS rate of carbon ion radiotherapy was 33% in the 9602 protocol and 50% in the 0007 protocol. This shows that there

has been a tendency for the results of concomitant and adjuvant chemotherapy to improve the response (Protocol 0007) (Fig. 2).

Table 2. Clinical characteristics of reported cases of mucosal malignant melanoma

	Authors		N	5-year OS (%)
Radiotherapy	Gilligan [13]	1991	28	18
(+/- Surgery)	Shibuya [14]	1992	28	25
Surgery	Chang [15]	1998	163	32
(+/- RT, +/- Chemo)	Patel [16]	2002	59	35
	Lund [17]	1999	58	28
Carbon ion alone	NIRS	2013	102	33
Carbon ion + Chemo	NIRS	2013	116	50

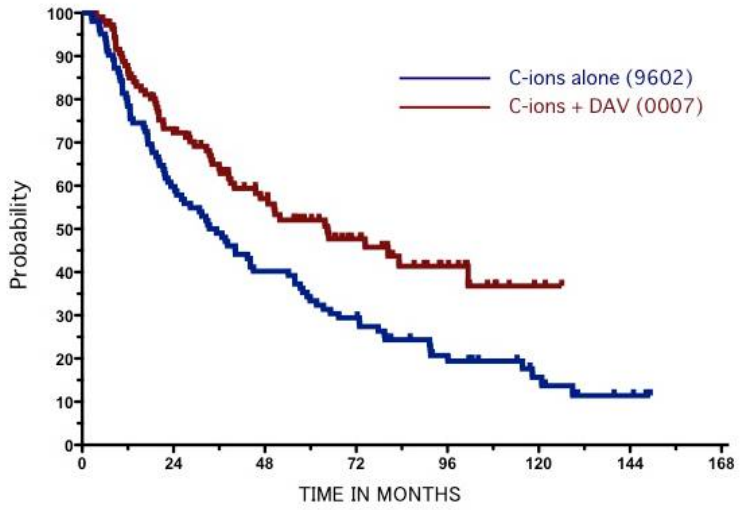

Figure 2. Overall Survival of Mucosal Malignant Melanomas

Conclusion

Malignant head-and-neck tumors are therapeutically very diverse because of the many important organs present in this region and the great variety of tissue types involved. Carbon ion radiotherapy requires considerable versatility in terms of the use of a specific radiation dose suited for the particular histological type and the application of concurrent chemotherapy. At present, efforts are being made to increase the numbers of patients in order to produce results that can provide cogent clinical evidence.

References

［1］ Mizoe J, Tsujii H, Kamada T, et al: Dose escalation study of carbon ion radiotherapy for locally advanced head-and-neck cancer. Int J Radiat Oncol Biol Phys. 2004; 60: 358-364.

［2］ Mizoe J, Hasegawa A, Jingu K, et al: Results of carbon ion radiotherapy for head and neck cancer. Radiother Oncol. 2012; 103: 32-37.

［3］ Iseli TA, Karnell LH, Graham SM, et al: Role of radiotherapy in adenoid cystic carcinoma of the head and neck. J Laryngol Otol. 2009; 123: 1137-1144.

［4］ Mendenhall WM, Morris CG, Amdur RJ, et al: Radiotherapy alone or combined with surgery for adenoid cystic carcinoma of the head and neck. Head Neck. 2004; 26(2): 154-162.

［5］ Kamada T, Tsujii H, Tsuji H, et al: Efficacy and safety of carbon ion radiotherapy in bone and soft tissue sarcomas. J Clin Oncol. 2002; 20: 4466-71.

［6］ Willers H, Hug EB, Spiro IJ, et al: Adult soft tissue sarcomas of the head and neck treated by radiation and surgery or radiation alone: patterns of failure and prognostic factors. Int J Radiat Oncol Biol Phys. 1995; 33: 585-593.

［7］ Mendenhall WM, Mendenhall CM, Werning JW, et al: Adult head and neck soft tissue sarcomas. Head Neck. 2005: 27: 916-922.

［8］ Le QT, Fu KK, Kroll S, et al: Prognostic factors in adult soft-tissue sarcomas of the head and neck. Int J Radiat Oncol Biol Phys. 1997; 37: 975-984.

［9］ Barker JL Jr, Paulino AC, Feeney S, et al: Locoregional treatment for adult soft tissue sarcomas of the head and neck: an institutional review. Cancer J. 2003; 9: 49-57.

［10］ Chen SA, Morris CG, Amdur RJ, et al: Adult head and neck soft tissue sarcomas. Am J Clin Oncol. 2005; 28: 259-263.

［11］ Mendenhall WM, Amdur RJ, Hinerman RW, et al: Head and neck mucosal melanoma. Am J Clin Oncol. 2005; 28: 626-630.

［12］ Lengyel E, Gilde K, Remenár E, et al: Malignant Mucosal Melanoma of the Head and Neck -a Review- Pathology Oncology Research. 2003; 9: 7-12.

［13］ Gilligan D, Slevin NJ: Radical radiotherapy for 28 cases of mucosal melanoma in the nasal cavity and sinuses. Br J Radiol. 1991; 64:1147-1150.

［14］ Shibuya H, Takeda M, Matsumoto S, et al: The efficacy of radiation therapy for malignant melanoma in the mucosa of the upper jaw: an analytic study. Int J Radiat Oncol Biol Phys. 1992; 25: 35-39.

［15］ Chang AE, Karnell LH, Menck HR: The National Cancer Data Base Report on cutaneous and noncutaneous melanoma. Cancer. 1998; 83: 1664-1678.

［16］ Patel SG, Prasad ML, Escrig M, et al: Primary mucosal malignant melanoma of the head and neck. Head Neck. 2002; 24: 247-257.

［17］ Lund VJ, Howard DJ, Harding L, et al: Management options and survival in malignant melanoma of the sinonasal mucosa. Laryngoscope. 1999; 109: 208-211.

Carbon Ion Radiotherapy for Skull Base and Upper Cervical Spine Tumors

Masashi Koto, Azusa Hasegawa, Ryo Takagi, Hiroaki Ikawa, Hirohiko Tsujii, and Tadashi Kamada

Research Center for Charged Particle Therapy, National Institute of Radiological Sciences, Chiba, Japan.

e-mail address: koto@nirs.go.jp

Abstract

Purpose: To estimate the toxicity and efficacy of carbon ion radiotherapy for skull base and upper cervical spine tumors.

Patients and Methods: A phase I dose escalation study for skull base and upper cervical spine tumors was initiated in April 1997. The patients were treated with 16 fractions over four weeks, with a total dose of 48.0, 52.8, 57.6, or 60.8 Gy equivalents (GyE). In April 2004, a phase II study was initiated with an irradiation schedule of 60.8 GyE in 16 fractions over four weeks. There were 84 patients included in the analysis. Histologically, 51 patients had chordoma, 15 chondrosarcoma, nine olfactory neuroblastoma, seven meningioma and two had other types. The patients were treated with a dose of 48.0 GyE (four patients), 52.8 GyE (six patients), 57.6 GyE (nine patients) or 60.8 GyE (65 patients).

Results: The follow-up periods ranged from four to 179 months, with a median period of 62 months. The five-year local control and overall survival rates for all patients were 86% and 85%, respectively. The five-year local control and overall survival rates for chordoma patients were 87% and 90%, respectively. At the time of the analysis, there was no evidence of any serious acute (Grade $\geq$ 4) reactions. Regarding late reactions, a grade 4 brain injury developed in one patient and a grade 4 optic nerve neuropathy developed in one patient.

Conclusion: A carbon ion dose of 60.8 GyE in 16 fractions was effective and safe for the treatment of skull base and upper cervical spine tumors.

Introduction

The management of skull base and upper cervical spine tumors is challenging, because they lie in close proximity to critical structures such as the brainstem, spinal cord and anterior optic pathways. These anatomical structures often limit surgical access and resectability, as well as the delivery of high-dose radiations. In addition, some tumors that originate from the skull base region have different dose requirements. For example, more than 70 Gy of radiation is needed to achieve local control of chordoma, and more than 60 Gy is needed for chondrosarcoma [1]. New treatment techniques, such as intensity-modulated radiotherapy and stereotactic radiotherapy, have improved the dose distribution and are being used for skull base tumors. However, the clinical results are still unclear.

On the other hand, proton therapy with its superior physical spatial distribution has provided a major improvement in local control with regard to possible dose escalations. Several studies reported promising results of using proton therapy for skull base tumors. Munzenrider et al. reported that the 10-year local control rate for

chondrosarcoma treated with proton therapy was 94% [2]. Wenkel et al. reported that the 10-year local control rate for meningioma treated with combined proton and photon therapy was 88% [3]. However, in chordoma patients, local control with proton therapy, even at elevated doses, is difficult to achieve. The reported five-year local control rates for chordoma treated with proton therapy ranged from 46 to 81% [2, 4-6]. Therefore, the high linear energy transfer of carbon ion radiotherapy has promising potential for the treatment of skull base chordoma [7, 8]. In this study, we estimated the toxicity and efficacy of carbon ion radiotherapy for skull base and upper cervical spine tumors.

Methods and Materials

1. Protocol

A phase I dose escalation study for skull base and upper cervical spine tumors was initiated in April 1997. The patients were treated with 16 fractions over four weeks with a total dose of 48.0, 52.8, 57.6 or 60.8 Gy equivalents (GyE). In April 2004, a phase II study was initiated with an irradiation schedule of 60.8 GyE in 16 fractions over four weeks. Chordoma, chondrosarcoma, meningioma, and other tumors arising from the skull base or paracervical spine located superior to the C2 vertebra were targeted. Only patients with residual tumors after surgery or with inoperable tumors were permitted to enroll in the carbon ion radiotherapy study. The eligibility criteria for enrollment in this clinical trial were the presence of a histologically proven tumor, patient age ranging from 15 to 80 years, a KPS of 60% or more, neurological function of grade I or II, the absence of anti-cancer chemotherapy within the previous four weeks, asurvival expectancy of six months or more and no distant metastasis.

2. Treatment planning

A set of 2.5-mm-thick CT images was taken for treatment planning, with the patient placed in a custom-made immobilization device with a dental mouthpiece. The metals in the oral cavity were removed before the treatment planning CT to avoid artifacts on CT images including the tumor. The gross tumor volume (GTV) was delineated on the CT images using CT-MRI fusion. The clinical target volume was defined with an adequate safety margin for the GTV. A margin of 5 mm was usually added to the CTV to create the planning target volume. In cases where the tumor was close to critical organs, such as the brain stem or spinal cord, the CTV margin was reduced to spare these organs. The limiting doses for critical normal tissues were set as 30 GyE for the spinal cord and brain stem and 40 GyE for the optic chiasm and optic nerves. When the ipsilateral optic nerve was located very close to the tumor, the dose limitation for the optic nerve was ignored. A limiting dose for the brain was not provided. However, it was recommended that brain volumes receiving more than 50 GyE of radiation should be less than 5 mL to reduce the risk of developing brain necrosis. Three-dimensional treatment planning was performed with the HIPLAN software program (National Institute of Radiologic Sciences, Chiba, Japan) designed for carbon ion radiotherapy. Carbon ion radiotherapy was given once daily, four days a week. The patients were treated with two to five ports. One port was used in each treatment session. At every treatment session, the patient's position was verified with a computer-aided on-line positioning system. The patient was positioned on a treatment couch with the immobilization devices, and digital orthogonal X-ray TV images in that

position were taken and transferred to the positioning computer. They were compared with the reference image on the computer screen, and the differences were measured. The treatment couch was then moved to the matching position until the largest deviation from the field edge and iso-center position was less than 2 mm.

3. Patients

The carbon ion dose was escalated in successive stages: 48 GyE in four patients, 52.8 GyE in six patients, 57.6 GyE in nine patients and 60.8 GyE in nine patients. The phase I clinical trial was concluded in February 2004, and in April 2004, a phase II clinical trial was initiated under the Highly Advanced Medical Technology scheme, with an irradiation schedule of 60.8 GyE in 16 fractions over four weeks. 56 patients were enrolled in this trial until June 2012. The total 84 patients included in the analysis consisted of 40 males and 44 females. Their ages ranged from 16 to 78 years, with a median of 51 years. Histologically, 51 patients had chordoma, 15 chondrosarcoma, nine olfactory neuroblastoma, seven meningioma, one giant cell tumor and one had neuroendocrine carcinoma. Sixty-six tumors were located in the skull base region and 18 in the upper cervical spine region.

4. Statistical analysis

Acute toxicity was assessed based on the Radiation Therapy Oncology Group (RTOG) score, and late toxicity was determined based on the RTOG/European Organisation for Research and Treatment of Cancer (EORTC) score. The follow-up time was calculated from the first date of irradiation. The local control and overall survival rates were calculated according to the Kaplan-Meier method.

Results

1. Toxicity

Acute reactions were of a minor nature, as one of the patients in the 48 GyE group showed a grade 3 skin reaction, and one patient in the 57.6 GyE group and three patients in the 60.8 GyE group developed a grade 3 mucosal reaction.

Regarding late reactions, one patient was scored as having grade 4 brain morbidity and two as grade 2. The patient with grade 4 developed left paresis due to a cystic formation originating from radiation-induced brain necrosis. However, the patient received cyst enucleation twice and is still alive without any paresis or disease. A grade 4 optic nerve neuropathy was observed in one patient and grade 3 neuropathy was observed in another. One patient with cervical spine chordoma developed grade 3 radiation myelitis.

2. Local control and survival

The follow-up periods ranged from four to 179 months, with a median period of 62 months. Local control was defined as showing no evidence of tumor regrowth by MRI, CT, physical examination or biopsy. The five-year local control and overall survival rates for all patients were 86% and 85%, respectively. The five-year local control rate according to the histological types was 87% for the 51 chordomas, 81% for the 15 chondrosarcomas, 89% for the nine olfactory neuroblastomas and 83% for the seven meningiomas. The five-year overall survival

rate was 90% for patients with chordomas, 76% for chondrosarcomas, 73% for olfactory neuroblastomas, and 86% for those with meningiomas. The five-year local control and overall survival rates for the patients treated with a dose of 60.8 GyE were 86% and 84%, respectively.

3. Chordomas

Of the 84 patients, 51 patients (61%) had chordomas. The follow-up period ranged from 13 to 163 months, with a median of 63 months. The five-year and 10-year local control rates of all chordoma patients were 87% and 80%, respectively (Fig. 1). The five-year local control rates of the patients treated with a dose of 60.8 GyE was 89%. Of the 51 patients, seven patients developed in-field recurrence. The local recurrence (in-field) patterns for chordomas were analyzed (Table 1). All of the recurrent sites were located on the edge of the tumors. There were no patients with in-field recurrence from the center of the tumor. In the seven patients who developed in-field recurrence, five of the recurrent sites were very close to an organ at risk, such as the brain stem or spinal cord.

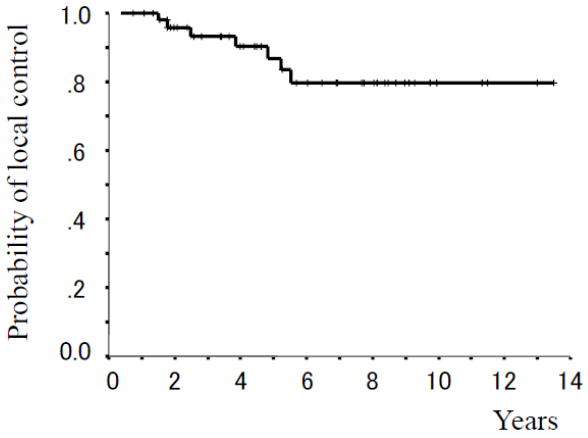

Fig. 1. The local control rate of skull and upper cervical spine chordomas treated with carbon ion radiotherapy (n=51).

Table 1. The local recurrence patterns of chordomas

	Age	Gender	Tumor location	Dose (GyE)	Recurrent site
1	47	F	C	48.0	Marginal (spinal cord)
2	64	F	C	57.6	Marginal (pharynx)
3	63	M	C	60.8	Marginal (pharynx)
4	67	F	C	60.8	Marginal (spinal cord)
5	47	F	S	52.8	Marginal (brain stem)
6	30	M	S	60.8	Marginal (brain stem)
7	49	M	S	60.8	Marginal (brain stem)

* C: cervical, S: skull base

Discussion

A carbon ion dose of 60.8 GyE showed excellent local control for skull base and upper cervical tumors. Beginning in April 2004, a phase II trial using carbon ion radiotherapy was initiated under the Highly Advanced Medical Technology scheme with an irradiation schedule of 60.8 GyE in 16 fractions over four weeks.

High LET charged particles, such as carbon ions, have excellent dose localizing properties, and this can cause severe damage to the tumor while minimizing the effects on normal tissues. When the tumor was located close to critical organs, delineation of the clinical target volume was done in an effort to prevent damage to these organs. In particular, when both optic nerves were involved in the high dose area, treatments were planned to spare the contralateral optic nerve and chiasm based on our previous dose criteria [9]. For tumors close to the brain stem or spinal cord, we recommended surgical resection to create a space between the tumor and these organs before carbon ion radiotherapy was administered. This allowed for better prevention of severe toxicity to the brain stem and spinal cord, and may have improved the local control rate. Most local recurrences of chordomas developed from the marginal site adjacent to these critical organs.

Shultz-Ertner et al. previously showed the dose-response curve of chordomas for local control rates based on several reported studies and their clinical results [8]. A prescribed dose of 60.8 GyE in 16 fractions contains 88.2 GyE in terms of the conventional fraction. Our data, which was an 89% at five-year for local control rate for chordomas, corresponded to the expected value based on their curve.

Tumors such as chordomas can be judged based on the results of the long-term prognosis. Consequently, it will take more time to reach a definitive conclusion about the efficacy of the carbon ion radiotherapy in our series of patients. However, it is already clear that, compared with photon or other charged particle radiotherapy, carbon ion radiotherapy will provide higher local control rates (Table 2) [2,4-6,10-14]. Notably, the 10-year local control rate of chordomas is 80% for this study.

Table 2. The clinical characteristics of the previously reported cases of skull base chordoma

			Median	Median f/u	Local control rate (%)		
	Authors	N	dose	(y)	3-y	5-y	10-y
Photon	Catton et al . [10]	24	50	5.2		23	15
	Romero et al. [11]	18	50	3.1		17	
	Forsyth et al. [12]	39	50	8.3		39	31
	Magrini et al. [13]	12	58	6		25	25
Proton (+/- photon)	Munzenrider et al. (MGH) [2]	169	66-83	3.4		73	54
	Noel et al (CPO) [4]	100	67	2.6	86 (2y)	54 (4y)	
	Igaki et al. (Tsukuba) [5]	13	72	5.8	67	46	
	Ares et al. (PSI) [6]	42	73.5	3.2 (mean)		81	
Helium	Castro et al. (LB) [14]	53	65	4.3		63	
Carbon	Shults-Ertner et al. (GSI) [8]	96	60	2.6 (mean)	81	70	
	NIRS	51	60.8	5.3		87	80

Conclusion

In this phase I/II clinical study for skull base and upper cervical spine tumors, a dose escalation study was performed up to the fourth-stage dose level. Finally, a dose fractionation regimen of 60.8 GyE in 16 fractions over four weeks was recommended. Our data from a phase I/II study have demonstrated that a carbon ion dose 60.8 GyE was effective and safe for the treatment of skull base and upper cervical spine tumors.

References

[1] Debus J, Schulz-Ertner D, Schad L, et al Stereotactic fractionated radiotherapy for chordomas and chondrosarcomas of the skull base. Int J Radiat Oncol Biol Phys. 2000; 47: 591-96.

[2] Munzenrider JE, Liebsch NJ. Proton therapy for tumors of the skull base. Strahlenther Onkol. 1999; 175: 57-63.

[3] Wenkel E, Thornton AF, Finkelstein D, et al Benign meningioma: partially resected, biopsied, and recurrent intracranial tumors treated with combined proton and photon radiotherapy. Int J Radiat Oncol Biol Phys. 2000; 48: 1363-70.

[4] Noël G, Habrand JL, Jauffret E, et al Radiation therapy for chordoma and chondrosarcoma of the skull base and the cervical spine. Prognostic factors and patterns of failure. Strahlenther Onkol. 2003; 179: 241-8.

[5] Igaki H, Tokuuye K, Okumura T, et al Clinical results of proton beam therapy for skull base chordoma. Int J Radiat Oncol Biol Phys. 2004; 60: 1120-26.

[6] Ares C, Hug EB, Lomax AJ, et al Effectiveness and safety of spot scanning proton radiation therapy for chordomas and chondrosarcomas of the skull base: first long-term report. Int J Radiat Oncol Biol Phys. 2009; 75: 1111-8.

[7] Mizoe J, Hasegawa A, Takagi R, et al Carbon ion radiotherapy for skull base chordoma. Skull Base. 2009; 19: 219-24.

[8] Schulz-Ertner D, Karger CP, Feuerhake A, et al Effectiveness of carbon ion radiotherapy in the treatment of skull-base chordomas. Int J Radiat Oncol Biol Phys. 2007; 68: 449-57.

[9] Hasegawa A, Mizoe J, Mizota A, Tsujii H. Outcomes of visual acuity in carbon ion radiotherapy: analysis of dose–volume histograms and prognostic factors. Int J Radiat Oncol Biol Phys. 2006; 64: 396-401.

[10] Catton C, O'Sullivan B, Bell R, et al Chordoma: Long-term follow-up after radical photon irradiation. Radiother Oncol. 1996; 41: 67-72.

[11] Romero J, Cardenes H, la Torre A, et al Chordoma: Results of radiation therapy in eighteen patients. Radiother Oncol. 1993; 29: 27-32.

[12] Forsyth PA, Cascino TL, Shaw EG, et al Intracranial chordomas: A clinicopathological and prognostic study of 51 cases. J Neurosurg. 1993; 78: 741-7.

[13] Magrini SM, Papi MG, Marletta F, et al Chordoma- natural history, treatment and prognosis. The Florence Radiotherapy Department experience (1956-1990) and a critical review of the literature. Acta Oncol. 1992; 31: 847-51.

[14] Castro JR, Linstadt DE, Bahary JP, et al Experience in charged particle irradiation of tumors of the skull base: 1977-1992. Int J Radiat Oncol Biol Phys. 1994; 29: 647-55.

Carbon Ion Radiotherapy in a Hypofractionated Regimen for Stage I Non-Small Cell Lung Cancer

Naoyoshi Yamamoto

Research Center for Charged Particle Therapy, National Institute of Radiological Sciences, Chiba, Japan
e-mail address: nao_y@nirs.go.jp

Abstract

Beginning in 1994, we conducted a phase I/II clinical trial for stage I non-small cell lung cancer (NSCLC) by using carbon ion beams alone, demonstrating optimal doses of 90.0 GyE in 18 fractions over six weeks and 72.0 GyE in nine fractions over three weeks for achieving more than 95% local control with minimal pulmonary damage. Following this schedule, we conducted phase II clinical trials for stage I NSCLC from 1999 to 2003. In the present study, the total dose was fixed at 72.0 GyE in nine fractions over three weeks, and at 52.8 GyE for stage IA and 60.0 GyE for stage 1B in four fractions in one week. We also conducted a phase I/II single fractionation clinical trial as a dose escalation study. The total dose was increased from 28.0 GyE to 50.0 GyE.

In the first and second phase II trials, the local control rate for all patients was 91.5%, and those for patients with T1 and T2 tumors were 96.3% and 84.7%, respectively. The five-year overall survival rate was 45.3%. No adverse effects greater than grade 2 occurred in the lung.

In a single fractionation trial, the five-year local control rate for 151 patients was 79.2%, and the control rates for T1 and T2 tumors were 83.6% and 72.2%, respectively. No adverse effects greater than grade 2 occurred in the lung.

Carbon beam radiotherapy, an excellent new modality in terms of a high quality of life and activities of daily living, was proven to be a valid alternative to surgery for patients with stage I cancer, especially for elderly and inoperable patients.

Introduction

In 1998, lung cancer became the leading cause of cancer-related death in Japan, as it had been in Western countries. Surgery plays a pivotal role in the curative treatment for non-small cell lung cancer (NSCLC), but it is not necessarily the best treatment for elderly patients and/or patients with cardiovascular and pulmonary complications. Conventional radiotherapy as an alternative, however, produces a five-year survival rate of merely 10-30% due to poor control of the primary tumor. Dose escalation is essential to improve the effectiveness of radiotherapy, but this involves increasing the risk of pulmonary toxicity. Carbon ion radiotherapy (CIRT) is a promising modality because of its excellent dose localization and high biological effect on the tumor. Our previous clinical trials led us to conclude that irradiation with heavy particle beams, notably carbon ion beams, offers a significant potential for improving tumor control without increasing the risk of toxicity.

Between 1994 and 1999, a phase I/II study of the treatment of stage I NSCLC by CIRT was first conducted using a dose escalation method to determine the optimal dose. An additional purpose was to develop correct, reliable and safe irradiation techniques for CIRT. As reported in our phase I/II study [1,2], the following results were obtained: 1) The local control rate was dose-dependent, reaching more than 90% at 90.0 GyE with a regimen of 18 fractions over six weeks and at 72.0 GyE with nine fractions given over three weeks. Both

regimens were determined to be optimal. It was found that setting the provisional target by adding a small margin to the gross target volume to generate a clinical target volume could prevent marginal recurrence [3]. 2) Damage to the lung was minimal, with grade 3 radiation pneumonitis occurring in 2.7% of the cases. Respiratory-gated and 4-portal oblique irradiation directions excluding opposed ports proved successful for reducing the incidence of radiation pneumonitis. 3) Survival was strongly influenced by local control and the size of the primary lesion. The early detection of nodal and intralobar metastasis, followed by irradiation with carbon beams, can prevent the survival rate from decreasing further. Local failure, distant metastasis and malignant pleurisy were responsible for decreases in survival.

In the present study, a phase II clinical trial and a phase I/II dose escalation clinical trial are reported. In the phase II clinical trial, the total dose was fixed at 72.0 GyE in nine fractions given over three weeks [4], and at 52.8 GyE for stage IA NSCLC and 60.0 GyE for stage IB NSCLC in four fractions in one week [5]. Using this optimal schedule, the phase II clinical trial was initiated in April 1999 and closed in December 2003, accruing a total of 127 patients.

The phase I/II dose escalation clinical trial was initiated in April 2003. The initial total dose was 28.0 GyE, administered in a single fraction using respiratory-gated and 4-portal oblique irradiation directions, with the total irradiation dose being escalated in increments of 2.0 GyE each, up to 50.0 GyE. This clinical trial is still in progress. This article describes the intermediate steps of the phase I/II clinical trial and the results of the phase II clinical trial in terms of the local control and survival after CIRT.

Materials and Methods

1. Phase II clinical trial

One hundred and twenty-nine patients with 131 primary lesions were treated with CIRT. Fifty-one primary tumors of 50 patients were treated by carbon ion beam irradiation alone using a fixed total dose of 72 GyE in nine fractions over three weeks (#9802 protocol [4]). The remaining 79 patients had 80 stage I tumors (#0001 protocol [5]). For the survival analysis, 127 patients were evaluated, since two patients had been treated twice, one in the first protocol (#9802), and one in the second protocol (#0001). The IA and IB stage tumors were treated with fixed doses of 52.8 GyE and 60.0 GyE in four fractions in one week, respectively. The mean patient age was 74.5 years, and the gender breakdown was 92 males and 37 females. The tumors were 72 T1 and 59 T2. The mean tumor size was 31.5 mm in diameter. By type, there were 85 adenocarcinomas, 43 squamous cell carcinomas, two large cell carcinomas and one adenosquamous cell carcinoma. Medical inoperability stood at 76%.

2. Phase I/II clinical trial (single fractionation)

One hundred and fifty-one patients were treated in this clinical trial between April 2003 and March 2012. As mentioned above, the intermediate steps of the phase I/II clinical trial included a total dose of 36.0 GyE or more, and the local control rate was as high as 80%. The 151 primary tumors were treated by carbon ion beam irradiation alone using a total dose of 36.0 GyE (n=18), 38.0 GyE (n=14), 40.0 GyE (n=20), 42.0 GyE (n=15), 44.0 GyE (n=44), 46.0 GyE (n=20), 48.0 GyE (n=10) or 50.0 GyE (n=10) per single fractionation. The mean patient age was 73.9 years, and the gender breakdown was 51 females and 100 males. The tumors were 91 T1 and 60 T2. The mean tumor size was 29.0 mm in diameter. By type (the cancer type was determined by biopsy), there were 104 adenocarcinomas, 46 squamous cell carcinomas, and one large cell carcinoma. The medical inoperability rate was 55.6%.

3. Planning

The same system of carbon ion beam irradiation was used in both the phase II and phase I/II clinical trials. The targets were usually irradiated from four oblique directions without prophylactic elective nodal irradiation (ENI). A greater than 10 mm margin was set outside the gross target volume (GTV) to determine the clinical target volume (CTV). The planning target volume (PTV) was established by adding an internal margin (IM) to the CTV. The IM was determined by extending the target margin in the head and tail directions by a width of 5

mm, leading to a successful prevention of marginal recurrence, possibly resulting from respiration movement [3]. A respiratory-gated irradiation system was used in all irradiation sessions.

Results

1. Phase II clinical trial (#9802, #0001)

All patients were followed up until death, with a median follow-up time of 50.8 months, ranging from 2.5 months to 70.0 months. The local control rate for the 131 primary lesions was 91.5%, those for T1 (n=72) and T2 (n=59) tumors were 96.3% and 84.7%, and those for squamous cell type (Sq) (n=43) and non-squamous cell type (Non-Sq) (n=88) tumors were 87.1% and 93.8%, respectively. While there was a significant difference (p=0.0156) in the tumor control rate between T1 and T2 tumors, there was no significant difference (P=0.1516) between squamous and non-squamous tumors in T1+T1 patients, nor between T1 and T2 tumors. However, with respect to squamous cell type cancer, the local control rate was 100% for T1 (n=17) and 78.0% for T2 (n=26), tumors, which was a near-significant difference (p=0.0518). The local control of non-squamous tumors was 95.3% for T1 (n=55) and 91.0% for T2 (n=33), which was not significantly different (p=0.3364).

The five-year cause-specific survival rate of the 127 patients was 67%, breaking down into 84.8% for stage IA and 43.7% for stage IB tumors. The five-year overall survival rate was 45.3%, breaking down into 53.9% for stage IA and 34.2% for stage IB tumors.

Toxicities to the skin and lungs caused by CIRT were assessed according to RTOG (early) and RTOG/EOTRC (late). Early skin reactions were assessed for 131 lesions and late skin reactions for 128 lesions. Of the early reactions in the lesions, 125 were grade 1 and six were grade 2. Among the late reactions in the lesions, 126 were grade 1, one was grade 2 and one was grade 3. The lung reaction was clinically assessed in a total of 129 patients. One hundred twenty-seven patients had grade 0 and two had grade 2 early reactions. Late effects were evaluated in 126 patients: seven patients had grade 0, 116 patients had grade 1 and three patients had grade 2 reaction. No reaction higher than grade 2 was observed.

Fifty-three of the 127 patients (41.7%) had recurrence, all between one and 54 months (median, 10.5 months) after the commencement of therapy. No reoccurrence was observed in the other 74 patients (58.3%). The nine primary recurrences (7.1%) and 11 regional metastases (8.7%) consisting of seven regional nodes (5.5%), one intrabronchial (0.8%) and three cases with intralobar metastases (PM1) (2.4%) occurred in loco-regional sites. In one patient, primary recurrence was seen at the tumor margin, while in another, it occurred in-field.

The cause of death was as follows: 62 out of the 127 patients (48.8%) died, half of disease progression. Among the patients with recurrence, five of the nine with primary recurrence (55%) died from disease progression. Ten of the 11 patients with regional metastases were re-treated, nine with CIRT and one with photons. Seven of these patients, although they had no further recurrence, died due to intercurrent disease, and one with nodal metastasis but no re-treatment died of disease progression. Eight of the 11(72%) patients with regional metastases (72%) died, and nine of the 10 patients (90%) with malignant pleurisy and 17 of the 23 patients (74%) with distant metastases died of disease progression. Five of them died due to primary recurrence, and 26 due to metastasis and dissemination. For the remaining 31 patients, intercurrent diseases were the cause of death [4, 5, 6].

2. Phase I/II clinical trial (single fractionation)

All patients were followed up until death, with a median follow-up time of 45.6 months, ranging from 1.6 months to 88.4 months. The five-year overall local control rate for the 151 primary lesions was 79.2%, and those for the T1 (n=91) and T2 (n=60) tumors were 83.6% and 72.2%, respectively. The overall survival rate was 55.1%, and the cause-specific survival rate was 73.1% (Fig. 1).

Toxicities of CIRT to the skin and lung were assessed according to the NCI-CTC (early) and RTOG/EOTRC (late). Early skin reactions were assessed for 151 lesions and late skin reactions for 148 lesions. Of the early reactions in lesions, 146 were grade 1 and three were grade 2. Among the late reactions in lesions, 143 were

grade 1 and one was grade 2. Lung reactions were clinically assessed in all 151 patients. Forty-seven had grade 0, 101 had grade 1 and three had grade 2 early reactions. Late reactions were followed up in 146 patients, with 134 showing grade 1 reactions and one showing a grade 2 reaction. There were no adverse effects greater than grade 2.

The clinical course of a 71-year-old female is shown in Figures 2 and 3. Tumor shrinkage and slight lung fibrosis were apparent, and a grade 1 skin reaction was observed.

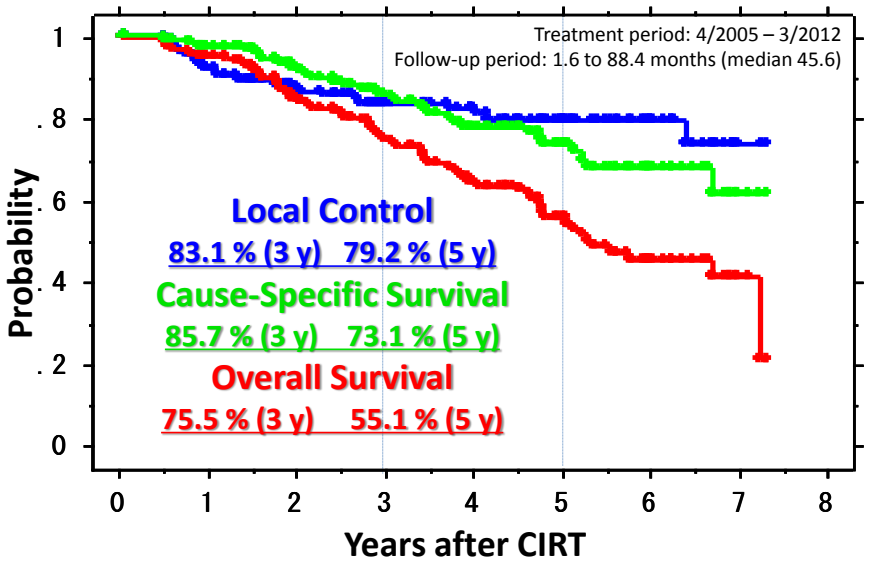

Fig.1. The survival and local control rates after CIRT using single fractionation

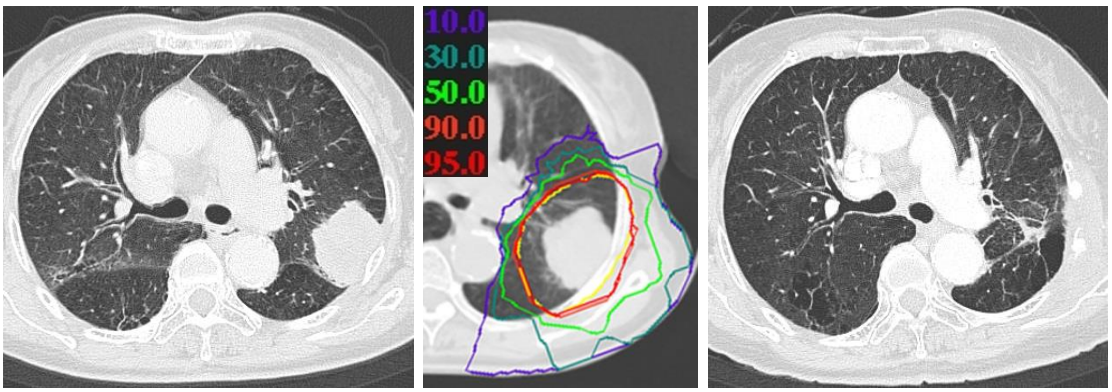

Fig. 2. The clinical course of a 71-year-old female (T2N0M0 squamous cell carcinoma) after CIRT (40 GyE/ single fractionation). Shown are an image taken prior to CIRT (left side), the dose distribution on the planning CT image (center), and a CT scan taken 18 months after CIRT (right side). Apparent tumor shrinkage was observed, without severe lung fibrosis.

Fig.3. The skin reaction after CIRT (40.0 GyE/1 fr). Grade 1early and late reactions were observed.

Conclusions

One hundred twenty-seven stage I NSCLC patients with 131 primary tumors were treated with CIRT using a total dose of 72 GyE in a regimen of nine fractions over three weeks, with 52.8 GyE administered to stage IA and 60 GyE for stage IB tumors in four fractions over one week. In addition, 151 stage I NSCLC patients with 151 primary tumors were treated with single-fraction CIRT using total doses ranging from 36.0 GyE to 50.0 GyE.

Carbon beam radiotherapy, an excellent new modality in terms of a high quality of life and activities of daily living, was proven to be a valid alternative to surgery for stage I cancer patients, especially for elderly and inoperable patients.

References

[1] Miyamoto T, Yamamoto N, Nishimura H, et al. Carbon ion radiotherapy for stage I non-small cell lung cancer. Radiother Oncol 2003;66:127-140.

[2] Yamamoto N, Miyamoto T, Nishimura H, et al. Preoperative carbon ion radiotherapy for non-small cell lung cancer with chest wall invasion - pathological findings concerning tumor response and radiation induced lung injury in the resected organs. Lung Cancer 2003;42:87-95.

[3] Koto M, Miyamoto T, Yamamoto N, et al. Local control and recurrence of stage I non-small cell lung cancer after carbon ion radiotherapy. Radiother Oncol 2004;71:147-156.

[4] Miyamoto T, Baba M, Yamamoto N, et al. Curative treatment of stage I non-small cell lung cancer with carbon ion beams using a hypo-fractionated regimen. Int J Radiat Oncol Biol Phys 2007;67:750-8.

[5] Miyamoto T, Baba M, Sugane T, et al. Carbon ion radiotherapy for stage I non-small cell lung cancer using a regimen of four fractions during 1 week. J Thorac Oncol 2007;2:916-26.

[6] Sugane T, Baba M, Imai R, et al. Carbon ion radiotherapy for elderly patients 80 years and older with stage I non-small cell lung cancer. Lung Cancer (2008), doi:10.1016/j.lungcan.2008.07.007.

Carbon Ion Radiotherapy for Bone and Soft Tissue Sarcomas

Reiko Imai

Research Center for Charged Particle Therapy, National Institute of Radiological Sciences, Chiba, Japan
e-mail address: r_imai@nirs.go.jp

Abstract

A clinical trial was first initiated in 1996 to evaluate the safety and efficacy of carbon ion radiotherapy for bone and soft tissue sarcomas not suitable for surgery. As of March 2013, over 900 patients were enrolled in the clinical trials. Through a dose escalation trial and a subsequent fixed dose trial, it was revealed that carbon ion radiotherapy provided definite local control and offered a survival advantage without unacceptable morbidity for patients with bone and soft tissue sarcomas that were either difficult or impossible to cure using other modalities. The most commonly treated sarcoma at NIRS was sacral chordoma, followed by axial high-grade bone and soft-tissue sarcomas. This part deals with carbon ion radiotherapy for unresectable sarcomas below C2.

Introduction

Malignant tumors that originate in the bone and soft tissues (e.g., muscle and adipose tissue) are termed sarcomas, which differ from carcinomas (e.g., lung cancer and stomach cancer). Sarcomas have a much lower incidence than other cancers. In Japan, some 500 and 2000 patients are diagnosed every year with malignant tumors originating from the bone and soft tissue, respectively (1,2). Unlike carcinomas, sarcomas are not lifestyle-related, and they occur at a considerably high rate among young subjects. Sarcomas involve a wide variety of histological types (e.g., osteosarcoma, chondrosarcoma, liposarcoma) and can develop in any part of the body. Depending on the combination of the histological type and the original site of the tumor, the therapeutic approaches vary, and the same treatment can result in different outcomes in different patients depending on these and other factors (3).

Multidisciplinary approaches including surgery, chemotherapy (anti-cancer drugs), and radiotherapy have been most successful for the treatment of bone and soft-tissue tumors in the last 30 years. In particular, the survival rate has been greatly improved for patients with osteosarcomas of the extremity due to progress in chemotherapy (4). In addition, dramatic advances in surgical techniques and prosthetic technology have markedly increased the limb salvage rate. The first-line treatment for bone and soft-tissue tumors is inevitably surgery. However, not all cases are resectable, depending on the tumor site, size, and depth of invasion. The resection of tumors of the extremities is often curative, whereas tumors involving the spine, pelvis, and other axial parts of the body are generally not amenable to surgery, especially advanced cases. Some patients undergoing surgical resection may also run the risk of being deprived of excretory function or suffering a major loss of ambulatory ability (5).

Until recently, unresectable tumors were treated with external radiation therapy and/or brachytherapy combined with chemotherapy. However, chemotherapy was not always effective for the treatment of a wide variety of sarcomas, and conventional radiotherapy achieved good results for only a few types of sarcomas. Therefore, unresectable sarcomas had a very poor prognosis due to the lack of any effective local treatment (6).

Clinical trials of carbon ion radiotherapy for bone and soft tissue sarcomas

Between June 1996 and February 2000, a phase I/II study was carried out to evaluate the efficacy and safety of carbon ion radiotherapy for bone and soft tissue sarcoma (7). This study presented a dose escalation trial using 16 fractionations starting from a total dose of 52.8 GyE (3.3GyE per fraction). The eligibility criteria for the study are shown in Table 1. Following the trial, a fixed –dose phase II trial was launched in April 2000 using a total

dose of 70.4GyE or 73.6GyE. While the phase II trial included patients with radiation–associated sarcoma, patients with intravascular tumor thrombosis were excluded. A central review of the surgical or biopsy specimens was carried out for all candidates. In October 2003 carbon ion radiotherapy was approved as Advanced Medicine by the Japanese Ministry of Health, Labor and Welfare and then the protocol has been employed. Four protocols related to carbon ion radiotherapy for sarcoma are ongoing. All patients enrolled in the trials signed an informed consent form approved by the local institutional review board (7-11).

Table 1. Eligibility for carbon ion radiotherapy

- Pathological confirmation as sarcoma
- Gross measurable lesion
- Lesion size < 15 cm in maximum diameter
- Unresectable tumor judged by referring surgeons
- Expected long prognosis
  - Others are depends on protocols.
  - No preplanned irradiation combined with surgery

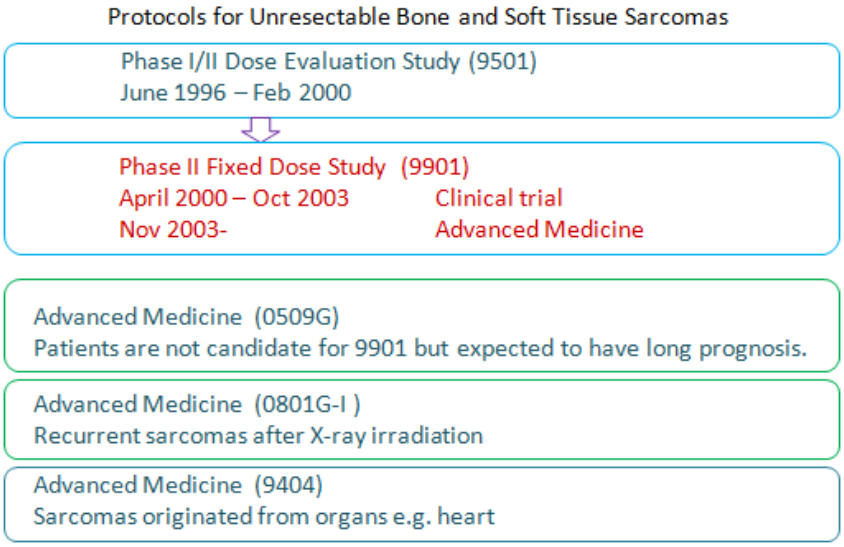

Figure1. Ongoing protocols on carbon ion radiotherapy for sarcomas

Carbon ion radiotherapy for bone and soft tissue sarcomas

The carbon ion beam has higher biological effectiveness and more favorable dose distribution profiles than ordinary radiation beams, like x-ray. The use of the particles provides the target tumor site with a large amount of irradiation possessing a high tumoricidal effect. Three-dimensional treatment planning was performed with the HIPLAN software program (National Institute of Radiological Sciences, Chiba, Japan) specifically designed for planning carbon ion radiotherapy. The standard protocol for the treatment of bone and soft-tissue tumors consists of 16 irradiation sessions delivered over four weeks, once daily four times per week, from Tuesday to Friday Tuesday to Friday. A total dose ranging 52.8 to 73.6 GyE (GyE= carbon physical dose (Gy) x Relative Biological Effectiveness (RBE) was administered. The fraction dose was modified to be 3.3-4.6GyE. Energies of 350 and 430MeV/n are used mainly for the treatment for axial bone and soft tissue sarcomas, respectively. A margin of 5mm was usually added to the clinical target volume to create the planned target volume. The clinical target volume was covered by at least 90% of the prescribed dose. The patients were usually treated with 3 ports to avoid severe reactions in the normal tissue. One port was used in each session. During the irradiation, the patients lie down in either the supine or prone position with tailor-made immobilization devices on the treatment couch for 20 to 30 minutes in the treatment room. The irradiation with the carbon ion beams lasts for a few minutes.

Results

The phase I/II dose escalation study was carried out on 64 lesions of 57 patients between June 1996 and February 2000 (7). This study produced a favorable tumor control rate of 89% at 1 year, and 63% at 3 years and 5 years, respectively. The overall survival rates were 82% at 1 year, 47% at 3 years, and 37% at 5 years, respectively. The median survival was 31 months. There was a significant difference in the results for the local control rate achieved with a total dose of 57.6GyE or less and that with 64.0GyE or more. As 7 of the 17 patients treated with 73.6GyE were found to have Grade 3 RTOG acute reactions in the skin, the dose escalation was halted at this dose level. These findings made it clear that with a dose fractionation regimen of 16 fractions over 4 weeks, a total dose of 70.4GyE was the maximum applicable dose in patients for whom there was sufficient skin close to the tumor, while a total dose of 73.6GyE was possible in other cases. When we started using at least three portals in order to reduce the dose delivered to the skin, such severe reactions were no longer observed. In view of these findings, the recommended dose for axial bone and soft tissue sarcomas was fixed at 70.4 GyE in 16 fractions over 4 weeks.

In the subsequent fixed-dose phase II study started in April 2000, 575 candidates (594 sarcomas) have been enrolled as of August 2013. The 589 lesions of 570 patients followed for six months or longer were analyzed. The clinical characteristics of those patients are summarized in Table 2.

Table 2

The patients characteristics of the phase II study (n=589 sarcomas of 570 pts)

Age	Median	58 (11-87)
Tumor sites		
	Pelvis	443
	Spine/Para-spine	112
	Extremities/others	34
Prescribed dose / 16 fractions		
	64.0	42
	67.2	115
	70.4	422
	73.6	10
Pathology		
	Bone	455
	Chordoma	212
	Chondrosarcoma	90
	Osteosarcoma	89
	Others	64
	Soft Tissue	134
	MFH	33
	Synovial	14
	MPNST	12
	Lipo	11
	Others	64

The prescribed dose of 73.6GyE (4.6GyE /fraction) was applied in the two clinical trials, however it has been closed due to grade >3 acute and late reactions. Total doses of 64.0GyE (4.0GyE /fractions) and 67.2GyE (4.2GyE/fractions) are used for spinal sarcomas and chordomas, respectively. The 422 patients were treated with a total dose of 70.4GyE (4.4gyE/fraction) which was resulted to be a workable dose after the two clinical trials. As

of August 2013, the 2-year and 5-year local control rates were 84% and 69%, respectively. The two–year and 5-year overall survival rates were 78% and 58%, respectively (Fig2). There were none of recurrent tumors irradiated at the total dose 73.6GyE. The types of radiation-related toxicity are summarized in Table 3. The toxicity was acceptable level at 2% skin/soft tissue late G3/4 toxicity. Late skin toxicities including grade 3 in 6 patients and 4 in 1 patient were also observed. These late skin reactions suggested that in addition to a total dose, there were other risk factors as follows: 1) subcutaneous tumor invasion, 2) a large tumor volume, 3) sacrococcygeal involvement, 4) previous surgery, 5) additional chemotherapy and 6) irradiation using 2 ports. It would be possible to prevent the skin reactions by irradiation using over 3 ports in order to reduce the dose administered to the skin surface (12). The incidence of Grade 3 and higher late akin reactions in the patients receiving a total dose of 70.4GyE with over 3 ports has been within the acceptable level for the past several years.

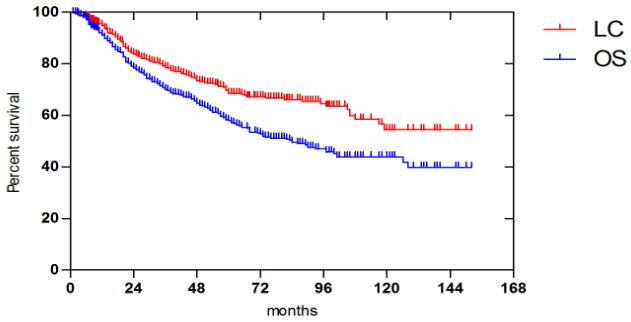

Figure2. Actual local control and overall survival rate in the 589 sarcomas of 570 patients with bone and soft tissue sarcomas enrolled to phase II study. The 5-year local control rates was 69% and the 5-year overall survival rates was 58%.

Table3 Late radiation morbidities in the phase II study

	n	0	1	2	3	4	5
Skin	589	6	526	41	6	1	0
GI tract	482	476	3	0	0	3	0
Peripheral nerves	430	375	31	21	3	0	0
Spinal cord	54	49	1	2	2	0	0

Sacral Chordoma

Among the bone and soft-tissue sarcomas treated with carbon ion radiotherapy at NIRS, sacral chordoma accounted for the largest proportion. Sacral chordoma is a rare tumor. Surgery is the first-choice of treatment, but it is not always possible. Since sacral chordomas usually develop gradually, they are often left undetected until they start to cause pain and other symptoms. A lot of patients referred to our hospital presented with a sacral chordoma over 10 cm in diameter. The sacrum houses the sacral nerves, which innervate the excretory functions and ambulation. Depending on the level of the tumor involvement to the sacral bone, excision of these nerves causes permanent gait, excretory and other disabilities, and it impairs the patients' quality of life. Therefore, curative surgery for sacral chordoma (sacrectomy) is one of the most invasive surgeries. Sacral chordomas frequently occur among the elderly population, who are also often contraindicated for surgery because of either comorbid diseases or overall frailty. Between 1996 and Mach of 2012,175 patients with sacral chordoma who didn't undergo prior surgery were enrolled in the trials on carbon ion radiotherapy. The median age of the 175

patients was 67 years. The median tumor diameter was 9 cm. The carbon ion dose ranged from 64.0GyE to 73.6 GyE. The cranial extension of tumor was at S2 or higher level in 70% of the patients. The median clinical target volume was 340cm^3. The median follow up period was 62 months. Five-year overall survival and 5-year local control rates were 82% and 76%, respectively (Fig3). The median local recurrent time was 40 months ranging from 13 to 119. The ambulatory in 97% of the patients remained with or without supportive devices. Six patients experienced severe sciatic nerve complications disturbing ambulatory and had impairment of their ordinary life. According to the better overall survival rate than local control rate at 5 years in Figure 3, as for chordoma, longer survival is expected than other high grade sarcomas due to the slow-growing tumor characteristics. The sustainability of good quality of life provided by carbon ion radiotherapy is important.

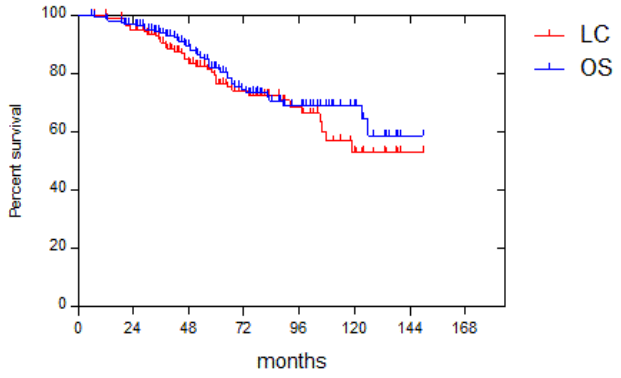

Figure3. Actual local control and overall survival rate in the 175patietns with sacral chordoma.
The 5-year local control rate was 76% and the 5 year overall survival rate was 82%.

Osteosarcoma

Osteosaromas of the trunk constituted the third largest group among our study. For the treatment of osteosarcomas of the extremity, which develop with a high incidence among youth, the paradigm based on a combination of surgery and chemotherapy has been well-established, and carbon ion radiotherapy is unlikely to outweigh their advantages. The 5-year local control and 5-year overall survival rates for the 78 patients with unresectable osteosarcoma of the trunk were 62% and 33%, respectively (13). Tumor sites included the pelvis in 61 patients, the spine and paraspinal region in 15 patients, and other sites in 2 patients. The median applied dose was 70.4GyE in a total of 16 fixed fractions over 4 weeks. The median diameter of the tumors was 9 cm. As reported in the literature, in the cases of unresectable osteosarcoma, the survival rate was 10% or less. Therefore, carbon ion radiotherapy appears to provide a survival benefit for unresectable osteosarcomas. The tumor volume was a prognostic factor for the survival and local control rate. Thirty-eight patients who had a clinical target volume <500 cm^3 had a 5-year overall survival rate of 46% and a 5-year local control rate of 88%, while 40 patients who had a clinical target volume >500 cm^3 had a 5-year overall survival rate of 19% and a 5-year local control rate of 31%. Except for 3 patients who experienced severe skin/soft tissue complications requiring skin grafts, no other severe toxicities were observed. Among 9 patients who were continuously disease free for >5 years, 8 were able to walk with or without the help of a cane, and 6 were free from pain killers. For unresectable osteosarcoma, carbon ion radiotherapy will be the mainstay treatment.

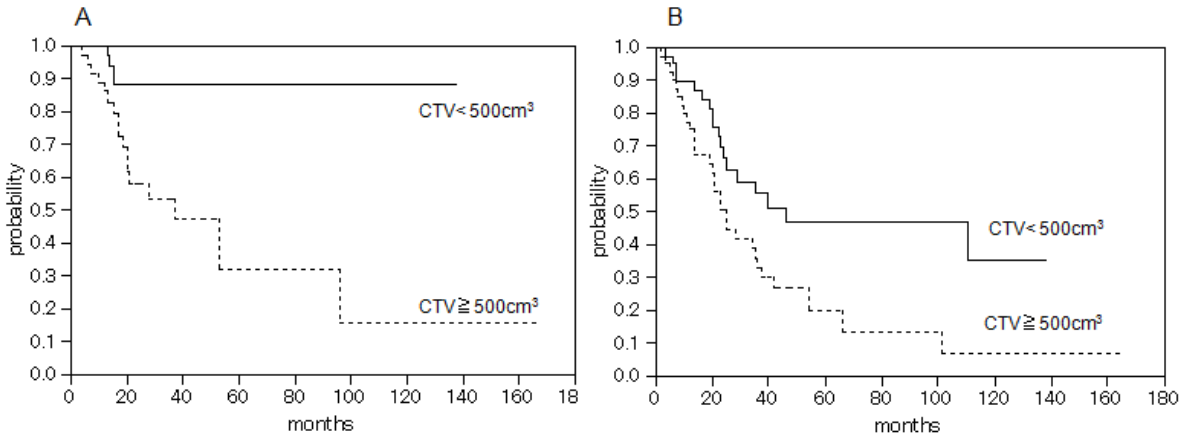

Figure4. Actual local control and overall survival rates of two groups divided by tumor volume in the 78 patients with osteosarcoma of the trunk. A) The 5-year local control rats of CTV<500cm^3 and >500cm^3 were 88 and 31%, respectively. B) 5-year overall survival rates of CTV<500cm^3 and >500cm^3 were 46% and 19%, respectively.

Chondrosarcoma

Chondrosarcoma is the second most common primary malignant bone tumor. Surgery has been considered the main form of treatment for chondrosarcoma, and the definitive en bloc resection of the tumor is mandatory to obtain long term disease free survival. However, radical surgical intervention for chondrosarcoma of the trunk has sometimes been associated with substantial morbidities. We evaluated 75 patients treated with carbon ion radiotherapy for 78 chondrosarcomas, including 2 limbs. None of the patients had metastasis at the time of referral to our hospital, and the tumors were deemed unresectable by the referring surgeons. The median patient age was 56 years. Of the 78 lesions, 85% were of a histological grade greater than 2. The median irradiated total dose was 70.4 GyE administered in 16 fractions over 4 weeks. The CTV ranged between 25 and 2900 cm^3 (median, 496 cm^3). The median follow-up time was 41 months (range, 3–117 months) for all patients, and all living patients were followed up for more than 2 years. At 5 years, the actuarial local control and overall survival rates were 55% and 57%, respectively. Four patients experienced skin/soft tissue late reactions of grade 3 or 4. Among 16 patients aged more than 70 years, 10 survived over a 3-year follow-up period and remained ambulatory (14).

Spinal sarcoma

Treatment of spinal sarcoma makes the best use of the characteristics of the charged particle beam. The treatment of such tumors is complicated by the proximity of lesions to the spinal cord. A “patch combination technique” is used in patients to optimize the dose distribution within tumors of an irregular volume and lying close to the spinal cord. The target volume is divided into 2 segments, and each segment is treated by a separate radiation field—an anterior/posterior field and a lateral field. By utilizing the sharp dose fall-off after the Bragg peak, the distal edge of 1 field is matched with the lateral edge of the second field. The dose constraint of the carbon ion beams directed to the cross-sections involving the spinal cord is 30 GyE administered in 16 fractions, however radiation-induced myelopathy was quite rare especially in limited experience of CIRT, more accumulation of cases and further analysis are needed in the future (Fig5). In our study, as of 2012, carbon ion radiotherapy was employed in 48 cases with spinal sarcomas, excluding sacral lesions. The patient median age was 53 years. In principal a total dose of 64 GyE in 16 fractions was applied for spinal sarcomas. Thirty-five patients were without prior treatment. The median follow-up time was 25 months, and the median survival time was 44 months (range, 5.2-148 months). The 5-year local control, overall survival, and progression free rates were 79%, 52%, and 48%, respectively. One patient each had a grade 3 late skin reaction and a grade 4 late skin reaction. Vertebral body compression was observed in 7 patients. One patient had

a grade 3 late spinal cord reaction. Ambulatory without supportive devices in 22 of the surviving 28 patients who had primary tumors remained (15).

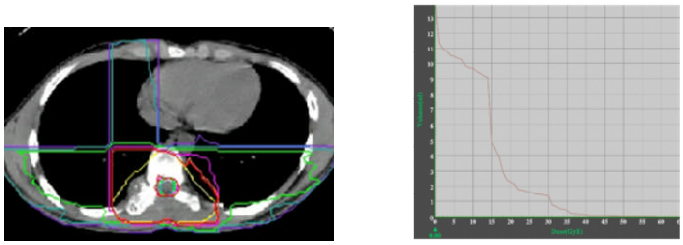

Figure5. A dose distribution and a dose volume histogram on the spinal cord of a spinal sarcoma

Conclusion

In this study, carbon ion radiotherapy was well tolerated and demonstrated substantial activity against sarcomas. These results were obtained in patients with advanced and/or chemo-resistant gross lesions not suited for surgical resection, and were located mainly in the trunk. The results of carbon ion radiotherapy using a total dose of 64GyE to 70.4GyE in 16 fractions over four weeks were satisfactory, considering the candidates were disqualified from surgery. However, it is imperative to continue with long term follow-up to assess the safety and efficacy of carbon ion radiotherapy.

Reference

[1] General rules for clinical and pathological studies on malignant bone tumors, the 3rd edition, The JOA committee of tumors

[2] General rules for clinical and pathological studies on malignant soft tissue tumors, the 3rd edition, The JOA committee of tumors

[3] Jaffe N. Osteosarcoma: review of the past, impact on the future. The American experience .Cancer Treat Res. 2009;152:239-62.

[4] Kawai A, Huvos AG, Meyers PA, et al. Osteosarcoma of the pelvis. Oncologic results of 40 patients. Clin Orthop Relat Res. 1998 ;348:196-207.

[5] Ozaki T, Flege S, Kevric M, et al. Osteosarcoma of the pelvis: experience of the Cooperative Osteosarcoma Study Group. J Clin Oncol. 2003 ;21(2):334-41.

[6] Ritter J, Bielack SS. Osteosarcoma. Ann Oncol. 2010 ;21 Suppl 7:vii320-5.

[7] Kamada T, Tsujii H, Tsuji H, et al. Efficacy and safety of carbon ion radiotherapy in bone and soft tissue sarcomas. J Clin Oncol. 2002 ;20(22):4466-71.

[8] Imai R, Kamada T, Sugahara S, et al. Carbon ion radiotherapy for sacral chordoma.Br J Radiol. *in press*

[9] Imai R, Kamada T, Tsuji H,et al. Effect of carbon ion radiotherapy for sacral chordoma: results of Phase I-II and Phase II clinical trials.Int J Radiat Oncol Biol Phys. 2010;77(5):1470-6.

[10] Imai R, Kamada T, Tsuji H, et al. Carbon ion radiotherapy for unresectable sacral chordomas. Clin Cancer Res. 2004;10(17):5741-6.

[11] Serizawa I, Kagei K, Kamada T, et al. Carbon ion radiotherapy for unresectable retroperitoneal sarcomas. Int J Radiat Oncol Biol Phys. 2009;75(4):1105-10.

[12] Yanagi Kamada T, Tsuji H, Dose-volume histogram and dose-surface histogram analysis for skin reactions to carbon ion radiotherapy for bone and soft tissue sarcoma. Radiother Oncol. 2010;95(1):60-5.

[13] Matsunobu A, Imai R, Kamada T, et al. Impact of carbon ion radiotherapy for unresectable osteosarcoma of the trunk.Cancer. 2012;118:4555-63.

[14] Maruyama K, Imai R, T Kamada et al (2012) Carbon Ion Radiation Therapy for Chondrosarcoma. Int J Radiat Oncol Biol Phys 84:S139.
[15] Matsumoto K, Imai R, Kamada T, et al. Impact of carbon ion radiotherapy for primary spinal sarcoma.Cancer. 2013;119:3496-503.

Carbon Ion Radiotherapy in Patients with Prostate Cancer

Hiroshi Tsuji, Takuma Nomiya, Katsuya Maruyama, Tadashi kamada, Hirohiko Tsujii

Research Center for Charged Particle Therapy, National Institute of Radiological Sciences, Chiba, Japan,
e-mail address: h_tsuji@nirs.go.jp

Abstract

A clinical trial of carbon ion radiotherapy (C-ion RT) for prostate cancer was started in 1995 at the National Institute of Radiological Sciences (NIRS), taking advantage of the quality of carbon ion beams to distinguish dose concentrations and establish a high anticancer efficacy. First, two phase I/II dose escalation studies with a fractionation of 20 fractions over five weeks were conducted to establish techniques using carbon ion beams to determine the optimal dose of fractionation. Then, a phase II study of 20 fractions was performed to validate the feasibility and efficacy of C-ion RT delivered in 20 fractions, which was successfully completed in 2003. Thereafter, a study of hypofractionated C-ion RT in16 fractions over four weeks was performed. Consequently, the incidence of late radiation toxicity decreased without an increase in tumor recurrence. Currently, hypofractionated radiotherapy in 12 fractions over three weeks with scanning irradiation is being evaluated in clinical practice.

Up to February 2013, 1,733 patients underwent C-ion RT, including 552 patients treated with 20 fractions, 1,107 patients treated with 16 fractions, and 64 patients treated with 12 fractions. Of these patients, 53% were categorized as high-risk. The five-year overall survival rate and biochemical relapse-free rate in the entire group were 95.1% and 90.7%, respectively. All risk factors had a significant influence on both biochemical control and patient survival. Biochemical control was not affected by the alteration of dose fractionation; however, the incidence of late radiation toxicity decreased in association with a decrease in the fraction number.

1. Introduction

Localized prostate cancer, particularly locally advanced cancer, is a good indication for carbon ion therapy. Carbon ion beams can offer the most concentrated dose distribution among the various types of state-of-the-art radiation therapies, including intensity-modulated radiotherapy (IMRT), stereotactic body radiotherapy (SBRT), and proton radiotherapy. Furthermore, an improvement in the therapeutic ratio can also be expected with higher biological effects of carbon ion beams. In order to evaluate the possible advantages of carbon ion beams in the treatment of prostate cancer, the National Institute of Radiological Sciences (NIRS) conducted clinical trials of carbon ion radiotherapy (C-ion RT).

2. Materials and methods

Between July 1995 and December 1997, the first dose escalation study of C-ion RT for locally advanced prostate cancer was carried out at the NIRS to determine the optimum dose level for C-ion RT administrated in 20 fractions over five weeks, and the second phase I/II study for both early and advanced prostate cancer was started in January 1998. The second study was successfully completed in March 2000, with no Grade 3 or worse late complications [1~6]. After these results were taken into consideration, a phase II clinical study was designed to further confirm the effectiveness of C-ion RT using a fixed dose fractionation schedule of 66 GyE in 20 fractions

over five weeks [3,7,8]. This clinical trial was conducted between April 2000 and October 2003. At the end of the study, approval for advanced medicine from the Japanese government was given to C-ion RT at the NIRS, and a further move in the direction toward a more hypofractionated regimen of 16 fractions over four weeks was started. A total dose of 57.6 GyE in 16 fractions was adopted, and the effectiveness and safety of C-ion RT with this dose fractionation was confirmed [8]. Furthermore, a new clinical trial of C-ion RT with 12 fractions over three weeks was carried out in 2010 to establish a more hypofractionated regimen for C-ion RT. Forty-six patients were enrolled, none of whom developed Grade 2 or worse toxicity or biochemical recurrence. Although the observation period was too short to evaluate the efficacy of this new fractionation, the incidence of toxicity was sufficiently low; therefore, the NIRS decided to apply this fractionation in all cases of prostate cancer starting in April 2013.

A total of 1,733 patients with prostate cancer underwent C-ion RT up to March 2013, including 96 patients treated in the early dose escalation trials and 175 patients treated in the phase II clinical trial. Thereafter 1,462 patients were treated using the approved highly advanced medical technology or in a new clinical trial of 12 fraction treatment. The annual number of patients has gradually increased, particularly in 2003, when we obtained approval for the highly advanced medical technology, and in 2007, when we shortened the therapy term from 20 times in five weeks to 16 times in four weeks (Figure 1).

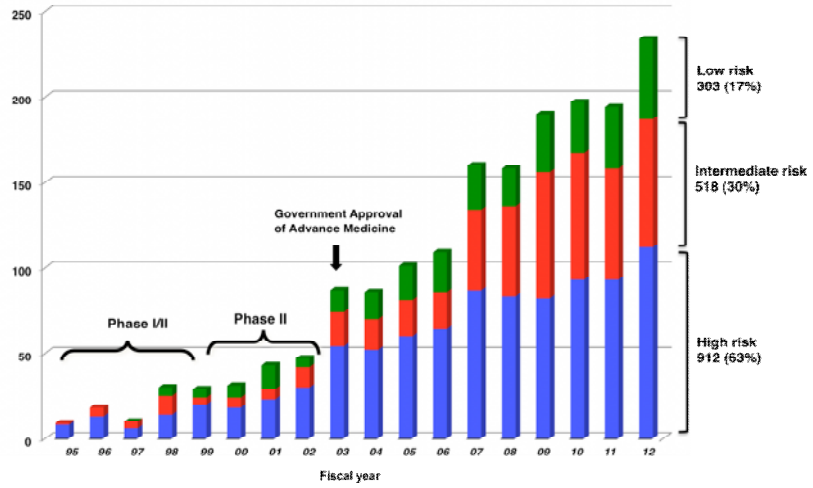

Figure 1. Changes in the number of prostate cancer carbon ion radiotherapy cases according to the fiscal year.

The eligible patients had no metastases, and the pathological diagnosis was confirmed to be prostate cancer. In the current approach to therapy, the patients were classified into three groups (high-risk, intermediate-risk and low-risk) according to the clinical stage, initial PSA value, and pathological Gleason score. For the high-risk and intermediate-risk groups, we combined long-term and short-term endocrine therapy, respectively. Among the treated patients, the high-risk group accounted for more than one half of all patients (Figure 1). The analysis objects included 1,479 patients treated in and after the phase II clinical trial and observed for six months or more. Of these patients, 466 received C-ion RT in 20 fractions, 967 received C-ion RT in 16 fractions, and 46 were treated with new fractionation at 12 fractions.

The clinical target volume (CTV) is defined as the area comprising the prostate and seminal vesicle (SV), as demonstrated on CT images, irrespective of the T-stage and risk factors. However, the whole SV is not always included in the CTV in patients with a low risk. Furthermore, anterior and lateral safety margins of 10 mm and a posterior margin of 5 mm are added to the CTV to create the initial planning target volume (PTV1). In order to reduce the dose to the anterior rectal wall, a rectum-sparing target volume (PTV2) is used for the latter half of the C-ion RT, with the posterior margin reduced to the anterior boundary of the rectum. A dose-volume histogram (DVH) is calculated to evaluate the planned dose distribution, particularly for the rectum. A reference DVH of the

rectum was obtained from the initial toxicity study on C-ion RT at the NIRS [2], which includes the average DVH of patients with Grade I or less rectal toxicity in the first and second dose escalation trials. A plan for a new patient is then compared with the reference DVH in order to prevent the rectal DVH from exceeding the reference DVH, especially at the high-dose level.

The C-ion RT is carried out once a day, with four fractions per week. Verification of the field is performed at every treatment session with a computer-aided online positioning system to maintain a positioning error within less than 2 mm.

Beam delivery with spot scanning became available in 2011at the NIRS. Currently, all patients with prostate cancer are treated with this spot scanning method based on our judgment that spot scanning provides better dose distribution than the passive beam method in the treatment of prostate cancer. Figure 2 shows the dose distribution of passive beam (a) and scanning beam (b) therapy. The plan using passive beam irradiation is calculated for the anterior and two lateral directions. The plans for scanning beam irradiation are made using only two lateral beams. The dose to the hip joint is apparently reduced in the plan for scanning beam irradiation with two ports compared to the plan using passive beam irradiation with three ports.

(a) (b)

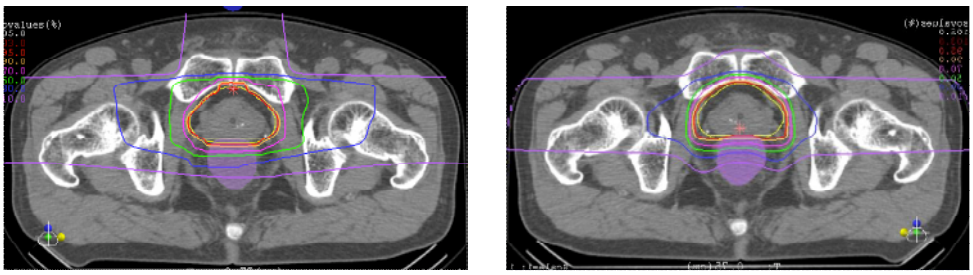

Figure 2. Dose-distribution of C-ion RT. (a) Passive irradiation, (b) Scanning irradiation.

In addition, the irradiated volume of the rectum can be a little smaller in the plan using scanning irradiation than in the plan using passive irradiation, as demonstrated by the DVH (Fig. 3).

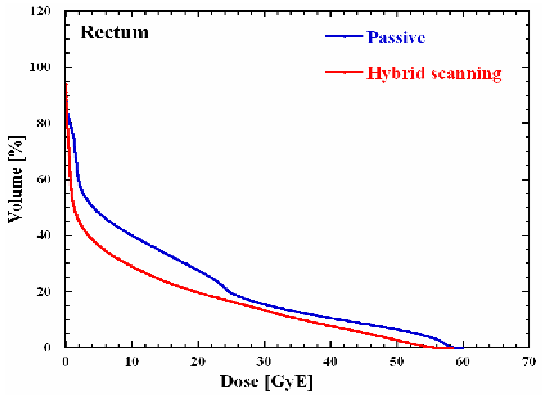

Figure 3. A dose-volume histogram (DVH) of the rectum.

The irradiated volume in the area of scanning irradiation (red) is slightly smaller than that observed in the area of passive irradiation (blue).

3. Results

2-1) Toxicity

Regarding late radiation toxicities, the incidence of late gastrointestinal (GI) and genitourinary (GU) morbidities and Grade 2 or worse morbidities in the 63.0 GyE/20 Fr and 57.6 GyE/16 Fr groups were 2.3% and 0.4% at the rectum and 6.1% and 2.4% in the GU system, respectively. The results of comparisons of the late toxicity incidence in various radiotherapies and carbon ion radiotherapy are shown in Table1 [9~14]. Compared with other various radiotherapies, carbon ion radiotherapy was associated with a lower rate of toxicity, particularly a significantly low rate of rectal toxicity. As for the rate of toxicity in the lower urinary tract system, carbon ion radiotherapy consisting of 63.0GyE/20 fractions, intensity modulated radiation therapy and proton therapy were associated with approximately the same rates; however, a lower incidence was observed for the 57.6GyE/16 fractions. As for toxicity in the rectum, even at 63.0GyE, a lower rate was observed compared to that for X-ray or proton therapy. Treatment with 57.6GyE further reduced this rate.

			No. of	Morbidity ≥ G2	
Institutes	Radiotherapy	Dose (Gy/f)	pts.	Rectum	GU
Christie H.[9]	IMRT	60.0/20	60	9.5%	4.0%
Princess Margaret H.[10]	IMRT	60.0/20	92	6.3%	10.0%
Cleveland CF.[11]	IMRT	70.0/28	770	4.4%	5.2%
Stanford U.[12]	SRT	36.25/5	41	15.0%	29.0%
RTOG9406[13]	3DCRT	68.4-79.2/38-41	275	7-16%	18-29%
	3DCRT	78.0/39	118	25-26%	23-28%
Loma Linda U.[14]	Proton	75.0/39	901	3.5%	5.4%
NIRS [8]	C-ion	63.0/20	216	2.3%	6.1%
	C-ion	57.6/16	967	0.3%	2.4%

2-2) Relapse-free and survival rates

The overall survival rate in the entire group was 95.1% at five years and 79.6% at 10 years according to a Kaplan-Meier estimation (Figure 4). The 5-year and 10-year biochemical relapse-free rates were 90.7% and 83.0%, respectively. Of 1,479 patients, 773 (52.3%) belonged to the high-risk group; therefore, the outcomes for tumor control are quite satisfactory. Based on the data available for 1,144 patients, the T-stage and Gleason score were found to have a significant influence on the biochemical relapse-free rate. Furthermore, the T-stage, initial PSA level and Gleason score affected patient survival. Concerning the effects of the dose-fractionation of C-ion RT on biochemical control, no differences were observed in the biochemical relapse-free rate between the 20-fraction group and the 16-fraction group. Although the observation period in the 12-fraction group was very short and the number of patients was small, no patients have developed biochemical relapse to date.

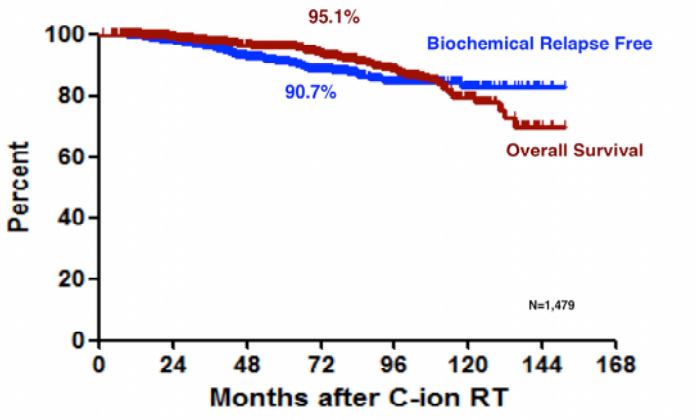

Figure 4. Overall survival and biochemical relapse-free rates in the prostate cancer patients treated with C-ion RT at the NIRS.

4. Discussion

We introduced the treatment results for carbon ion radiotherapy in an established therapeutic approach after a phase II trial.

As for treatment morbidity, in the genitourinary system, the incidence of morbidity was approximately the same as that observed with the 63.0GyE/20 fraction carbon ion radiotherapy, intensity modulated radiation therapy and proton therapy. This finding is interesting in that it shows that this dose has a comparable impact on lower urinary tract tissues. Meanwhile in the 57.6GyE/16 fractions, a lower incidence was realized as a real outcome for shortening the treatment term. As for rectal toxicity, even the 63.0GyE therapy was associated with a lower rate than X-ray or proton therapy. This is thought to be proof of eminent dose convergence of carbon ion beams. In addition, treatment with 57.6GyE further reduced the incidence. By adding shortening to high-dose convergence, a significant reduction in toxicity was obtained.

Regarding antitumor effects, high survival rates were observed, especially in the high-risk group. This is due to the carbon ion's excellent curative effects along with the superior treatment strategy. There were no differences in the relapse-free or survival rate between the 20-fraction and 16-fraction groups, although the rate of toxicity was lower in the 16-fraction groups. Therefore reducing the fractions to 16 made it possible to achieve improvements not only in efficiency, but also in outcomes from therapy.

5. Conclusion

Carbon ion radiotherapy is an ideal therapeutic approach as a method of radiation therapy against prostate cancer. Furthermore, regarding toxicity and curative effects, previous outcomes strongly illustrate this fact. Shortening the treatment period also resulted in a better outcome; therefore, further shortening and promotion of streamlining can be expected. Prostate cancer is a target disease of therapy utilizing the characteristics of carbon ion beams, and is anticipated to play a significant role in popularizing carbon ion radiotherapy.

References

［1］ Tsuji H, Yanagi T, Ishikawa H et al (2005) Hypofractionated radiotherapy with carbon ion beams for prostate cancer. Int J Radiat Oncol Biol Phys 63:1153–60

［2］ Akakura K, Tsujii H, Morita S et al (2004) Phase I/II clinical trials of carbon ion therapy for prostate cancer. Prostate 58: 252–8

［3］ Ishikawa H, Tsuji H, Kamada T et al (2006) Carbon ion radiation therapy for prostate cancer: Results of a prospective phase II study. Radiother Oncol 81:57–64

［4］ Ishikawa H, Tsuji H, Kamada T et al (2006) Risk factors of late rectal bleeding after carbon ion therapy for prostate cancer. Int J Radiat Oncol Biol Phys 66:1084–91

［5］ Ishikawa H, Tsuji H, Kamada T et al (2008) Adverse effects of androgen deprivation therapy on persistent genitourinary complications after carbon ion radiotherapy for prostate cancer. Int J Radiat Oncol Biol Phys 72:78–84

［6］ Okada T, Kamada T, Tsuji H et al (2010) Carbon ion radiotherapy: Clinical experiences at National Institute of Radiological Science (NIRS). J Radiat Res 51:355–64

［7］ Ishikawa H, Tsuji H, Kamada T et al (2012) Carbon-ion radiation therapy for prostate cancer. Int J Urol 19:296–305

［8］ Okada T, Tsuji H, Kamada T et al (2012) Carbon ion radiotherapy in advanced hypofractionated regimens for prostate cancer: From 20 to 16 fractions. Int J Radiat Oncol Biol Phys 84: 968–72

[9] Coote JH, Wylie JP, Cowan RA et al (2009) Hypofractionated intensity-modulated radiotherapy for carcinoma of the prostate: analysis of toxicity. Int J Radiat Oncol Biol Phys 74:1121–7

[10] Martin JM, Rosewall T, Bayley A et al (2007) Phase II trial of hypofractionated image-guided intensity-modulated radiotherapy for localized prostate adenocarcinoma. Int J Radiat Oncol Biol 69:1084–9

[11] Kupelian PA, Thakkar VV, Khuntia D et al (2005) Hypofractionated intensity-modulated radiotherapy (70 gy at 2.5 Gy per fraction) for localized prostate cancer: Long-term outcomes. Int J Radiat Oncol Biol Phys 63:1463–8

[12] King CR, Brooks JD, Gill H et al (2009) Stereotactic body radiotherapy for localized prostate cancer: interim results of a prospective phase II clinical trial. Int J Radiat Oncol Biol Phys 73: 1043–8

[13] Michalski JM, Bae K, Roach M et al (2010) Long-term toxicity following 3D conformal radiation therapy for prostate cancer from the RTOG 9406 phase I/II dose escalation study. Int J Radiat Oncol Biol Phys 76:14–22

[14] Schulte RW, Slater JD, Rossi CJ Jr et al (2000) Value and perspectives of proton radiation therapy for limited stage prostate cancer. Strahlenther Onkol 176:3–8

Carbon-ion Radiotherapy for Hepatocellular Carcinoma

Shigeo Yasuda, Mayumi Harada, Shigeru Yamada, Miho Shiomi, Tetsurou Isozaki, Tadashi Kamada

Research Center Hospital for Charged Particle Therapy, National Institute of Radiological Sciences, Chiba, Japan
e-mail address: yasudash@nirs.go.jp

Abstract

Clinical trials of carbon ion radiotherapy (C-ion RT) for hepatocellular carcinoma (HCC) were conducted at the National Institute of Radiological Sciences (NIRS) in Japan between April 1995 and August 2005. In four clinical studies, we tried to determine the optimal dose and to shorten the treatment duration using five different fractionation schedules comprising 15, 12, eight, four and two fractions. There have been no treatment-related deaths and no severe adverse events. As a result of these studies, the duration of treatment could be reduced from five weeks to two days. Two-fraction therapy is currently ongoing, licensed as a Highly Advanced Medical Technology. Between April 2003 and August 2012, 133 patients with HCC underwent two fraction C-ion RT. There were no cases of grade 4 toxicity. The local control rates were 98% and 83% at one and three years, respectively, with a total dose of 45.0 GyE. Because of the low toxicity and good local control rate, C-ion RT is a promising radical and minimally invasive therapeutic option for HCC.

Introduction

Hepatocellular carcinoma (HCC) is one of the most common malignancies worldwide, and various locoregional therapies are presently available. The standard therapies used for HCC are hepatectomy, transcatheter arterial embolization (TAE), percutaneous ethanol injection (PEI), radio-frequency ablation (RFA) and liver transplantation. According to the Survey and Follow-up Study of Primary Liver Cancer in Japan, the relative use of these therapies in the treatment records of all patients in the two-year period from January 1, 2004 through December 31, 2005 were: hepatectomy in 32% of cases, TAE in 32% and percutaneous local therapy involving PEI, percutaneous microwave coagulation therapy (PMCT) and RFA in 31%. Each of these procedures has merits and drawbacks. For example, while hepatectomy provides the best certainty of removing cancer cells, the procedure also results in serious stress to both the liver and the body as a whole. TAE is clinically useful, and has a relatively low degree of invasiveness, but is of limited radicality. PEI and RFA, on the other hand, are simple procedures offering a high degree of radicality, but their effect is limited to comparatively small tumors (less than 3 cm in diameter).

The use of radiotherapy for HCC has been considered difficult in view of the problems associated with radiation-induced hepatic insufficiency [1, 2]. However, progress in the development of irradiation devices in recent years has made it possible to achieve highly localized irradiation, reducing the degree of toxicity [3-6]. This has spurred advances in radiotherapy research for liver cancer [7-12]. Carbon ion beams possess the Bragg peak, and have advantageous biological and physical properties that result in a higher cytocidal effect than that of photons and protons [13-16]. Carbon-ion radiotherapy (C-ion RT) has been performed for the treatment of HCC since April 1995.

Four clinical studies were carried out to determine the optimal dose based on a dose-escalating protocol using four different fractionation schedules comprising 15, 12, eight and four fractions. Most of the subjects enrolled under these protocols had been judged not to be amenable to, or as having had recurrence after, other treatments, or as having no prospects for an adequate treatment effect with any of the existing therapies. Following these studies, we conducted a phase II study using a fixed total dose of 52.8 GyE in four fractions. This study revealed the high safety and effectiveness of the treatment. Following that, we are now offering even shorter-course radiotherapy of two fractions give over only two days for patients with HCC. Therefore, the duration of treatment could be safely reduced from five weeks to two days.

Two-fraction therapy is currently ongoing, and is licensed as a Highly Advanced Medical Technology.

Methods and materials

Before the treatment planning, one or two metal markers (0.5 × 3 mm) made of iridium wire were inserted near the tumor under ultrasound imaging guidance as landmarks for target volume localization. These markers were visible not only in CT images, but also in orthogonal x-ray images (Fig. 1). To accurately reproduce the patient position, a low-temperature thermoplastic sheet and a customized cradle were used. The supine or prone position was selected according to the location of the tumor. Patients were forbidden from eating and drinking before acquisition of the treatment planning CT images and prior to each treatment. This is because the position of the liver would be changed depending on the volume of the stomach.

Three-dimensional treatment planning with 2.5-mm CT images was performed using the HIPLAN, which was originally developed for 3D treatment planning [17]. The planning target volume (PTV) was defined so as to include a 1- to 1.2-cm margin around the gross tumor volume. A dose-volume histogram was used to evaluate the probability of liver damage (Fig. 2). Double right-angled field geometry was used for irradiation in most patients. Respiratory gating was employed for CT image acquisition and irradiation stages to ensure more accurate delivery of the radiation [18]. To assess the accuracy of patient positioning and target volume localization, orthogonal fluoroscopy and radiography were used immediately prior to each treatment session.

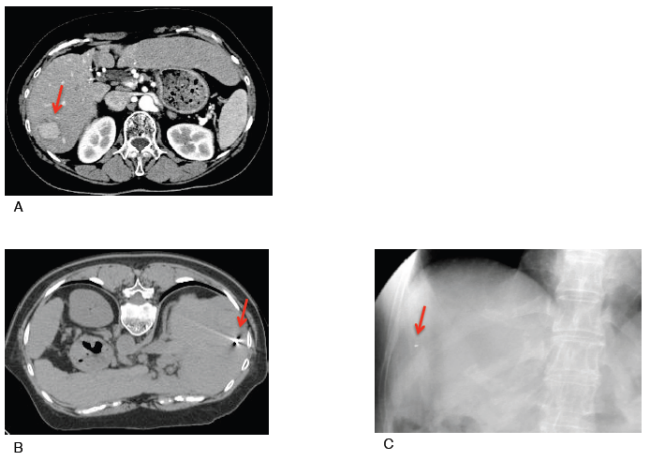

Fig. 1. A patient with hepatocellular carcinoma 5.5 cm in maximum diameter in the right posterior interior segment of the liver

A. A CT scan obtained before the treatment. **B**. A CT image used for treatment planning: the arrow shows a metal marker implanted near the tumor. **C**. An x-ray image. The metal marker can be seen in the x-ray (arrow).

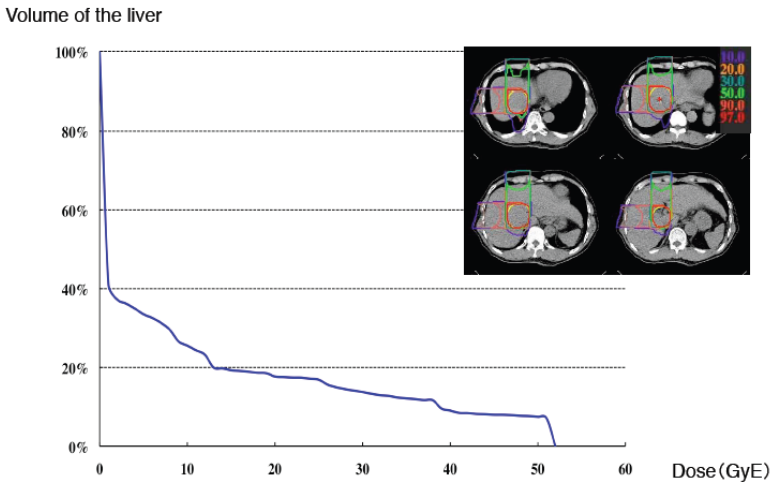

Fig. 2. The dose distribution and dose-volume histogram of the liver

During the treatment planning, a dose-volume histogram was used to evaluate the probability of liver damage.

Results

Between April 2003 and August 2012, 133 patients with HCC underwent two fraction C-ion RT. The background data of the patients and tumors are presented in Table 1. The patients consisted of 91 males and 42 females. Their median age was 72 years (range, 44-87). The median maximum tumor diameter was 42 mm (range, 14-140 mm). One hundred twenty-three patients were classified into Child-Pugh A and 10 into Child-Pugh B. All 133 patients were treated with a total dose range of 32.0-45.0 GyE.

No treatment-related deaths occurred in the hypofractionation trial. There were no cases of grade 4 hepatic toxicity. With regard to the Child-Pugh score, in the late phase (three months after treatment), an increase of two points or more occurred in 6% and 3% in the smaller tumor group (≤ 5 cm) and the larger tumor group (> 5 cm), respectively. There were no significant differences between the two groups (P=0.678). This demonstrated that the changes in liver function remained minor after C-ion RT was performed. No serious adverse effects were noted in the digestive organs. There was no other grade 4 or higher toxicity (Table 2).

The local control rates were 98% and 90% at one year, and were 83% and 76% at three years, in the higher dose group (45.0 GyE) and the lower dose group (≤ 42.8 GyE), respectively. There was no significant difference according to the total dose (P=0.1099) (Fig. 4). In the higher dose group, the local control rates were 97% and 100% at one year, and were 81% and 80% at three years in the smaller tumor group (≤ 5 cm) and the larger tumor group (> 5 cm), respectively. Local control was not dependent on the tumor size (P=0.892) (Fig. 5).

The overall survival rates were 95% and 96% at one year, and were 71% and 59% at three years, in the higher dose group (45.0 GyE) and the lower dose group (≤ 42.8 GyE), respectively. There was no significant difference between the groups (P=0.4674) (Fig. 6). In patients with a single lesion 5 cm or larger in diameter, the overall survival rates were 88% at one year, 61% at three years and 43% at five years after C-ion RT. According to the Report from The Liver Cancer Study Group of Japan [19], in patients with a single lesion 5-10 cm in diameter, the overall survival rates were 82% at one year, 59% at three years and 44% at five years after hepatic resection.

Our outcomes seem to be comparable to those of hepatic resection.

Table 3 shows the results of proton and C-ion RT for HCC. The local control rates were similar, but C-ion RT had smaller fraction numbers.

Table 1. The patient and tumor characteristics in the two fractions C-ion RT study

Characteristics	Total (n=133)
Age (years)	
Median	72
Range	44-87
Sex, n (%)	
Male	91 (68)
Female	42 (32)
Etiology of cirrhosis, n (%)	
HCVAb positive	92 (69)
HBsAg positive	12 (9)
Neither	30 (23)
Both	1 (1)
Child-Pugh classification, n (%)	
A	123 (92)
B	10 (8)
UICC^{5th} stage, n (%)	
I	19 (14)
II	97 (73)
IIIA	15 (11)
IVA	2 (2)
Number of tumors, n (%)	
Single	118 (89)
Multiple	15 (11)
Maximum tumor diameter (mm)	
Median	42
Range	14-140
AFP (ng/ml)	
Mean ± SD	2350.3 ± 11891.4
PIVKA-2 (mAU/ml)	
Mean ± SD	5256.3 ± 43838.0

HCVAb, hepatitis C virus antibody; HBsAg, hepatitis B surface antigen; UICC, Union for International Cancer Control; AFP, alpha-fetoprotein; SD, standard deviation.

Table 2. Acute and late toxicities after C-ion RT

	Acute (n=133)					Late (n=132)				
	Grade					Grade				
	0	1	2	3	4	0	1	2	3	4
Skin	0	130	3	0	0	7	124	1	0	0
Liver	68	35	25	4	0	50	48	26	4	0
Gastrointestinal	133	0	0	0	0	132	0	0	0	0
Lung	104	29	1	0	0	78	53	1	0	0

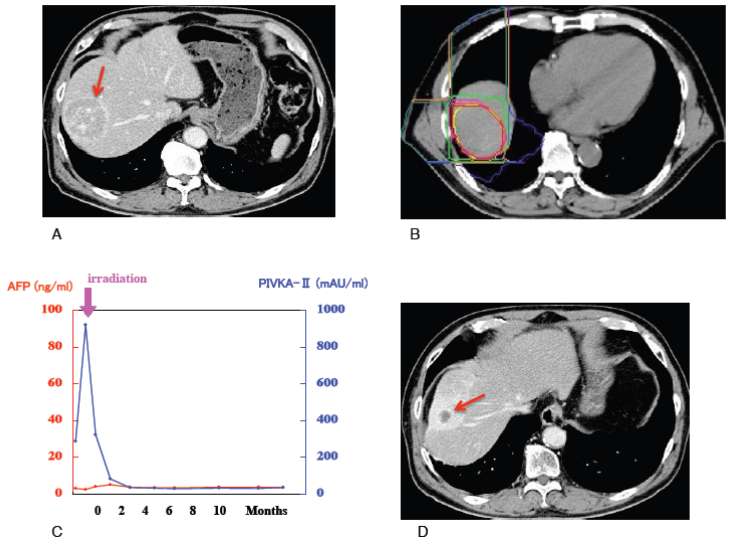

Fig. 3. A case with hepatocellular carcinoma 5.5 cm in maximum diameter in the right anterior superior segment of the liver.

A. A CT scan obtained before treatment **B**. The dose distribution: The beam was delivered using a combination of the anterior and lateral portals (dose ratio 1:1). The planning target volume was defined so as to include a 1.2-cm margin around the gross tumor volume, except for the right side, where the margin was narrower to exclude the ribs from the high dose area. **C**: The changes in the serum tumor marker levels: The serum PIKA-II value promptly decreased after the treatment. **D**: A CT scan obtained nine months after treatment showed that the tumor had regressed remarkably. There were no rib fractures after the treatment.

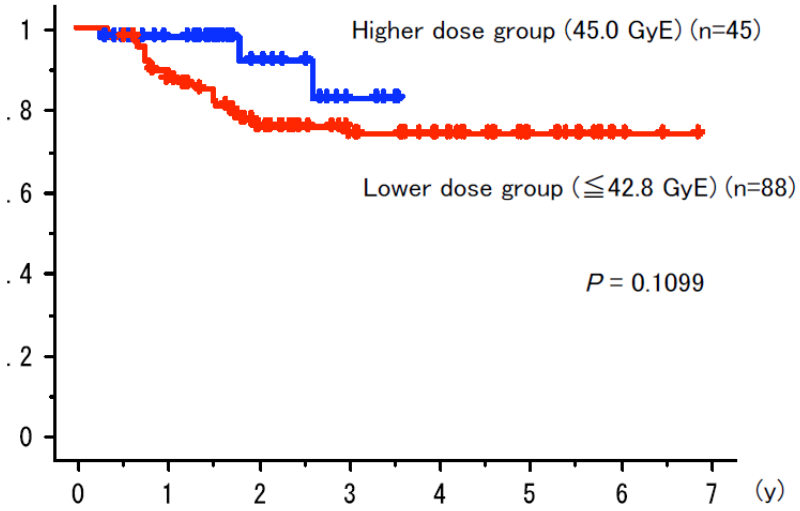

Fig. 4. The local control rates achieved by a total dose in two fractions of C-ion RT for hepatocellular carcinoma
The one- and three-year local control rates were 98% and 83% in the higher dose group (45.0 GyE) and 90% and 76% in the lower dose group (≤ 42.8 GyE), respectively (P=0.1099).

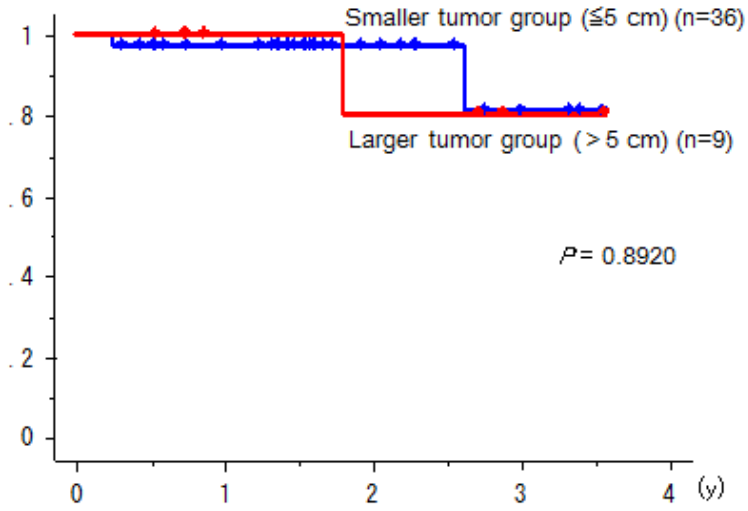

Fig. 5. The local control rates by tumor size following C-ion RT (45 GyE/2 fr) for hepatocellular carcinoma
The one- and three-year local control rates were 97% and 81% in the smaller tumor group (≤ 5 cm) and 100% and 80% in the larger tumor group (>5 cm), respectively. Local control was not dependent on the tumor size (P=0.892)

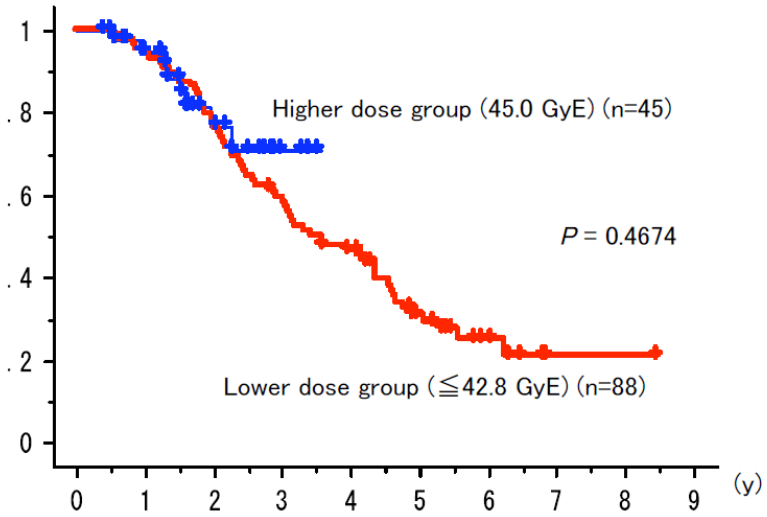

Fig. 6. The overall survival rates achieved by the total dose in two fractions of C-ion RT for hepatocellular carcinoma

Discussion

We have already reported that C-ion RT used for the treatment of HCC is safe and effective, and that it causes only minor liver damage [16]. We investigated the reasons why the liver function is retained, and found that the non-irradiated regions of the liver are considered to contribute to the retention of liver function [20]. For patients with extensive infiltration and those with multiple lesions, it is difficult to achieve a radical cure with C-ion RT alone. C-ion RT is therefore indicated for patients with a level of liver function corresponding to Child-Pugh grade A or B. For small lesions 3 cm or less, however, other minimally-invasive, effective and low-cost therapies, such as PEI and RFA, are available. In contrast, lesions larger than 3 cm are difficult to treat with PEI or RFA alone, making them ideal targets for C-ion RT. Moreover, even for lesions less than 3 cm in diameter adjacent to the porta hepatis, the use of minimally invasive treatment without complications is an important issue. We compared the efficacy and toxicity of C-ion RT of 52.8 GyE in four fractions for patients with HCC in terms of the tumor location (adjacent to the porta hepatis or not) and found that there were no significant differences in liver toxicity. Excellent local control was obtained independent of the tumor location. Therefore, in certain patients with a higher risk of injury to the bile duct when undergoing RFA, C-ion RT appears to offer a promising therapeutic alternative [21].

Table 3. The results of proton and C-ion RT for hepatocellular carcinoma

Type of radiation	Proton	Proton	Carbon
Facility	National Cancer Center Hospital East	University of Tsukuba	National Institute of Radiological Sciences
Number of patients	40	51	45
Maximum tumor diameter (mm)			
Median	45	28	35
Range	25-82	8-93	15-95
Total dose / fractionation	76 GyE / 20 fr	66 GyE / 10 fr	45 GyE / 2 fr
Local control rate	2y 96%	3y 94.5%	2y 94%
		5y 87.8%	
Overall survival rate	3y 66%	3y 49.2%	3y 73%
		5y 38.7%	
Reference	[19]Kawashima et al. J Clin Oncol 2005:23:1839-46	[20]Fukumitsu et al. Int J Radiat Oncol Biol Phys 2009:74:831-6	

Conclusion

C-ion RT is a safe and effective modality, and it seems to be a definitive and minimally invasive radiation therapy for HCC. However, further careful follow-up is still needed to confirm its clinical efficacy in practical medicine.

References

[1] Ingold DK, Reed GB, Kaplan HS, et al. Radiation hepatitis. Am J Roentgenol 1965;93:200-208.

[2] Phillips R, Murikami K. Primary neoplasms of the liver. Results of radiation therapy. Cancer 1960;13:714-720.

[3] Stillwagon GB, Order SE, Guse C, et al. 194 hepatocellular cancers treated by radiation and chemotherapy combinations: Toxicity and response: a Radiation Therapy Oncology Group study. Int J Radiat Oncol Biol Phys 1989;17:1223-1229.

[4] Robertson JM, Lawrence TS, Dworzanin LM, et al. Treatment of primary hepatobiliary cancers with conformal radiation therapy and regional chemotherapy. J Clin Oncol 1993;11:1286-1293.

[5] Xi M, Liu MZ, Deng XW, et al. Defining internal target volume (ITV) for hepatocellular carcinoma using four-dimensional CT. Radiother Oncol 2007;84:272-278.

[6] Sato K, Yamada H, Ogawa K, et al. Performance of HIMAC. Nucl Phys 1995;A588:229-234.

[7] Ohto M, Ebara M, Yoshikawa M, et al. Radiation therapy and percutaneous ethanol injection for the treatment of HCC. In: Okuda K, Ishak KG, editors. Neoplasm of the Liver. Tokyo: Springer-Verlag; 1987. p. 335-341.

[8] Yasuda S, Ito H, Yoshikawa M, et al. Radiotherapy for large HCC combined with transcatheter arterial embolization and percutaneous ethanol injection therapy. Int J Oncol 1999;15:467-473.

[9] Cheng J C-H, Chuang VP, Cheng SH, et al. Local radiotherapy with or without transcatheter arterial chemoembolization for patients with unresectable HCC. Int J Radiat Oncol Biol Phys 2000;47:435-442.

[10] Guo W-J, Yu E-X. Evaluation of combined therapy with chemoembolization and irradiation for large HCC. Br J Radiol 2000;73:1091-1097.

[11] Kawashima M, Furuse J, Nishio T, et al. Phase II Study of Radiotherapy Employing Proton Beam for HCC. J Clin Oncol 2005;23:1839-1846.

[12] Fukumitsu N, Sugahara S, Nakayama H, et al. A prospective study of hypofractionated proton beam therapy for patients with hepatocellular carcinoma. Int J Radiat Oncol Biol Phys 2009:74:831-836.

[13] Kanai T, Furusawa Y, Fukutsu K, Itsukaichi H, Eguchi-Kasai K and Ohara H. Irradiation of mixed beam and design of spread-out Bragg peak for heavy-ion radiotherapy. Radiat Res 1997;147:78-85.

[14] Kanai T, Endo M, Minohara S, et al. Biophysical characteristics of HIMAC clinical irradiation system for heavy-ion radiation therapy. Int J Radiat Oncol Biol Phys 1999;44:201-210.

[15] Tsujii H, Morita S, Miyamoto T, et al. Preliminary results of phase I/II carbon ion therapy. J Brachyther Int 1997;13:1-8.

[16] Kato H, Tsujii H, Miyamoto T, et al. Results of the first prospective study of carbon ion radiotherapy for hepatocellular carcinoma with liver cirrhosis. Int J Radiat Oncol Biol Phys 2004;59:1468-1476.

[17] Endo M, Koyama-Ito H, Minohara S, et al. HIPLAN-A HEAVY ION TREATMENT PLANNING SYSTEM AT HIMAC. J. Jpn. Soc. Ther Radiol Oncol 1996;8:231-238.

[18] Minohara S, Kanai T, Endo M, et al. Respiratory gated irradiation system for heavy-ion radiotherapy. Int J Radiat Oncol Biol Phys 2000;47:1097-1103.

[19] Kudo M, Arii S, Ikari I, et al. Report of the 18th nationwide follow-up survey of primary liver cancer in Japan. Kanzo 2010;51:460-484.

[20] Imada H, Kato H, Yasuda S, et al. Compensatory enlargement of the liver after treatment of hepatocellular carcinoma with carbon ion radiotherapy – Relation to prognosis and liver function. Radiother Oncol 2010;96:236-242.

[21] Imada H, Kato H, Yasuda S, et al. Comparison of efficacy and toxicity of short-course carbon ion radiotherapy for hepatocellular carcinoma depending on their proximity of the porta hepatis. Radiother Oncol 2010;96:231-235.

Carbon Ion Radiotherapy for Postoperative Recurrence of Rectal Cancer

Shigeru Yamada, Satoshi Endo, Kohtaro Terashima,
Makoto Shinoto, Shigeo Yasuda, Miho Shiomi and Tetsuro Isozaki

Research Center for Charged Particle Therapy, National Institute of Radiological Sciences, Chiba, Japan
e-mail address:s_yamada@nirs.go.jp

Abstract

To improve long-term local control and survival of locally recurrent rectal cancer, we have initiated a radiation dose-escalation trial using carbon ion beams. The purpose of this study is to evaluate the tolerance for and effectiveness of carbon ion radiotherapy in patients with locally recurrent rectal cancer. Between April 2001 and August 2012, 198 lesions at 189 patients were treated with C-ion RT. The dose was determined as 67.2 GyE and escalated to 70.4 GyE and 73.6 GyE. The local control rates in 197 lesions are 94 % at 3 years and 89 % at 5 years. Local control rate and survival rate at 5 years were 97 % at 73.6 GyE and 51 % at 73.6 GyE. In the literature, the reported 5-year survival rates for locally recurrent rectal cancer treated with resection were 20–40 %. Carbon ion radiotherapy seems to be a safe and effective modality in the management of locally recurrent rectal cancer, providing good local control and offering a survival advantage without acceptable morbidity. In this chapter, the treatment methods and the up-to-date outcomes of carbon ion radiotherapy (C-ion RT) for the recurrent rectal cancer at the NIRS are introduced.

Keywords

Carbon-ion • Rectal cancer • Recurrence

Introduction

The large intestine starts at the ascending colon, which is connected to the small bowel, and ends at the rectum, which extends from the sacral promontory to the anal canal. In 2008, approximately 43,000 patients died of colorectal cancer in Japan, which is the third most common cause of cancer deaths, after lung and stomach cancers. Approximately 100,000 patients were diagnosed with colorectal cancer in 2004, thus making it the second most common type of cancer after stomach cancer. The analysis of the postoperative recurrence rates of colorectal cancer indicates a higher rate for rectal cancer than colon cancer. When compared by the site of recurrence, rectal cancer had a more than three times higher local recurrence rate than colon cancer. With the recent advances in surgical techniques and procedures, the pelvic recurrence rate of rectal cancer has been

decreasing; however, the postoperative recurrence rate is still 5–20 % today. Surgical resection is the first choice for locally recurrent rectal cancer, although total pelvic exenteration or another highly invasive procedure is often required. In many cases, locally recurrent rectal cancers are not completely resectable so generally surgical resections are not selected. The comparison of resection rates by the type of tumors shows that the resection rates were in the range of 40–50 % for liver metastases and 20–40 % for lung metastases, whereas the rate was 10–40 % for locally recurrent colorectal cancers [1, 2]. Curative resection of these tumors will lead to a survival rate similar to those for other types of recurrences and metastases.

Clinical Trial in Recurrent Rectal Cancer at NIRS

The first clinical trial of the C-ion RT at the National Institute of Radiological Sciences (NIRS) for the recurrent rectal cancer was started in 2000. It was a phase I/II dose-searching study and the dose was escalated from the starting dose of 67.2 to 73.6 GyE in 16 fractions. A total of 38 patients were treated and the results indicated that the C-ion RT could be a sufficiently safe and effective treatment for the recurrent rectal cancer. This study was finished in 2004 and the second trial with the recommended dose determined by the first trial was initiated immediately. One hundred and fifty-two patients were treated in the second study until 2004 and the satisfactory results could be obtained as well. In November 2003 the approval of the Japanese government for the advanced medicine was given to the C-ion RT at the NIRS, and after the end of the second trial, the recurrent rectal cancer was added to the indication of the advanced medicine.

Methods of Carbon Ion Radiation Therapy

A set of 2.5–5.0-mm-thick CT images throughout the pelvis was taken for treatment planning, with the patient placed in immobilizing devices and with respiratory gating. Clinical target volume (CTV) was determined by setting the margin 5 mm outside the GTV and included the regional lymph nodes (LN). The LN areas that should be considered the target volume include the internal iliac, the external iliac, and the presacral node. The current recommended dose was 73.6 GyE/16 fractions. One hundred percent of the prescribed dose is given at the maximum dose point of each portal. The dose constraints of the maximum dose for the intestine and bladder were 30 GyE in 9 fractions and 60 GyE in16 fractions, respectively. Prophylactic nodal areas of risk are usually treated to 37.8–41.4 GyE in 9 fractions of 4.2–4.6 GyE before irradiation field is reduced in size. The target volume includes the primary tumor, adjacent lymph nodes, and presacral region. Target volumes are based on known pattern of local recurrence in locally recurrent rectal cancer. MRI and methionine PET are useful to distinguish the tumor from postoperative fibrosis and the bowels. Planning target volume (PTV) is defined as the CTV plus at least 5 mm margin in all directions; however, the margins are modified if the critical organs, such as skin or bowels, exist near the tumor.

Results of the C-Ion Therapy for Patients with Pelvic Recurrence of Rectal Cancer

Between April 2001 and August 2012, 198 lesions at 189 patients were enrolled onto this study. Criteria for trial eligibility include confirmation of locally recurrent rectal cancers without distant metastases based on CT, MRI, and PET findings. The dose was determined as 67.2 GyE and escalated to 70.4 and 73.6 GyE. The predominant sites of relapse were 75 presacral, 77 lymph nodes, 28 perineal, and 9 anastomosis. Ten patients received radiation dose at 67.2 GyE, 18(+3) at 70.4 GyE, and 161(+6) at 73.6 GyE. All toxicities in the 198 lesions at 189 patients were relatively few and mild in these patients. No grade 3–5 acute toxicity was observed. The local control rates in 197 lesions are 94 % at 3 years and 89 % at 5 years. Local control rates at 5 year were 97 % at 73.6 GyE. In terms of symptomatic response within 3 months after treatment, pain improved in 97 % of the symptomatic cases. The 3- and 5-year overall survival rates in 188 patients were 72 % and 47 %, respectively. Survival rates at 5 years were 20 % at 67.2 GyE, 24 % at 70.4 GyE, and 51 % at 73.6 GyE. In the literature, the reported 5-year survival rates for locally recurrent rectal cancer treated with conventional radiation and with resection were 0–40 % (Table 1) [3-10]and 20–40 % (Table 2) [10-11], respectively. Most of our patients were inoperable, so our results seem to be better than surgery. Carbon ion radiotherapy seems to be a safe and effective modality in the management of locally recurrent rectal cancer, providing good local control and offering a survival advantage without acceptable morbidity.

Study & Reference	Year	Number	Dose (Gy)	Survival Rate		Local Control
				2y	5y	
LybeertMLM	1992	76	6-66	61%(1y)	3%	28%(3y)
Knol HP	1995	50	60	27%	8%	-
Murata	1997	18	12-60	44%(1y)	-	46%(2y)
Hu JB	2006	23	55-66	50%(2y)	18%(3y)	
Kim MS	2008	23	30-51/3f	82%	23%	74%(5y)
Lee JH	2011	22	54-66	66%	40%	56%(5y)
NIRS	2012	136	73.6	87%	45%	93%(5y)

Table 1. The results on the radiation therapy of locally recurrent rectal cancer reported by other studies

Study & Reference	Year	Number	Survival Rate		
			1y	2y	5y
Garcia-A J	1999	42	88%	62%	35%
Wanebo	1999	53	91%	62%	31%
Salo JC	1999	71	88%	75%	31%
Saito N	2003	43	91%	78%	39%
Moriya	2004	48	95%	76%	36%
Melton	2007	29	92%	65%	20%
NIRS	2013	136	99%	87%	45%

Table 2. The results of the surgical treatment reported by other studies

Indication of Spacer in the C-Ion RT for the Recurrent Rectal Cancer

Pelvic recurrent tumors are often located in close proximity to the digestive tract. Consequently, a significant proportion of patients were often judged as ineligible for carbon ion radiotherapy, because the digestive tract could not be excluded from the irradiation field. At our hospital, therefore, we adopted a surgical preparatory procedure, to place a spacer between the target tumor and the digestive tract before

conducting carbon ion radiotherapy, when the tumor was located close to a sensitive organ. To exclude the small intestine and colon from the clinical target volume (CTV) and reduce the exposure of them, we use expanded polytetrafluoroethylene (Gore-Tex soft-tissue patch, W. L. Gore & Assoc Inc, Flagstaff, Ariz) which is a strong and easy-to-use material and does not need to be removed after the conclusion of radiotherapy (Fig. 24.2). Mesenterium, muscle cutaneous flap, or omentum instead of Gore-Tex sheet is used at infectious lesion. From 2003, 73 patients are treated with the spacer. Most of tumor sites were the sidewall or presacrum. Eight of grade 3 acute toxicities were observed. This rate is higher than without spacer. All patients completed the scheduled treatment course. Local control rate is 96 % at 2 years and 88 % at 5 years. This is almost the same as without spacer. The survival curves of patients with locally recurrent rectal cancer are similar between with and without spacer. The case was of a 59-year-old Japanese female and referred to the NIRS hospital with a diagnosis of postoperative recurrence of the rectal cancer (Fig. 1). CT scan revealed a tumor mass in the sidewall of the pelvis and in contact with the intestine. After placing Gore-Tex sheet, this dose distribution revealed the dose of the surrounding intestine is extremely low. She did not experience any major toxicity. The tumor size on CT scan decreased 24 M after treatment.

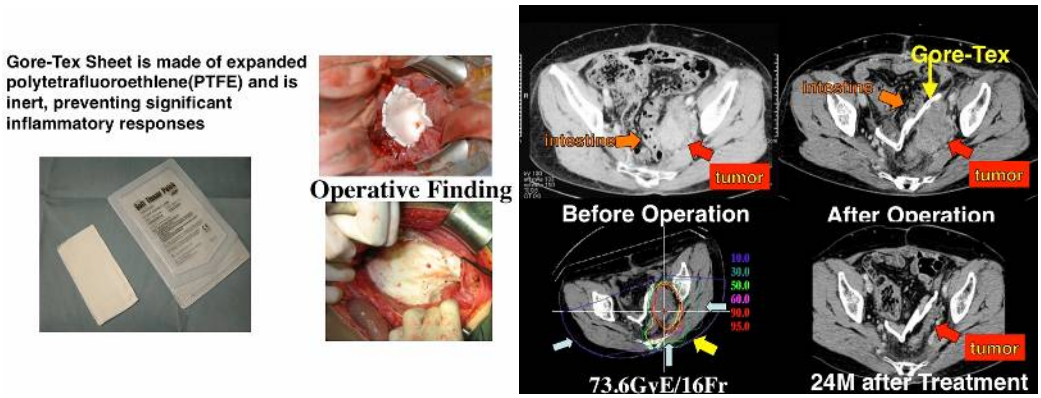

Fig. 1. Right: The photograph of Gore-Tex soft-tissue patch and operative findings using it. Left: This patient is a 59-year-old female with locally recurrent rectal cancer. CT scan revealed a tumor mass in the sidewall of the pelvis and in contact with the intestine. After placing Gore-Tex sheet, the dose distribution revealed the dose of the surrounding intestine is extremely low. The tumor size on CT scan decreased 24 M after treatment. She did not experience any major toxicity

Carbon Ion Radiotherapy for Locally Recurrent Rectal Cancer in Patients with Prior Pelvic Irradiation

Among gastrointestinal malignancies, many studies have shown the safety and efficacy of pelvic reirradiation for rectal cancer [10–14]. Reirradiation to the pelvis could potentially play a role in palliation of symptoms or local control. Local recurrences are located close to critical organs such as the small intestine, colon, and bladder, and in these patients reirradiation would be expected to be associated with a higher risk of acute and late toxicity at these organs than primary irradiation. The purpose of this study was to assess carbon ion radiation therapy performed as reirradiation in patients with locally recurrent rectal cancer. Twenty-three patients were treated with carbon ion RT as reirradiation for locally recurrent rectal cancer. Nine relapses originated in the presacral region,

8 in the pelvic sidewalls and 6 in the perineal region. The total dose range of 70.4 Gy equivalent (GyE) was administered in 16 fixed fractions over 4 weeks (4.4 GyE/ fraction). All patients completed the scheduled treatment course. Grade 3 toxicities occurred in 6 (26 %) patients. The major late toxicities were peripheral neuropathy and infection. No other severe acute reactions (grade ≥3) were observed at this study (Table 24.4). The 1- and 3-year overall survival rates were 83 % (95 % CI, 68–98 %) and 65 % (95 % CI, 43–87 %), respectively. The 1- and 3-year disease-free survival rates were 71 % (95 % CI, 51–91 %) and 51 % (95 % CI, 27–75 %), respectively. Carbon ion radiotherapy as reirradiation appears to be a safe and effective modality in the management of locally recurrent rectal cancer, providing good local control and offering a survival advantage without unacceptable morbidity.

Case Study

The case was of a 65-year-old Japanese male referred to the NIRS hospital with a diagnosis of postoperative recurrence of rectal cancer. He underwent the surgery 4 years before and the initial stage was IIIa. The CT scan and PET scan revealed a tumor mass in the right sidewall of the pelvis and infiltratedpelvic bone (Fig. 2). The C-ion RT was performed with three ports of left oblique lateral, right oblique lateral, and oblique posterior, and the total dose was 73.6 GyE in 16 fractions. Twelve months later, the CT and the methionine accumulation after treatment demonstrated disappearance of the tumor and osteogenesis in the osteolytic lesion.

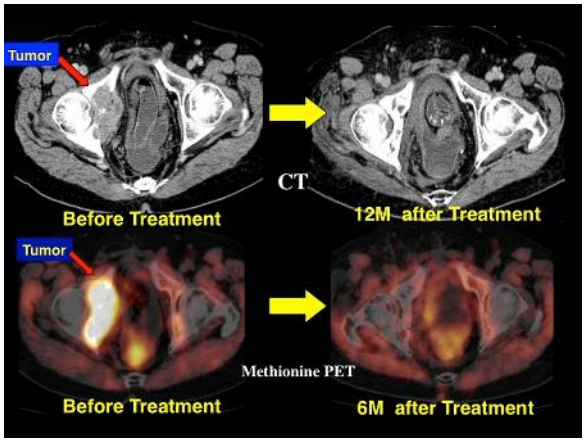

Fig. 2. This patient is a 65-year-old male with locally recurrent rectal cancer.

References

[1] Kobayashi H, Hashiguchi Y, Ueno H. Follow-up for recurrent colorectal cancer. J Ppn Soci Coloproctology. 2006;59:851–6.

[2] Sugihara K. Guidelines for treatment of recurrent rectal cancer. Tokyo: Nankodo Co. Ltd; 2003. p. 89–149.

[3] Lybeert ML, Martijn H, de Neve W, et al. Radiotherapy for locoregional relapses of rectal carcinoma after initial radical surgery: definite but limited influence on relapse-free survival and survival. Int J Radiat Oncol Biol Phys. 1992;24:241–6.

[4] Knol HP, Hanssens PE, Rutten HJ, et al. Effect of radiation therapy alone or in combination with surgery and/or chemotherapy on tumor and symptom control of recurrent rectal cancer. Strahlenther Onkol. 1997;173(1):43–9.

[5] Murata T, Fujii I, Yoshino M. Radiation therapy with or without chemotherapy and hyperthermia for recurrent rectal cancer. J Jpn Soc Ther Radiol Oncol. 1997;9:63–71.

[6] Hu JB. Int J Radiat Oncol Biol Phys. 2006;23:241.

[7] Kim MS, Choi C, Yoo S, et al. Stereotactic body radiation therapy in patients with pelvic recurrence from rectal carcinoma. Jpn J Clin Oncol. 2008;38:695–700.

[8] Lee JH, Kim YS, Yang SW, et al. Radiotherapy with or without surgery for patients with idiopathic sclerosing orbital inflammation refractory or intolerant to steroid therapy. Int J Radiat Oncol Biol Phys. 2012;84:52–8.

[9] Garcia-Aguilar J, Cromwell JW, Marra C, et al. Treatment of locally recurrent rectal cancer. Dis Colon Rectum. 2001;44: 1743–8.

[10] García-Aguilar J, Belmonte MC, Javier PJ, et al. Incontinence after lateral internal sphincterotomy: anatomic and functional evaluation. Dis Colon Rectum. 1998;41:423–7.

[11] Wanebo HJ, Antoniuk P, Koness JR, et al. Pelvic resection of recurrent rectal cancer: technical considerations and outcomes. Dis Colon Rectum. 1999;42:1438–48.

[12] Salo JC, Paty PB, Guillem J, et al. Surgical salvage of recurrent rectal carcinoma after curative resection: a 10-year experience. Ann Surg Oncol. 1999;6:171–7.

[13] Saito N, Koda K, Takiguchi N, et al. Curative surgery for local pelvic recurrence of rectal cancer. Dig Surg. 2003;20:192–200.

[14] Moriya Y, Akasu T, Fujita S, et al. Total pelvic exenteration with distal sacrectomy for fixed recurrent rectal cancer in the pelvis. Dis Colon Rectum. 2004;47:2047–54.

[15] Melton GB, Paty PB, Boland PJ, et al. Sacral resection for recurrent rectal cancer: analysis of morbidity and treatment results. Dis Colon Rectum. 2006;49:1099–107.

Carbon Ion Radiotherapy for Pancreatic Cancer

Shigeru Yamada, Kohtaro Terashima, Makoto Shinoto,
Shigeo Yasuda, Miho Shiomi, and Tetsuro Isozaki

Research Center for Charged Particle Therapy, National Institute of Radiological Sciences, Chiba, Japan
e-mail address:s_yamada@nirs.go.jp

Abstract

Pancreatic cancer is the fifth leading cause of cancer death and is considered to be one of the most lethal cancers in Japan. Complete surgical resection is the only curative treatment. Even if curative resection is performed, the disease usually recurs, and 5-year survival rates are less than 20 %. Chemotherapy or chemoradiotherapy is selected as a standard treatment for unresectable pancreatic cancer. However, since pancreatic cancer is often resistant to chemotherapy and radiotherapy, the local control and survival rates are very low. We conducted a phase I/II clinical trial using carbon ion radiotherapy (C-ion RT) for patients with operable and locally advanced pancreatic cancer. This was delivered preoperatively in 8 fractions over 2 weeks, was well tolerated, and resulted in excellent local control and survival rates. C-ion RT for patients with locally advanced pancreatic cancer was also well tolerated, even when concomitantly administered with the highest dose of gemcitabine (1,000 mg/m2), and likewise resulted in a good survival rate. We discuss current treatment methods and the results of C-ion RT for pancreatic cancer at the National Institute of Radiological Sciences.

Keywords
Carbon-ion • Pancreatic cancer • Radiation

Introduction

More than 26,000 people die of pancreatic cancer in Japan each year, and this number continues to increase [1]. Pancreatic cancer is also the fifth leading cause of cancer death and is considered to be one of the most lethal cancers in Japan. Complete surgical resection is the only curative treatment. However, only a small percentage of patients (10–20 %) are candidates for surgical resection because of local progression or metastatic spread at the time of diagnosis [2]. Even if a curative resection is performed, the disease usually recurs and 5-year survival rates are less than 20 % [3]. In cases where the cancer cannot be resected, chemotherapy and chemoradiotherapy are the standard treatments [4]. However, since pancreatic cancer is often resistant to both these treatments, the local control rate is very low. Recently, along with the development of new anticancer agents, more advanced radiotherapy techniques have also been introduced [5, 6]. However, these therapies still fail to provide a satisfactory outcome in most cases, and the median survival is still only approximately 10 months.

Carbon Ion Radiotherapy

Koong measured the oxygen concentration in seven pancreatic tumors intraoperatively using the Eppendorf polarographic needle electrode system [8]. All seven of these tumors were revealed to have significant hypoxia, in contrast to the adjacent normal pancreas that had a normal oxygen concentration [7]. Hypoxic cells are 2–3 times more resistant

than cancer cells exposed to normal oxygen levels [8]. Tumor hypoxia has been shown to be a major biological cause of local treatment failure after radiation therapy. However, when using carbon ion radiotherapy (C-ion RT), the radiosensitivities of hypoxic cells and normoxic cells are almost the same. Carbon ions are more effective at killing hypoxic cells. Furthermore, although pancreatic cancer stem cells have been shown to be resistant to conventional chemotherapy and radiation [9], carbon ion beams have greater efficacy for killing this cell type. This may be due to the prolonged induction of DNA damage caused by C-ion RT compared toX-rays [10].

Carbon ion beams are also safer than conventional radiological approaches. There are complicated neuroplexus structures around the main arteries of the pancreas, and these are the site of most local recurrences. These sites therefore need to be irradiated, even though they are close to radiosensitive organs such as the stomach, duodenum, and spinal cord. Heavy-ion beams exhibit unique depth-dose curves that offer the potential advantage of safely delivering a biological effective dose to the tumor whilst sparing these organs. Figure 1 shows the dose distribution for a cancer of the pancreatic head. The patient received a 48 GyE carbon ion beam dose. A sufficient dose can be delivered to the tumor and neuroplexus without increasing the dose to surrounding organs such as the stomach and duodenum.

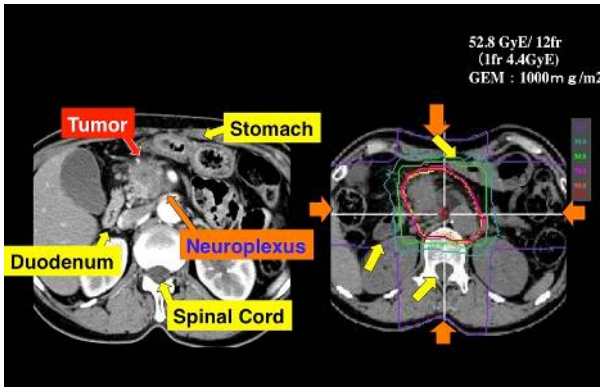

Fig. 1. Typical dose distribution for pancreatic cancer. The image is from a case of a 75-year-old man with cancer in the head of the pancreas that received 52.8 GyE/12 fr. It is possible to deliver a high dose to the tumor and neuroplexus whilst minimizing the dose to the surrounding organs such as the stomach or duodenum

The Pancreatic Cancer Trial at National Institute of Radiological Sciences

We started a phase I/II clinical trial for preoperative C-ion RT delivered in 16 fractions over 4 weeks for resectable pancreatic cancer in 2000 (Fig. 2). The purpose of this treatment was to reduce the risk of postoperative local recurrence, which accounts for approximately 50 % of all recurrences. We established the tolerance and effectiveness of preoperative C-ion RT and performed an additional clinical trial aimed at reducing the number of fractions to 8, delivered over 2 weeks beginning in 2003 (protocol 0203). In addition, we started a phase I/II clinical trial for patients with locally advanced pancreatic cancer (protocol 0204) and showed that the treatment was safe and provided excellent local control rates. As a result, we are currently performing a clinical trial using C-ion RT combined with gemcitabine (protocol 0513).

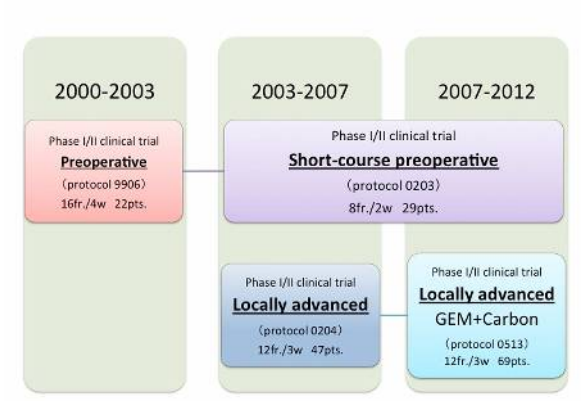

Fig. 2. The clinical trial pathway for C-ion RT in pancreatic cancer

Methodology at National Institute of Radiological Sciences

A set of 2.5-mm-thick CT images along the whole abdomen were taken for treatment planning, with the patient placed in immobilizing devices and with respiratory gating. Field arrangements were generally designed using a 3- or 4-field plan. The current recommended dose is 55.2 GyE delivered in 12 fractions for locally advanced pancreatic cancer and 35.2 GyE delivered in 8 factions for resectable pancreatic cancer. The gross tumor volume (GTV) was established using CT images and margins for possible subclinical tumor spread, and magnetic resonance imaging (MRI) and fludeoxyglucose (FDG)-positron emission tomography were used to diagnose tumor spread. The clinical target volume (CTV) was defined as the gross volume plus 0.5 or 0 cm (in contact with the duodenum or stomach). The CTV included the GTV, neuroplexus, and regional lymph nodes the latter consisted of the celiac, superior mesenteric, common hepatic and peri-pancreatic lymph nodes (Fig. 1). At least 50 % of the functioning renal parenchyma received a dose of 15 GyE or less, and the spinal cord dose was limited to 30 GyE or less. Planning target volume (PTV) is defined as the CTV with a margin of at least 5 mm in all directions, although these margins are modified if critical organs, such as the skin or bowels, are close to the tumor.

Results of Carbon Ion Radiotherapy

Preoperative Carbon Ion Radiotherapy for Patients with Resectable Pancreatic Cancer

The purpose of this study was to evaluate the safety and efficacy of C-ion RT as preoperative treatment and to determine the optimum dose needed to reduce the risk of postoperative local recurrence without causing unacceptable damage to normal tissue. The eligibility criteria for this study were that the pancreatic cancer was judged radically resectable and that it did not involve the celiac trunk or superior mesenteric artery. We performed C-ion RT with 8 fractions over 2 weeks, followed by resection 2–4 weeks later. The first dose was 30 GyE over 8 fractions, and this was then increased in 5 % increments. Twenty-six patients were enrolled between April 2003 and December 2010, and the initial dose of 30 GyE was ultimately escalated to 36.8 GyE. We administered C-ion RT to all patients as scheduled. The clinical stage according to the UICC was IIA in 15 cases and IIB in 11 cases. Twenty-one out of 26 patients received curative resection (resection rate 81 %), although the remaining five patients did not undergo surgery due to liver metastases or refusal of treatment. Although grade 3/4 toxicities were noted in 2 patients (liver abscess in one and PV thrombus in the other), neither were directly related to C-ion RT. No other serious adverse effects were observed. In the 21 surgical cases, the 5-year local control and overall survival rates were 100 and 52 %, respectively (Fig. 3). In the literature, the reported 5-year survival rates for pancreatic cancer treated with resection were 20–30 %.

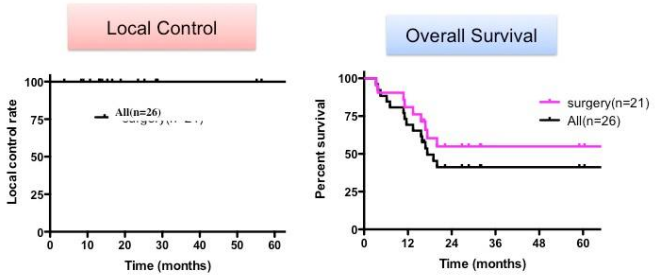

Fig. 3. Local control and overall survival. The local control rate in all patients was 100 %. There were no cases of recurrence within the irradiated lesion. The 5-year OS rate among patients who underwent resection was 55 %

Carbon Ion Radiotherapy for Patients with Locally Advanced Pancreatic Cancer

The phase I/II trial of C-ion RT (12 fractions/3 weeks) for locally advanced pancreatic cancer was performed in order to evaluate its safety and efficacy and to determine the optimum dose. Between April 2003 and February 2007, 47 patients with stage IVa or IVb cancer but without distant metastases, as defined by the staging criteria of the Japanese Committee on Cancer (corresponding to stage III based on the TNM classification), were enrolled into this trial. One patient was excluded because he received chemotherapy before treatment, and thus, a total of 46 patients were eligible for this analysis. Patients eligible for study entry had histologically or cytologically confirmed locally advanced and unresectable pancreatic ductal carcinoma. The basis on which the tumor was judged to not be resectable was a CT finding of tumor encasement of the celiac trunk and/or superior mesenteric artery. C-ion RT was administered once daily, 4 days a week to give a total of 12 fractions in 3 weeks. The dose was set at 38.4 GyE and escalated to 52.8 GyE at 5 % increments. All patients completed the scheduled treatment course. One grade 3 late toxicity and seven grade 3 acute toxicities were observed. Six of the seven grade 3 acute toxicities were anorexia and the other was cholangitis. Tumor response was evaluated in 46 lesions. A CR was achieved in 1 lesion, a PR in 7, SD in 37, and PD in a single lesion. The 1-year overall local control rate and the 1-year control rate for patients receiving at least 45.6 GyE were 76 and 95 %, respectively. The 1-year overall survival estimate for the 46 analyzed patients was 43 %. The maximum grade 3 acute reaction occurred in two-thirds of the patients (67 %) receiving 52.8 GyE. From these results, we concluded that the maximum tolerated dose of carbon ions is 52.8 GyE/12 fractions/3 weeks. On the basis of previous studies of drugs that can sensitize tumors to heavy-particle beam radiation, further studies were scheduled in an effort to find even more effective treatment modalities based on a combination of chemotherapy and radiotherapy. We started a phase I/II clinical trial of gemcitabine combined with carbon ion radiotherapy (C-ion RT) for patients with local advanced pancreatic cancer from April 2007.

Gemcitabine Combined with Carbon Ion Radiotherapy for Patients with Locally Advanced Pancreatic Cancer

The purpose of this trial was to establish the optimum dose of gemcitabine (a standard anticancer agent for advanced pancreatic cancer) and C-ion RT and to evaluate the safety and efficacy of this combination. The eligibility requirement for this study was that patients should have locally advanced pancreatic cancer involving the celiac trunk or superior mesenteric artery without distant metastasis. All patients had histologically or cytologically proven pancreatic adenocarcinoma or adenosquamous carcinoma. The radiation fractions were fixed at 12 fractions over 3 weeks, and the dose of gemcitabine and radiation was gradually increased. The radiation dose was fixed at 43.2 GyE/8 fractions and the initial gemcitabine dose was 400 mg/m2, which was increased to 700 and then to 1,000 mg/m2. Subsequently, the gemcitabine dose was kept at 1,000 mg/m2 and the radiation dose was increased in 5 % increments. Gemcitabine was administered once a week for three consecutive weeks. The irradiation field was set to include the primary tumor, perineural lesions, and a prophylactic regional lymph node area. Sixty patients were enrolled from April 2007 through February 2011. Patients were treated with C-ion RT at five dose levels together with concurrent weekly gemcitabine over three dose levels. Their clinical stage based on the UICC was III in 54 cases and IV in 6 cases. Dose-limiting toxicity developed as an early adverse event in only three of these 60 patients. One patient treated at the 50.4 GyE dose level suffered a grade 3 gastric ulcer 10 months after C-ion RT, but subsequently recovered with conservative management. No other serious side effects were noted. Treatment combinations that included full-dose gemcitabine (1,000 mg/m2) did not result in any increased incidence of adverse effects with dose escalation. The 2-year local control rate and 2-year overall survival rate were 26 and 32 %, respectively, and the median survival time was 19.3 months. The local control and overall survival increased with increasing C-ion RT dose. In the high-dose group, in which patients were irradiated with at least

45.6 GyE, the 2-year local control and 2-year overall survival rates were 58 and 54 %, respectively (Fig. 4). In the literature, the reported 2-year survival rates for locally advanced pancreatic cancer were 10–25 %.

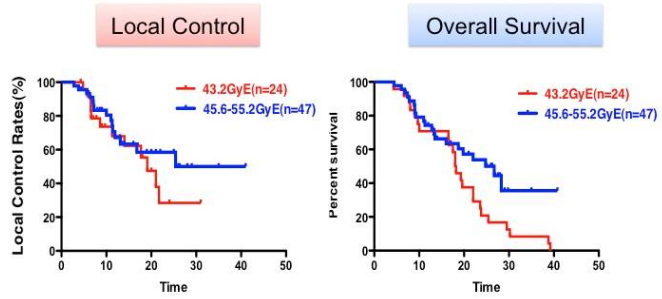

Fig. 4. Local control and overall survival by total dose. For doses greater than 45.6 GyE, the 2-year local control rate was 58 % and the overall survival rate was 54 %, both of which are higher than in the low-dose group

Future Perspectives

In 2011, beam delivery using spot scanning became available at the NIRS. It continues to be used to target lesions without significant respiratory movement at the time of writing (April 2013). However, spot-scanning irradiation for mobile targets is currently under development and will be realized in the near future. Further improvements in the long-term outcome of treatment are expected with further dose escalation. Scanning irradiation can provide even better dose distribution than the passive method in the treatment of a number of tumor types because it is much more flexible. When using passive irradiation, a uniform length of the spread-out Bragg peak must be used in each field, but this often gives rise to an unnecessarily high dose to the surrounding normal tissue. The use of scanning irradiation avoids this and it is in fact possible to reduce the dose to the normal tissue even more by accepting the high-dose spot inside the target, if desirable. Figure 5 shows the dose distribution using both broad and scanning beams; the latter results in a lower dose to the spinal cord and kidney. A further advantage of broad-beam irradiation is the lack of any requirement for collimator or compensation bolus, reducing the preparation time between CT acquisition and the start of treatment and reducing the total cost of the procedure. In addition, a rotating gantry can be used with the carbon ion beam. As a result, patients need not be immobilized in an uncomfortable, inclined position, as they do currently when C-ion RT with passive irradiation is used.

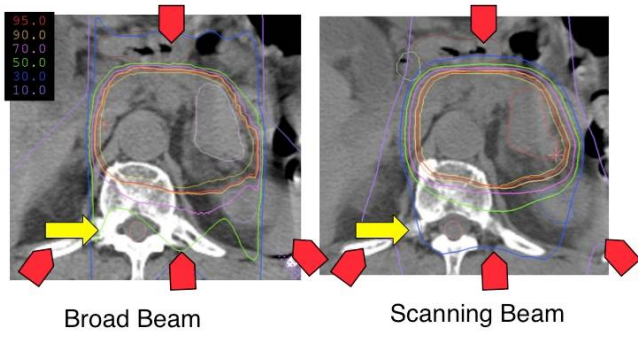

Fig. 5. The difference between broad-beam and scanning beam irradiation. The left and right panels show the dose distribution by broad-beam and scanning beam irradiation, respectively. Broad-beam delivery results in a lower dose to the spinal cord and the kidney

Case Study

The case was a 66-year-old Japanese man who was referred to the NIRS with a diagnosis of pancreatic cancer (Fig. 6). The C-ion RT was performed with four anterior-posterior (A-P), P-A, and bilateral ports and the total dose was 50.4 GyE

in 12 fractions. The CT at 40 months post treatment and the FDG accumulation at 6 months post treatment both demonstrated the disappearance of the tumor. The patient remains disease free 70 months after treatment and currently does not require medication.

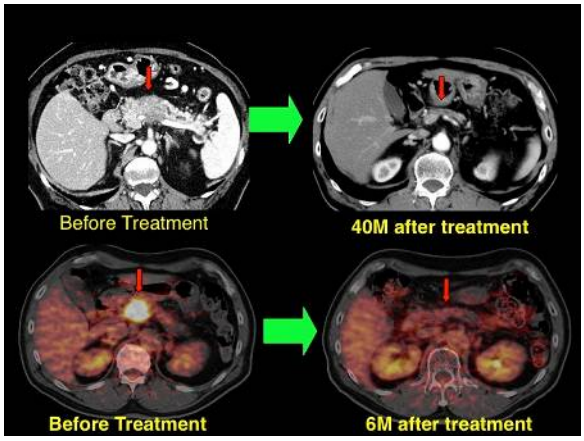

Fig. 6. This patient is a 65-year-old male with locally recurrent rectal cancer. A CT scan and PET scan revealed a tumor mass in the right sidewall of the pelvis and infiltrated pelvic bone

References

[1] Registration committee of pancreatic cancer. Annual report of nationwide survey of pancreatic cancer. J Jpn Panc Surg. 2003;18:1–169.

[2] Lillemoe KD, Cameron JL, Hardacre JM, et al. Is prophylactic gastrojejunostomy ndicated for unresectable periampullary cancer Ann Surg. 1999;230:22–330.

[3] Griffin JF, Smalley SR, Jewell W, et al. Patterns of failure after curative resection of pancreatic carcinoma. Cancer. 1990;66:56–61.

[4] Lillemoe KD, Cameron JL, Hardacre JM, et al. Is prophylactic gastrojejunostomy indicated for unresectable periampullary cancer Ann Surg. 1999;230:322–30.

[5] Roldan GE, Gunderson LL, Nagorney DM, et al. External beam versus intraoperative and extrabeam irradiation for locally advanced pancreatic cancer. Cancer. 1988;61:1110–6.

[6] Moertel CG, Gundeson LL, Mailliard JA, et al. Early evaluation of combined fluorouracil and leucovorin as a radiation enhancer for locally unresectable, residual, or recurrent gastrointestinal carcinoma. J Clin Oncol. 1994;12:21–7.

[7] Koong AC, Mehta VK, Le QT. Pancreatic tumors show high levels of hypoxia. Int J Radiat Oncol Biol Phys. 2000;48:919–22.

[8] Ando K, Koike S, Ohira C, et al. Accelerated reoxygenation of a murine fibrosarcoma after carbon-ion radiation. Int J Radiat Biol. 1999;75:505–12.

[9] Lee CJ, Dosch J, Simeone M. Pancreatic cancer stem cells. J Clin Oncol. 2008;26:2806–12.

[10] Oonishi K, Cui X, Hirakawa H. Different effects of carbon ion beams and X-rays on clonogenic survival and DNA repair in human pancreatic cancer stem-like cells. Radiother Oncol. 2012;103:32–7.

[11] Kamada T, Tsujii H, Tsuji H, et al. Efficacy and safety of carbon ion radiotherapy in bone and soft tissue sarcomas. J Clin Oncol. 2002;20:4466–71.

Session 2: Radiobiology of Carbon Ion Radiotherapy

Modeling of the Biological and Clinical Response to Carbon Ion Radiotherapy

Naruhiro Matsufuji and Taku Inaniwa

Research Center for Charged Particle Therapy, National Institute of Radiological Sciences, Chiba, Japan
e-mail address: matufuji@nirs.go.jp

Abstract

To achieve precise and accurate dose delivery of carbon ion radiotherapy (C-ion RT) and to better understand the resultant response, we have carried out a study on a biological model to be implemented in the routine C-ion RT and to evaluate the cellular response to fractionated irradiation. We have updated the model from the original pragmatic model to a new, modified microdosimetric kinetic model (MKM). We herein describe a method to calculate the relative biological effectiveness in mixed radiation fields of therapeutic ion beams using the modified MKM. In addition, we show the procedure for integrating the modified MKM into a treatment planning system for a scanned carbon beam. With this procedure, the model is fully integrated into our research version of the treatment planning system. The depth-survival curve of our standard HSG cells were measured and compared with the results of the modified MKM prediction. The good agreement between the two curves proved that the proposed method is a candidate for calculating the biological effects in treatment planning for C-ion RT.

To understand the overall biological response of normal cells to carbon beam irradiation, a fractionated cell survival experiment was carried out with normal human fibroblast cells. The response was well reproduced by introducing the potentially lethal damage repair (PLDR) and sublethal damage repair (SLDR) effects into a conventional LQ model. The model analysis suggested that PLDR occurs after irradiation, ranging from 30 to 90% depending on the radiation type. The SLD was perfectly repaired during the fraction interval for the lower LET irradiation, but remained at about 30% for the high-LET irradiation.

Updating the RBE Model for C-ion RT (the modified MKM) [1]

1. Introduction

The precise and accurate modeling of the biological / clinical effectiveness (RBE) of the therapeutic carbon-ion beam is a requisite for the success of C-ion RT. At the National Institute of Radiological Sciences (NIRS), the RBE is estimated by a method proposed by Kanai *et al* [2] that is based on the linear-quadratic (LQ) model. Starting from the LQ parameters, α and β, for a mono-energetic carbon beam derived from the empirical linear energy transfer (LET)-α and LET-β tables [3], dose-averaged coefficients of α and β for a mixed beam are calculated. For patient planning, the *in vitro* human salivary gland (HSG) tumor cell survival response, *i.e.*, the information in the LET-α and LET-β tables, is used to obtain the radiobiological RBE distribution under the assumption that the moderate radiosensitivity of HSG cells reflects a typical response of tumors to the carbon beam. All the radiobiological RBE values are then rescaled to clinical RBE values according to the RBE observed in a clinical study with fast neutron treatment, to account for the difference between the *in vitro* response and clinically required *in vivo* response. The validity of this pragmatic procedure

was evaluated with tumor control probability curves for non-small cell lung cancer [4].

Another approach for predicting the cell survival response after ion irradiation is the microdosimetric kinetic model (MKM) originally developed by Hawkins [5]. In the MKM, the surviving fraction of cells can be predicted from the specific energy, z, deposited to a subcellular structure, referred to as a 'domain' for any kind of radiation. The MKM was recently modified by revising the saturation correction for expressing the decrease of the RBE due to the overkill effect in a very high specific energy *z* region [6]. The attractive point of the modified MKM over the original pragmatic approach is that it enables a mechanistic estimate of the biological effect of any kind of radiation to be made based on its measurable, and therefore verifiable, physical quantities. In contrast, it is essentially indispensable in the framework of the original model to conduct biological experiments with the beam, otherwise inter- or extrapolation of adjacent data is needed. We consider that more precise and accurate estimation of the biological effects of the therapeutic carbon ion beam can be realized using the modified MKM, and have decided to integrate the modified MKM as our RBE model for C-ion RT. Based on the recent progress in this direction, we describe a new method to predict the RBE of therapeutic ion beams by the modified MKM, with biological verification.

2. The modified microdosimetric kinetic model (modified MKM)

The mathematical procedure to predict the cell survival fraction after ion irradiation by the modified MKM was previously described in detail [6]. Therefore, the explanation of the procedure is kept to a minimum here. In the MKM, the survival fraction of a cell, S, is equal to the probability that the number of lethal lesions is zero in the cell nucleus and can be expressed as the negative exponential of the number of lethal lesions in the nucleus $\langle L_n \rangle$, averaged over the cellular population:

$$S = \exp(-\langle L_n \rangle) \quad (1)$$

$\langle L_n \rangle$ can be calculated as:

$$\langle L_n \rangle = (\alpha_0 + \beta z_{1D}^{*})D + \beta D^2 \quad (2)$$

where α_0 is the constant that represents the imaginary value at LET = 0, and D is the absorbed dose. The parameter β is treated as a constant independent of the radiation type in the MKM. The variable z^*_{1D} denotes the saturation corrected dose-mean specific energy of the domain delivered in a single event and described as:

$$z_{1D}^{*} = \int z_{sat} z f_1(z) dz \,/\, \int z f_1(z) dz \quad (3)$$

where $f_1(z)$ is the probability density of z deposited by a single energy-deposition event of the domain, and z_{sat} represents the saturation-corrected specific energy derived as follows:

$$z_{sat} = z_0^2/z^2(1 - \exp(-z^2/z_0^2)) \quad (4)$$

with the saturation coefficient z_0:

$$z_0 = (R_n/r_d)^2/\sqrt{\beta(1 + (R_n/r_d)^2)} \quad (5)$$

In equation (5), R_n and r_d are the radii of the cell nucleus and the domain, respectively. These biological parameters were determined using our reference cells, HSG [6]. Physical parameters, such as the z^*_{1D} for any kind of mono-energetic ions along the ion track (*x*-direction), can be derived by using the x–$z_{sat}(x)$ and x–$z(x)$ relationships. In the active scanning delivery of carbon ion beams, the prescribed dose distribution at a position *i* can be achieved by superimposing the dose at position *i* given by the beam *j*, d_{ij}, according to the weight of the beam intensity determined by the planning, w_j, for the beam. To obtain the radiation quality of the scanned carbon beams, we used Monte Carlo simulations (PTSsim), which is a simulation code for particle therapy based on Geant4. The validity of the Monte Carlo simulations for therapeutic carbon beams was

examined and concluded to be satisfactory [7].

3. Application of the modified MKM for the response of HSG cells

To verify that the method could predict the RBE in mixed radiation fields, cell irradiation experiments were conducted for mixed radiation fields with scanned carbon beams. Some experimental results implied that the radiosensitivity of the HSG cell line has changed over time. To account for the change, we assumed that not R_n and r_d, but only α_0, can be adjusted. To obtain the value of α_0 for the current HSG cells, we measured the survival curve for a mono-energetic 290 MeV/n carbon-ion beam and found that value of α was 0.282 Gy^{-1} from the linear coefficient fitted by the LQ model with a fixed value of $\beta = 0.0615$ Gy^{-2}. The z^*_{1D} at that point was 3.43 Gy, so the value of α_0 was derived as $\alpha_0 = \alpha - \beta z^*_{1D} = 0.0708$ Gy^{-2}. To verify the proposed method to predict the RBE in mixed radiation fields, we performed cell irradiation experiments. The modified MKM was fully integrated into the research version of the treatment planning system developed by Inaniwa *et al.* [8]. The biological dose distribution for HSG cells was optimized therein for a cylindrical target volume 100 mm in diameter and 60 mm in length positioned in the center of a 116 mm space in water. A 290 MeV/n carbon beam was used for the irradiation. The prescribed dose was set to be 5.79 Gy (RBE) at the clinical dose, or 3.99 Gy (RBE) as the biological dose for HSG cells.

Next, the HSG cells in flasks were positioned around the isocenter of the active scanning system developed at the HIMAC. In addition to the depth-survival curve, the survival curve at the center of the spread-out Bragg peak (SOBP), *i.e.*, 116 mm water equivalent depth, was measured. A 290 MeV/n carbon beam with a beam intensity of 1.5×10^8 particles/s was used for cell exposures. After the irradiation, the samples were assayed to estimate the survival probability by the colony-formation method.

4. Results and discussion

The dose distributions measured with a calibrated parallel-plate ionization chamber (PTW 34045) in combination with an electrometer (Unidos PTW) were compared with the planned ones, as shown in Figure 1. The measured absorbed dose distributions showed good agreement with the planned ones within an accuracy of ±1% in the whole region. Figure 2 shows the measured and predicted survival values as a function of the water equivalent depth for the cell irradiation experiments. In this figure, the survival values for four measurements at each depth are plotted, in addition to their average. The predicted survival fractions showed equivalently good agreement with the measured ones in the whole region from the plateau to the fragment tail, and very good agreement was observed between the survival curve measured at the center of the SOBP and the predicted one, as shown in Figure 3. The slight underestimations of survival observed in the target could

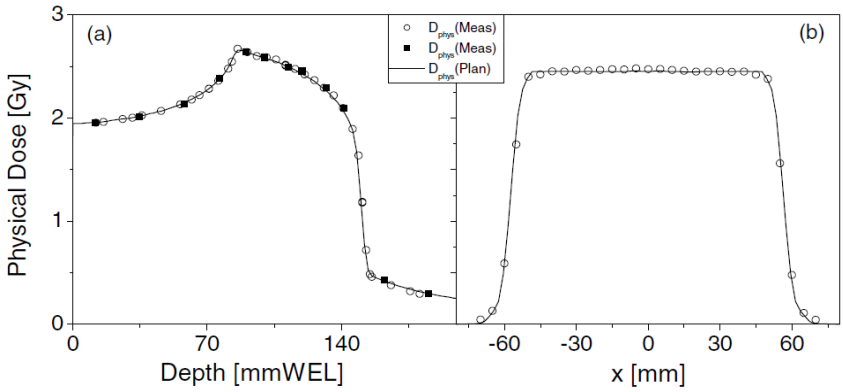

Fig. 1. The planned and measured dose distributions on the central beam axis (a) and on the transverse axis

be attributed to not correcting the parameters R_n and r_d for radiosensitivity.

Next, the biological dose distribution was optimized based on the original RBE model [1]. In this optimization, the 10.0% survival of the 'old' HSG cells was selected as an endpoint corresponding to the 4.04 Gy (RBE) biological dose. The predicted survival curve is shown in Figure 4 with a dashed curve. According to the optimized irradiation parameters, the cell irradiation experiments were performed using the 'current' HSG tumor cells. The experimental setup and its procedures were the same as described above. The measured survival fractions are shown in Figure 4, with symbols. We recalculated the survival fractions based on the modified MKM, in which the current response of HSG tumor cells was reflected through the value of α_0. The recalculated survival curve, shown by a solid line in the figure, reproduces the measured survival fractions very well. From this study, we concluded that the modified MKM was fully integrated into the treatment planning for the carbon beam at our facility. The therapeutic dose given in routine C-ion RT is now designed using the modified MKM.

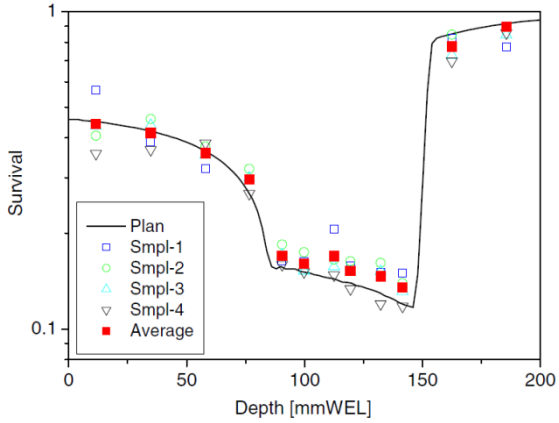

Fig. 2. The planned (using the modified MKM) and measured HSG cell survival distributions

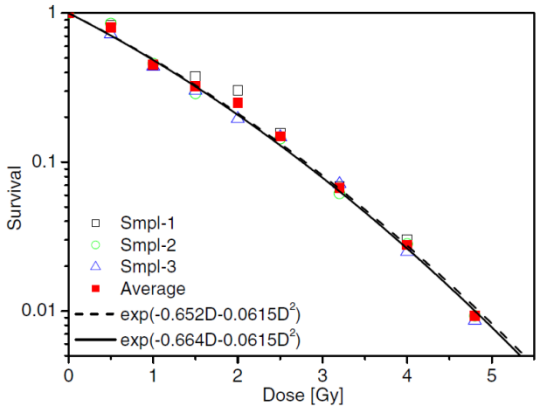

Fig. 3. The planned (using the modified MKM) and measured HSG cell survival at the middle of the SOBP.

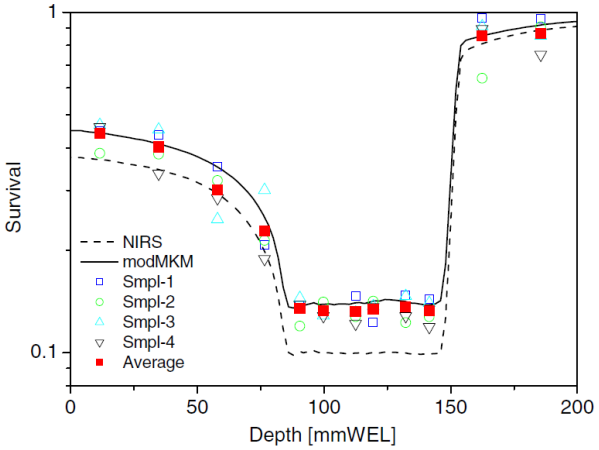

Fig. 4. The HSG cell survival distributions, recalculated for the original response using the modified MKM.

Cell survival response to fractionated irradiation [9]

1. Introduction

Radiation therapy is usually carried out on a fractionated irradiation basis to avoid serious side effects. C-ion RT is no exception; however, due to its superior dose localization to the tumor, hypofractionation is considered to be feasible. In fractionated therapeutic irradiation strategies, repair is thought to be completed before the subsequent irradiation. In other words, the dose response is considered to be identical among irradiations. However, in some experiments, a difference in response has been observed between single and fractionated irradiations with a high LET heavy-ion beam [10]. In order to understand these results, we carried out an *in vitro* fractionated irradiation experiment with carbon ion beams that mimicked the clinical schedule with human cells. A delayed-assay experiment was also conducted with the cells in order to reveal the extent of damage repair. The results were analyzed by integrating the damage repair process into the linear-quadratic (LQ) model.

2. Cell survival response model to fractionated irradiation

The LQ model has been widely used as a dose response model for cell survival. In the LQ model, the cell survival probability, S_n, for n fractionated irradiations with a single dose, d, is given by implicitly assuming the full recovery between the fractionations as:

$$\mathrm{S}_n = \exp[-n(\alpha d + \beta d^2)] \tag{6}$$

It is regarded that radiation causes two types of DNA damage. One is potentially lethal damage (PLD). In principle, PLD is considered fatal, and the initial yield is estimated by the LQ formula. However, some part of the PLD can be repaired, depending on the environment after the irradiation [11]. The other type of damage is sublethal damage (SLD), which can be repaired in hours unless additional sublethal damage occurs. Lethal damage originates from unrepaired PLD and SLD. In this study, we considered the simultaneous actions of both repair processes following fractionated irradiation. For the sake of simplicity, we started with two fraction irradiations. In this case, the survival, S_2, can be considered as:

$$log\mathrm{S}_2 = -[\gamma(\alpha d + \beta d^2) + (\alpha d + \beta d^2) + \beta d^2 h_n(\theta)] \tag{7}$$

$$h_n(\theta) = (2/n)[\theta/(1-\theta)][n - (1-\theta^n)/(1-\theta)] \tag{8}$$

where θ represents the extent of SLDR (between 0 (full SLDR) and 1 (no SLDR)). The last term in eq. (8) corresponds to the extent of SLDR based on the Incomplete Repair (IR) model [12] and γ corresponds to the extent of PLDR (between 0 (full PLDR) and 1 (no PLDR)) [13]. The first term corresponds to the lesions remaining after the PLDR process: for the second irradiation, the γ is not given if the cells were immediately assayed after the irradiation. The β value was assumed to be constant throughout the irradiation. When generalizing eq. (7) to n fractions, the survival, S_n, is given as:

$$log\mathrm{S}_n = -\{(n-1)[\gamma(\alpha d + \beta d^2) + \beta d^2 h_{n-1}(\theta)] + (\alpha d + \beta d^2) + 2\beta d^2[\theta(1-\theta^{n-1})/(1-\theta)]\} \tag{9}$$

Again, in this fractionated experiment, the irradiated cells were immediately assayed after the final irradiation. Therefore, PLDR does not take place after the final irradiation; i.e. PLDR is repeated *(n−1)* times for n fractionated irradiations. Here, we assume that both the PLDR and SLDR take place independently; *i.e.*, the cross term between the PLDR and SLDR is not taken into consideration.

In fractionated irradiation experiments, it is not possible to derive γ and θ separately, because the observed cell survival response is affected by both processes. On the other hand, the PLDR can be evaluated separately by comparing the immediate plating (normal single fraction) and delayed plating (delayed assay) survival. Thus, we first tried to evaluate the parameter γ by a delayed-assay experiment with α and β values of the immediate assay. Then, in order to reproduce the response in fractionated irradiations, we searched for the θ which gave the best fit (in the least squares sense) to the experimental data with the derived γ. This approach is based on the assumption that PLDR occurs prior to SLDR.

3. Biological experiments

Two human normal cell lines, NB1RGB (normal human skin fibroblast cell line) and HFL-I (normal embryonic lung fibroblast cell line) were chosen. Biological experiments with carbon ion beams were carried out at the biology experiments port of the HIMAC. The initial energy of the carbon beam was 290 MeV/n, and the dose rate at the point of irradiation was controlled in the range of 0.1–7.0 Gy/min in order to maintain dosimetric precision. Incident beams were broadened uniformly to 10 cm in diameter at the isocenter. Cells were irradiated at two different irradiation depths where the dose-averaged LET was approximately 13 and 75 keV/μm, respectively, adjusted by inserting an energy absorber made of polymethyl methacrylate (PMMA) upstream from the cells. The cells were almost 100% confluent by the first day of irradiation. For the fractionations, doses of 0.15–5.5 Gy were delivered to each cell flask placed at the isocenter for the single-, two-, three-, or four-dose fractionated irradiation over a 24-h interval. Within an hour after the final irradiation, the cells were re-plated onto a new dish, then incubated for two weeks to allow them to form colonies. For the delayed assay, the cells were incubated for 24 h post-irradiation to determine cell survival as a function of the delayed plating time. The experiment was carried out also with X-rays as a reference for the carbon beam.

4. Results and discussion

The cell survival curves for fractionated irradiation (Figure 5) show the surviving fractions of each cell line. The lines in the figure correspond to the survival curve calculated with eq. (6) based on the α and β values of single irradiation. It is obvious from the figure that the cell survival response to fractionated irradiation is not a simple repeat of that following single irradiation. Table 1 summarizes the SLDR and PLDR parameters. Concerning the SLDR, the SLD was completely repaired for X-rays, but about 30% of the SLDs were left unrepaired following exposure to 75 keV/μm carbon ions. The γ values derived by best fits were almost identical with those derived from the delayed assay, except for the HFL-I for 13 keV/μm. Figure 6 shows the cell survival fit based on the parameters in Table 1.

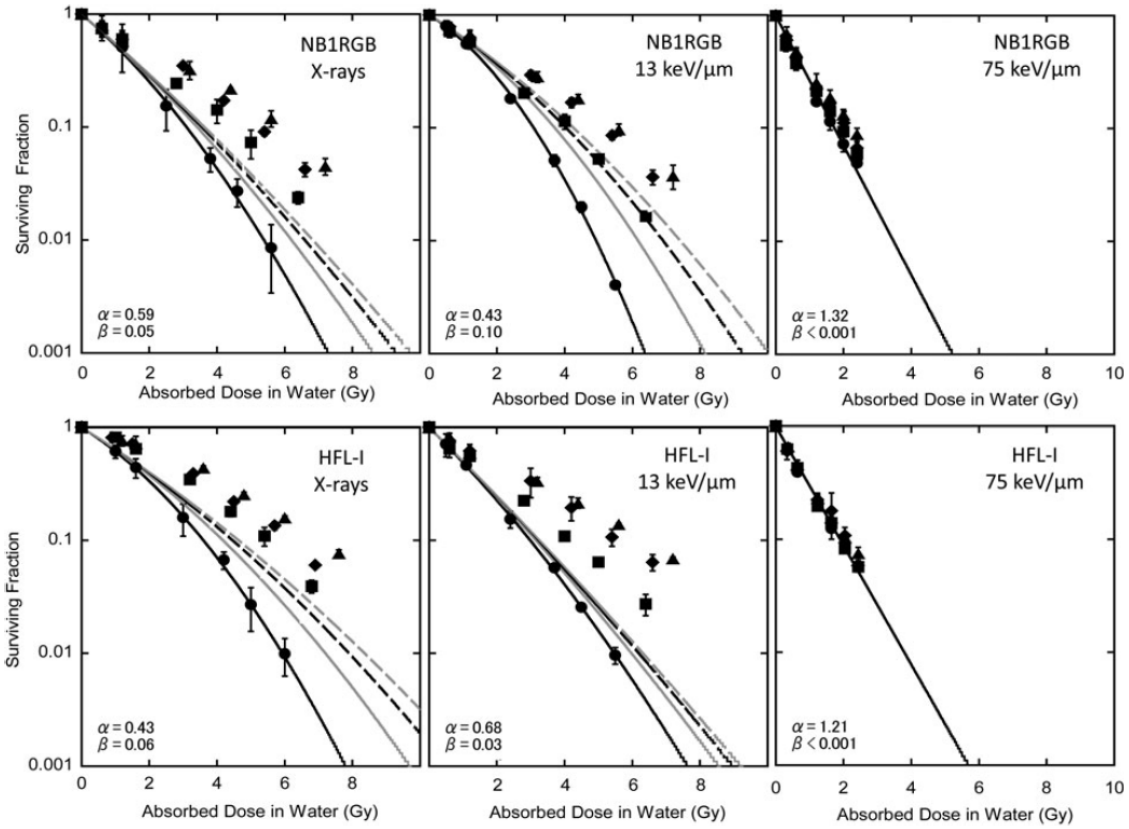

Fig. 5. The survival of NB1RGB and HFL-I cells following exposure to a single fraction up to four fractions of X-ray or carbon ion radiation. The lines in the figures correspond to the fit with eq. (6).

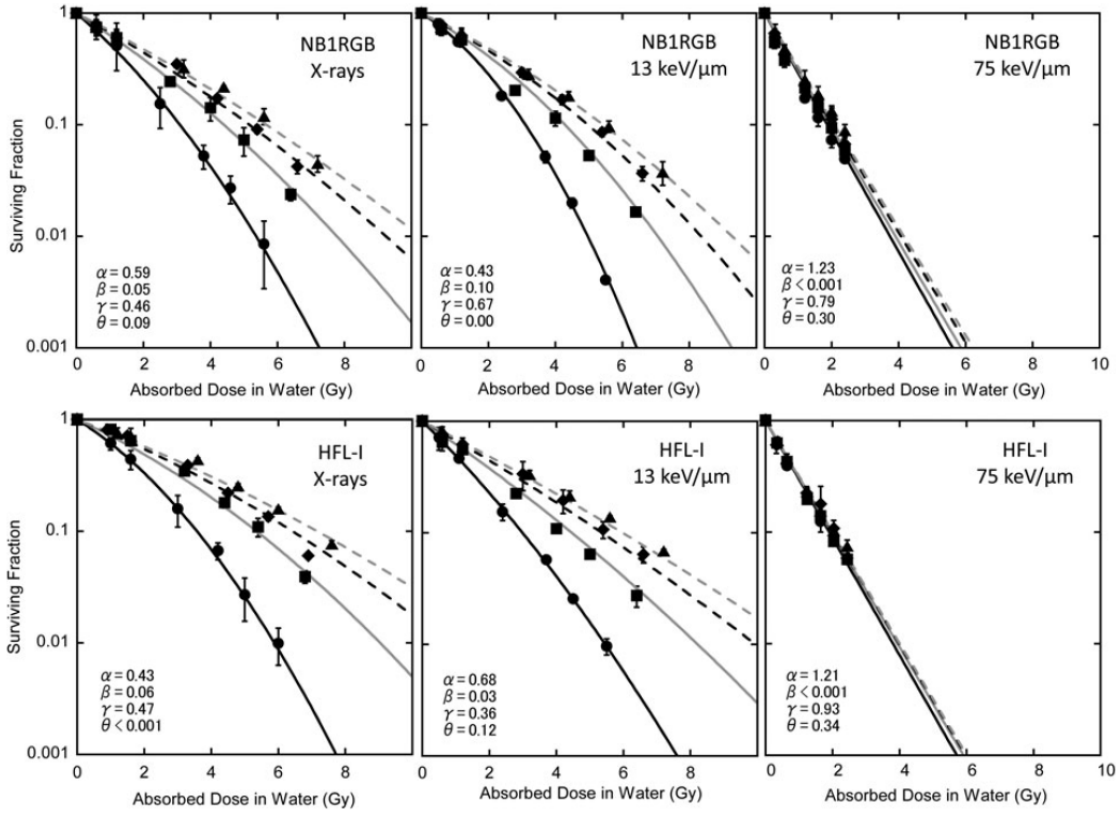

Fig. 6. The survival of NB1RGB and HFL-I cells following exposure to a single fraction up to four fractions of X-ray or carbon ion radiation. The lines in the figures correspond to the fit with eq. (9).

Again, as indicated in the figures, the cell survival response to fractionated irradiation was not reproduced as a simple repeat of the single irradiation. This suggests that the repair process plays an important role in the response to fractionated irradiation. Concerning the PLDR, the delayed assay after 24 h revealed that PLDR repair occurs in normal cells. The PLDR factor γ tended to increase with an increasing LET. This means that PLDR is less likely to occur at high LET. The LET dependency of the PLDR has already been reported in studies of mouse embryos and Ehrlich ascites tumor cells. The present results also suggest that not only PLDR, but also SLDR, should be taken into consideration to reproduce the overall cell survival response to fractionated irradiation, at least for higher LET: the SLD was almost fully repaired in response to low-LET beams, such as X-rays or 13 keV/μm carbon-ions.

Here, the γ values of HFL-I cells exposed to 13 keV/μm irradiation derived by best fits were different from those derived from the delayed assay. As explained, in this study, the cross term between the PLDR and SLDR was not taken into consideration, which likely caused the discrepancy. The other possibility is that the repair capacity could change over time during fractionated irradiation [14], while we assumed a fixed repair capacity. These factors, i.e. the repair kinetics of PLD and SLD and their cross effect, are worth studying to enable more accurate modeling in the future. The results of SLDR and PLDR clearly suggest that both types of damage induced by high-LET radiation are less frequently repaired than those caused by low-LET radiation. High-LET radiation is likely to form cluster-like damage in the cell nucleus, and such damage is generally not repaired by non-homologous end joining (NHEJ), which is the major repair mechanism for human cells. Thus, chromatin damage, as a consequence of clustered DNA damage, cannot be repaired perfectly, and cell division is consequently suppressed. The damaged cells are thus likely to die during replication.

In this study, we focused on the response of normal cells. Marchese reported that PLDR works even in tumor cells [13]. They estimated the PLDR factor, γ, in six malignant cell lines, and indicated that it ranged from 0.62–0.93. As their experimental data were derived from 6-h-interval experiments, the effect of repopulation was regarded to be negligible. In a 24-h-interval irradiation, however, it is necessary to take into account both repopulation and repair effects.

In conclusion, by introducing repair effects into an LQ model, it was possible to estimate the response of normal cells to carbon ions. Our analysis suggested that PLDR-like repair can take place following any radiation, while SLDR-like repair was significantly suppressed for the higher-LET irradiation. In this study, we assumed that there was constant PLDR and SLDR as a function of time; however, in the future, it would be worthwhile to study their time-course in order to better understand the repair mechanisms.

Table 1. Parameters in eq. (9) to fit the experimental data shown in Fig. 6.

		α (Gy^{-1})	β (Gy^{-2})	γ	θ
NB1RGB	X-rays	0.59 ± 0.17	0.05 ± 0.02	0.46 ± 0.00	0.09 ± 0.06
	13 keV/μm	0.43 ± 0.05	0.01 ± 0.01	0.67 ± 0.05	0.00 ± 0.00
	75 keV/μm	1.32 ± 0.04	<0.001	0.79 ± 0.06	0.30 ± 0.02
HFL-I	X-rays	0.43 ± 0.14	0.06 ± 0.02	0.47 ± 0.04	<0.001
	13 keV/μm	0.68 ± 0.07	0.03 ± 0.02	0.36 ± 0.09	0.12 ± 0.14
	75 keV/μm	1.21 ± 0.04	<0.001	0.93 ± 0.06	0.34 ± 0.13

References

［1］ Inaniwa, T., Furukawa, T., Kase, Y. *et al*. Treatment planning for a scanned carbon beam with a modified microdosimetric kinetic model. *Phys. Med. Biol.* 2010;**55**: 6721-6737.

［2］ Kanai, T., Endo., M., Minohara, S. *et al.* Biophysical characteristics of HIMAC clinical irradiation system for heavy-ion radiation therapy *Int. J. Radiat. Oncol. Biol. Phys.* 1999; **44**: 201–210.

［3］ Furusawa, Y., Fukutsu, K., Aoki, M. *et al*. Inactivation of aerobic and hypoxic cells from three different cell lines by accelerated He-, C- and Ne-ion beams. *Radiat. Res.* 2000;**154**: 485–496.

［4］ Kanai, T., Matsufuji, N., Miyamoto, T. *et al.* Examination of GyE system for HIMAC carbon therapy *Int. J. Radiat. Oncol. Biol. Phys.* 2006; **64**: 650–656.

［5］ Hawkins, R. B. A microdosimetric-kinetic model for the effect of non-Poisson distribution of lethal lesions on the variation of RBE with LET *Radiat. Res.* 2003; **160**: 61–69.

［6］ Kase, Y., Kanai, T., Matsufuji, N. *et al.* Biophysical calculation of cell survival probabilities using amorphous track structure models for heavy-ion irradiation. *Phys. Med. Biol.* 2008; **53**: 37–59.

［7］ Inaniwa, T., Furukawa, T., Sato, S. *et al.* Development of treatment planning for scanning irradiation at HIMAC. *Nucl. Instrum. Methods. Phys. Res. B* 2008; 266: 2194–2198

［8］ Toshito, T., Inaniwa, T., Furukawa, T. *et al.* Introduction of Monte Carlo method to treatment planning for scanning carbon beam therapy. *Proc. 99th Scientific Meeting of JSMP* 2010: 125–126.

［9］ Wada, M., Suzuki, M., Liu, C. *et al.* Modeling the biological response of normal human cells, including repair processes, to fractionated carbon beam irradiation. *J. Radiat. Res.* 2013; **54**: 798–807.

［10］ Ando, K., Koike, S., Uzawa, A. *et al*. Repair of skin damage during fractionated irradiation with gamma rays and low-LET carbon ions. *J. Radiat. Res.* 2006; **47**: 167–74.

［11］ Arlett, C. F. and Priestley, A. Defective recovery from potentially lethal damage in some human fibroblast cell strains. *Int. J. Radiat. Biol.* 1983; **43**: 157–67.

［12］ Thames H. D. An ’incomplete-repair’ model for survival after fractionated and continuous irradiations. *Int. J. Radiat. Biol. Relat. Stud. Phys. Chem. Med.* 1985; **47**: 319–39.

［13］ Marchese, M. J., Zaider, M. and Hall, E. J. Potentially lethal damage repair in human cells. *Radiother. Oncol.* 1987; **9**: 57-65.

［14］ Ngo, F. Q., Youngman, K., Suzuki, S. *et al.* Evidence for reduced capacity for damage accumulation and repair in plateau-phase C3H 10T1/2 cells following multiple-dose irradiation with gamma rays. *Radiat. Res.* 1986; **106**: 380–95.

Genetic Variations in Cancer Cells and Effects of Carbon-ion Irradiation

Takashi Imai

Advanced Radiation Biology Research Program, Research Center for Charged Particle Therapy

National Institute of Radiological Sciences, Chiba, Japan

e-mail address:imait@nirs.go.jp

Abstract

Many favorable outcomes have been reported in clinical trials for carbon-ion radiotherapy against several types of malignant tumors. However, some biological issues still remain to be resolved for the improvement of the long-term patient survival. We have studied the following fundamental biological issues: (1) Certain tumor cells are pathologically indistinguishable from others, despite sometimes showing radio-resistance. What makes these tumor cells radio-resistant? (2) What causes distant metastases after local treatment? If the metastatic cells are affected by irradiation, what are the molecular mechanisms? What is the most suitable therapy to be used concurrently with carbon-ion radiotherapy to suppress metastasis? (3) Can radioprotective agents, such as anti-reactive oxygen species or some growth factors, protect normal tissues surrounding the tumor cells from the effects of carbon-ion radiotherapy? Through these studies, we have considered the effects of the genetic differences in individuals or in the experimental materials, such as cell lines and mouse strains, on the radio-sensitivity.

In this symposium, I would like to focus on the analyses of pancreatic cancer cell lines that showed different invasive potentials after irradiation. We first analyzed the migration and invasion of the cells under X-ray-irradiated or carbon-ion-irradiated conditions; the results showed that MIAPaCa-2 cells have greater invasiveness than Panc-1 cells under both X-ray-irradiated and non-irradiated conditions. Surprisingly, the invasiveness of PANC-1 cells was enhanced by carbon-ion irradiation. Both cell lines showed the ability to undergo the mesenchymal (elongated mode)–amoeboid (rounded mode) transition and to move through the extracellular matrix by either the elongated or the rounded modes. Therefore, to suppress the radiation-induced invasiveness of these cells, the simultaneous use of particular protease inhibitors for the elongated mode and a Rho-kinase inhibitor for the rounded mode may be helpful. The identification of genetic differences in the cell lines that are related to the different responses to the irradiation is necessary to develop new prognostic factors for tumors with invasive potential, as well as to identify novel therapeutic targets.

Introduction

Pancreatic cancer is one of the most aggressive malignant diseases, with an extremely low five-year survival rate [1,2]. Most pancreatic cancer patients have advanced disease at the time of diagnosis, and the major clinical problem regarding its treatment is its inherent resistance to conventional chemotherapy and radiotherapy [1–3]. Carbon-ion radiotherapy offers several advantages over conventional photon radiotherapy, including a more accurate dose distribution [4–6] and higher biological efficiency in tumor cell killing [7–9]. Therefore, carbon-ion irradiation is expected to improve the clinical outcome in pancreatic cancer patients.

Metastasis is the main factor underlying cancer treatment failure, and is responsible for nearly 90% of cancer

deaths. However, the molecular mechanism underlying tumor metastasis is a complex multistage process, and a better understanding of the mechanism is required to decrease the number of cancer deaths. In the radiation-biology field, the effects of irradiation complicate the invasion of cancer cells. For example, some studies have suggested that irradiation itself induces the metastasis of tumor cells both *in vitro* and *in vivo*, although other studies have not supported these findings. It has also been reported that carbon-ion irradiation diminished the invasive potential of several cancer cell lines, whereas photon irradiation enhanced the metastatic potential of tumor cells [10-13]. We have found many differences in the experimental conditions utilized among these reports, including differences in cell lines, irradiation conditions and evaluation methods.

Therefore, we tried to systematically test a total of 32 cell lines derived from eight different types of human tumor or normal tissues with regard to their irradiation-induced invasiveness by using the conventional transwell method. The main variables in these experiments were the differences in the cell lines and the radiation types (X-ray or carbon-ion beams; unpublished data).

It is known that tumor cells invade by two different modes of motility, mesenchymal and amoeboid [14-17]. Tumor cells with the mesenchymal mode of motility are known to use proteolytic enzymes, such as matrix metalloproteinases (MMPs) and serine proteases (SerPs), to create a path to move through the extracellular matrix (ECM). In contrast, cells with the amoeboid mode of motility, which are rounded, exhibit a protease-independent mechanism of invasion; this mechanism is based on actomyosin contractility and is dependent on Rho/Rho-kinase (ROCK) signaling. Evidence has shown that cells can shift between these two modes of motility depending on the environmental conditions [18,19].

In this study, we analyzed the effects of the proteases that were induced by X-ray or carbon-ion irradiation, and the effects of Rho-kinase, with regard to the radiation-induced invasiveness of MIAPaCa-2 and PANC-1 cell lines, which were both derived from pancreatic ductal cancer.

Materials and Methods

Cell culture and reagents

Human pancreatic cancer cell lines, MIAPaCa-2, BxPC-3, AsPC-1 and PANC-1, were purchased from the ATCC (Manassas, VA, USA). GM6001, aprotinin, bestatin, E-64, leupeptin and pepstatin A were purchased from Calbiochem-Novabiochem International (La Jolla, CA, USA), and Y27632 was obtained from Wako (Osaka, Japan).

Irradiation

Carbon-ions were accelerated by the heavy-ion medical accelerator in Chiba (HIMAC) at the National Institute of Radiological Sciences (NIRS), Japan [6]. The initial energy of the carbon-ion beams was 290 MeV/ u, and the LET value was 80 keV/μm; a mono-energetic beam with a narrow Bragg peak was applied at a depth of 10 cm, and cells were irradiated with 0, 0.5, 1, 2 or 4 Gy. All radiation treatments were carried out at a dose rate of approximately 1 Gy/min. X-ray irradiation was carried out as described previously [20].

Immunoblotting

Immunoblotting was carried out as described previously [20]. Primary antibodies against human MMP2 (Daiichi Fine Chemical, Toyama, Japan), plasminogen (Santa Cruz Biotechnology, Santa Cruz, CA, USA), urokinase type plasminogen activator (uPA) (Santa Cruz Biotechnology) and glyceraldehyde-3-phosphate

dehydrogenase (GAPDH) (Trevigen, Gaithersburg, MD, USA) with anti-mouse IgG conjugated with horseradish peroxidase (Amersham Biosciences, Buckinghamshire, UK) were used for the analysis.

Quantitative real-time polymerase chain reaction

Quantitative real-time PCR (qRT–PCR) was carried out in a LightCycler 480 instrument with the Probes Master Mix (Roche Diagnostics, Indianapolis, IN, USA), as described previously [21].

Migration ability and invasion assay

The migration ability and invasiveness of the cells were examined by using transwell chambers containing a 6.5-mm filter with a pore size of 8 μm (Corning, Horseheads, NY, USA) [22], as described previously [20]. The MIAPaCa-2 or PANC-1 cells and BxPC-3 or AsPC-1 cells were suspended in the appropriate medium containing 0.35% BSA and seeded into each well at 1 x 10^5 and 2 x 10^5 cells/well, respectively, and the migration and invasion assays were carried out for 24 h from day 2 to day 3 (Fig. 1). On day 3, the cells that reached the undersurface of the transwell membrane were fixed and stained with Diff Quick (Sysmex, Kobe, Japan). The number of migrated or invaded cells in four random fields was counted using a microscope. The percentages of both viable and dead cells were determined by a FACS analysis with a cell viability double-staining kit (Dojindo Molecular Technologies, Tokyo, Japan)[23]. We calculated the number of viable cells among the total seeded cells by multiplying the ratio of viable cells by the total number of seeded cells. We then determined the percentage of migrated or invaded cells.

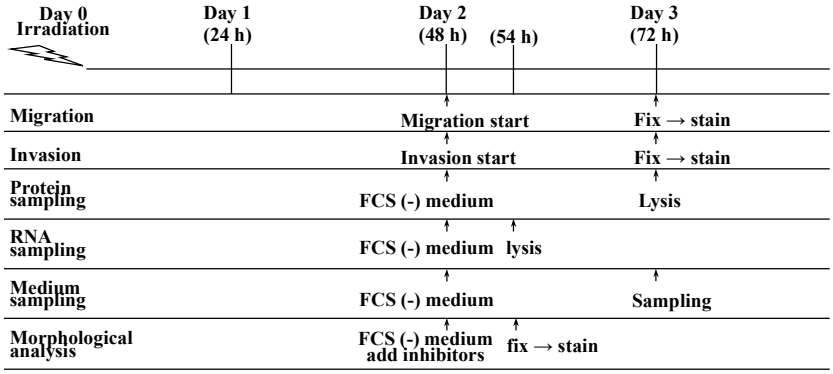

Figure 1. An outline of the experimental procedures.

Determination of the serine protease and urokinase type plasminogen A activity

To investigate the activity levels of serine protease, a Serine Protease Detect Zymo Electrophoresis kit (Life Laboratory, Yamagata, Japan) was used. On day 2, the conditioned medium was replaced with serum-free DMEM, and the cells were incubated for 24 h (Fig. 1). On day 3, the supernatant was collected, mixed with sample buffer without heating or reduction, and applied to casein-polyacrylamide gels. Bands for plasmin, pancreatic elastase chymotrypsin and trypsin were visualized at the molecular weight values of 91, 26, 25 and 23 kDa, respectively. To assess the uPA activity, the conditioned medium was analyzed by a colorimetric assay in the presence of Spectorzyme UK (American Diagnostica, Stamford, CT, USA) as described previously [24]. For inhibitor treatment, the uPA inhibitor, amiloride hydrochloride hydrate (Sigma-Aldrich, St. Louis, MO, USA) was added to samples before the analysis with Spectorzyme UK.

Statistical analysis

The statistical analyses were carried out using unpaired Student's t-test or the Mann–Whitney U-test. A *P*-value <0.05 was considered to be significant.

Results

Four pancreatic cancer cell lines, AsPC-1, BxPC-3, MIAPaCa-2 and PANC-1, were assayed for the effects of C-ion irradiation on their migration ability and invasiveness. C-ion irradiation suppressed the migration of AsPC-1, BxPC-3 and MIAPaCa-2 cells, and diminished the MIAPaCa-2 cell invasion. In contrast, 2 Gy irradiation induced invasiveness in the PANC-1 cells, without altering their migration (Fig. 2). The responses of the MIAPaCa-2 and PANC-1 to the X-ray or carbon-ion irradiation dose in terms of the invasiveness are shown in Figure 3. X-ray irradiation enhanced the invasiveness of both the MIAPaCa-2 and PANC-1 cell lines, but the invasion ratio of MIAPaCa-2 cells was much higher than that of PANC-1 cells. Carbon-ion irradiation almost completely suppressed the invasion of MIAPaCa-2 cells, but induced the invasion of PANC-1 cells. Based on these data, we further characterized the MIAPaCa-2 and PANC-1 cells to identify molecules important for invasiveness.

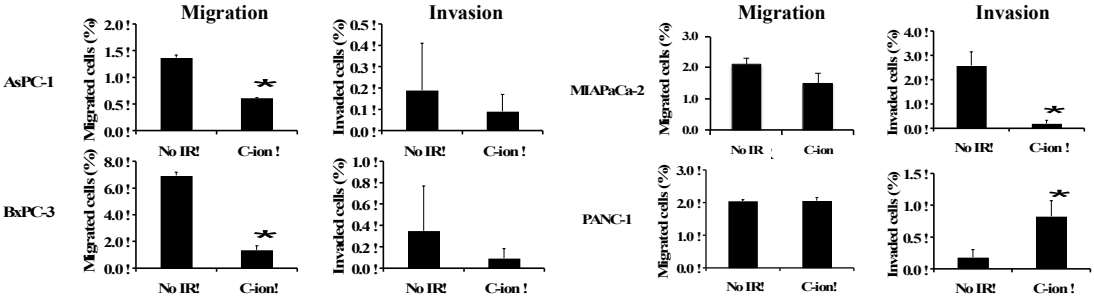

Figure 2. The effects of carbon-ion irradiation (2 Gy) on the migration and invasiveness of pancreatic cancer cell lines.

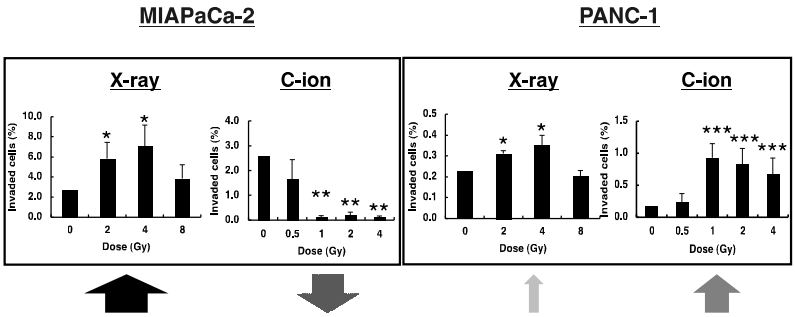

Figure 3. The effects of X-ray or carbon-ion irradiation on the invasiveness of MIAPaCa-2 and PANC-1 cells.

We found that the X-ray-induced MIAPaCa-2 invasion was associated with the induction of MMP-2 expression and activity, and induced the amoeboid-mesenchymal transition to some extent. MIAPaCa-2 cells are morphologically heterogeneous, including cells migrating by both the mesenchymal (elongated) and amoeboid (rounded) modes (Fig. 4). In accordance with this, we demonstrated that the combination of a MMPI and ROCK inhibitor (ROCKI), which blocks both mesenchymal and amoeboid movements, was needed to suppress the MIAPaCa-2 invasion, whereas the single use of the MMPI only slightly reduced the invasiveness, and in the case of ROCKI, it actually enhanced the invasion (Fig. 5). Carbon-ion irradiation, on the other hand, suppressed the

expression and activation of MMP-2, which resulted in reduced invasion [25]. The effects of carbon-ion irradiation on the amoeboid type of invasion are still unknown, and further research is needed on this topic.

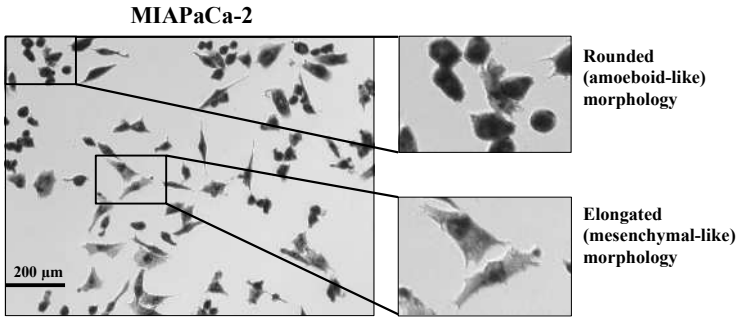

Figure 4. MIAPaCa-2 cells with a typical mesenchymal-type and amoeboid-type morphology are shown.

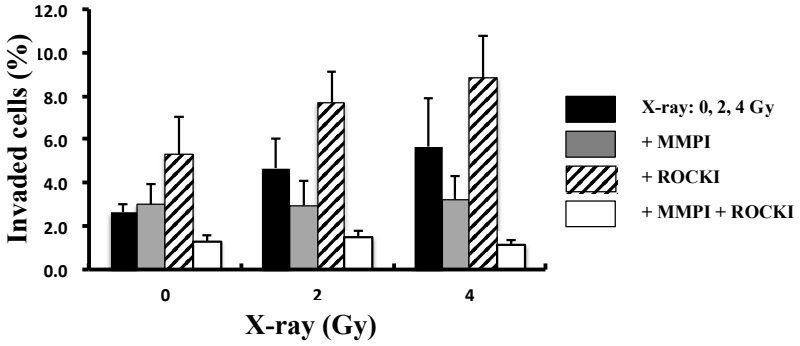

Figure 5. The effects of the MMPI and ROCKI on the invasiveness of MIAPaCa-2 cells. The invasion assay was performed with the addition of the inhibitors. Data represent the mean+/-SD (n = 6).

The PANC-1 cultures had no rounded cells, which suggested that PANC-1 invasiveness is dependent on proteolysis. Indeed, MMP-2 was found to be significantly associated with the X-ray-induced PANC-1 invasion [20]. However, in contrast to MIAPaCa-2, carbon-ion irradiation enhanced the PANC-1 invasion via the activation of serine proteases (SerP), such as plasmin, and uPA (Fig. 6). Inhibition of the functioning protease, SerP, however, failed to reduce the carbon-ion-enhanced PANC-1 invasion, because the carbon-ion-irradiated PANC-1 cells exhibited the ability to undergo the mesenchymal-amoeboid transition. To block both the mesenchymal and amoeboid invasions of carbon-ion-irradiated PANC-1 cells, we treated PANC-1 cells with a SerP inhibitor plus a ROCK inhibitor; this resulted in effective reduction of the invasion of carbon-ion-irradiated PANC-1 cells (Fig. 7).

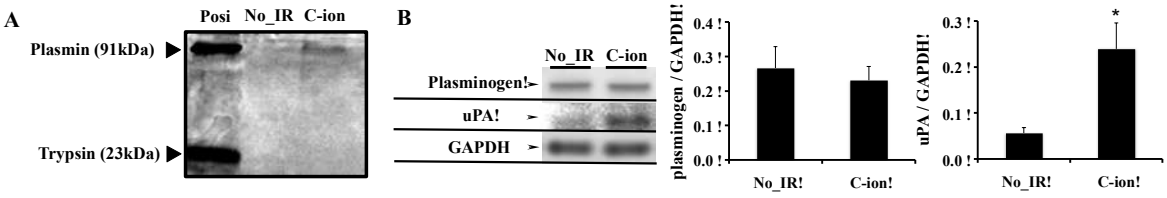

Figure 6. The key protease responsible for the carbon-ion-irradiated PANC-1 invasion at the dose of 2 Gy. (A) The enzyme activities of serine proteases were determined using a Serine Protease Detect Zymo Electrophoresis

Kit. (B) The protein expression levels of plasminogen and uPA were determined by a Western blot analysis. These data represent the means +/- SD of samples (n = 5).

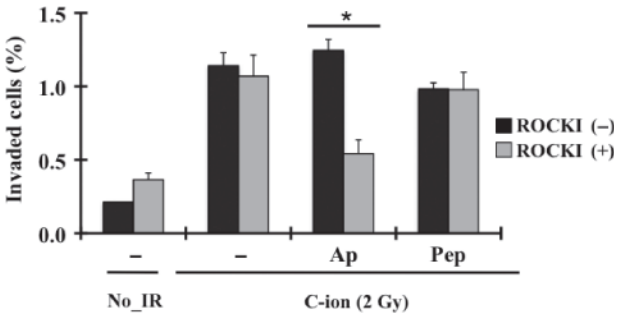

Figure 7. The effects of serine protease inhibitors plus a ROCKI on the invasiveness of carbon-ion-irradiated PANC-1 cells. The invasion assay was performed with the addition of the ROCKI or with the ROCKI plus one of the serine protease inhibitors. The data represent the means ± SD of samples (n = 6). *P< 0.05 vs. control.

Discussion

Studies have shown that the invasiveness of tumor cells is enhanced by X-ray irradiation via the induction of proteases, which degrade the ECM [10-13]. Recent reports have suggested that tumor cells can be classified into those that predominantly take on an elongated or mesenchymal morphology, a rounded or amoeboid morphology, or an intermediate (oval) type of morphology [14-16,26,27]. Because the cells with mesenchymal morphology invade via a mechanism depending on proteolysis of the ECM, this type of invasion is expected to be suppressed by treatment of the cells with protease inhibitors.

The invasion of cells with the amoeboid mode of motility is expected to be blocked by a ROCKI. The ROCKI used in the present study can block the Rho-mediated activation of myosin and suppress the invasiveness of several cancer cell lines [28,29]. Wyckoff et al. suggested that the effects of ROCKI may be related to the dramatic alteration in the localization of myosin light chains; instead of forming bundles around the cell cortex and behind the invasive edge, myosin light chains spread diffusely in the cytoplasm, except in certain localized areas around the cell margin [30].

In the present study, we showed that MMP2 is a key factor involved in X-ray-induced MIAPaCa-2 cell invasion, and that MMP2 is also an important mediator of PANC-1 cell invasion induced by X-ray irradiation. In contrast, SerP, such as uPA and uPAR, rather than MMP2, appear to be the key factors involved in carbon-ion-induced PANC-1 cell invasion. Notably, the expression levels of uPA and uPAR were reduced in carbon-ion-irradiated MIAPaCa-2 cells (data not shown); however, we have not yet determined whether these reductions played any role in the carbon-ion-induced suppression of MIAPaCa-2 cell invasion. Interestingly, both MIAPaCa-2 and PANC-1 cells have potential to switch between the amoeboid–mesenchymal and mesenchymal-amoeboid modes. This switching results in a failure to suppress the irradiation-induced invasiveness by the use of single inhibitors for each mode of invasion. Therefore, we suggested that the simultaneous use of inhibitors of both the amoeboid and mesenchymal movement of cells would more effectively suppress the invasiveness of cells under both X-ray and carbon-ion irradiated conditions.

Although the present study involved only an *in vitro* analysis, the results showed that cancer cells have differences in their response to radiation based on their different phenotypes, such as their type of invasiveness.

If specific genetic mutations related to these invasive phenotypes can be identified in human cancers, it may be possible to develop new prognostic markers and molecular-targeted drugs for the proliferation of cells with invasive potential, which can be used concurrently with suitable radiotherapy.

Conclusion

Irradiation alters the invasive potential of MIAPaCa-2 and PANC-1 via altering the functioning protease expression and activity levels, and it also affects the mesenchymal and amoeboid mode transition. Since the ability to transition between these two modes of motility can allow the cells to invade adjacent tissues via either protease-dependent or protease-independent mechanisms, depending on the environmental conditions, blocking both the mesenchymal and amoeboid modes of invasion is necessary. We found that PANC-1 cells were the only cells that showed enhanced invasion after the carbon-ion irradiation among the four pancreatic cancer cell lines tested in this study. It is still unclear how carbon-ion irradiation generates such cell-specific effects, and further investigations, such as research on the genetic background of target tumors, will be required to determine the mechanisms underlying these effects.

Acknowledgements

I would like to thank Drs. M. Fujita, F. Nakayama, K. Ishikawa, T. Shimokawa and K. Sato of the Advanced Radiation Biology Research Program and Dr. S. Yamada of the Research Center Hospital for helpful discussions and advice, and Ms. K. Imadome, Y. Ohtsuka, T. Suga and A. Ishikawa for technical assistance. This work was performed as a Research Project with Heavy Ions at the NIRS-HIMAC.

References

［1］ Wong HH, Lemoine NR. Pancreatic cancer: molecular pathogenesis and new therapeutic targets. Nat Rev Gastroenterol Hepatol 2009; **6**: 412–422.

［2］ Lau WY, Lai EC. Development and controversies of adjuvant therapy for pancreatic cancer. Hepatobiliary Pancreat Dis Int 2008; **7**: 121–125.

［3］ Krishnan S, Rena V, Janjan NA et al. Prognostic factors in patients with unresectable locally advanced pancreatic adenocarcinoma treated with chemoradiation. Cancer 2006; 107: 2589–2596.

［4］ Okada T, Kamada T, Tsuji H et al. Carbon ion radiotherapy: clinical experiences at National Institute of Radiological Science (NIRS). J Radiat Res 2010; 51: 355–364.

［5］ Fokas E, Kraft G, An H, Engenhart-Cabillic R. Ion beam radiobiology and cancer: time to update ourselves. Biochim Biophys Acta 2009; 1796: 216–229.

［6］ Schulz-Ertner D, Tsujii H. Particle radiation therapy using proton and heavier ion beams. J Clin Oncol 2007; 25: 953–964.

［7］ Tobias CA, Blakely EA, Alpen EL et al. Molecular and cellular radiobiology of heavy ions. Int J Radiat Oncol Biol Phys 1982; **8**: 2109–2120.

［8］ Matsui Y, Asano T, Kenmochi T, Iwakawa M, Imai T, Ochiai T. Effects of carbon-ion beams on human pancreatic cancer cell lines that differ in genetic status. Am J Clin Oncol 2004; 27: 24–28.

［9］ Hamada N, Imaoka T, Masunaga S et al. Recent advances in the biology of heavy-ion cancer therapy. J Radiat Res 2010; 51: 365–383.

［10］ Qian LW, Mizumoto K, Urashima T et al. Radiation-induced increase in invasive potential of human pancreatic cancer cells and its blockade by a matrix metalloproteinase inhibitor; CGS27023. Clin Cancer Res 2002; 8: 1223–1227.

［11］ Ogata T, Teshima T, Kagawa K et al. Particle irradiation suppresses metastatic potential of cancer cells. Cancer Res 2005; 65: 113–120.

［12］ Akino Y, Teshima T, Kihara A et al. Carbon-ion beam irradiation effectively suppresses migration and invasion of human non-small-cell lung cancer cells. Int J Radiat Oncol Biol Phys 2009; 75: 475–481.

［13］ Goetze K, Scholz M, Taucher-Scholz G, Mueller-Klieser W. The impact of conventional and heavy ion irradiation on tumor cell migration in vitro. Int J Radiat Biol 2007; 83: 889–896.

［14］ Wolf K, Mazo I, Leung H et al. Compensation mechanism in tumor cell migration: mesenchymal-amoeboid transition after blocking of pericellular proteolysis. J Cell Biol 2003; 160: 267–277.

［15］ Yamazaki D, Kurisu S, Takenawa T. Involvement of Rac and Rho signaling in cancer cell motility in 3D substrates. Oncogene 2009; 28: 1570–1583.

［16］ Narumiya S, Tanji M, Ishizaki T. Rho signaling, ROCK and mDia1, in transformation, metastasis and invasion. Cancer Metastasis Rev 2009; 28: 65–76.

［17］ Mishima T, Naotsuka M, Horita Y, Sato M, Ohashi K, Mizuno K. LIM-kinase is critical for the mesenchymal-to-amoeboid cell morphological transition in 3D matrices. Biochem Biophys Res Commun 2010; 392: 577–581.

［18］ Victoria Sanz-Moreno Gadea G Ahn J et al. Rac activation and inactivation control plasticity of tumor cell movement. Cell 135:510-23, 2008.

［19］ Croft and Olson. Regulating the conversion between rounded and elongated modes of cancer cell movement. Cancer Cell 14: 349-351, 2008.

［20］ Fujita M, Otsuka Y, Yamada S, Iwakawa M, Imai T. X-ray irradiation and Rho-kinase inhibitor additively induce invasiveness of the cells of the pancreatic cancer line, MIAPaCa-2, which exhibits mesenchymal and amoeboid motility. Cancer Sci 2011; 102: 792–798.

［21］ Imadome K, Iwakawa M, Nojiri K et al. Upregulation of stress-response genes with cell cycle arrest induced by carbon ion irradiation in multiple murine tumors models. Cancer Biol Ther 2008; **7**: 208–217.

［22］ Albini AY, Iwamoto H, Kleinman KG et al. A rapid in vitro assay for quantitating the invasive potential of tumor cells. Cancer Res 1987; 47: 3239–3245.

［23］ Kaneshiro ES, Wyder MA, Wu YP, Cushion MT. Reliability of calcein acetoxy methyl ester and ethidium homodimer or propidium iodide for viability assessment of microbes. J Microbiol Methods 1993; 17: 1–16.

［24］ Deshet N, Lupu-Meiri M, Espinoza I et al. Plasminogen-induced aggregation of PANC-1 cells requires conversion to plasmin and is inhibited by endogenous plasminogen activator inhibitor-1. J Cell Physiol 2008; 216:632–639.

［25］ Fujita M, Otsuka Y, Imadome K, Endo S, Yamada S, Imai T. Carbon-ion radiation enhances migration ability and invasiveness of the pancreatic cancer cell, PANC-1, *in vitro*. Cancer Sci 2012; 103: 677–683.

［26］ Pinner S, Sahai E. PDK1 regulates cancer cell motility by antagonizing inhibition of ROCK1 by RhoE. Nat Cell Biol 2008; 10: 127–137.

［27］ Friedl P, Wolf K. Plasticity of cell migration: a multiscale tuning model. J Cell Biol 2010; 188: 11–19.

［28］ Liu S, Goldstein RH, Scepansky EM, Rosenblatt M. Inhibition of rho- associated kinase signaling prevents breast cancer metastasis to human bone. Cancer Res 2009; 69: 8742–8751.

［29］ Micuda S, Ro¨sel D, Ryska A, Brabek J. ROCK inhibitors as emerging therapeutic candidates for sarcomas. Curr Cancer Drug Targets 2010; 10: 127–134.

［30］ Wyckoff JB, Pinner SE, Gschmeissner S, Condeelis JS, Sahai E. ROCK- and myosin-dependent matrix deformation enables protease-independent tumor- cell invasion in vivo. Curr Biol 2006; 16: 1515–1523.

The Oxygen Effect in Carbon Ion Radiotherapy

Ryoichi Hirayama[1], Akiko Uzawa[1], Yoshitaka Matsumoto[1], Yumiko Kaneko[2], Masakuni Ozaki[1], Kei Yamashita[1], Huizi Li[1], Yoshiya Furusawa[1,2]

[1]*Research Center for Charged Particle Therapy,* [2]*International Open Laboratory, National Institute of Radiological Sciences, Chiba, Japan*

e-mail address:hirayama@nirs.go.jp

Abstract

We measured the RBE (relative biological effectiveness) and OER (oxygen enhancement ratio) and evaluated their correlations with the cell survival within implanted solid tumors following exposure to 290 MeV/nucleon clinical carbon-ion beams. SCCVII (squamous cell carcinoma) cells were transplanted into the right hind legs of syngeneic C3H/He male mice. Irradiation with either carbon-ion beams with a 6-cm spread-out Bragg peak (SOBP) or X-rays was delivered to tumors 5mm or smaller diameter. We used two different oxygen conditions for the irradiated tumors. Hypoxic or normoxic conditions in tumors were produced by clamping the leg to stop the blood flow or by leaving the leg clamped. After irradiation, single-cell suspensions were prepared from excised and trypsinized tumors, and were used for *in vivo-in vitro* colony formation assays to obtain cell survival curves. The OER value was 1.87 after X-irradiation. The OER values (1.20 ~ 1.52) of carbon-ion irradiated samples were smaller than those of X-ray irradiated samples. However, no significant changes of the OER at the proximal, middle or distal positions within the SOBP carbon-ion beams were observed. To conclude, we found that the OER values changed little with increasing LET within the SOBP carbon-ion beams. Therefore, the OERs within the SOBP carbon-ion beams can be considered to be constant values in the patient treatment plan.

Introduction

The Heavy Ion Medical Accelerator in Chiba (HIMAC) was constructed at the National Institute of Radiological Sciences (NIRS), Chiba, Japan in 1993 to perform advanced radiotherapy. Clinical trials were started using carbon ions in June, 1994. A total of 7,339 patients had been treated with HIMAC carbon ions by March, 2013. Carbon ions are superior to photon radiation, such as X-rays, in two major points: the physical and the biological characteristics for cancer treatment [1, 2]. For example, carbon ions show a larger RBE (relative biological effectiveness) and a smaller OER (oxygen enhancement ratio) for DNA damage and cell killing than X-rays [2-13].

Exposure of mammalian cells to ionizing radiation leads to a large number of different types of DNA damage, such as base damage, single-strand breaks (SSB) and double-strand breaks (DSB). Most of the DNA damage is repaired by biological processes, but a small fraction is not. In the case of DSB, they are mainly repaired via homologous recombination (HR) or nonhomologous end joining (NHEJ) [14-17]. It is generally believed that the majority of the non-reparable damage is SSB with DSB, such as multiple or clustered lesions [18-22], while the SSBs are considered to be faithfully repaired [23]. However, the actual fraction of non-reparable DSBs is not known, and non-reparable DNA damage/lesions could be an important factor related to the RBE and OER of cell lethality.

The radiation resistance of a cell under low oxygen conditions is critical to cancer treatment, and therefore

clarifying the mechanisms underlying of the oxygen effect is important. Three major relationships between the OER for cell lethality and linear energy transfer (LET) have become obvious; 1) the OER for cell lethality decreases with increasing LET, 2) the OER-LET spectrum is not usually dependent on the cell types, and tends to shift to the high LET side by increasing the particle charge Z and 3) the oxygen effect is almost lost at a LET of 300 keV/μm or higher [10, 24].

There is general agreement that oxygen acts via the information of free radicals. In a word, radio-chemical reactions are generally believed to be the fundamental mechanisms underlying the oxygen effects [25, 26]. In particular, the OH radical-mediated indirect actions to induce DNA base damage are important for low LET radiation [27]. Oxygen is useful for the fixation of DNA damage [28, 29].

In this report, we measured the OER for cell lethality *in vivo* after X-ray or clinical carbon-ion beams (6-cm SOBP carbon ions) irradiation.

Methods and Materials

1. Mice and cancer cells

The squamous cell carcinoma (SCCVII) cells derived from C3H/HeMsNrsf mice were cultured *in vitro* in Eagle's minimum essential medium (SIGMA) supplemented with 15% heat-inactivated fetal bovine serum under humidified air with 5% CO_2 at 37°C. Male C3H mice (8-10 weeks of age) were used in this study, and were produced and maintained in specific pathogen-free (SPF) facilities. Tumor cells (1.0×10^6 cells/10 μl) were transplanted intramuscularly into the right hind legs of syngeneic mice five days before the irradiation. Irradiation sessions were performed when the tumor diameters were 5 mm or less [5]. All animal experiments were carried out in accordance with the Guidelines for Animal Experimentation at NIRS, Chiba, Japan.

2. Irradiation

Carbon ions ($^{12}C^{6+}$) were accelerated by the HIMAC synchrotron to 290 MeV/nucleon. Irradiation was conducted using horizontal carbon beams with a dose rate of ~4 Gy/min. Three different LET values of the carbon ions in a 6-cm spread-out Bragg peak (SOBP) were generated by selecting the depth along the irradiation path using a polymethyl methacrylate (PMMA) range shifter (93.35, 114.28 and 136.34 mmH_2O). We chose both low and high LET points in the SOBP beam (Fig. 1).

Dose-averaged LETs were set to deliver 46, 50 and 80 keV/μm at the proximal and distal portions of the SOBP, respectively. X-ray irradiations were performed using an X-ray generator (Shimadzu, Pantac HF-320S) operating at 200 kV, and 20 mA, with a filter of 0.5 mm aluminum and 0.5 mm copper at a dose rate of ~4 Gy/min.

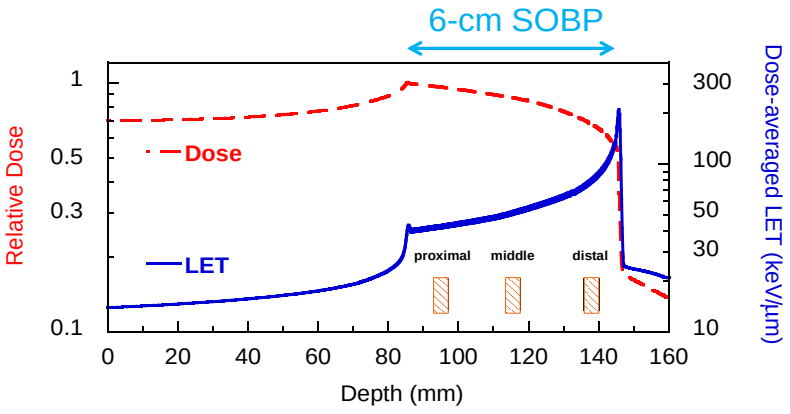

Fig. 1. The distributions of the relative dose and dose-averaged LET curves measured in water.

3. Assessment of the clonogenic cell survival by an *in vitro-in vivo* colony formation assay

The survival of SCCVII cells was measured in mice using an *in vitro-in vivo* colony formation assay method immediately after irradiation [4]. To aid in immobilizing mice on a board, Nembutal solution at 5 mg/ml was intraperitoneally injected at 0.1 ml/10 g body weight 20 min before the start of irradiation. The tumors in the legs

were made totally hypoxic by clamping them on the proximal side of the tumor for 15 minutes before and during irradiation (hypoxic condition) [30, 31]. Clamped or non-clamped (normoxic condition) tumor-bearing mice were sacrificed by cervical dislocation immediately after irradiation, and the whole bodies of the sacrificed mice were rapidly cooled in ice-water, and then the tumors were excised. We summarized the flow of the experiments in Fig. 2. In brief, tumors were excised, minced and disaggregated by stirring for 20 min at 37ºC in PBS containing 0.25% trypsin. Appropriate numbers of tumor cells from the single-cell suspensions resulting from three different irradiated conditions were seeded in triplicate into 60- or 100-mm-diameter culture dishes at densities to give approximately 100 colonies per dish. After 11 days of incubation, the colonies were fixed with 10% formalin and stained with 1% methylene blue in water. Colonies consisting of more than 50 surviving cells were scored. The RBE and OER were calculated using the following equations:

$$RBE_{normoxic} = D_{10} \text{ for Carbon ions, } {}_{(normoxic)}/D_{10} \text{ for X-rays, } {}_{(normoxic)} \quad (1)$$

$$RBE_{hypoxic} = D_{10} \text{ for Carbon ions, } {}_{(hypoxic)}/D_{10} \text{ for X-rays, } {}_{(hypoxic)} \quad (2)$$

$$OER = D_{10} \text{ under hypoxic}/D_{10} \text{ under normoxic} \quad (3)$$

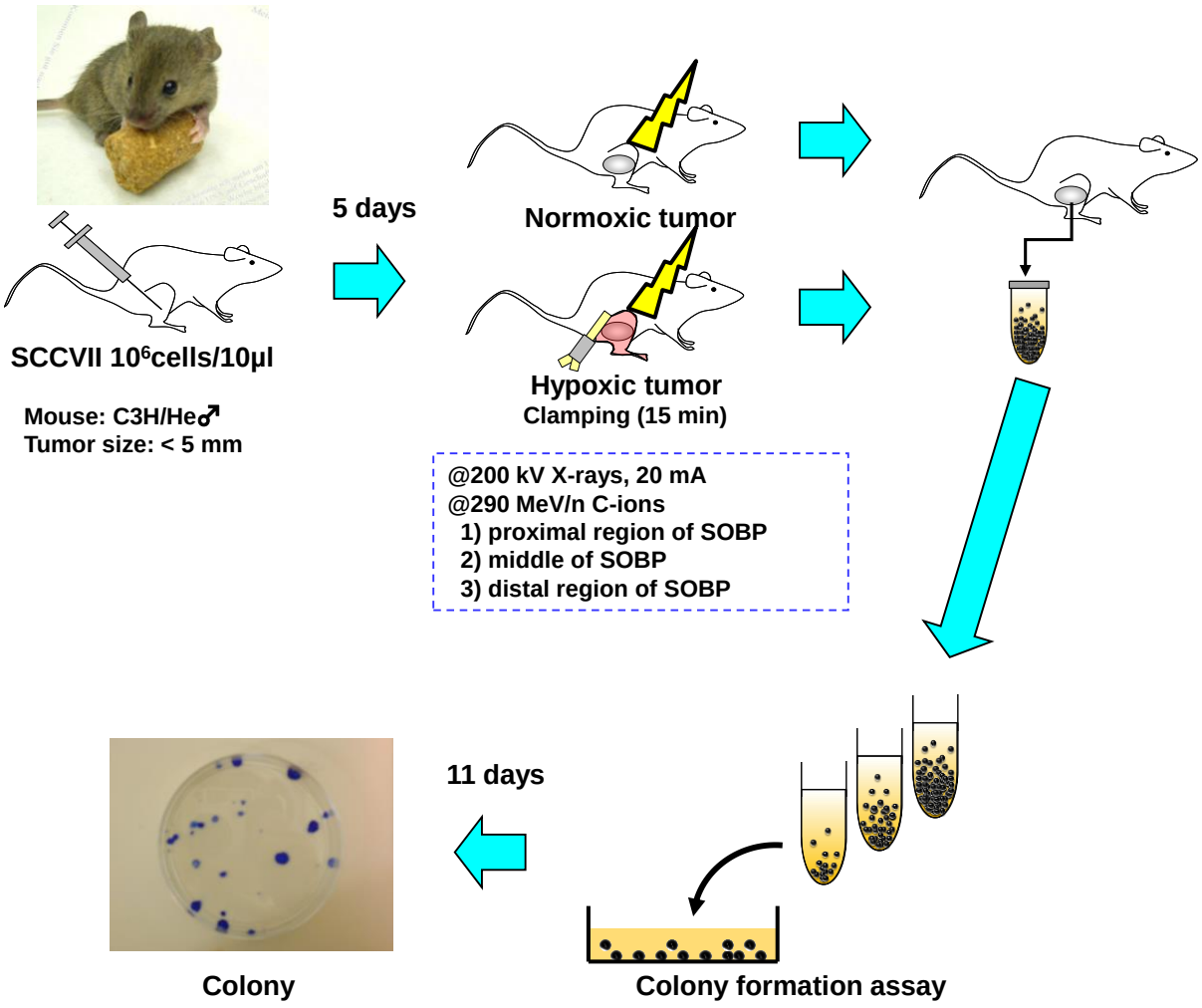

Fig. 2. A flow chart of the experiment

4. Hypoxic fraction assessment

The paired survival curve method [32] was used to assess the hypoxic fraction in SCCVII tumors. In brief, survival curves were determined for tumor cells under non-clamped (normoxic condition) and clamped (hypoxic

condition) tumors, and the hypoxic fraction was evaluated by a comparison of these survival curves. Clamping the blood supply to the tumor produced the hypoxic condition. After irradiation, tumors were excised from the mouse legs and the tumor cells were suspended and assayed using the *in vitro-in vivo* colony formation assay. The survival data under hypoxic and normoxic conditions were fitted by the equations:

$$SF_h = m_h \cdot \exp(-\alpha_h \cdot D) \quad (4)$$

$$SF_n = m_n \cdot \exp(-\alpha_n \cdot D) \quad (5)$$

where SF_h, m_h and α_h (Gy^{-1}) are the survival parameters under hypoxic conditions and SF_n, m_n and α_n (Gy^{-1}) are the survival parameters under normoxic conditions, respectively. If we assume that hypoxic and normoxic curves become parallel ($\alpha_h = \alpha_n$), the hypoxic fraction (HF) can be estimated by the equation:

$$\log(HF) = \log(m_n) - \log(m_h) \quad (6)$$

2.5. Statistical analysis

The values represented the mean and standard error (mean ± SE) of three or more independent experiments. The differences between groups were determined by Student's t-test or the Kruskal-Wallis test.

Results

1. Tumor cell survival

We first examined the dose-response curve of SCCVII cell survival after exposure toX-rays and carbon-ion beams in the two different oxygen states. The plating efficiencies of hypoxic and normoxic tumors were 0.45 ± 0.04 and 0.44 ± 0.05, respectively. Therefore, the plating efficiencies were not affected by the different oxygen conditions ($P > 0.1$, by the Kruskal-Wallis test). Carbon-ion beams with an LET at 80 keV/μm showed the highest radiosensitivities in all positions. We observed that all survival curves had shoulders, whereas the curves for X-rays showed a curvature for high doses, indicating a more radioresistant subgroup of cells. The RBE values of carbon ions in the two different oxygen conditions (hypoxic and normoxic) increased with increasing LET values (Figs. 3A and B). The maximum RBE values were 2.23 under hypoxic and 1.76 under normoxic conditions in several positions within the SOBP carbon-ion beams, respectively. The RBE values under hypoxic conditions were larger than those under normoxic conditions in the SOBP beams. The OER values were also calculated based on the D_{10} values, and the OER values of carbon ions were smaller than those of X-rays. However, the OER values of carbon ions showed no significant changes ($P > 0.3$, by the t-test) at three positions within the SOBP beams (Fig. 3C).

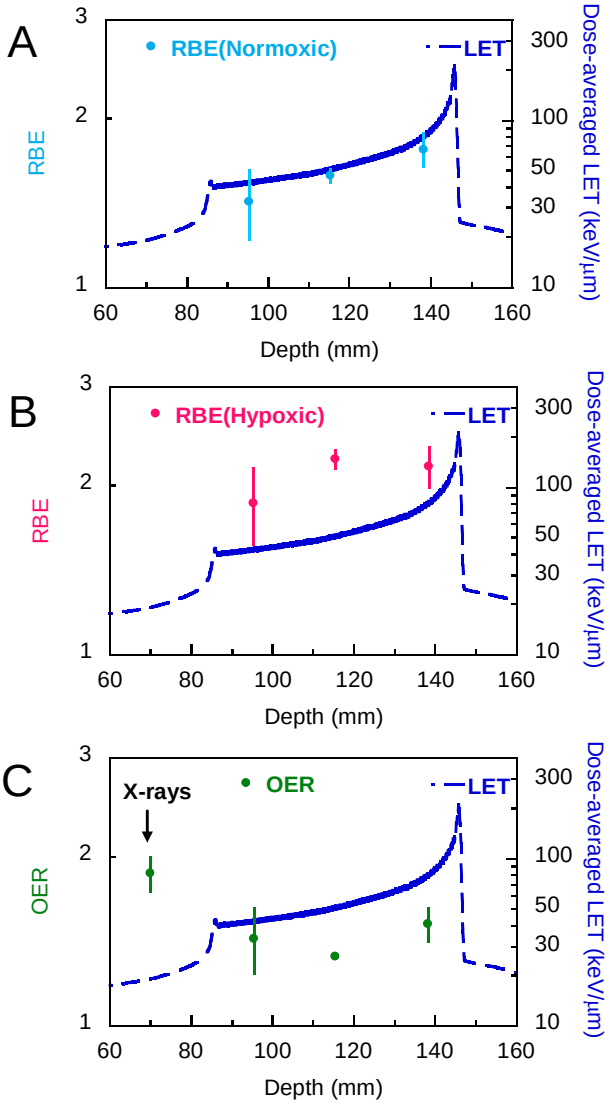

Fig. 3. The RBE under normoxic (A) and hypoxic (B) and the OER (C) in several positions within the SOBP carbon-ion beams.

2. Hypoxic fraction

The survival curve assay, survival curves for the hypoxic and normoxic tumors irradiated with X-rays are shown in Fig. 4. The hypoxic fraction in normoxic tumor was found to be 10 ± 3% from equation (6). The radio-resistance of the tumors to X-rays may be partly explained by the presence of hypoxic cells in the SCCVII tumor samples.

Discussion

The RBE values for previous *in vivo* [33-41] and *in vitro* [40-42] experiments increased with increasing LET values within the SOBP of the carbon-ion beams. Our data also showed a similar trend (Figs. 3A and B). Utilizing the enhanced biological effectiveness of carbon-ion beams, carbon-ion therapy has yielded significant therapeutic benefits. We found that the calculated RBE values for hypoxic cells from clamped tumors were the highest in comparison to the other conditions tested. This trend has also been reported by other researchers [8-10, 43]. The reason for this could be that a large RBE value is dependent on the spatial and temporal distributions of energy deposited from accelerated carbon ions. Additionally, we found that hypoxia-induced radioresistance to X-rays can be overcome by carbon-ion beams. In the case of X-rays, the calculated OER value was 1.87 ± 0.13 in the present study. The OER values of carbon-ion beams were smaller than the OER for *in vitro* experiments. This finding concurred with a previous report [44]. One of the reasons is that a small normoxic tumor always contains a few hypoxic cells. In fact, the normoxic tumors (< 5 mm diameter) contained approximately 10% hypoxic cells (Fig. 4). In other words, the cells in the normoxic tumors are not in an entirely oxygenated condition. Furthermore, the immobilization of mice on the board and use of anesthesia might raise the hypoxic fraction [45, 46].

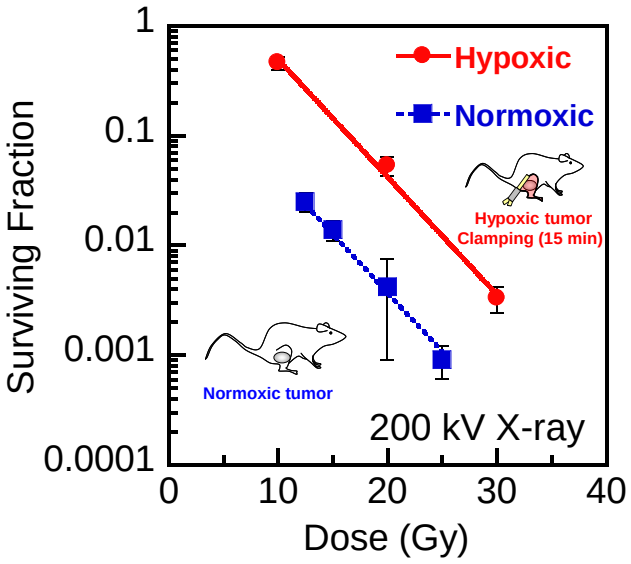

Fig. 4. The paired survival curves for clamped (hypoxic) and non-clamped (normoxic) tumors irradiated with 200 kV X-rays.

The OER values for carbon-ion beams showed no significant change in the SOBP (Fig. 3C). In previously published *in vitro* studies, the OER values for low-LET radiation were ~3. With an increasing LET value there was a decrease in the OER values starting at around 50 keV/μm and falling below 2 at around 100 keV/μm [10, 24, 43, 44]. The OER values for previously published *in vivo* experiments in the low-LET region were ~2, and with increasing LET, the OER values gradually decreased to around 1.5 at around 100 keV/μm [31, 44, 47, 48]. The LET-dependent changes in the OER values for the previously published *in vivo* experiments were small, and our data agree with those in the previous studies.

Conclusion

In this study, we found that the RBE values for cell survival increased with increasing LET values, and that the OER values changed little with increasing LET within the SOBP carbon-ion beams. Therefore, the OERs within the SOBP carbon-ion beams can be considered to be constant values in the patient treatment plan.

References

[1] Chen GT, Castro JR, Quivey JM. Heavy charged particle radiotherapy. Annu Rev Biophys Bioeng. 1981;10: 499-529.

[2] Durante M, Loeffler JS. Charged particles in radiation oncology. Nat Rev Clin Oncol. 2010;7(1): 37-43.

[3] Tinganelli W, Ma NY, Von Neubeck C, et al. Influence of acute hypoxia and radiation quality on cell survival. J Radiat Res. 2013;54 Suppl 1: i23-30

[4] Hirayama R, Uzawa A, Takase N, et al. Evaluation of SCCVII tumor cell survival in clamped and non-clamped solid tumors exposed to carbon-ion beams in comparison to X-rays. Mutat Res. 2013;30;756(1-2): 146-151.

[5] Hirayama R, Uzawa A, Matsumoto Y, et al. Induction of DNA DSB and its rejoining in clamped and non-clamped tumours after exposure to carbon ion beams in comparison to X rays. Radiat Prot Dosimetry. 2011;143(2-4): 508-512.

[6] Usami N, Kobayashi K, Hirayama R, et al. Comparison of DNA breaks at entrance channel and Bragg peak induced by fast C6+ ions--influence of the addition of platinum atoms on DNA. J Radiat Res. 2010;51(1): 21-26.

[7] Ma NY, Tinganelli W, Maier A, et al. Influence of chronic hypoxia and radiation quality on cell survival. J Radiat Res. 2013;54 Suppl 1: i13-22.

[8] Hirayama R, Furusawa Y, Fukawa T, et al. Repair kinetics of DNA-DSB induced by X-rays or carbon ions under oxic and hypoxic conditions. J Radiat Res. 2005;46(3): 325-332.

[9] Staab A, Zukowski D, Walenta S, et al. Response of Chinese hamster v79 multicellular spheroids exposed to high-energy carbon ions. Radiat Res. 2004;161(2):219-227.

[10] Furusawa Y, Fukutsu K, Aoki M, et al. Inactivation of aerobic and hypoxic cells from three different cell lines by accelerated (3)He-, (12)C- and (20)Ne-ion beams. Radiat Res. 2000;154(5): 485-496. Erratum in: Radiat Res. 2012;177(1): 129-131.

[11] Blakely EA. Cell inactivation by heavy charged particles. Radiat Environ Biophys. 1992;31(3): 181-196.

[12] Roots R, Yang TC, Craise L, et al. Rejoining capacity of DNA breaks induced by accelerated carbon and neon ions in the spread Bragg peak. Int J Radiat Biol Relat Stud Phys Chem Med. 1980;38(2): 203-210.

[13] Roots R, Yang TC, Craise L, et al. Impaired repair capacity of DNA breaks induced in mammalian cellular DNA by accelerated heavy ions. Radiat Res. 1979;78(1): 38-49.

[14] Ma L, Kazama Y, Inoue H, et al. The type of mutations induced by carbon-ion-beam irradiation of the filamentous fungus Neurospora crassa. Fungal Biol. 2013;117(4): 227-238.

[15] Taleei R, Nikjoo H. The non-homologous end-joining (NHEJ) pathway for the repair of DNA double-strand breaks: I. A mathematical model. Radiat Res. 2013;179(5): 530-539.

[16] Lan L, Ui A, Nakajima S, et al. The ACF1 complex is required for DNA double-strand break repair in human cells. Mol Cell. 2010;40(6): 976-987.

[17] Iijima K, Ohara M, Seki R, et al. Dancing on damaged chromatin: functions of ATM and the .RAD50/MRE11/NBS1 complex in cellular responses to DNA damage. J Radiat Res. 2008;49(5): 451-464.

[18] Frankenburg-Schwager M, Harbich R, Beckonert S, et al. Half-life values for DNA double-strand break rejoining in yeast can vary by more than an order of magnitude depending on the irradiation conditions. Int J Radiat Biol. 1994;66(5): 543-547.

[19] Frankenberg-Schwager M, Frankenberg D, Harbich R, et al. Evidence against the "oxygen-in-the-track" hypothesis as an explanation for the radiobiological low oxygen enhancement ratio at high linear energy transfer radiation. Radiat Environ Biophys. 1994;33(1): 1-8.

[20] Lobrich M, Rydberg B, Cooper PK. Repair of x-ray-induced DNA double-strand breaks in specific Not I restriction fragments in human fibroblasts: joining of correct and incorrect ends. Proc Natl Acad Sci 1995;92(26): 12050-12054.

[21] Dahm-Daphi J, Dikomey E. Rejoining of DNA double-strand breaks in X-irradiated CHO cells studied by constant- and graded-field gel electrophoresis. Int J Radiat Biol. 1996;69(5): 615-621.

[22] Baumstark-Khan C, Heilmann J, Rink H. Induction and repair of DNA strand breaks in bovine lens epithelial cells after high LET irradiation. Adv Space Res 2003;31(6): 1583-1591.

[23] Sakai K, Suzuki S, Nakamura N, et al. Induction and subsequent repair of DNA damage by fast neutrons in cultured mammalian cells. Radiat Res. 1987;110(3): 311-320.

[24] Blakely EA, Tobias CA, Smith KC, et al. Inactivation of human kidney cells by high-energy monoenergetic heavy-ion beams. Radiat Res. 1979;80(1): 122-160.

[25] Alper T. The Modification of damage caused by primary ionization of biological targets. Radiat Res. 1956;5(6): 122-160.

[26] Sonntag Cv. DNA and double-stranded oligonucleotides: The ‘oxygen effect’, chemical repair and sensitization. In: Schreck S editor. Free-Radical-Induced DNA Damage and Its Repair. 1st edition, Heidelberg: Springer, 2006;432-442.

[27] Hirayama R, Furusawa Y, Murayama C et al. LET dependence of the formation of oxidative damage 8-hydroxy-2’-deoxyguanosine (8-OHdG) in 2’-deoxyguanine aqueous solution irradiated with heavy ions. Radiat Phys Chem. 2009;78(12): 1207-1210.

[28] Chapman JD, Reuvers AP, Borsa J, et al. Chemical radioprotection and radiosensitization of mammalian cells growing in vitro. Radiat Res. 2012;178(2): AV214-22.

[29] Millar BC, Sapora O, Fielden EM, et al. The application of rapid-lysis techniques in radiobiology. IV. The effect of glycerol and DMSO on Chinese hamster cell survival and DNA single-strand break production. Radiat Res. 1981;86(3): 506-514.

[30] Masunaga S, Ono K. Significance of the response of quiescent cell populations within solid tumors in cancer therapy. J Radiat Res. 2002;43(1): 11-25.

[31] Ando K, Koike S, Ohira C, et al. Accelerated reoxygenation of a murine fibrosarcoma after carbon-ion radiation. Int J Radiat Biol. 1999;75(4): 505-512.

[32] Moulder JE, Rockwell S. Hypoxic fractions of solid tumors: experimental techniques, methods of analysis, and a survey of existing data. Int J Radiat Oncol Biol Phys. 1984;10(5): 695-712.

[33] Ando K, Koike S, Nojima K, et al. Mouse skin reactions following fractionated irradiation with carbon ions. Int J Radiat Biol. 1998;74(1): 129-138.

[34] Koike S, Ando K, Oohira C, et al. Relative biological effectiveness of 290 MeV/u carbon ions for the growth delay of a radioresistant murine fibrosarcoma. J Radiat Res. 2002;43(3): 247-255.

[35] Koike S, Ando K, Uzawa A, et al. Significance of fractionated irradiation for the biological therapeutic gain of carbon ions. Radiat Prot Dosimetry. 2002;99(1-4): 405-408.

[36] Kagawa K, Murakami M, Hishikawa Y, et al. Preclinical biological assessment of proton and carbon ion beams at Hyogo Ion Beam Medical Center. Int J Radiat Oncol Biol Phys. 2002;54(3): 928-938.

[37] Gueulette J, Octave-Prignot M, De Costera BM, et al. Intestinal crypt regeneration in mice: a biological system for quality assurance in non-conventional radiation therapy. Radiother Oncol. 2004;73 Suppl 2: S148-S154.

[38] Uzawa A, Ando K, Furusawa Y, et al. Biological intercomparison using gut crypt survivals for proton and carbon-ion beams. J Radiat Res. 2007;48 Suppl.A: A75-A80.

［39］ Masunaga S, Ando K, Uzawa A, et al. The radiosensitivity of total and quiescent cell populations in solid tumors to 290 MeV/u carbon ion beam irradiation in vivo. Acta Oncol. 2008;47(6): 1087-1093.
［40］ Uzawa A, Ando K, Koike S, et al. Comparison of biological effectiveness of carbon-ion beams in Japan and Germany. Int J Radiat Oncol Biol Phys. 2009;73(5): 1545-1551.
［41］ Ando K, Kase Y. Biological characteristics of carbon-ion therapy. Int J Radiat Biol. 2009;85(9): 715-28.
［42］ Frese MC, Yu VK, Stewart RD, et al. A mechanism-based approach to predict the relative biological effectiveness of protons and carbon ions in radiation therapy. Int J Radiat Oncol Biol Phys. 2012;83(1): 442-450.
［43］ Weyrather WK, Kraft G. RBE of carbon ions: experimental data and the strategy of RBE calculation for treatment planning. Radiother Oncol. 2004;73 Suppl 2: S161-169.
［44］ Wenzl T, Wilkens JJ. Modelling of the oxygen enhancement ratio for ion beam radiation therapy. Phys Med Biol. 2011;56(11): 3251-3268.
［45］ Ando K, Koike S, Fukuda N, et al. Independent effect of a mixed-beam regimen of fast neutrons and gamma rays on a murine fibrosarcoma. Radiat Res. 1984;98(1): 96-106.
［46］ Cullen BM, Walker HC. The effect of several different anaesthetics on the blood pressure and heart rate of the mouse and on the radiation response of the mouse sarcoma RIF-1. Int J Radiat Biol Relat Stud Phys Chem Med. 1985;48(5): 761-71.
［47］ Masunaga S, Hirayama R, Uzawa A, et al. The effect of post-irradiation tumor oxygenation status on recovery from radiation-induced damage in vivo: with reference to that in quiescent cell populations. J Cancer Res Clin Oncol. 2009;135(8): 1109-1116.
［48］ Masunaga S, Hirayama R, Uzawa A, et al. Influence of manipulating hypoxia in solid tumors on the radiation dose-rate effect in vivo, with reference to that in the quiescent cell population. Jpn J Radiol. 2010;28(2):132-142.

Session 3: Present Status at Med-Austron & European Networks

The Actual Status of MedAustron

Ulrike Mock, Ramona Mayer

EBG MedAustron Ltd., Wiener Neustadt, Austria
Corresponding Author: Ulrike Mock,
e-mail address: ulrike.mock@medaustron.at

Abstract:

The MedAustron ion beam center of treatment and research in Wiener Neustadt, Austria will be the fourth facility worldwide equipped with dual beams offering protons and carbon ions under the same technical conditions. The company EBG MedAustron GmbH has the overall responsibility for the construction and operation of the MedAustron center. Realization of the particle accelerator facility, based on a synchrotron for the delivery of protons and carbon ions, is realized in cooperation with the European Organization for Nuclear Research (CERN). The construction of the building was completed in October 2012 and installation of the synchrotron and the technical infrastructure is currently ongoing. MedAustron will consist of three medical treatment rooms with different beam arrangements. One room is equipped with a horizontal fixed beam, one room with a horizontal and vertical fixed beam. In both rooms irradiation with protons or carbon ions is possible. In the third medical treatment room a proton gantry will be installed. In addition to this a fourth irradiation room offers the possibility for non-clinical research activities in the fields of experimental- or medical physics and radiobiology. According to the time schedule the next two years are dedicated to physical and medical commission and certification of the facility. Treatment of the first patient is intended by the end of 2015. In the full operational phase MedAustron will be capable to irradiate 1.200-1.400 patients per year. This text illustrates the main components and structures of the MedAustron facility.

Introduction

In Wiener Neustadt the Federal State of Lower Austria is currently building the MedAustron ion beam center of treatment and research through the EBG MedAustron Ltd., which has the overall responsibility for the construction and operation of the facility. The company PEG MedAustron Ltd. is responsible for building up the non-clinical research infrastructure enabling scientific projects related to protons or carbon ions for national or international research institutions.

Technical and functional description of MedAustron

1. Building

Figure 1: The MedAustron ion beam center of treatment and research building

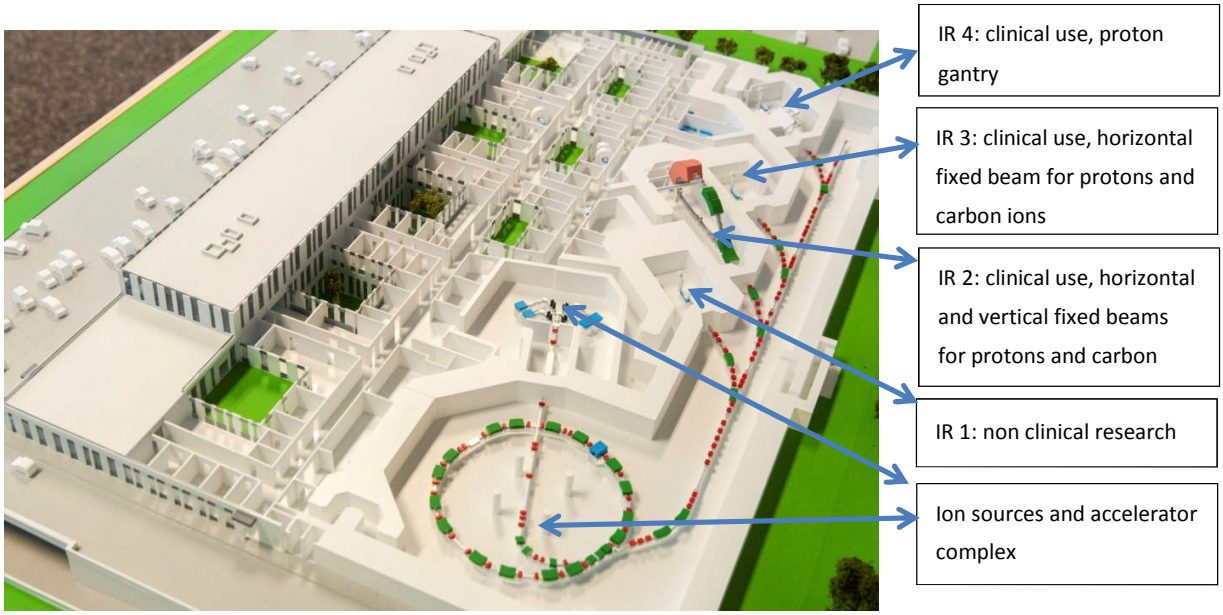

Figure 2: Illustration of the building with regard to the accelerator complex and the different irradiation rooms (IR1-4)

The ground floor consists of all rooms necessary for medical patients` treatment. In addition to this the non-clinical research area and the accelerator unit are on the same floor.

2. The accelerator complex

Main components of the accelerator complex are the injector, the linear accelerator unit, the synchrotron and the extraction lines.

The injector is equipped with three ion sources and the potential to install a fourth source. Two sources serve as the standard configuration for the intended medical applications and therefore consist of one source for protons and

one source for carbon ions. The other two sources function as reserve or can be used for non-clinical research activities on the basis of other ion species. Sources are connected with the drift tube linear accelerator which accelerates the beam up to the required injection energy of the synchrotron. These parts of the accelerator complex have already been installed and tested with regard to technical and physical functionality.

Based on the CERN Proton Ion Medical Machine Study (PIMMS) the synchrotron was designed and technically developed within the Italian CNAO project. For MedAustron this concept was adapted according to needs with regard to proton energy ranges of 60-250 MeV for medical applications and 60-800 MeV for non-clinical research activities. In addition the synchrotron enables carbon ion applications in the range of 120MeV per nucleon to 400 MeV per nucleon.

Installation of the synchrotron will be finished by the end of 2013 and will be followed by a period of commissioning the machine. In order to perform the necessary physical evaluations IR 3 -which will be the first available treatment room for medical applications- is currently equipped with all components and beam testing in this room is supposed to start in spring 2014.

3. Medical Concept

At MedAustron all patients are treated within clinical studies, which enable a variety of clinical research activities. As examples for the intended evaluations comparisons between protons and carbon ions in different tumor entities or the determination of acute and late treatment related side effects can be mentioned but have to be regarded only as a small spectrum of all research options.

Patient treatment in 2015 will start in IR 3, which is equipped with a horizontal beam line. Regarding beam quality, protons will be available in the startup phase. Parallel to the implementation of patient therapy in this room, commissioning of the other two rooms and the carbon ion beams will be processed. In 2016 the second treatment room with a horizontal and a vertical beam line is going to be commissioned. Additionally it is planned to provide carbon ions for patient treatment in the same year.

Based on the availability of beam arrangements patients suffering from tumors of the brain, scull base area and prostate can be regarded as the main initial indications for treatment at MedAustron. Parallel to the operational availability of the other treatment rooms , the number of patients and tumor types will steadily increase.

3. 1 Medical equipment

3.1.1 Medical imaging

With regard to treatment planning in house imaging can be performed using a 64-slice large bore CT, a 3,0 Tesla MRI and ultrasound. CT and MRI have already been ordered and will be installed by the end of 2013. In addition to initial treatment planning, plan modification may become necessary during the treatment course because of variable effects like weight loss, changes in organ filling or changes in tumor shapes due to response. Therefore imaging devices will also be used for adaptive and image guided therapy strategies at MedAustron.

Additionally a PET-CT is installed close to the irradiation room area, enabling measurement of tissue activation caused by beam application during treatment.

3.1.2 Medical beam lines at MedAustron

Within the three irradiation rooms beam line arrangements differ. One room (IR 3) is equipped with a horizontal fixed beam offering protons and carbon ions. In the second room (IR 2) treatment can be applied by using the

horizontal and vertical beams. Treatment can consist of protons and carbon ions. The third room (IR 4) treatment will be provided by using a proton gantry. Casing of this gantry is already in place.
By the end of 2015 patient treatment will start in IR3 using protons. Carbon ion irradiation in this room is supposed to start by the end of 2016.

The second treatment room for medical applications (IR2) will be available in autumn 2016 Initial treatment will be performed using protons, carbon ion applications will start in spring 2017.
Concerning IR4 the installation of the gantry has already started. Nonetheless this room will only be available after starting operation of IR1-3. Consequently irradiation using the proton gantry is supposed to be possible by autumn 2018.
Parallel to the commissioning of the medical treatment rooms, non clinical research activities will be implemented and corresponding projects can start in the non clinical research room (IR1) in spring 2016.

3.1.2. Treatment planning

Beam delivery technology is based on active beam scanning which will be implemented on all beam lines offering a greater flexibility in plan optimization during treatment planning. This superior dose distribution will reduce neutron dose at the patient level significantly.
The treatment planning system is provided by RaySearch and will initially be able to perform dose calculation for photons, electrons and protons. Within an updated version available in 2016 treatment planning based on carbon ions will be possible.

3.1.3 Patient positioning and irradiation rooms

For each medical treatment room there are 2-3 pre-immobilization rooms. This concept enables to optimize the treatment procedure by immobilizing the patients outside the irradiation rooms and transferring them into the irradiation room by shuttles.

At MedAustron patient`s treatment can be performed in three different irradiation rooms. All rooms are equipped with specifically designed treatment tables from BEC. The tables are mounted on the ceiling and table movements along six axes of freedom and another ceiling mounted linear axis are possible. As a consequence a high flexibility in patient positioning with regard to the fixed beams is given. Imaging of the patient is supposed to be performed prior to each treatment session and the corresponding imaging ring for x-rays and cone beam CT is directly fixed at the table and can move along the table axis as needed.

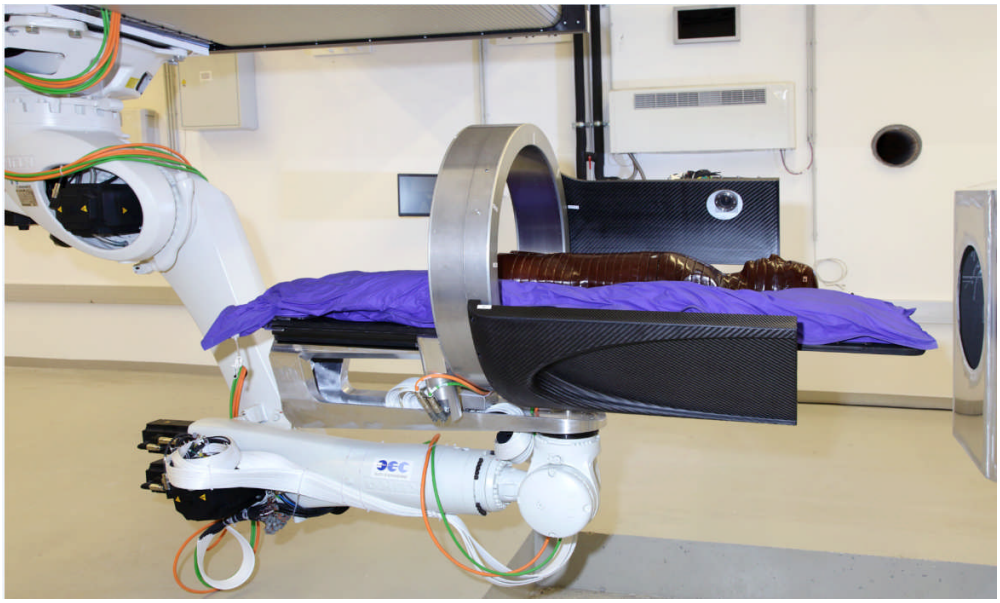

Figure 3: Ceiling mounted treatment table with imaging ring

3.1.4 Personal concept at MedAustron

Implementation of national co-operations with the Austrian University hospitals in Vienna, Graz and Salzburg and other radiotherapy departments is a major concern of MedAustron. As a consequence five physicians and seven physicists in training have been hired as MedAustron employees and are currently trained in different facilities. After becoming specialists in radio-oncology or medical physicists they will continue their work at MedAustron.

Biological Basis of Combined Ion Beam and Chemotherapy

Ira-Ida Skvortsova

Head of Laboratory for Experimental and Translational Research on Radiation Oncology (EXTRO-Lab), Dept. of Therapeutic Radiology and Oncology, Innsbruck Medical University, Innsbruck, Austria
e-mail address: Ira.Skvortsova@i-med.ac.at

Radiation therapy (including ion beam therapy) plays an important role in the management of malignant tumors, however the problem of radiation resistance resulting in tumor recurrences after treatment is still unsolved. Therefore, the improvement of tumor response and clinical outcome after application of radiotherapy is urgently needed. It is generally believed that limited radiation sensitivity leading to the development of tumor relapses could be associated with carcinoma stem cell persistence (CSC) within the tumor (1). CSCs are characterized by their increased capacities to survive and repopulate after exposure to cytotoxic agents and enhanced abilities for metastatic spread (1, 2). Hence, anti-cancer treatment approaches should effectively destroy CSCs in order to avoid disease recurrences. Although it was already shown that carbon ion radiation has superior potential to kill CSCs compared to conventional photon therapy, ion therapy was not able to eliminate all CSCs (3, 4). It is suggested that use of CSC-specific chemotherapeutic agents can successfully eradicate CSCs and improve radiation therapy results.

In recent years, combination of chemotherapy and radiotherapy has become a standard strategy in the treatment of various malignant tumors. Concomitant use of ionizing radiation and chemotherapeutic agents allows to improve local-regional, distant control and survival rates in a number of cancers such as lung, head and neck, esophageal, colo-rectal carcinomas and malignant gliomas. Despite large clinical experience with combined-treatment modalities using photon radiation therapy, little is known about the effective scheduling, dosage and mechanisms of activity when chemotherapeutic drugs are used in combination with ion beam radiation therapy. Furthermore, it is still unknown which chemotherapeutic agents could effectively kill CSCs. In order to know which therapeutic compounds could reveal anti-CSC activity when used alone or in combination with radiotherapy, it is necessary to elucidate intracellular molecular perturbations in CSCs, especially upon treatment with ionising radiation. Analysis of molecular features of CSCs could help to predict aggressive behaviour of malignant tumors, inclination for metastatic spread and limited sensitivity to anti-cancer treatment approaches. Proteomic approach could be widely used to identify proteins associated with activation of CSCs leading to cancer radiation resistance. It is logical to suggest that predicted treatment insensitivity requires consideration of more aggressive ion-beam-based schedules to treat malignant tumors with increased number of CSCs.

Taken together, identification of biomarkers of higher risk of radiation resistance and CSC persistence within the tumor could be effectively used in pre-clinical and clinical settings. Analysis of intracellular/intratumoral signaling pathways that are specifically affected in CSCs could provide additional clinical opportunities to stratify cancer patients to apply different therapeutic approaches. Thus, patients with CSC-related molecular features could be treated using more aggressive therapeutic strategies, such as ion beam therapy in combination with CSC-targeted chemotherapeutics.

Reference List

1 Clevers,H. The cancer stem cell: premises, promises and challenges, Nat.Med., *17:* 313-319, 2011.

2 Kranenburg,O., Emmink,B.L., Knol,J., van Houdt,W.J., Rinkes,I.H. and Jimenez,C.R. Proteomics in studying cancer stem cell biology, Expert.Rev.Proteomics., *9:* 325-336, 2012.

3 Bertrand,G., Maalouf,M., Boivin,A., Battiston-Montagne,P., Beuve,M., Levy,A., Jalade,P., Fournier,C., Ardail,D., Magne,N., Alphonse,G. and Rodriguez-Lafrasse,C. Targeting Head and Neck Cancer Stem Cells to Overcome Resistance to Photon and Carbon Ion Radiation, Stem Cell Rev., 2013.

4 Ogawa,K., Yoshioka,Y., Isohashi,F., Seo,Y., Yoshida,K. and Yamazaki,H. Radiotherapy targeting cancer stem cells: current views and future perspectives, Anticancer Res., *33:* 747-754, 2013.

Ion Beam Therapy Technology Developments at MedAustron

Stanislav Vatnitsky, Ramona Mayer, Bernd Mößlacher.

EBG MedAustron, Wiener Neustadt, Austria
e-mail address:stanislav.vatnitsky@medaustron.at

Abstract

The MedAustron - a centre for ion beam therapy and research - is in establishing phase in Wiener Neustadt, Austria. It is planned to treat first patient at the end of 2015. The development of the equipment, that is installed and will be used at the MedAustron, is performed under co-operations with several industrial and scientific partners. The paper describes the major developments in ion beam therapy technology as an outcome of these co-operations. The MedAustron accelerator facilities based on synchrotron and developed in collaboration with the European Organization for Nuclear Research (CERN) will be used for the delivery of protons and light ions to four irradiation rooms (IR) for cancer treatment as well as for clinical and non-clinical research. All IRs are supplied with the continuous scanning beam delivery systems developed in cooperation with CNAO Foundation. Each irradiation room is equipped with a robotic patient alignment system (PAS) developed in cooperation with B-E-C (Reutlingen, Germany) and medPhoton (Salzburg, Austria). The PAS combines robotic positioner with a sliding imaging ring system (PAIR). The system enables volumetric cone beam computed tomography (CBCT) and also offers 2-D/3-D imaging. The Institute for research and development on advanced radiation technologies (radART) of the Paracelsus Medical University in Salzburg is developing open source software - ORAion suite for the MedAustron. A range of components of this suite will be integrated with the treatment planning software from RaySearch Laboratories, Sweden, that will be used for planning of all treatments with protons and carbon ions as well as for conventional treatments as a back-up.

1. Introduction

The EBG MedAustron GmbH, a publically owned corporation, is establishing a centre for ion beam therapy and research, the MedAustron, in Wiener Neustadt in the county of Lower Austria. It is planned to treat first patient at the end of 2015 and bring the centre to full capacity in 2020. The development of the equipment, that is installed and will be used at the MedAustron, is performed under co-operations with several industrial and scientific partners, where the MedAustron contributed in the preparation of concepts and technical specifications, documents and procedures for acceptance testing and medical commissioning. It is foreseen that the major components of medical equipment will be delivered as medical devices, certified by the correspondent suppliers. After equipment delivery and acceptance the MedAustron will be responsible for its medical commissioning. The paper describes the major developments in ion beam therapy technology as an outcome of these co-operations.

2. The major components of medical equipment at MedAustron

The MedAustron centre comprises an accelerator facility based on a synchrotron for the delivery of protons and light ions to four irradiation rooms (IR) for cancer treatment and for clinical and non-clinical research. The planning and development of the accelerator facilities was performed in collaboration with the European Organization for Nuclear Research (CERN), Geneva. For clinical purposes protons from 60 MeV to 250 MeV

and carbon ions from 120 MeV/u to 400 MeV/u will be used in three irradiation rooms (IR2 - IR4). The separate room – IR1 is dedicated to non-clinical research, where in addition to the protons and carbon ions with energies for clinical use, also protons up to 800 MeV can be used. The first and the third IRs (IR1 and IR3) are equipped with a fixed horizontal beam line for carbon ions and protons. The second IR - IR2 is equipped with a horizontal and a vertical beam line for carbon ions and protons. The fourth IR - IR4 features a proton gantry that allows irradiation from various angles. Collaboration has been established with the Paul Scherrer Institute (PSI), Villigen, to implement the technology of PSI Gantry 2 at MedAustron. Substantial modifications were required for setting up of this device in a clinical environment. The mechanical structures of MedAustron Gantry are already installed and the treatments in this room are planned to start in 2018. All IRs are supplied with the continuous scanning beam delivery systems developed in cooperation with CNAO Foundation. Each irradiation room is equipped with a robotic patient alignment system (PAS) developed in cooperation with B-E-C (Reutlingen, Germany) and medPhoton (Salzburg, Austria). The PAS combines robotic positioner with a sliding imaging ring system (PAIR). The system enables volumetric cone beam computed tomography (CBCT) and also offers 2-D/3-D imaging. The Institute for research and development on advanced radiation technologies (radART) of the Paracelsus Medical University (PMU) in Salzburg is developing open source software - ORAion suite for the MedAustron. A range of components of this suite will be integrated with the treatment planning software from Research Laboratories, Sweden that will be used for planning of all treatments with protons and carbon ions and for the conventional treatments as a back-up.

2.1 Beam delivery systems

All IRs will be supplied with the continuous scanning beam delivery system, that is part of the accelerator facility, which also includes a synchrotron with a control and an energy selection system as well as a beam transport system – MedAustron Particle Therapy Accelerator (MAPTA). MAPTA as a medical device will be certified by MedAustron. The main task of MAPTA is to provide beams of ions with the physical properties to comply the prescription of the treatment plan, ensuring beam switch off in a defined time limit, if those physical properties are outside defined tolerances, providing means for beam switch off in a defined time limit, if any other device or system, which is interfaced to MAPTA, transmits an interlock signal, and providing data needed for treatment records.

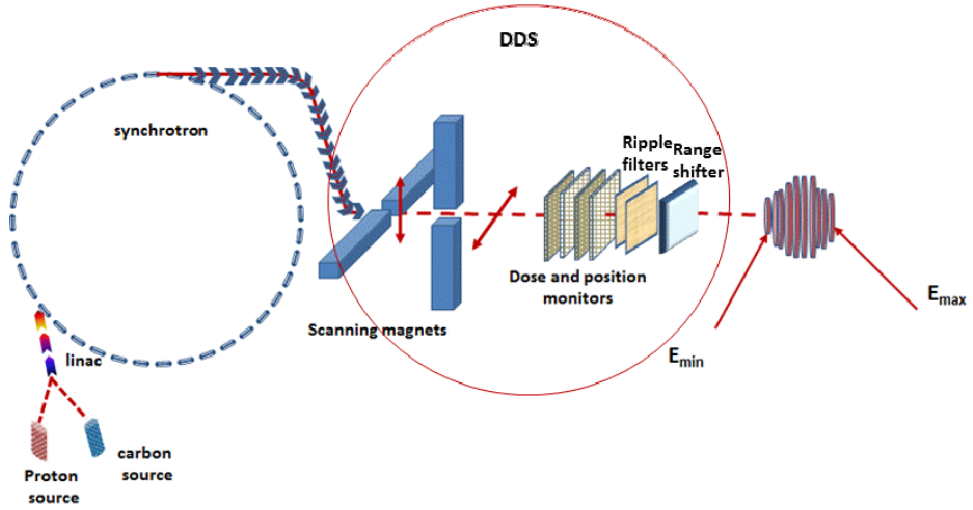

Figure 1. Schematic view of the beam delivery system. Using modulated scanning technique the tumour is divided into several layers and each layer is treated with the correspondent number of spots at the same energy

from E_{min} to E_{max}. Depending on the energy, beams have different characteristics that can be modified by ripple filter and range shifter.

A Medical Front End of MAPTA – dose delivery system (DDS) is developed in cooperation with CNAO Foundation; however, its integration within MAPTA will be done by MedAustron. The first system will be installed at MedAustron in 2014 and commissioned for treatment in 2015. As shown in Figure 1, DDS is the part of MAPTA, which is installed in IR just before the patient. The DDS is managing ion beams for radiation treatments when the modulated scanning mode is used. Using the scanning magnets the DDS steers the beam delivered by the accelerator system in the right position, and by using beam monitoring system it releases the correct amount of energy to the tumour volume. DDS is equipped with range shifter and ripple filters, which modify the longitudinal properties of the ion beam. For treatments using a single beam entry direction, the modulated scanning technique delivers a dose distribution that is more conformal to the proximal surface of the target and more conformal avoidant to the proximal critical structures compared to a passive scattering technique. The most important use of the modulated scanning technique is probably for cases where irregularly shaped target and normal tissues are intertwined and multi-portal optimization can be used to mix the flux and energy of large number of spots coming from different directions [1].

2.2 Patient Alignment System

The major components of the Patient Alignment System (PAS) are the patient positioner (PP), devices to register the patient to the PP, devices to immobilize the patient with respect to the PP, a collision avoidance and detection system (CADS), and the patient localization and verification system that itself consists of x-ray sources, image capture devices, image processing software, and alignment software. A robotic ceiling-mounted PAS that will be installed at MedAustron in all IRs is developed in cooperation with B-E-C (Reutlingen, Germany) and medPhoton (Salzburg, Austria) [1]. The advantage of a ceiling mounted robotic system for patient alignment is that it can offer larger working spaces (figure 2), than pit-mounted PAS.

Figure 2. left: Ceiling mounted robotic PP from B-E-C (Reutlingen, Germany) installed in one of the IR at MedAustron. Right: PAIR installed for testing at MedAustron.

The B-E-C PP uses an industrials robot from KUKA Roboter GmbH, with 7 degrees of freedom, modified to meet the requirements of medical devices. These requirements include reducing the speed of travel and operating in a reasonably slow mode; implementation of teaching modes, i.e. when the user moves the positioner in a specific way and the robot "learns" the path; and finally, implementation of CADS with functional and passive safety features. The PAS combines robotic PP and a sliding Imaging Ring system (PAIR) – Figure 3, which is comprised of an x-ray source independently rotating from the flat panel detector.

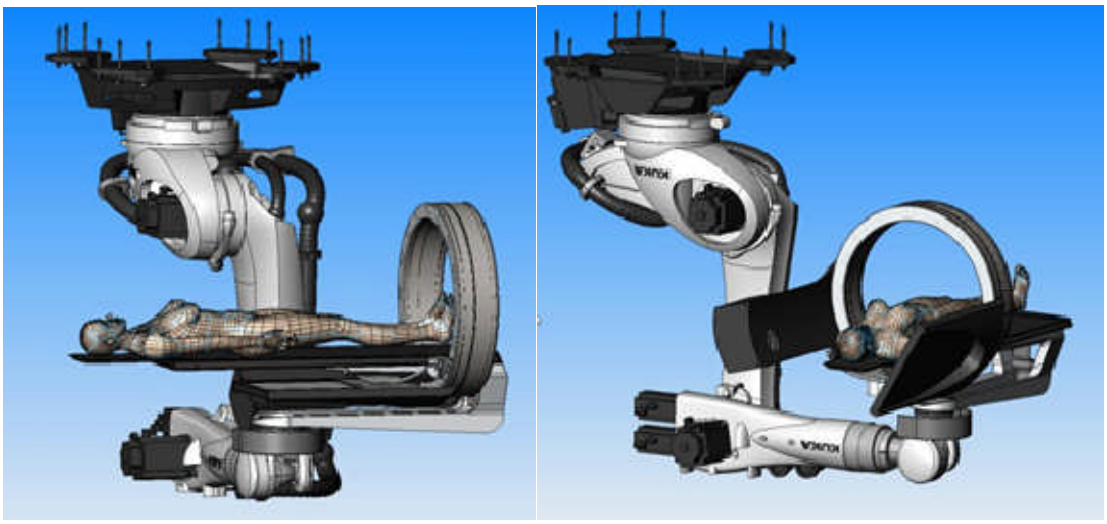

Figure 3: left: In the parking position of the imaging system, the ring is retracted away from the treatment region with the imaging panel and tube stored underneath the table-top. Right: In the imaging position, shown here for treatment of a head, CBCT may be performed for any region of interest inside the ring. In addition, 2D projections may be acquired in any direction perpendicular to the patient axis [1]. Figures courtesy of H. Deutschmann.

The PAIR system enables accelerated volumetric cone beam computed tomography (CBCT with up to 5 rotations/min) and offers ultrafast 2D/3D imaging and registration protocols (maximum frame rate of 30 Hz). The imaging ring is 78 cm in diameter and equivalent to the maximum field of view (FOV) of 78 cm in the central plane, however, the full resolution maximum FOV is limited to 60.5 cm (360° acquisition). Furthermore, the system is capable of dual energy X-ray imaging to improve soft tissue or bone contrast and was developed for 4D tracking applications to allow motion compensation intra-fractionally. During movements, imaging, and irradiation, the system is tracked optically from the floor to compensate for load dependent flex, thus maintaining accurate alignment of the target with respect to the ion beam.

The CADS developed by B-E-C and medPhoton solves in each IR two major tasks. The first task is to provide collision avoidance. This is accomplished by software that models in three dimensions the room environment and then calculates a safe path for the devices to move. The software enables the user to create a representative avatar of the patient. The avatar is computed based of the basic anthropometrical data of each patient. Using configurable catalogue of fixation devices and table-tops, the generated patient setup can be associated with a treatment plan which in turn enables the Record&Verify - system to check the planned patient setup. The CADS must take into account all the current and prescribed setup parameters of different objects (gantry, positioner with patient, imaging devices etc.) and compute the possibility for a collision. The second task is to detect collisions with special touch guards that control the movements and, if a collision is detected, stop further movements.

The developed CADS supports the treatment technology when the patients will be treated non-isocentrically. The nozzles at MedAustron do not have movable snouts that are used at other facilities to control air gap between nozzle and patient surface. Therefore after verification of the planned patient setup,

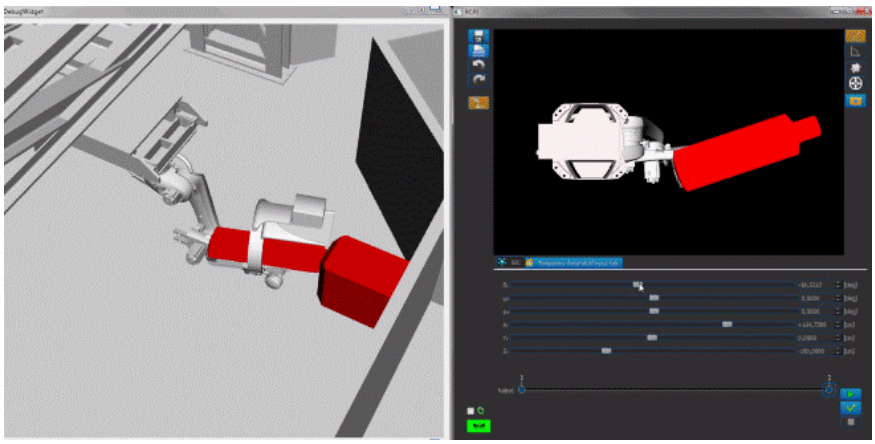

Figure 4. Illustration of collision indication during patient setup with ORAion.
Figure courtesy of P. Steininger

robotic PP will move the patient along beam axis towards the nozzle under CADS control to enable the smallest possible air gap. The CADS will be integrated into the safety system of each IR. The first complete PAS will be installed in 2014 and be commissioned for treatment in 2015.

2.3 Open radART ion suite - ORAion

The Institute for research and development on advanced radiation technologies (radART) of the Paracelsus Medical University (PMU) Salzburg has a scientific collaboration with the EBG MedAustron GmbH in the field of developing, integrating and commissioning an open source software suite for the MedAustron.

The radART institute's software package open-radART ion (ORAion) is furnished with specially developed modules for ion beam therapy process and patient information management at the MedAustron, see Figure 5. Basically, ORAion is designed to be the foremost patient administration system implying all aspects required for efficient patient management in clinical radiotherapy: patient appointment and resource workload scheduling, activity recording for billing, clinical document management, patient and equipment identification management, medical image / structure / treatment plan / treatment record management and archiving, web-services for safe extramural patient data exchange, diagnostic and verification image review as well as tight integration with the treatment planning system (TPS).

The mentioned features related to the Oncology Information System (OIS) component of ORAion are tightly integrated with its modules for patient treatment where the RadioTherapy Software System (RTS²) package constitutes the central component. The RTS² coordinates the treatment workflow by bi-directionally interfacing the irradiation-room-specific ORAion "plugins" (PIs) and "modules" (-Ms): Nozzle Element PlugIn (NEPI), Gantry PlugIn (GAPI), PAIR Robotic Couch PlugIn (RCPI), PAIR Imaging Ring PlugIn (IRPI), X-Ray PlugIn (XRPI), Flat Panel PlugIn (FPPI), 2D/3D Registration Module (REG23-M), Cone Beam CT Module (CBCT-M), etc. An irradiation room's plugins are tied together by an instance of the ORAion Treatment Control System (TCS) which allows the RTS² to communicate with all connected software pieces in a well-coordinated and directed fashion. The RTS² can be considered as workflow manager for all activities in immediate association with the treatment process.

In addition to providing a flexible and configurable TCS-based environment compatible with infrastructure of each MedAustron IRs, ORAion comprises a very specific plugin, the MedAustron PlugIn (MAPI). This is a bi-directionally designed software gate for accessing the MAPTA. Via this port delivery information in the form of machine-specific files and commands are communicated for execution to MedAustron Accelerator Control System (MACS), and simultaneously on-line beam and status information from the accelerator are received. Both collaborating parties, radART and EBG MedAustron, work together on integrating different MAPTA's components and gateways by developing and testing the MedAustron Delivery and Allocation Manager (MADAM) which constitutes the accelerator's medical software frontend towards ORAion's MAPI.

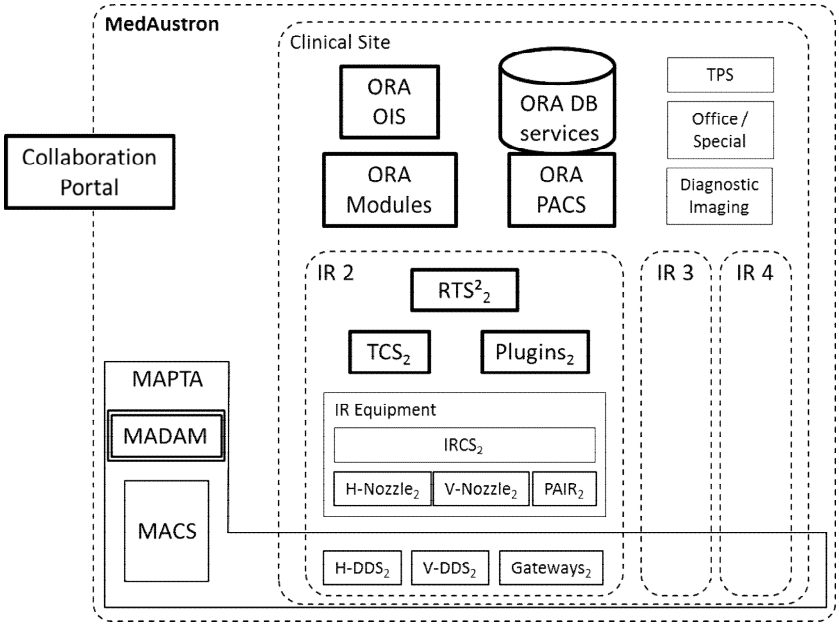

Figure 5. High-level overview of ORAion planned to be installed at MedAustron [2]. Details are in text.

More detailed description of the components of the medical software suite ORAion is presented in the paper by P. Steininger et al. 2013 [2]. The delivery and acceptance testing of the major components of ORAion suite is planned in 2014 and medical commissioning should be completed by the end of 2015.

2.4 Treatment planning support

The RaySearch Laboratories (RSL), Sweden, was selected as provider of the TPS for planning of all treatments at the MedAustron including treatments with protons and carbon ions and also for the conventional treatments as a back-up. This decision was supported by the assurance of RSL to develop and implement in RayStation® new features specific for MedAustron beam delivery system and treatment workflow.

The most important one is the development of carbon planning capability. For carbon treatments RayStation® will allow optimization of biologically effective dose. To develop this functionality, RSL has entered into a license agreement with GSI Helmholtzzentrum für Schwerionenforschung in Darmstadt, Germany (GSI) regarding techniques for calculating radiobiological effective dose in ion beam treatments with Local Effect Model (LEM) where the survival of cells irradiated with ion beams is predicted based on their response to photons. Both the LEM I and LEM IV versions are planned to be implemented. The carbon ion planning module builds on the pencil beam scanning (PBS) functionality for protons. Optimization of PBS uses multi-field optimization, single field uniform dose and distal edge tracking techniques. The PBS module

optimizes spot weights and the scanning pattern for discrete line scanned beams used at MedAustron. Such characteristics of the MedAustron beam delivery system, like dose rate and spot size, will also be subject to optimization.

In addition to PBS algorithm for physical dose calculation RayStation® will use also Monte Carlo, to serve both normal clinical use as well as research needs. Physical dose calculations will include, among other things, tools for robust optimization regarding uncertainties in range (density) and position (isocenter shifts, target shifts etc.). The application of Multi-Criteria Optimization (MCO) to compute a selection of plans from which the planner can chose the most suitable balance between target cover and irradiation of adjacent normal tissue will ensure the development of the optimal plan in the fastest possible time.

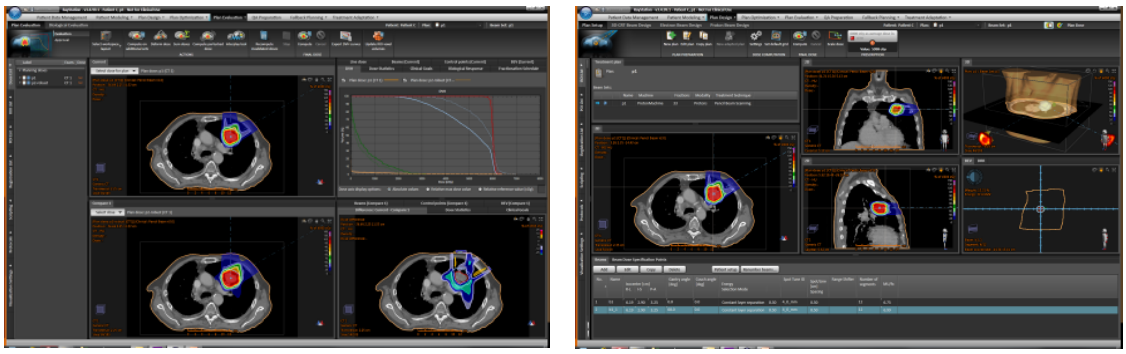

Figure 6. Graphical users interface for proton planning with RayStation®. Figures courtesy of E. Traneus.

A range of medical software components of ORAion will be integrated at MedAustron with the treatment planning software from RSL. These components are related to support as general workflow in data and image management via Picture Archiving and Communication System (PACS)/OIS. MedAustron is also looking forward to implementing RSL scripting capabilities through treatment panning process. Even RayStation® itself supports automation of plan creation, structure definitions, beam placement, etc., scripting will allow for more customization especially in setting up plan verification and QA procedures. The delivery of proton planning RayStation is scheduled in 2014 and proton module will be commissioned for treatment in 2015, while the carbon planning functionality will be delivered in 2015 and will be commissioned for treatment in 2016.

References

［1］ Vatnitsky S. and Moyers M. Radiation therapy with light ions. In: J. Van Dyk editor. The Modern Technology of Radiation Therapy Volume 3. Medical Physics Publishing, Madison Wisconsin, 2013 183-223.

［2］ Steininger P. et al. "The open-radART ion (ORAion) Software Suite" These proceedings, 2013

ENLIGHT Collaboration

Manjit Dosanjh

CERN, Switzerland
e-mail address: Manjit.Dosanjh@cern.ch

The European Network for Research in Light-Ion Hadron Therapy (ENLIGHT) which had its inaugural meeting at CERN in February 2002, was established to coordinate European efforts in using light-ion beams for radiation therapy. Funded by the European Commission (EC) for three years, ENLIGHT has created a multidisciplinary platform, uniting traditionally separate communities so that clinicians, physicists, biologists and engineers with experience in ions could work together with a common goal.

In 2006, a brainstorming amongst clinicians, oncologists, physicists, radiobiologists, information and communication technology experts and engineers—from around 20 European countries—took place at CERN. The community felt that ENLIGHT was a key ingredient for future progress, and therefore should be maintained and broadened, called ENLIGHT++. The aim of ENLIGHT++ network is twofold: to maintain and enlarge the European network of Institution and specialist which work in the field of Light Ion Therapy and to sponsor the research in fields of common interests for the development of the cutting edge and technically advanced clinical facilities.

It provides a common European platform for fostering and co-ordinating collaborations between national research activities related to hadrontherapy, encompassing such various fields as proton and light ion accelerators, detectors, image reconstruction and processing, radiobiology, oncology, and clinical research. ENLIGHT permits a critical mass of physicians, radiobiologists, medical physicists and biomedical engineers from different European countries, involved in the development of hadrontherapy.

Under the umbrella of ENLIGHT, there are currently four EC funded projects:

PARTNER

A Particle Training Network for European Radiotherapy (PARTNER) was established in response to the critical need for reinforcing research in ion therapy and the training of professionals in the rapidly emerging field of hadron therapy. This was an interdisciplinary, multinational initiative, which has the primary goal of training young researchers who will help to improve the overall efficiency of ion therapy in cancer treatment, and promote clinical, biological and technical developments at a pan-European level, for the benefit of all European inhabitants. This need was particular urgent since two particle therapy facilities have become operational in Heidelberg and in Pavia. PARTNER is funded under the Marie Curie-ITN (Initial Training Network) and offers outstanding training opportunities for future careers of the young researchers. For further details see

http://cern.ch/PARTNER

ULICE

This is a 4-year research project which started on 1st September 2009 and is funded by the European Commission for 8.4 millions Euros. This project is coordinated by CNAO (the Italian hadron therapy facility) and involves 21 European institutions. All the existing and planned heavy ion facilities participate together with two physics research centres (CERN and GSI) and two industrial companies (Siemens and IBA). The project is built around three pillars. The first one," Joint Research Activities", is focused on improving the performances of the facilities. It will deal with technical issues such as:

- Design of a lower cost heavy ion rotating gantry, or development of the optimal strategy to cope with organ motion and anatomy changes;
- Creation of a "clinical research infrastructure", i.e. a framework to produce scientifically sound evidence on the efficacy of heavy ion therapy.

The second pillar," Networking Activities", deals with the dissemination of the project results to the wider community of people involved in cancer care.

The last pillar, "Trans-national Access", is lead by HIT and will provide access to external researchers to the existing ion therapy facilities in order to perform their own preclinical research. It will also produce agreed protocols for multi centric clinical trials and will allow external clinical researchers to participate in those trials. This pillar is intended to maximize availability of a scarce resource to all European researchers and will utilize advanced e-science grid technology.

http://cern.ch/ULICE

ENVISION

This is a 4-year project set up by 17 leading European research organisations, including 2 leading European industrial partners (Siemens and IBA), The project started on 1st February 2010, is funded by the EC for 6M Euros and CERN is the project coordinator. ENVISION tackles simultaneously the problems of real-time Dose Monitoring and of performing accurate Quality Assurance tests by developing novel imaging modalities and dose calculation engines that can study the very sharp changes in dose deposition. These tools will allow to better assess the treated volume as well as to derive reliable indicators of the actual delivered dose. The project also focuses on the detection of nuclear reaction products resulting from the interaction of the beam with atomic nuclei of the tissue (positron emitting nuclides for in-beam PET, photons or light charged particles.

http://cern.ch/ENVISION

ENTERVISION

ENTERVISION People ITN project is providing training for 12 Early-Stage Researchers and 4 Experienced Researchers in the field of online Digital Imaging technologies for cancer Hadron radiation therapy. A step-change in online Digital Imaging technology to monitor dose delivery and quality assurance is needed both for conventional X-ray therapy as well as for hadron-radiation treatment (with protons or light-ion beams) of cancer patients. At the same time, whilst the emerging digital imaging field clearly shares common ground with image guided X-ray therapy, the unique properties of hadron beams raises new challenges for training of researchers and exciting opportunities to work on novel hardware applications. Project started in February 2011.

http://cern.ch/ENTERVISION

These and future initiatives involve integrating clinical, biological and technical knowledge as well as training the future generation at a European level, so that hadron therapy becomes widely available for the benefit of all European inhabitants.

ENLIGHT's key vision is the promotion and the optimisation of hadron therapy for cancer treatment at a pan-European level www.cern.ch/ENLIGHT

Acknowledgement:

ENLIGHT only exists because of the community it represents, so I would like to thank all members of the community and PARNTER, ULICE, ENVISION and ENTERVISION consortia, as well as the EC for the funding of these projects

Initiation of an International Ion Therapy Research Board

Richard Pötter[1], Maximilian Schmid[1], Jacques Balosso[2], Michael Baumann[3], Stephanie E. Combs[4], Jürgen Debus[4], Wolfgang Dörr[1], Manjit Dosanjh[5], Piero Fossati[6], Dietmar Georg[1], Jean-Louis Habrand[7], Ramona Mayer[8], Ulrike Mock[8], Roberto Orecchia[6], Guillaume Vogin[9], André Wambersie[10], Thomas Schreiner[11]
On behalf of ULICE Workpackage 2.3 and the International Ion Therapy Research Board

[1]*Department of Radiation Oncology, Comprehensive Cancer Center, Medical University of Vienna, Vienna, Austria*
Währinger Straße 18-20, Vienna, Austria, e-mail address: richard.poetter@akhwien.at
[2]*Grenoble Joseph Fourier University and Etoile, France HADRON*
[3]*Technical University of Dresden*
[4]*Heidelberg University and HIT*
[5]*CERN*
[6]*CNAO and European Institute of Oncology*
[7]*Archade, France HADRON*
[8]*EBG MedAustron*
[9]*Centre Régional de lutte contre le cancer Léon Bérard, Lyon*
[10]*Université Catholique de Louvain, Brussels*
[11]*PEG MedAustron*

Abstract

The experimental nature of carbon ion therapy still requires extensive clinical and translational research which includes biology, medical physics and technology as well as advanced clinical research on diagnosis, prognosis, treatment, oncological outcome, morbidity and quality of life for various forms of malignancies. In regard of the limited number of carbon ion therapy facilities in Europe and worldwide, this can only be successfully realised if joint efforts and appropriate structures between carbon ion therapy centres are initiated, implemented and pursued. The European ULICE FP 7 Research project has recently provided a frame for building up future research infrastructure in this field. In consequence, a first concept based on the comprehensive work of ULICE WP2 could be set up which has included the implementation of an International Ion Therapy Research Board to establish and promote continuous joint scientific and clinical efforts in the field of carbon ion therapy in Europe and worldwide. In this paper background, aims, tasks, tools, composition and first steps of this International Ion Therapy Research Board (IONTREB) are summarized.

Introduction and background

Carbon ion therapy due to its distinct biological characteristics has to be considered as a relatively novel and so far under-investigated therapeutic application in radiation oncology ("new radiation drug") in comparison to photon therapy and even proton therapy. Therefore extensive research requiring phase I-IV trials are necessary to clarify and quantify the clinical gain of carbon ion therapy versus advanced photon beam therapy techniques as well as proton beam therapy, also including advanced clinical research in regard to the scientific progress in the overall diagnostic and therapeutic areas of oncology. However, currently, a very limited number of carbon ion centres is in operation in Europe (n=2) and worldwide (n=5). Taking in addition those centres into consideration which are currently under installation or preparation, the total number will be still very slowly increasing in the near and intermediate future [1]. Consequently, overall and in each centre, only a relatively low number of patients can be expected to be included in clinical carbon ion research activities, thus hindering the scientific evaluation of the clinical outcome [2-3]. This situation appears to be highly problematic – in particular facing the challenges of evidence based medicine [4-6] – for the performance of high quality clinical research and threatens the development and promotion of carbon ion therapy in general, even if specific forms of clinical research in particular for technology assessment may be considered [7-8]. Therefore, joint efforts between European and International carbon ion therapy centres urgently need to be established to facilitate and enhance multicentre clinical and translational research in the field of ion beam therapy. (This may also apply to some degree to the increasing number of proton therapy centres [9-10]). This requires the installation of an adequate and comprehensive research structure and network, respectively, as started in some European FP7 Research Projects for carbon ion therapy during the recent period, such as ULICE, ENVISION, ENTERVISION, PARTNER [11-14]. Based on the analysis of the current situation of international ion beam therapy research, one work package of ULICE (WP2) was in particular dedicated to prepare and establish a comprehensive research infrastructure for Ion Beam Therapy Research on the European level and beyond. This WP included topics on "Concepts and terms for dose volume parameters and for outcome assessment in hadron-therapy integrating applied biology, medical physics and clinical medicine" (WP 2.1), "Development of Standard Operating Procedures (SOP) for clinical trial design in hadron-therapy" (WP 2.2) and "Design and implementation of a clinical research infrastructure" (WP 2.3). Altogether 11 deliverables had been planned for this WP for various topics and 10 have been already provided. The "International Ion Therapy Research Board" which has been one of the major sub-tasks of WP 2.3 is outlined in this paper (Deliverable 2.3, 2.6, 2.11) [15].

Aims of the International Ion Therapy Research Board (IONTREB)

The main objective of the IONTREB is the coordination, supervision and guidance of multicentre carbon ion therapy studies, starting with activities related to the existing and upcoming centres in Europe. The mid and long term aim is to include the majority of patients treated with ion beam therapy into prospective multicentre studies. The IONTREB will focus on the implementation and supervision of high-quality prospective multi-centre clinical research programmes targeting (carbon) ion-beam radiotherapy. These activities aim at comprehensive and valid clinical study structure and databases in order to demonstrate the potential of ion therapy and to provide clinical evidence regarding disease outcome, morbidity and quality of life. Specific tools for designing, planning, performing, and evaluating such high-level research, as incorporated into IONTREB activities, are

regarded as an essential prerequisite of a basic framework for a comprehensive multi-centre research infrastructure (see deliverables 1-10, WP2). The aim is to embed such international board into the frame of existing and upcoming ion beam therapy centers which are at present in Europe well represented in the European Network of Light Ion Hadron Therapy (ENLIGHT) which has followed the FP5 ENLIGHT project which took place from 2002-2006 [16].

Tasks of the International Ion Therapy Research Board (IONTREB)

The major tasks of IONTREB are related to international prospective multi-centre cooperative phase I, II, and III trials and an international multi-centre joint database research structure, in which comprehensive parameters on patient, tumour, imaging (including anatomical mapping), treatment, morbidity, quality of life and disease outcome characteristics are prospectively collected. General considerations on infrastructure, organisation and specific responsibilities for such coordinated research need to be defined. This also includes a coordinated tissue databank initiative which is under consideration and has to be designed in cooperation with other European (radio-) oncological tissue database activities (e.g. GENEPI) [17].

The following specific tasks will be carried out by the IONTREB:

- to guide the design, implementation, operation and continuous evaluation of a prospective multi-centre database for patients treated in a defined consortium of centres with carbon ions, protons, advanced photons;
- to guide the design and the performance of database orientated research including the publication of results;
- to design, to decide and to follow up on multi-centre phase I, II, and III clinical studies performed in the carbon-ion centres alone or in combination with photon and/or proton facilities;
- to link translational research activities with regard to all the various areas of current and potential future interest and to research groups that are currently active in this field to on-going and projected clinical trial and database orientated research in ion beam therapy.

Composition of the European IONTREB

A core group for the IONTREB was founded in 2013 within the ULICE (Union of Light Ion Centres in Europe) project to enable the design, implementation and the operation of coordinated research. This core group comprises at present the major representatives of the different facilities in operation and preparation all over Europe (Figure 1). This composition should allow for and ensure adequate contribution of specific study protocols from all individual centres and – provided approval by the IONTREB – all centres have expressed their interest then to recruit patients into these various multicentre clinical studies. This will enable in mid and long term perspective that a considerable number of patients treated at the participating centres will be included into these multicentre prospective clinical trials approved by an international expert board. Moreover, under the auspices of IONTREB also translational research and technology development for currently unresolved issues will be addressed and promoted.

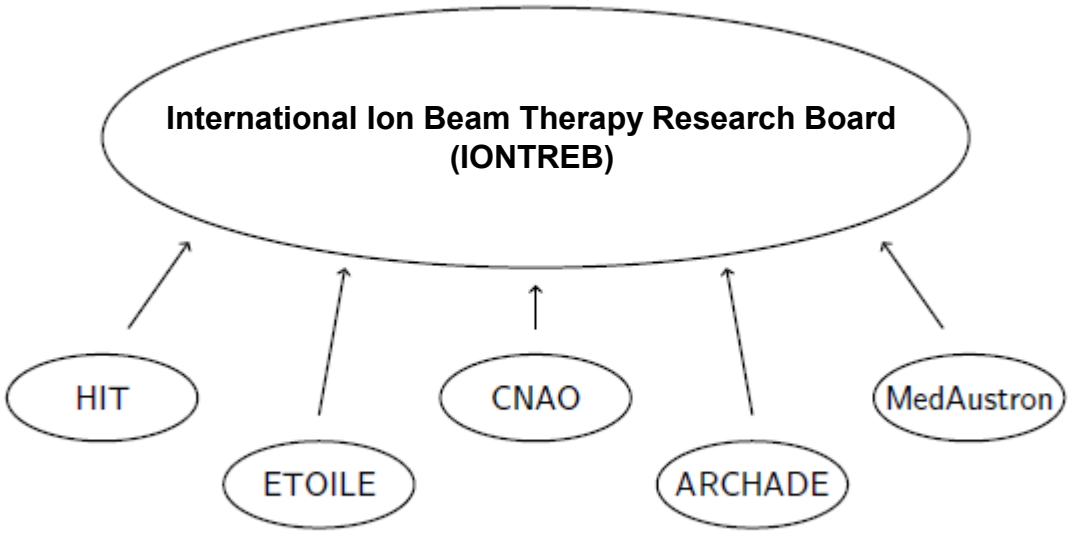

Figure 1: Composition of the European International Ion Therapy Research Board (IONTREB)

In addition to the core group, representatives of various other different disciplines will be necessary for the successful performance of an international coordinated carbon ion therapy research such as:

- radiation oncology specialists: carbon ion, proton, and advanced photon radiotherapy; psycho-oncology;
- translational research specialists: tumour and normal tissue radiobiology, medical radiation physics, medical imaging sciences;
- cancer diagnosis specialists: pathology, radiology, nuclear medicine;
- medical oncology specialists: anti-neoplastic drugs;
- organ specialists: various disease sites, combined treatment, and OAR assessment;
- clinical trial specialists: methodologists, statistician, data manager, clinical research technician, study nurse, quality assurance;
- basic physics and technology specialists: beam diagnostic and control, quality assurance, radiation protection.

Steps

After implementation of the European IONTREB in Vienna in February 2013 it was agreed upon that joint cooperative prospective clinical trials should be implemented in the running and upcoming carbon ion beam centers with 5 such protocols being activated until 2017 following a road map with HIT 2013, CNAO 2014, Marburg 2015, MedAustron 2016, France Hadron 2017. The protocol for a given indication would have to be followed and put into practice by each of the five European centres. The protocol itself will be designed by a Principal Investigator (PI), who has to be nominated by the specific centre. The protocol will be proposed to

IONTREB and discussed and approved by IONTREB. Such protocol is then implemented in the running centres and continuously supervised by a PI who coordinates the data collection, QA procedures and the scientific evaluation of data in close cooperation with the other participating centres. The PI reports in regular intervals to the IONTREB. It is appreciated, if upcoming centres and groups will also bring in patients already in their preparatory phase before opening the centre (model: study on adenoid cystic carcinomas, chordomas and sarcomas between France HADRON and HIT or CNAO). Through this procedure an efficient start for the initiation of joint clinical trials on carbon ion therapy is facilitated and embedded into an international frame or research coordination by linking it to the IONTREB.

Other issues have been discussed at the IONTREB level such as the build up of a joint database going beyond the performance of specific clinical trials [18] following the terms and concepts for reporting as defined in WP2 of ULICE. A short form of all the deliverables as provided in ULICE WP2 was decided to be provided and published until the end of the ULICE project (August 2014).

Conclusion

A common international clinical research structure and network focusing on carbon ion therapy and radiation oncology need to be defined, established and activated for the successful implementation and future development of this innovative and highly promising therapeutic instrument on a multicentre international level. This network also requires close contact to translational research activities in the field. One first step forward in this aspect was realised by the initiation of the European International Ion Therapy Research Board. This structural instrument will coordinate, supervise and guide multicentre European (international) clinical studies on the administration of carbon ion therapy in radiation oncology in order to guarantee high-quality clinical research and to ensure sustainable structures for multicentre carbon ion therapy research.

References

[1] Webpage PTCOG - http://ptcog.web.psi.ch/

[2] Combs SE, Laperriere N, Brada M. Clinical controversies: proton radiation therapy for brain and skull base tumors. Semin Radiat Oncol. 2013;23(2):120-6.

[3] Brada M, Bortfeld T. Proton therapy: the present and the future. Semin Radiat Oncol. 2013;23(2):75-6.

[4] Brada M, Pijls-Johannesma M, De Ruysscher D. Proton therapy in clinical practice: current clinical evidence. J Clin Oncol. 2007;25(8):965-70.

[5] De Ruysscher D, Mark Lodge M, Jones B, Brada M, Munro A, Jefferson T, Pijls-Johannesma M. Charged particles in radiotherapy: a 5-year update of a systematic review. Radiother Oncol. 2012;103(1):5-7.

[6] Lodge M, Pijls-Johannesma M, Stirk L, Munro AJ, De Ruysscher D, Jefferson T. A systematic literature review of the clinical and cost-effectiveness of hadron therapy in cancer. Radiother Oncol. 2007;83(2):110-22.

[7] Bentzen SM. Radiation therapy: intensity modulated, image guided, biologically optimized and evidence based. Radiother Oncol. 2005;77(3):227-30.

[8] Bentzen SM. Randomized controlled trials in health technology assessment: overkill or overdue? Radiother Oncol. 2008;86(2):142-7

[9] Langendijk JA, Lambin P, De Ruysscher D, Widder J, Bos M, Verheij M. Selection of patients for radiotherapy with protons aiming at reduction of side effects: the model-based approach. Radiother Oncol. 2013;107(3):267-73.

[10] Miller RC, Lodge M, Murad MH, Jones B. Controversies in clinical trials in proton radiotherapy: the present and the future. Semin Radiat Oncol. 2013;23(2):127-33.

[11] Combs SE, Dosanjh M, Pötter R, Orrechia R, Haberer T, Durante M, Fossati P, Parodi K, Balosso J, Amaldi U, Baumann M, Debus J. Towards clinical evidence in particle therapy: ENLIGHT, PARTNER, ULICE and beyond. J Radiat Res. 2013;54 Suppl 1:i6-12.

[12] Dosanjh M, Magrin G. Introduction to the EC's Marie Curie Initial Training Network (MC-ITN) project: Particle Training Network for European Radiotherapy (PARTNER). J Radiat Res. 2013;54 Suppl 1:i1-5.

[13] Kessel KA, Bougatf N, Bohn C, Habermehl D, Oetzel D, Bendl R, Engelmann U, Orecchia R, Fossati P, Pötter R, Dosanjh M, Debus J, Combs SE. Connection of European particle therapy centers and generation of a common particle database system within the European ULICE-framework. Radiat Oncol. 2012 ;7:115.

[14] Combs SE, Kieser M, Habermehl D, Weitz J, Jäger D, Fossati P, Orrechia R, Engenhart-Cabillic R, Pötter R, Dosanjh M, Jäkel O, Büchler MW, Debus J. Phase I/II trial evaluating carbon ion radiotherapy for the treatment of recurrent rectal cancer: the PANDORA-01 trial. BMC Cancer. 2012;12:137.

[15] Webpage ULICE - http://ulice.web.cern.ch/ULICE/cms/index.php?file=home

[16] Dosanjh M, Cirilli M, Greco V, Meijer AE. ENLIGHT: The European Network for Light Ion Hadron Therapy. Health Phys. 2012 Nov;103(5):674-80.

[17] Baumann M, Hölscher T, Begg AC. Towards genetic prediction of radiation responses: ESTRO's GENEPI project. Radiother Oncol. 2003;69(2):121-5.

[18] Kessel KA, Bougatf N, Bohn C, Habermehl D, Oetzel D, Bendl R, Engelmann U, Orecchia R, Fossati P, Pötter R, Dosanjh M, Debus J, Combs SE. Connection of European particle therapy centers and generation of a common particle database system within the European ULICE-framework. Radiat Oncol. 2012;7:115.

Session 4: Carbon Ion Radiotherapy in the World

Carbon Ion Therapy: Actual and Future Strategies at HIT

Klaus Herfarth and Jürgen Debus

Dept. of Radiation Oncology, University of Heidelberg, Germany
e-mail address:klaus.herfarth@med.uni-heidelberg.de

Abstract

The primary goal of the Heidelberg Ion Treatment center (HIT) is to assess the role of ion irradiation (primarily carbon ions and protons) in cancer treatment. Clinical trials have been established to broaden the evidence for the use of particle therapy and for looking in differences in the use of different particles. This articles focuses on the trials that have been started at HIT. Starting with tumors without movement, newer trials also deal with more movement of the target and the surrounding tissue. Future trials will also include a motion management.

Introduction

Heidelberg University treated the first patient with carbon ions in Germany in 1997. In these days, treatments with carbon ions were performed at the German society of heavy ions (GSI) in Darmstadt. There were 3 treatment slots counting 20 days each available for patient treatment each year. 440 patients had been treated at this facility between 1997 and 2008. Most of those patients had chordomas and chondrosarcomas of the skull base or adenoid cystic cancers of the salivary glands in clinical trials. The results of these trials had been published [1, 2] and results the long tern outcome will be presented in the near future. Among other arguments, the experience at the GSI initiated the development of the Heidelberg Ion Treatment facility HIT, the first real clinical heavy ion institution. The foundation stone was set in November 2003 and the first patient was treated 6 years later in November 2009. Over 1700 patients have been treated at HIT using carbon ions or protons. Many of those patients were included in clinical trials to proof and to confirm the value of heavy ion radiation therapy in the treatment of cancer. The article will focus on the actual trials at HIT and the future directions.

Methods and Materials

Fifteen clinical trials had been started at HIT since the first patient was treated on November 14, 2009. The trials will be described and future directions will be pointed out in the discussion section.

Results

One of the first initiated trials at HIT were the trials about chordomas and chondrosarcomas of the skull base. Very promising results could had been achieved during our treatment time at the GSI which seemed to be at least equally to the actual standard treatment using protons. Based on those experiences and the possibility to treat patients either with protons of carbon ions at HIT, two randomized phase III trials were established at HIT.

1. HIT-1 Trial for chordomas of the skull base

One of the first trials at HIT was a prospective randomized phase II trial for the treatment of skull base chordomas. This trial is testing for superiority of carbon ions irradiation against proton irradiation with respect to the local progression free survival (5 years local progression free survival 70% using protons and 80% using carbon ions). A dose of 72 GyE +/- 5% using protons in 2 GyE per fraction is defined a the standard treatment. Patient in the carbon ion arm receive a dose of 63 GyE +/- 5% in 3 GyE per fraction. The treatment will be carried out 5-6 times a week. Secondary objectives of this trial are overall survival, progression and metastasis free survival, patterns of recurrence and morbidity. We also like to determine prognostic factors. A total of 344 patients have to be enrolled (172 in each arm) and recruitment is under way. The design of the trial had been published by Nikoghysian et al.[3]

2. HIT Chondrosarcoma trial

This trial is also a prospective randomized phase II trial for the optimal treatment of skull base chondrosarcomas. Details concerning the details of this trial can be read elsewhere [4]. This trial wants to proof the equal effectivity of carbon ions and protons (The use of carbon ions is not inferior and at least as good as protons with respect to the 5 years local progression free survival). The planned dose in the standard arm is70 GyE +/- 5% using fraction doses of 2 GyE protons. The experimental arm is carried out using carbon ions in 3 GyE per fraction put o a total dose of 60 GyE +/- 5%. The treatment is performed 5-6 times a week. A total of 154 patients are need for this trial and recruitment is under way.

The other major indication at the GSI had been adenoid cystic carcinomas of the salivary gland. Very promising results of the combination of photon treatment with a carbon ion boost could had been achieved at GSI. The COSMIC trial resulted out of this experience.

3. COSMIC trial

The details of the COSMIC trial had been published elsewhere [5]. Goal of the trial was to evaluate toxicity in dose-escalated treatment with intensity-modulated radiotherapy (IMRT) and carbon ion boost for malignant salivary gland tumors (MSGT) of the head and neck. It was a prospective phase II trial. The dose to the primary target volume (boost volume) was increased to 8 x 3 GyE carbon ions compared to 6 x 3 GyE carbon ions at the GSI. The extended target volume of possible microscopic spread was treated using 25 x 2 Gy of photons in an IMRT technique. Primary endpoint was mucositis CTC°III, secondary endpoints were local control, progression-free survival, and toxicity. A total of 50 patients were included in this trial and recruitment was finished in April 2011. An interim analysis was published in May 2012 [6]. Actual results of the trial were presented at the ASTRO meeting 2013 and the PTCOG meeting 2013.

4. ACCEPT trial

The ACCEPT trial has followed the COSMIC trial in the treatment of adenoid cystic carcinomas (ACC) of the head and neck. However, in this trial only ACC patients with macroscopic residual disease can be included. Patients receive carbon ion boost of 6 x 3 GyE to the high risk area in conjunction with a 27 x 2 Gy photon IMRT of the extended CTC. In addition, all patients receive the EGFR antibody Cetuximab on a weekly basis. Primary endpoint is toxicity (mucosistis grade IV) to evaluate toxicity and feasibility of Cetuximab and carbon ion irradiation in the treatment of ACCs. Secondary endpoints are local control, metastases free survival and disease free survival. A total of 50 patients are planned for this study and recruitment is under way. More details about the trial has been published previously [7].

5. IMRT-HIT-SNT trial

This trial examines the effect of a carbon ion boost in the treatment of patients with unresected or incompletely resected nasal or paranasal sinus carcinomas [8]. It is a prospective non-randomized phase II trial evaluating the acute effects on the mucosa (rate of mucositis III°) as primary endpoint. Patients start with 8 x 3 GyE carbon ion boost, followed by 25 x 2 Gy photon IMRT. In addition, proteomic and genomic examinations were performed out of the peripheral blood of the treated patients.

6. TPF C-HIT trial

Locally advanced tumors of the oro-, hypo pharynx and larynx are suitable for this trial. Apart of a induction chemotherapy using Docetaxel, Cisplatinum and 5FU (TPF), the design is pretty similar to the accept trial. Patients receive a 8 x 3 GyE carbon ion boost to the primarily macroscopic tumor sites and a 25 x 2 Gy photon IMRT to the lymphatic drainage of the head and neck. Additionally, patients receive weekly Cetuximab. The primary endpoint is toxicity in this prospective mono-centric, non-randomized phase II trial. The recruitment of 50 patients was planned, however, the study had to be closed due to bad recruitment. Details of this trial can be read elsewhere (JENSEN, BMC).

Other early HIT trials are dealing with intracerebral tumors, escpacially with treatment of high grade gliomas or atypical meningeomas.

7. CLEOPATRA trial

This trial is a single center randomized phase II trial for the treatment of glioblastomas. Standard treatment is a radiochemotherapy of 30 x 2 Gy in combination with the drug temozolomide in addition to a resection (if possible). The aim of the trial to proof the overall survival (primary endpoint) for glioblastoma patients using a carbon ion boost dose escalation compared to the standard treatment. Patients receive a 5 x 2 GyE proton boost in the standard arm after 25 x 2 Gy 3D conformal photon treatment. The experimental arm consists of a 6 x 3 GyE carbon ion boost. All patients receive temozolomide 75 mg/m2 daily. The aim is to compare overall survival, progression free survival, toxicity and safety. The recruitment of 2 x 75 patients is planned and patient recruitment is going on. Details of this trial is published by S. Combs [9]

8. CINDERELLA trial

The effect of carbon ion irradiation in the treatment of recurrent gliomas after initial radiation treatment should be examined in the CINDERELLA trial. Details of the trial are published elsewhere [10]. This is a prospective randomized single-center phase I/II trial. There is no randomization in the phase I. The dose to the CTV is continuously increased from 10 x 3 GyE carbon ions to finally 16 x 3 GyE. Eight patients are treated in each of the 7 dose levels. The goal of this phase I is the determination of the recommended dose in the phase II. The next dose level is only entered if the previous dose level does not show an excess of dose limiting toxicity. The phase II will compare the results of a standardized stereotactic photon irradiation (18 x 2 Gy) against the on the phase I established dose level of carbon ions in a 2:3 randomization. Currently, recruitment of the phase I is still under way and the dose level of 14 x 3 GyE has been finished.

9. MARCIE trial

Atypical meningeomas have a much higher recurrence rate than meningeomas WHO grade 1. The Phase II-MARCIE-Study will evaluate a carbon ion boost applied to the macroscopic tumor in conjunction with photon radiotherapy in patients with atypical menigiomas after incomplete resection or biopsy. Patients with atypical meningeoma with macroscopic tumor avert biopsy or resection (Simpson grade 4 and 5). The treatment starts using photon irradiation of 25 x 2 Gy. This followed by a carbon ion boost of 6 x 3 GyE which results a higher

total dose than the standardized 30 x 2 Gy photon irradiation usually used. Primary endpoint is progression-free survival, secondary endpoints are overall survival, safety and toxicity. The study protocol is published elsewhere [11] and recruitment is under way.

The first trials at HIT have focused on tumors of the brain, skull base and the head& neck region, where movements can be minimized an no internal movement of the target is expected. The next generation of trials have focused on pelvic tumors.

10. IPI trial

The role of the use of ions in the primary treatment of prostate cancer is unknown. There are no prospective proton data. However, NIRS has published promising results in respect of the hypo fractionated use of carbon ions [12]. The IPI trial wants to confirm these Japanese data in a prospective randomized phase II trial. In addition, basis data of toxicity and biochemical progression free survival should be established for the use of hypofractionated ion treatment (carbon ions and protons) using raster scan technique. Patients with low of intermediate risk prostate are included in this trial. patients receive either 20 x 3.3 GyE carbons ions or 20 x 3 .3 GyE protons. All patients received a spacer gel between rectum and prostate for additional rectum protection and buffering internal prostate movement [13]. The protocol is currently under review for publication. Between May 2011 and October 2012 all planned 92 patients could have been recruited.

11. PROLOG trial

This trial focuses on the use of protons in the postoperative situation of prostate cancer (either as adjuvant treatment or as salvage treatment). An earlier trial looked at the effectivity and toxicity of a hypo fractionated photon IMRT to the prostatic bed in those patients (PRIAMOS trial [14]). PROLOG is the successor of this trial. Patients with pT3 and/or R1 status or patients with an PSA recurrence after surgery will receive 18 x 3 GyE protons to the prostatic bed. The main objective is to demonstrate the safety and feasibility of a hypofractionated proton irradiation of the prostate bed. Treatment safety will be judged by the incidence of NCI CTC AE grade 3–4 toxicity and by occurrence of treatment discontinuation. A total of 40 patients should be included in this trial and recruitment is currently continuing.

12. PANDORA trial

Patients with recurrent rectal cancer are still challenging. This trial should look upon the role of carbon ions in the re-irradiation of patients with recurrent rectal cancer. In the Phase I/II the recommended dose of carbon ion radiotherapy will be determined in the Phase I part, and feasibility and progression-free survival will be assessed in the Phase II part of the study [15]. AS in the above mentioned MARCIE trial, the phase I consists of a stepwise dose escalation for the determination of the dose limiting toxicity. The dose is escalated from 12 x 3 GyE carbon ions to 18 x 3 GyE carbon ions in 7 dose levels. There are a maximum of 45 patients planned for the phase I. The established dose of the phase one will be assessed in the phase II with the inclusion of maximal 39 patients.

13. ISAC trial

Imai et al published the NIRS data in respect of hypofractionated carbon ion irradiation of sacral chordoma [16, 17]. These tumors were treated with 16 fractions (4 times a week) up to a median dose of 70.4 GyE. The results were superior to surgical results. As in the IPI trial, we want to confirm this data using the raster scan method. Additionally, we like to know, if these results are an effect of the use of carbon ions or an effect of high and hypo fractionation. Patients with macroscopic tumor will be randomized to either 16 x 4 GyE carbon ions or 16 x 4 GyE protons. The total dose is slightly reduced to the NIRS data taking 5-6 fractions per week into

account. The primary endpoint of this prospective mono centric randomized phase II trial is safety and toxicity. Secondary endpoints are progression free survival, overall survive and quality of life. The trial has started recruitment in 2013.

14. OSCAR trial

This trial is a non-randomized therapy trial to determine the safety and efficacy of heavy ion radiotherapy in patients with non-resectable osteosarcoma. Up to date there is no curative treatment protocol for patients with non-resectable osteosarcomas. The primary endpoint of OSACAR is feasibility and toxicity in the ion treatment of unresectable osteosarcoma. It is a non-randomized prospective phase I/II trial. Details about this trial were published by Blattmann et al. 2010 [18]. However, at the time of publication, the recruitment had not started and due to a new consensus with collaborators, the dose scheme changed a bit. The desired target dose is 72 Cobalt Gray Equivalent (Gy E) with 27 x 2 GyE protons and a carbon ion boost of 6 x 3 GyE. There are 5-6 fractions per week scheduled. Furthermore, FDG-PET imaging characteristics of non-resectable osteosarcoma before and after PT/HIT will be investigated prospectively. Secondary endpoints are local tumor control, overall survival, disease free survival and assessment of FDG-PET as a response marker. A total of 20 patients are planned to be included in the study. Currently, the OSCAR trial is recruiting patients.

15. PROMETHEUS trial

The Prometheus trial is the first trial evaluating carbon ion radiotherapy delivered by intensity- modulated raster scanning for the treatment of HCC. Within this Phase I dose escalation study, the optimal dose of carbon ion radiotherapy will be determined. Dose escalation started from 4 x 10 GyE and will be increased up to 4 x 14 GyE to the macroscopic tumor in 5 incremental levels. The next dose level is entered if no dose limiting toxicity (DLT) occurred in 3 patients. In case of 1 DLT, the dose level is extended to further 3 patients. The movement of the target is determined individually and the delivery is performed using gating techniques if necessary. The primary objective is toxicity of carbon ion radiotherapy and the definition of a maximal tolerated dose for subsequent clinical investigation of carbon ion radiotherapy. Secondary endpoints are imaging response and progression-free survival. Details of the trial are published elsewhere [19]. The results of the first 6 patients were recently published by Habermehl et al. [20].

Discussion

After patient start in November 2009, a number of trials were initiated to assess the role of carbon ions and or protons in the treatment of a variety of cancers. The NIRS data set a founding stone in the design of new trials. Many of our trials want to confirm the NIRS data also using raster scanning technique and a more dense fraction schedule. However, other trials also look into the possible different effect of the RBE of protons and carbon ions. Many of the trials will take years for final conclusions, others will collect basic data for the development of larger phase III trials like those for skull base chondrosarcomas and chordomas.

Future trials at HIT will include more and more moving targets. Shortly, the INKA trial for neoadjuvant radiotherapy using raster scanned carbon ions in patients with locally advanced sulcus superior tumors will be initiated. The role of ion radiotherapy in the treatment of pancreatic cancer will also be assessed in trials as the use of carbon ions for inoperable esophageal cancer.

Conclusion

HIT wants to continue the work that NIRS has started: To bring ion radiotherapy of different cancer types to a evidence based level for the benefit of our patients.

References

1. Schulz-Ertner D, Karger CP, Feuerhake A, Nikoghosyan A, Combs SE, Jakel O, Edler L, Scholz M, Debus J: **Effectiveness of carbon ion radiotherapy in the treatment of skull-base chordomas**. *International journal of radiation oncology, biology, physics* 2007, **68**(2):449-457.
2. Schulz-Ertner D, Nikoghosyan A, Hof H, Didinger B, Combs SE, Jakel O, Karger CP, Edler L, Debus J: **Carbon ion radiotherapy of skull base chondrosarcomas**. *International journal of radiation oncology, biology, physics* 2007, **67**(1):171-177.
3. Nikoghosyan AV, Karapanagiotou-Schenkel I, Munter MW, Jensen AD, Combs SE, Debus J: **Randomised trial of proton vs. carbon ion radiation therapy in patients with chordoma of the skull base, clinical phase III study HIT-1-Study**. *BMC cancer* 2010, **10**:607.
4. Nikoghosyan AV, Rauch G, Munter MW, Jensen AD, Combs SE, Kieser M, Debus J: **Randomised trial of proton vs. carbon ion radiation therapy in patients with low and intermediate grade chondrosarcoma of the skull base, clinical phase III study**. *BMC cancer* 2010, **10**:606.
5. Jensen AD, Nikoghosyan A, Windemuth-Kieselbach C, Debus J, Munter MW: **Combined treatment of malignant salivary gland tumours with intensity-modulated radiation therapy (IMRT) and carbon ions: COSMIC**. *BMC cancer* 2010, **10**:546.
6. Jensen AD, Nikoghosyan AV, Lossner K, Herfarth KK, Debus J, Munter MW: **IMRT and carbon ion boost for malignant salivary gland tumors: interim analysis of the COSMIC trial**. *BMC cancer* 2012, **12**:163.
7. Jensen AD, Nikoghosyan A, Hinke A, Debus J, Munter MW: **Combined treatment of adenoid cystic carcinoma with cetuximab and IMRT plus C12 heavy ion boost: ACCEPT [ACC, Erbitux(R) and particle therapy]**. *BMC cancer* 2011, **11**:70.
8. Jensen AD, Krauss J, Potthoff K, Desta A, Habl G, Mavtratzas A, Windemuth-Kiesselbach C, Debus J, Munter MW: **Phase II study of induction chemotherapy with TPF followed by radioimmunotherapy with Cetuximab and intensity-modulated radiotherapy (IMRT) in combination with a carbon ion boost for locally advanced tumours of the oro-, hypopharynx and larynx--TPF-C-HIT**. *BMC cancer* 2011, **11**:182.
9. Combs SE, Kieser M, Rieken S, Habermehl D, Jakel O, Haberer T, Nikoghosyan A, Haselmann R, Unterberg A, Wick W *et al*: **Randomized phase II study evaluating a carbon ion boost applied after combined radiochemotherapy with temozolomide versus a proton boost after radiochemotherapy with temozolomide in patients with primary glioblastoma: the CLEOPATRA trial**. *BMC cancer* 2010, **10**:478.
10. Combs SE, Burkholder I, Edler L, Rieken S, Habermehl D, Jakel O, Haberer T, Haselmann R, Unterberg A, Wick W *et al*: **Randomised phase I/II study to evaluate carbon ion radiotherapy versus fractionated stereotactic radiotherapy in patients with recurrent or progressive gliomas: the CINDERELLA trial**. *BMC cancer* 2010, **10**:533.
11. Combs SE, Edler L, Burkholder I, Rieken S, Habermehl D, Jakel O, Haberer T, Unterberg A, Wick W, Debus J *et al*: **Treatment of patients with atypical meningiomas Simpson grade 4 and 5 with a carbon ion boost in combination with postoperative photon radiotherapy: the MARCIE trial**. *BMC cancer* 2010, **10**:615.
12. Tsuji H, Yanagi T, Ishikawa H, Kamada T, Mizoe J-e, Kanai T, Morita S, Tsujii H: **Hypofractionated radiotherapy with carbon ion beams for prostate cancer**. *International Journal of Radiation Oncology*Biology*Physics* 2005, **63**(4):1153-1160.
13. Uhl M, van Triest B, Eble MJ, Weber DC, Herfarth K, De Weese TL: **Low rectal toxicity after dose escalated IMRT treatment of prostate cancer using an absorbable hydrogel for increasing and maintaining space between the rectum and prostate: results of a multi-institutional phase II trial**. *Radiother Oncol* 2013, **106**(2):215-219.
14. Krause S, Sterzing F, Neuhof D, Edler L, Debus J, Herfarth K: **Hypofractionated helical intensity-modulated radiotherapy of the prostate bed after prostatectomy with or without the pelvic lymph nodes - the PRIAMOS trial**. *BMC cancer* 2012, **12**:504.
15. Combs SE, Kieser M, Habermehl D, Weitz J, Jager D, Fossati P, Orrechia R, Engenhart-Cabillic R, Potter R, Dosanjh M *et al*: **Phase I/II trial evaluating carbon ion radiotherapy for the treatment of recurrent rectal cancer: the PANDORA-01 trial**. *BMC cancer* 2012, **12**:137.
16. Imai R, Kamada T, Tsuji H, Sugawara S, Serizawa I, Tsujii H, Tatezaki S: **Effect of carbon ion radiotherapy for sacral chordoma: results of Phase I-II and Phase II clinical trials**. *International journal of radiation oncology, biology, physics* 2010, **77**(5):1470-1476.
17. Imai R, Kamada T, Tsuji H, Yanagi T, Baba M, Miyamoto T, Kato S, Kandatsu S, Mizoe JE, Tsujii H *et al*: **Carbon ion radiotherapy for unresectable sacral chordomas**. *Clin Cancer Res* 2004, **10**(17):5741-5746.

18. Blattmann C, Oertel S, Schulz-Ertner D, Rieken S, Haufe S, Ewerbeck V, Unterberg A, Karapanagiotou-Schenkel I, Combs SE, Nikoghosyan A *et al*: **Non-randomized therapy trial to determine the safety and efficacy of heavy ion radiotherapy in patients with non-resectable osteosarcoma**. *BMC cancer* 2010, **10**:96.
19. Combs SE, Habermehl D, Ganten T, Schmidt J, Edler L, Burkholder I, Jakel O, Haberer T, Debus J: **Phase i study evaluating the treatment of patients with hepatocellular carcinoma (HCC) with carbon ion radiotherapy: the PROMETHEUS-01 trial**. *BMC cancer* 2011, **11**:67.
20. Habermehl D, Debus J, Ganten T, Ganten MK, Bauer J, Brecht IC, Brons S, Haberer T, Haertig M, Jakel O *et al*: **Hypofractionated carbon ion therapy delivered with scanned ion beams for patients with hepatocellular carcinoma - feasibility and clinical response**. *Radiation oncology (London, England)* 2013, **8**:59.

Initial Results at CNAO

[1, 2]Roberto Orecchia, [1]Maria R. Fiore, [1, 2]Piero Fossati, [1]Alberto Iannalfi, [1]Barbara Vischioni, [1]Viviana Vitolo, [1]Mario Ciocca, [1]Alfredo Mirandola, [1]Andrea Mairani, [1]Silvia Molinelli, [1]Gloria Freixas Vilches, [1, 3]Guido Baroni, [1]Giulia Fontana, [3]Andrea Pella, [1, 3]Marco Riboldi, [1]Barbara Tagaste, [1]Cristina Bono, [1, 4]Marco Krengli, [1]Sandro Rossi.

[1]Italian National Center for Oncologic Hadrontherapy, Pavia, Italy; [2] European Institute of Oncology, Milan, Italy; [3]Politecnico di Milano, Milan, Italy; [4]University of Piemonte Orientale, Novara, Italy.

e-mail address:roberto.orecchia@cnao.it

Abstract

The clinical activity in CNAO started in September 2011 with proton beam and in November 2012 with Carbon ions. Up to date, about 150 patients have been treated enrolled in the clinical trials approved by the Italian Health Ministry. Some radiobiological tests have been conducted before the clinical activity started. Several clinical trials have been enrolling patients. The CE marking certificate has been obtained on the protontherapy treatments of skull base chordomas. The next step on the way to CE marks is on carbon therapy for sarcomas of skull base and trunk which is awaited for the end of the year.

Introduction

The running phase of the clinical activity of the Centro Nazionale di Adroterapia Oncologica (CNAO) is in the frame of the path suggested by the Italian Ministry of Health. During 2011, activities required were those of biologic characterization on cells for proton beams whose good positive results let CNAO get the approval by the consultation ministerial entity Consiglio Superiore di Sanità in July 2011 for treating patients with protons. The first patient started treatment on the 22 September 2011. It was a skull base chondrosarcoma in a young male. In the first semester 2012, experimental activities were concentrated on carbon ion beam, for their dosimetric and biological characterization on mice. In July 2012, CNAO got the authorization for treating patients with carbon ions. In fact on 13 November 2012 a re-irradiation of an adenoid cystic carcinoma of salivary glands, widely affecting the maxillary sinus, has been treated in a man.

The path followed by CNAO since the treatments started leads, according to the Ministerial procedure, to the CE marking of the general system in hadrontherapy that is to say the CE marking on the therapeutic application of the CNAO synchrotron.

Three are the treatment rooms. The treatment lines are four as the middle one has the vertical line too.

Methods and Materials

Up to now, the treatments with protons and with carbon ions are alternated during the day. All treated patients are enrolled in one of the clinical trials approved by the Ethics Committee of CNAO and then authorized by the Italian Ministry of Health. The clinical trials approved until now are 23. All the studies have been drawn with the aim of getting the EC marking of the CNAO system that it is to say the synchrotron and its therapeutic application as a medical device. According to the suggestions of the ministerial offices involved in the authorization procedure, the population of patients is small and the primary goals of the trials are

foreseen at short time. The primary goal of the certifying protocols is the evaluation of the device safety, through the reliability of the procedures, their reproducibility and, from a clinical point of view, the side effects incidence or eventual technical problems.

The table below describes the title of the clinical trials through which patients can be enrolled.

Trials	**Particle**	**Fractions**
Proton therapy of skull-base chordoma and chondrosarcoma	Proton	35-37
Proton therapy of spine chordoma and chondrosarcoma	Proton	35-37
Proton therapy of intracranial meningioma	Proton	30-33
Proton therapy of brain tumors	Proton	22-30
Proton therapy of head and neck relapses	Proton	n.a.
Proton boost in advanced head and neck cancer	Proton	8-15
Proton therapy of brain glioblastoma	Proton	37
Proton re-irradiation of spine relapses chordoma and chondrosarcoma	Proton	n.a.
Carbon ions therapy of adenoid cystic carcinoma of salivary glands	Carbon	16
Carbon ions re-irradiation of pleomorphic adenoma	Carbon	16
Carbon ions re-irradiation of recurrent rectal cancer	Carbon	dose escalation
Carbon ions therapy of head and neck sarcoma	Carbon	16
Carbon ions therapy of trunk sarcoma	Carbon	16
Carbon ions re-irradiation of head and neck	Carbon	10-30
Carbon ions therapy of malignant mucosal melanoma of head and neck	Carbon	16
Carbon ions therapy of high risk prostate carcinoma	Carbon	16
Carbon ions therapy of primary and secondary orbital tumors	Carbon	16
Pancreas tumors	Carbon	12
Malignant liver tumors	Carbon	12
Carbon ions re-irradiation of spine relapses chordoma and chondrosarcoma	Carbon	12-20
Proton therapy of eye melanoma	Proton	4
Multidisciplinary approach for poor prognosis sinonasal tumors: Phase II study of chemotherapy, surgery, photon and heavy ion radiotherapy integration for more effective and less toxic treatment in operable patients. SINTART1.	Proton/ Carbon	n.a.
Multidisciplinary approach for poor prognosis sinonasal tumors: Phase II study of chemotherapy, photon and heavy ion radiotherapy integration for more effective and less toxic treatment in inoperable patients. SINTART2.	Proton/ Carbon	n.a.

The experimental phase is going on in a satisfactory way as the reliability of the system safety and the device

safety concern. This, together with the good clinical results, is making CNAO supporting the shortening of the certifying procedure.

The scientific method followed in CNAO for all the treatments is based on the use of procedures, models and techniques able to realize the same experiences and data got in the other hadrontherapy centers. There is a precise evaluation of dose constraints to the target volume and to OAR. For carbon ions, together with NIRS, an analytical model for translating the biological dose efficacy on the CNAO device.

Prescription doses (GyE) **(16 fractions, 4 fractions per week)**								
Indication	NIRS dose	CNAO dose						
		Opposed ports		Orthogonal ports		Single port		
		quadratic errors		quadratic errors		quadratic errors		MC
		Cubes	Spheres	Cubes	Spheres	Cubes	Spheres	Spheres
Head and neck non mesenchymal cancer	3.60	4.20	4.15	4.20	4.15	4.20	4.15	4.19
Skull base chordoma and chondrosarcoma	3.80	4.35	4.30	4.35	4.30	4.35	4.30	4.33
Head and neck non mesenchymal cancer	4.00	4.50	4.40	4.50	4.45	4.50	4.45	4.47
Spinal chordoma and chondrosarcoma	4.20	4.65	4.60	4.70	4.60	4.70	4.60	4.64
Head and neck sarcoma	4.40	4.80	4.70	4.80	4.70	4.80	4.70	4.75
Bone and soft tissue sarcoma	4.40	4.80	4.75	4.80	4.75	4.80	4.75	4.78

Results

In the following table, it is described the distribution on tumours' type and sites disease of the 149 patients treated up to 1 October. All body districts are represented.

The figures include out trial patients as for a clinical need, 23 patients have been treated outside the running studies.

Disease	**Sites**	**149 cases**
Chordoma/chondrosarcoma	sacrum	14
Chordoma/chondrosarcoma	spine	18
Chordoma/chondrosarcoma	skull base	44
Meningioma	brain	4
Adenocarcinoma	salivary glands	17
Adenocarcinoma	prostate	3

Mucoepidermoid carcinoma	head and neck	1
Sarcoma	head and neck	17
Adenoid cystic carcinoma	orbit	1
Sarcoma	trunk	17
Carcinoma	rinopharinx	7
Carcinoma	oropharinx	2
Mucoepidermoid carcinoma	salivary glands	2
Melanoma	head and neck	2

The following image represents a treatment plan concerning a patient affected by high grade malignant peripheral nerve sheath tumour of the right brachial plexus treated with carbon ion radiotherapy at CNAO.

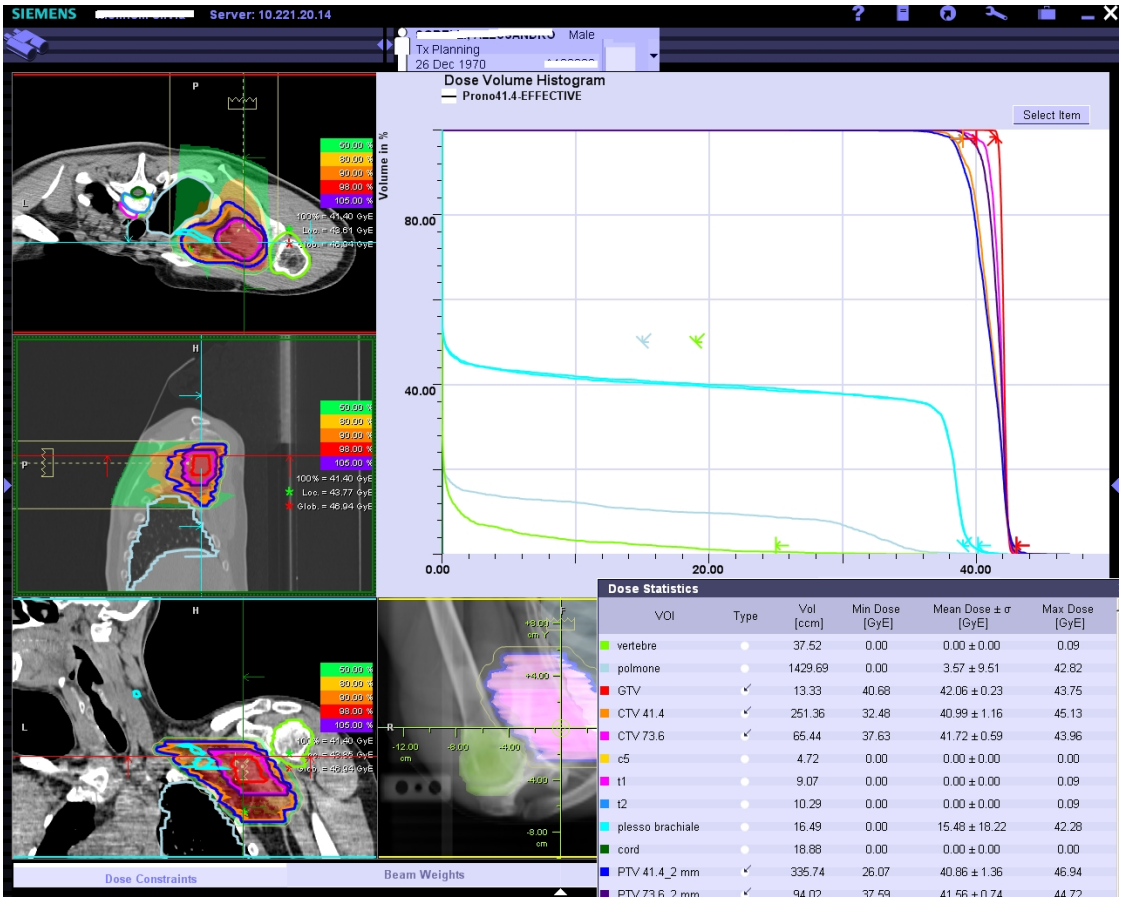

Up to 31 August 2013, 124 patients completed the treatment cycle. On them, a limited toxicity has been observed, on the whole less than expected. For the cited group of patients, the average follow up is of 4,6 months and the median one is of 3 months. The longest follow up is 21 months after the end of therapy.

As about the toxicity, 9 cases were with more than G2, according to CTCAE scale. 7 patients had G3 grade toxicity during the treatment. In 7 patients, the toxicity was of G3 grade during treatments: in one case it was a worsening of herpes zoster treated with antiviral systemic therapy per os. In the other 6 cases, it was a mucositis of the oral cavity of grade G3. In 4 of these patients, the toxicity retreated at the lower grade already at the end of the treatment cycle. In the 2 remaining patients, the G3 grade toxicity was no more at the moment of the first FU at 3 months.

There have been 2 other cases of late toxicity more than G2 grade. They were complete and monolateral of the visus deficit.

1) One case was a chordoma of clivus developing a toxicity with deficit of visus at grade G3 at 15 months and a complete loss of visus (G4) at 18 months from the end of therapy. The toxicity can be reported to the radiations' effect on the optic nerve. The neoplasm infiltrated the optic nerve and it has been intentionally irradiated with doses superior to those of the tolerance. The patient was well informed of the risk and gave her consent. At 18 months, there were no signs of disease and the controlateral visus was stable.
2) The second case was a poorly differentiated recurrent ethmoidal carcinoma already traeated with surgery, chemo and radiotherapy. After 3 months from the carbon ion reirradiation, the patient relapsed locally and at distance. The relapse at the apex of orbit caused the loss of visus, exophthalmos and paralysis of the III cranic nerve. Being not possible to define the concurrent role of the radiotherapy toxicity, the patient has been classified as G4, even if it seems more probable, also for the time of the onset, that the toxicity is linked to the tumour progression.

After one year from the end of the therapy, the rate of G2 toxicity can be estimated at around 33% (5 cases on 15). This fact can be related to:

1) radio induced pituitary deficit in 2 cases. In both patients, the pituitary gland was irradiated as the tumours were so close to the organ. The dose was more than the tolerance doses. So the toxicity was expected.
2) persistence of a neurologic deficit already known at the enrollment: the radiations damage cannot be excluded but the disease seems to be the most important cause of the toxicity.

The following table describes the overall data on toxicity.

	Toxicity								
	maximal during treatment	end of treatment	3 months	6 months	9 months	12 months	15 months	18 months	21 months
valuable patients	124	123	82	47	34	17	11	3	1
G0	20 % (25/124)	21% (26/123)	56% (46/82)	57% (27/47)	56% (19/34)	65% (11/17)	55% (6/11)	33% (1/3)	100% (1/1)
G1	31 % (38/124)	33% (41/123)	23% (19/82)	21% (10/47)	12% (4/34)	6% (1/17)	0% (0/11)	33% (1/3)	0% (0/1)
G2	44% (54/124)	43% (53/123)	19% (16/82)	21% (10/47)	32% (11/34)	29% (5/17)	36% (4/11)	0% (0/3)	0% (0/1)
G3	6% (7/124)	4% (3/123)	0% (0/82)	0% (0/47)	0% (0/34)	0% (0/17)	10% (1/11)	0% (0/3)	0% (0/1)
G4	0% (0/124)	0% (0/123)	1% (1/82)	0% (0/47)	0% (0/34)	0% (0/17)	0% (0/11)	33% (1/3)	0% (0/1)

Regarding the clinical trial about proton treatment of skull-base chordoma and chondrosarcoma, some results in term of volume reduction as illustrated in the following chart.

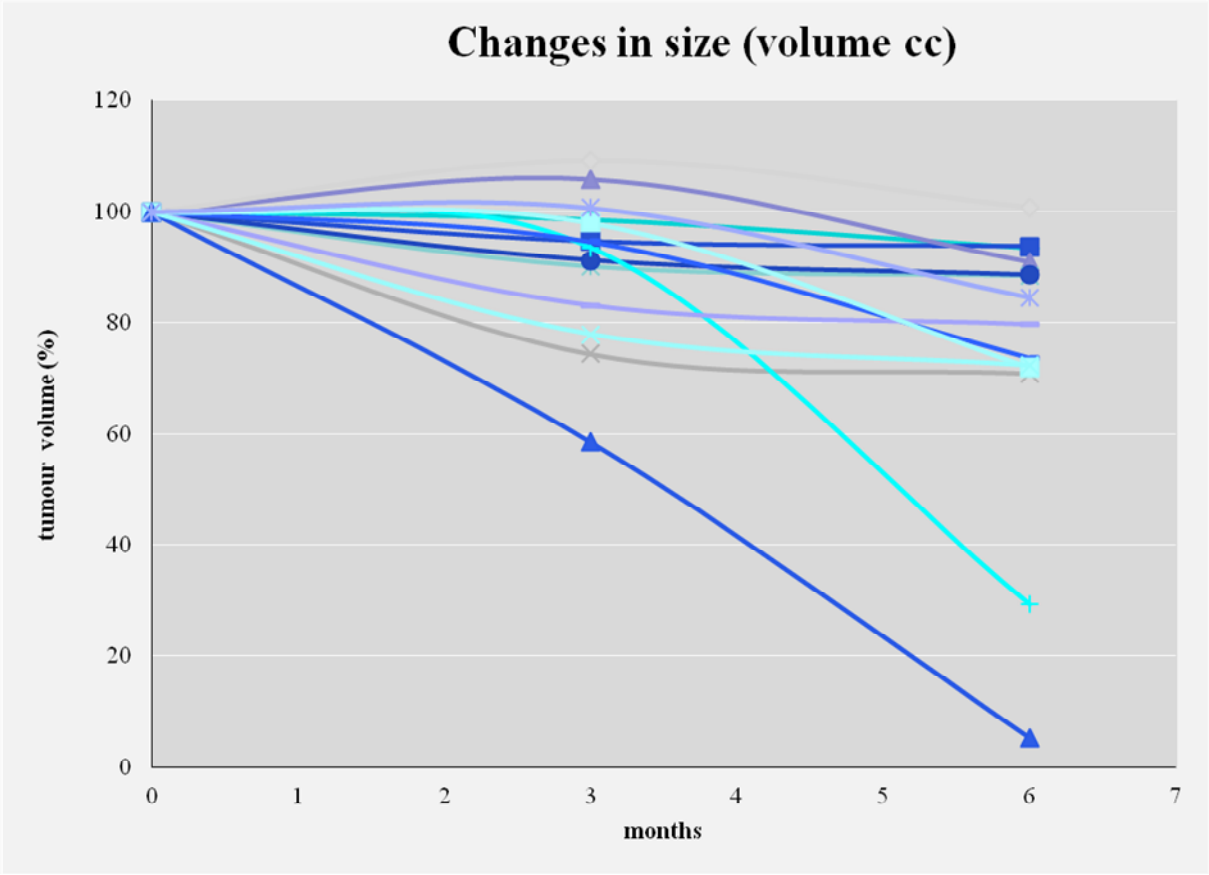

Discussion and Conclusion

The experimental initial phase of clinical activities in CNAO is characterized by the institutional and bureaucratic need to demonstrate to the Italian authorities that hadrontherapy is an important technology for the therapy of cancer.

The reported data on toxicity include both the toxicity related to hadrontherapy treatments both the one related to disease progression. The population consists also of relapses after previous conventional radiotherapy where the risk of reactions is higher. Nevertheless they have been enrolled in the clinical trials as there was a real therapeutic need. All the patients treated for relapses after conventional radiotherapy were all not eligible for re-irradiation with photons. In the number of patients, also out trial cases are considered, as non therapeutic alternatives were for them.

Although the negative bias of patient selection due to the heterogeneity of the pre - hadrontherapy patient treatment and clinical condition, the results show the safety and reliability of our treatment procedures.

References

[1] Fossati P, Molinelli S, Matsufuji N et al. H. Dose prescription in carbon ion radiotherapy: a planning study to compare NIRS and LEM approaches with a clinically-oriented strategy. Phys Med Biol. 2012 Nov 21;57(22):7543-54.

[2] Srivastava A, Vischioni B, Fiore MR et al .Quality of life in patients with chordomas/chondrosarcomas during treatment with proton beam therapy. J Radiat Res. 2013 Jul;54 Suppl 1:i43-8.

[3] Tuan J, Vischioni B, Fossati P et al., Srivastava A. Initial clinical experience with scanned proton beams at the Italian National Center for Hadrontherapy (CNAO). J Radiat Res. 2013 Jul;54 Suppl 1:i31-42.

［4］ Desplanques M, Tagaste B, Fontana G et al. A comparative study between the imaging system and the optical tracking system in proton therapy at CNAO. J Radiat Res. 2013 Jul;54 Suppl 1:i129-35.

［5］ Orecchia R, Srivastava A, Fiore MR et al. Proton beam radiotherapy: report of the first patient treated at the Centro Nazionale di Adroterapia Oncologica (CNAO) [National Center of Oncologic Hadron Therapy]. Tumori. 2013 Mar-Apr;99(2):e34-7.

［6］ Cantone MC, Ciocca M, Dionisi F et al. Application of failure mode and effects analysis to treatment planning in scanned proton beam radiotherapy. Radiat Oncol. 2013 May 24;8:127.

［7］ Molinelli S, Mairani A, Mirandola A et al. Dosimetric accuracy assessment of a treatment plan verification system for scanned proton beam radiotherapy: one-year experimental results and Monte Carlo analysis of the involved uncertainties. Phys Med Biol. 2013 Jun 7;58(11):3837-47.

Heavy Ion Therapy Project at GHMC

Takashi Nakano, MD, PhD

Gunma University Heavy Ion Medical Research Center
e-mail address: tnakano@med.gunma-u.ac.jp

At the present time in Japan, one in two people will suffer from cancer during their lifetime, making cancer care increasingly more and more important to medical welfare. The pressing issue of cancer care is not only the improvement of the long-term survival rate of patients, but also the establishment of minimally invasive cancer treatments that emphasize a high QOL (Quality Of Life).

In radiation therapy, remarkable progress has been made in advanced radiation therapy techniques for increasing the concentration of the dose on the cancerous lesion and so-called "radiation therapy for curing cancer while preserving the organ" is in the spotlight. Of these advanced radiation therapies, heavy ion radiotherapy has gained the spotlight for its superior dose convergence and high biological effectivity, and is one of the most minimally invasive treatments that give the best QOL after treatment in addition to having a strong ability to control cancer. A number of construction projects for heavy ion radiotherapy facilities have been scheduled throughout the world, which will make heavy ion therapy an important radiation therapy for cancer in the near future.

Heavy ion therapy is a treatment that accelerates ions with a molecular weight larger than helium, such as carbon ions, to nearly 70 percent of the speed of light and is used to treat cancer. Heavy ions have two major characteristics that differentiate them from X-rays, they have an excellent dose-distribution that is superior to X-rays, and therefore can treat tumors more precisely, and they have a 2 to 3 times stronger ability to kill cancer cells than X-rays or protons, and therefore they can more effectively control radiation-resistant tumors. Heavy ions can kill intensive cancer cells while sparing the surrounding normal tissue. Therefore, as an effective treatment that "cures cancer without compromising life activities through surgery" to provide excellent QOL, Heavy ion therapy is expected to be used for radiation-resistant types of tumors such as those associated with liver cancer, malignant melanoma, bone and soft tissue sarcoma.

According to the results of treatment in clinical trials using carbon ion beam therapy for over 5000 patients, which were started in June 1994 at NIRS in Chiba Japan, at present, lung cancer, liver cancer, head and neck cancer, prostate cancer, bone and soft tissue sarcoma and so on are considered to be good candidates for heavy ion therapy. This achievement has been evaluated as one of the most important scientific and technological breakthroughs in the 10-Year Strategy for Cancer Control, and the Japanese government has initiated a strategy for promoting the distribution of particle beam therapy across the country.

Research and development concerning the design of a compact heavy ion therapy facility was implemented at NIRS in 2004. Gunma University joined in the research and development of the compact heavy ion therapy facility in order to introduce a prototype machine at Gunma University. In addition, with strong support from local governments such as Gunma Prefecture, Gunma University completed construction of its compact heavy ion therapy facility in 2008 and started utilizing heavy ion therapy for cancers with the compact heavy ion therapy facility in March 2010. As of November 2013, more than 800 patients with various cancers have been

treated safely using this therapy. The present paper introduces the current status of heavy ion therapy at Gunma University and an outline of the Gunma heavy ion therapy project and its future prospects.

Outline of Gunma University heavy ion therapy facility

The heavy ion therapy facility designed for Gunma University is intended to deliver the practical compact heavy ion therapy facility, developed by the National Institute of Radiological Sciences, nation-wide as a basic specification **(Figure 1).** In addition, it provides another specification for the research and development of a carbon ion micro-surgery system as an option. The dimensions of the building are approximately 65m x 45m x 20m, housed within it is the ion source generator, the first-step linear accelerator, the synchrotron, which is the main accelerator and about 20m in diameter, the beam transfer lines, and three treatment rooms plus one research and development room. The treatment rooms consist of one with a horizontal irradiation port, one with horizontal and vertical irradiation ports, and one with a vertical irradiation port, while the research and development room micro-surgery system. The total construction budget is about 13 billion yen. In addition, as treatment support functions for planning the patient's series of treatments, it has a treatment planning room, a CT simulation room, an MRI room, and a PET/CT room. In this facility, the beam used for treatment consists only of carbon ions. The accelerator's design produces the beam intensity required for irradiating an exposure field of 15cm x 15cm at 5GyE/minute in the case of standard treatment conditions. The carbon ion beam can be accelerated up to 400MeV for each nucleus, which can penetrate about 25cm into water, and can cover treatment for most deep cancers.

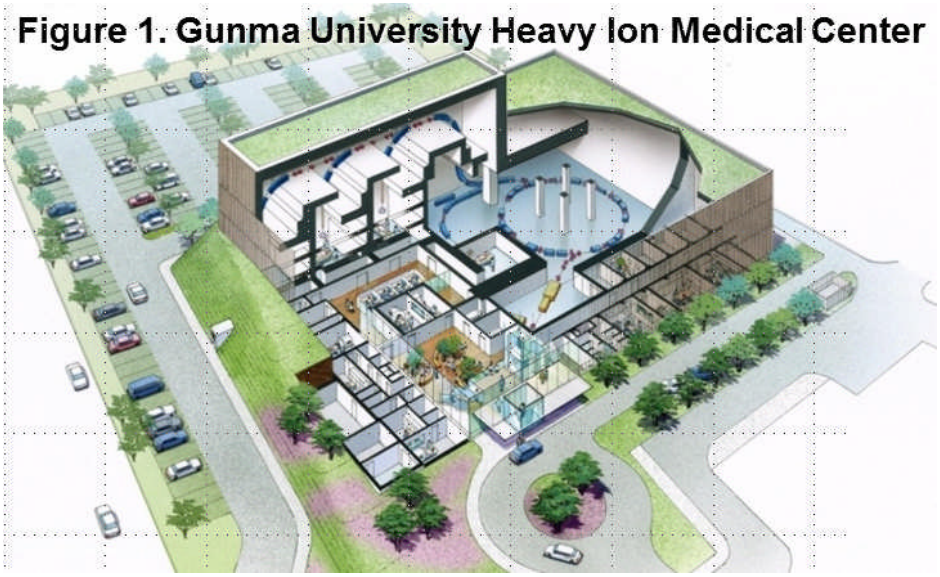

The beam is introduced into each irradiation chamber through the high energy beam transportation system, and tuned using various apparatus to form an irregular shaped dose distribution that encompasses the corresponding tumor. The passive broad beam delivery method is employed as a safe and easy method of forming the irradiation field. The narrow beam is expanded to a wide beam using the wobbler electromagnets and the scatterer, and a Spread Out Bragg Peak (SOBP) is created using the ridge filter system. A collimator and Bolus are used to shape the dose distribution according to the patient's treatment area. The staking layer irradiation method developed as a new irradiation method by the National Institute of Radiological Sciences is introduced into this beam line to improve the dose distribution, concentrating much more on the bulk of the tumor. The surrounding normal tissue can be much more spared from an unnecessary dose by dynamically moving the multi-leaf collimator and the range shifter in a coordinated fashion. In addition, the synchronous respiratory gating irradiation method, which matches the timing of irradiation to the patient's breath for the sake of internal organs that are adapted to the movement of the breath in order to improve the dose distribution on the tumor, and to decrease the side effects on normal tissue.

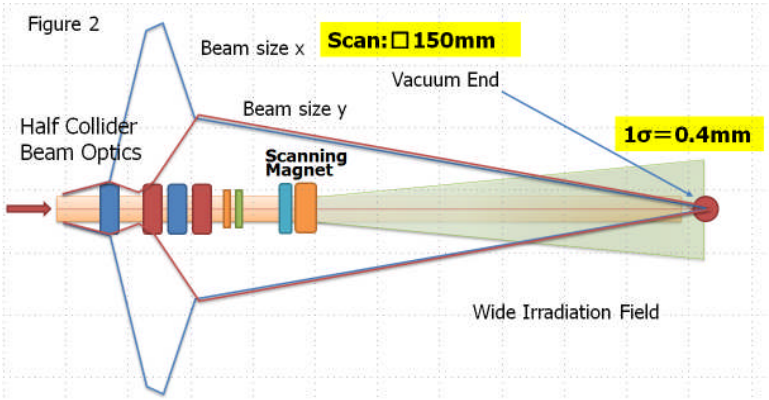

*Clinical results of patients treated with heavy ion therapy:

A total of 804 patients were treated with carbon beam therapy at GHMC from March 2010 up to September 2013. Classified according to the site of the tumor, there were 534 prostate cancers, 63 lung cancers, 51 liver cancers, 61 head and neck cancers, 45 bone and soft tissue sarcomas, and 50 other cancers. Although the median follow-up period was short, about a year, and was not enough to assess the full scope of the outcomes, severe acute and chronic radiation reactions have not occurred thus far.

The early clinical results were analyzed from a relatively large number of patients treated for prostate cancer with a mean observation period of 12.2 months. There were a total of 385 cases, of which, 181 cases were classified to be in a low-risk group, 17 cases were in a medium-risk group, 180 cases were in a high-risk group, and 7 cases were in a group of castration-resistant tumors). The 2-year overall survival rate was 98.4% (97.4-100), and the 2-year biochemical relapse-free rate was 98.7% (95.7-100). Based on these results, heavy ion therapy appears poised to become an important radiation treatment for cancer in the near future.

*Development of heavy-ion micro-surgery system at GHMC

The heavy ion therapy facility at Gunma University has a fourth treatment room for research and development. We are developing a high–precision heavy ion micro-surgery system in this room. The heavy ion micro-surgery system is a treatment technique for controlling the beam spot with a highly precise spatial position, on the order of millimeters, in order to take full advantage of the sharper and lower side scatter of carbon ions. High-precision heavy ion micro-surgery focuses a carbon beam down to a size of 1mm to 3mm φ, and can irradiate a minute targets in the body with the focused beam at a3 positional accuracy of less than 1mm, and thus treat the diseases. This technique is an innovative cutting-edge technique found nowhere else in the world, and we have already applied for a patent covering the principal elements of the method. This treatment technique can be extended to apply to the treatment of a variety of benign diseases other than cancers, such as vascular lesions and tumors adjacent to the spinal cord, pituitary tumors, acoustic neuromas, AVM, and age-related macular degeneration.

For those purposes, our group invented a novel beam focusing system, which uses a vertical irradiation port with 4 specialized focusing magnets to produce both a 0.4mm beam radius in 1-sigma size and 150mm square wide irradiation field with a positional accuracy of less than 1mm using a 3D spot scanning method.

Figure 2 represents the last 9m in the line of an irregular beam. With the conventional focusing system it is difficult to manage both the control of a small beam size and a wide irradiation field. The Gunma-type beam design is inspired by a "hadron collider", for example, the LHC at CERN. The collider strongly focuses a hadron beam and detects elementary particles with a huge detector, without using focusing magnets. In the Gunma design, the carbon beam size is expanded widely at first, and then strongly focused, in order to maintain its focus even when the beam is transmitted through the human body. Our group discovered how to design the beam to manage both a 0.4mm beam radius in 1-sigma size and a 150mm square wide irradiation field.

We have already achieved a $1\sigma = 1.4$ mm wide beam spot. Beam depth control with 0.1mm precision is achieved by incorporating the air gap from the surface of the body in order to modulate faint beam penetration.

Beam depth control with a precision of 0.1mm is another task in sub-mm carbon beam surgery. In particular,

the change in thickness of the range-shifter affects the beam size. We found that the air gap between the end of the range-shifter and the surface of the human body is appropriate for modulating small beam depth and size, because the density of the air is not zero but 1/1000 of water.

In addition, a sophisticated beam-range-control system was developed for treating age-related macular degeneration. The pretreatment scanning Bragg peak of carbons was used as the excitation light for fluorescence from the Indocianine green that accumulates in the lesion in order to set the penetration level of the beams accurately by determining the energy that generates the maximum fluorescence from the lesion.

Moreover, a CdTe Compton camera was developed to measure the gamma rays that scatter from the carbon ions in order to verify the exact beam positioning. We developed a three-dimensional image of multi-RI distributions and successfully obtained simultaneous images of two RIs administered to rats and confirmed the potential energy to be from at least Tc-99m γ-rays up to F-18 γ-rays.

The clinical experiment with carbon ion micro-surgery will be initiated with small beam spots of 2-3mm for a variety of diseases by 2018.

Reference

Suzuki Y, Yamaguchi M, Odaka H, Shimada H, Yoshida Y, Torikai K, Satoh T, Arakawa K, Kawachi N, Watanabe S, Takeda S, Ishikawa SN, Aono H, Watanabe S, Takahashi T, Nakano T. Three-dimensional and multienergy gamma-ray simultaneous imaging by using a Si/CdTe Compton camera. Radiology. 2013 Jun; 267(3):941-7.

Session 5: Medical Physics/ Technology

Development and Promotion of Carbon Ion Radiotherapy

Koji Noda

Research Center for Charged Particle Therapy, National Institute of Radiological Sciences, Chiba, Japan
e-mail address:noda_k@nirs.go.jp

Abstract

Carbon-ion radiotherapy (RT) with the HIMAC has been conducted since 1994, and the accumulated number of patients treated exceeded 7,500 in July 2013. On the basis of the HIMAC experience, NIRS developed a standard carbon-ion RT facility in order to boost the use of carbon-ion RT in Japan, and a pilot facility for this work was constructed at Gunma University and has been successfully operated since 2010. Toward the further development of the HIMAC treatment, NIRS has developed new treatment technologies, such as a fast 3D rescanning system using a pencil beam and a compact rotating gantry. These beam-delivery and accelerator technologies developed by NIRS have been applied to the following carbon-ion RT facility projects, including the Saga-HIMAT and Kanagawa prefectural projects.

1. Introduction

Heavy-ion beams are suitable for the treatment of deeply-seated cancer not only due to their high dose localization around the Bragg peak, but also due to the high biological effects in this region. Therefore, NIRS decided to construct HIMAC [1]. As the world's first heavy-ion accelerator facility dedicated to medical use, HIMAC has carried out cancer RT since June 1994. The HIMAC treatment has employed a single beam-wobbling method as the beam-delivery method because it is robust toward-beam errors, and because it offers easy dose management. The protocols were significantly increased after a respiratory-gated irradiation method was developed for moving-tumor treatments. As a result of the accumulated numbers of protocols, the Japanese government approved the carbon-ion RT at HIMAC as a highly advanced medical technology in 2003. Therefore, NIRS proposed the development of a standard carbon-ion RT facility [2] in order to boost the use of carbon-ion RT in Japan, with emphasis being place on a downsized version so as to reduce the cost. The design study and R&D work for the standard facility were carried out in FY 2004 and 2005. As the fruits of this work, a pilot facility was constructed at Gunma University, which has been successfully operated since 2010. NIRS, further, has also been engaged in a "new treatment research project" [3] since April 2006 for the further development of HIMAC treatments. One of most important purposes of this project is to realize an "adaptive cancer radiotherapy", which can accurately treat tumors even if there are changes in size and shape during the treatment period. For this purpose, NIRS has developed a fast 3D rescanning system with gated irradiation [4] to treatment both the static and moving tumors. In order to verify the newly developed technologies by a clinical study, a new treatment research facility, which is connected to the existing HIMAC accelerator complex, was constructed. The facility has been operated since May 2011, and more than 300 patients have been treated at this facility to date. The respiratory-gated 3D rescanning with the pencil-beam is scheduled to be used in FY 2013 for the moving-tumor treatment. Further, a compact heavy-ion rotating gantry with the pencil-beam 3D rescanning technology has been being developed with the superconducting technology in order to realize intensity-modulated carbon-ion RT for the more accurate and shorter-course treatments.

We herein report the development of HIMAC RT technologies and the promotion of carbon-ion RT in Japan.

2. Development of HIMAC

Carbon-ion RT has required a 3D irradiation field with several % of the uniformity on a tumor, while keeping the exposure to normal tissue as low as possible. For this purpose, beam-delivery methods have been developed, as well as the accelerator technology. The HIMAC beam-delivery system has employed a single beam-wobbling with a ridge filter method, which is one of the broad beam methods, in order to deliver its dose safely and reliably. The broad-beam method used by the HIMAC has continued to undergo development in order to improve the accuracy of the irradiation: these developments include the respiratory-gated irradiation and layer stacking methods. Toward more accurate and short-course RT, NIRS has developed pencil-beam 3D-scanning for both the static and moving tumors, as well as a carbon-ion rotating gantry with pencil-beam 3D scanning. NIRS has also developed the accelerator technologies related to the development of these beam-delivery technologies.

2.1 Development of beam-delivery technologies

2.1.1 Respiratory-gated irradiation method

Damage to normal tissues around the tumor was considered to be inevitable during the treatment of a tumor moving along with a patient's respiration. Therefore, a respiratory-gated irradiation system using the broad-beam method was developed [5]. In this scheme, an infrared-LED sensor is set on the surface of the patient's body, and its movement is monitored by a position-sensitive detector, which results in a respiratory signal. The beam should be delivered according to the gated signal produced only when the tumor is in the designed position. This scheme has been successfully applied since 1996.

2.1.2 Layer-stacking irradiation method

In a conventional beam-wobbling method, the fixed SOBP produced by a ridge filter results in undesirable dosage to the normal tissue in front of the target, because the thickness of an actual tumor varies within the irradiation field. In order to suppress this undesirable exposure, the layer-stacking irradiation method was developed [6]. This method conforms a variable SOBP to a target volume by dynamically controlling the conventional beam-modifying devices. The thin SOBP with several millimeters in the WEL, which is produced by a mini-ridge filter, is longitudinally scanned over the target volume in a stepwise manner. The target volume is longitudinally divided into slices, to each of which, the small SOBP is conformed using a multi-leaf collimator and a range shifter, and a variable SOBP coinciding to the target volume is formed. This method has been utilized routinely since 2004.

2.1.3 Phase-controlled rescanning method with fast 3D scanning

Adaptive cancer radiotherapy has strongly required a pencil-beam 3D scanning method for both the static and moving tumors. NIRS has thus developed a phase-controlled rescanning (PCR) method with a pencil-beam [4]. In the PCR method, rescanning completes irradiation on one slice during one gated period. Since the movement of the tumor is close to "zero" on average, a uniform dose distribution can be obtained even when irradiating a moving tumor. The PCR method is realized owing to mainly two technologies: 1) an intensity-modulation technique for a constant irradiation time on each slice having a different cross section and 2) a fast pencil-beam scanning technique for completing several rescans within a short time.

2.1.4 Rotating gantry

A compact heavy-ion rotating gantry [7] has been developed using superconducting technology in order to realize the use of intensity modulated carbon-ion RT (IMCT) combined with the pencil-beam 3D scanning to allow for more accurate and shorter-course treatment. A key point in the design was the use of combined-function superconducting magnets, thus allowing us to design a compact rotating gantry. Having optimized the layout of the gantry as well as the beam optics, the length and radius of the gantry were determined to be approximately 13 and 5.5 m, respectively.

2.2 Development of accelerator technologies

2.2.1 RF-KO slow extraction

For respiratory-gated irradiation with the broad-beam method, an essential technology in this scheme is the RF-KO slow extraction method [8], which can switch the beam on/off within 1 ms in response to respiration. The RF-KO method, based on transverse heating, originally had a huge ripple of kHz order in the time structure of the extracted beam due to the coherency in its extraction mechanism. However, the huge spill ripple has never disturbed the dose distribution in the beam-wobbling method, because the wobbling frequency of 50-60 Hz is much different from the ripple frequency. In the pencil-beam 3D scanning method, on the other hand, the spill ripple disturbs the dose distribution. NIRS thus improved the RF-KO slow extraction method [9] in order to significantly suppress the spill ripple. Further, the NIRS developed a method to suppress the fluctuation of the Hz order in the time structure by optimizing the AM function of the RF-KO system [10]. A beam-spill control system has been developed [11,12], based on the improvement of the time structure in the spill as mentioned above. Owing to this control system, the HIMAC synchrotron has given a low spill ripple and high reproducibility of the spill structure, which results in fast treatment planning for the fast 3D scanning at HIMAC. At present, the beam-control system has been upgraded so as to deliver an intensity modulated beam for the PCR method.

2.2.2 Intensity upgrade and extended flat-top operation

The beam intensity extracted from the synchrotron has been increased in order to complete single-fractional irradiation with one operation cycle. In this case, the efficiency of the gated irradiation is increased by a factor of about 2, because we can extend the flattop infinitely in principle. The extended flattop operation will save considerable time for the irradiation. In order to increase the beam intensity, we have thus developed a correction method for the third-order resonance that causes strong beam loss just after a beam injection into the synchrotron. In addition, the multi-harmonics operation of the RF acceleration system can also increase the intensity, because it suppresses the space-charge effect after bunching. Consequently, around 2×10^{10} carbon ions can be accelerated to the final energy. This intensity is sufficiently high to complete single-fractional irradiation for almost all tumors treated at the HIMAC when using the 3D-scanning method, with a beam-utilization efficiency of almost 100%.

2.2.3 Variable energy operation

Even when using the broad-beam method, quick energy changes have been required for an efficient operation. In the pencil-beam 3D scanning, variable energy operation by the accelerator itself has great advantages over using the range shifter method for slice changes because it helps keep the spot size small and suppresses secondary neutron production. GSI developed a variable energy operation using a cycle-by-cycle method. In this

case, it takes a few seconds of the operation cycle to change the energy for one slice change in the scanning method. The HIMAC synchrotron can be operated with variable energy in one operation cycle by applying a clock-stop technique to the synchrotron clock system [13]. As the first step, the HIMAC synchrotron has delivered beams with 11-step energies with the intensity modulation in one cycle operation for hybrid energy-scan RT [14]. As the second step, a full-energy scan is being developed, which has 201 energy steps ranging from 430 to 55 MeV/n. It will take less than 100 ms to change one slice.

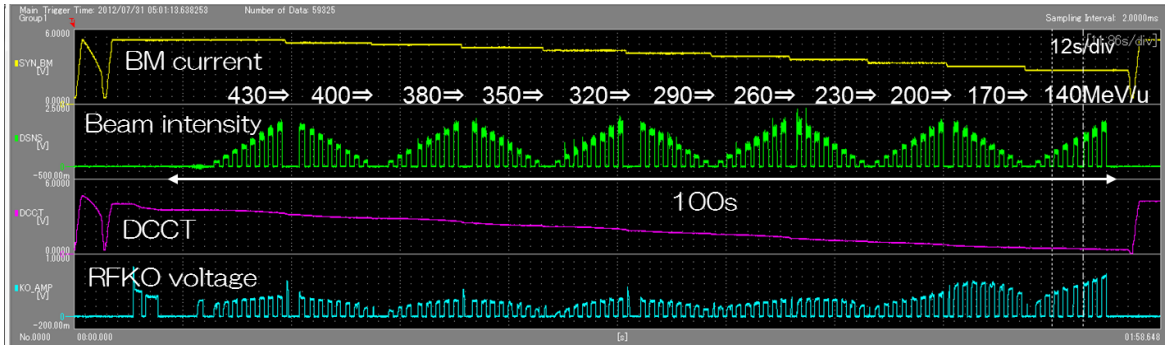

Fig. 1. The 11-step energy change with intensity modulation during one cycle of operation of the HIMAC synchrotron.

3. Promotion of carbon-ion RT facilities in Japan

For the widespread use of carbon-ion RT in Japan, NIRS designed a standard carbon-ion RT facility, which was a downsized version of the HIMAC facility, in order to reduce the construction cost. NIRS further developed key technologies for a standard facility from 2004 to 2005. GHMC (Gunma University Heavy-ion Medical Center), in collaboration with the NIRS, constructed a pilot facility in 2006, which was downsized to one-third compared with the HIMAC facility. Treatments at the pilot facility have been successfully carried out since March 2010. Following the pilot facility, two additional projects have been developed: the Saga-HIMAT (Saga Heavy-Ion Medical Accelerator in Tosu) and the i-ROCK (Ion-beam Radiation Oncology in Kanagawa). These projects employ the technologies developed for the standard facility and 3D scanning technology developed though the new treatment research projects promoted by the NIRS.

3.1 Pilot facility of the standard version

Considering the clinical statistics accumulated for more than ten years at HIMAC, specifications such as the residual range, maximum beam energy and irradiation-field size were determined so as to cover the HIMAC treatments [2]. The maximum residual range was designed to be 25 cm. The residual range depends not only on the beam energy, but also on the method used to form the lateral irradiation field. In the beam-wobbling method, carbon ions with energy of 400 MeV/n, corresponding to a 27.5 cm range in water, have a residual range of 25 cm, when the range loss mainly due to scattering can be suppressed to less than 2.5 cm. The spiral beam-wobbling method was thus developed [15]. As a result, the maximum energy was determined to be 400 MeV/n. On the other hand, the minimum energy was determined to be 140 MeV/n for eye melanoma treatment. A field diameter of 22 cm and an SOBP of 15 cm can cover almost all types of patients treated at HIMAC. A larger field size of more than 20 cm has mainly been required for the treatment of oblong tumors. In such cases, it is important to maintain the field length, rather than the diameter. The SOBP size should therefore be changeable from 4 to 15 cm. The dose rate of the new facilities needs to be 5 GyE/min/*l*, the same as that at the HIMAC. This dose rate corresponds to an intensity of 1.2×10^{9} pps extracted from the synchrotron, assuming a beam-utilization efficiency of 30% at the beam-delivery system. According to the beam-intensity schedule for the standard facility, the synchrotron requires a C^{6+} intensity of more than 200 eμA from the injector linac

cascade, and the ion source should provide a C^{4+} beam with an intensity of more than 260 eμA.

The annual number of patients treated at a new facility should be more than 600-800 patients for economic reasons, including the construction and running costs. Considering that there are six hours available for daily treatments, an occupancy time of 25 min for one session of fractional irradiation and 240 annual working days, the annual session number per room was estimated to be around 3400/year. Since the average fraction number is 12 at the HIMAC, the annual treatment number per room is estimated to be 280. Therefore, it was determined that the facility would require three treatment rooms in order to treat more than 800 patients/year. Further, the ratio of the treatment frequency with the horizontal irradiation port (H-port) to that with the vertical port (V-port) is around 5:4. Therefore, the three treatment rooms should be equipped with an H-port, V-port and H&V-ports. It was noted that the annual treatment number would exceed 1,000 patients when the occupancy time for the one-fractional irradiation could be reduced to less than 20 min owing to an automatic patient positioning system. The specifications for the standard carbon-ion RT facility in Japan are summarized in Table 1.

Table 1: Specifications of the standard C-ion RT facility

Ion Species	Carbon
Energy	400 – 140 MeV/n
Range/SOBP/Lateral-Size	250/40-150/220 mm
Max. Dose Rate	5 GyE/min/*l*
Beam Intensity	$1.2 \cdot 10^9$ pps
Treatment Rooms	3: H&V, H, V
Irradiation Method	Gating/Layer Stacking

The pilot facility has an ECR ion source, an RFQ and an APF-IH linac cascade, a synchrotron ring, three treatment rooms and one experimental room for basic research. In the pilot facility, a C^{4+} beam, which is generated by a compact 10-GHz ERC source [16], is accelerated to 4MeV/n through the injector cascade consisted of the RFQ and APF-IH linacs [17]. After the C^{4+} beam is fully stripped by a thin carbon foil, the C^{6+} beam is injected into the synchrotron through the multi-turn injection scheme, and is accelerated up to a maximum of 400 MeV/n. All magnets in the beam transport lines are made of laminated steel in order to permit a change in the beam line within one minute. The beam-delivery system employs both the single beam-wobbling and spiral beam-wobbling methods to provide uniform lateral dose distribution, while the ridge filter method is used for producing the SOBP.

3.2 New treatment research facility

The PCR method, which has been under development since 2006, needed to be verified by a clinical study. Therefore, NIRS constructed a new treatment research facility, which is connected to the existing HIMAC accelerator. In the treatment hall, located beneath the facility, three treatment rooms are prepared to treat more than 800 patients per year. Two of them are equipped with fixed beam-delivery systems in both the horizontal and vertical directions, while the other one will be equipped with a rotating gantry. Two treatment-simulation rooms are also prepared for patient positioning as a place for rehearsal, and for observing any changes of the target size and shape with x-ray or CT during the entire treatment. Furthermore, six rooms are devoted to patient preparation just before irradiation. A bird's-eye view of the new treatment facility at the HIMAC is shown in Fig. 2.

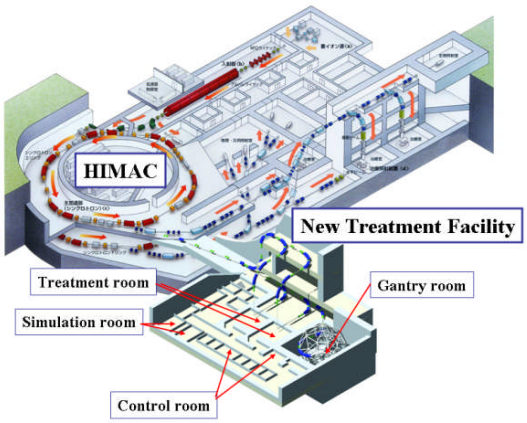

Fig. 2. A bird's-eye view of the new treatment research facility at HIMAC.

In order to carry out the clinical study in a manner identical to the existing HIMAC treatment, the residual range was required to be more than 25 cm. Thus, the maximum ion energy was designed to be 430 MeV/n, corresponding to the residual range of 30 cm in a carbon-ion beam and 22 cm in an oxygen-ion beam. The maximum lateral-field and SOBP sizes are 22 cm × 22 cm and 15 cm, respectively, in order to cover all treatments with the HIMAC. The rotating gantry system also employs a maximum energy of 430 MeV/n, a maximum lateral-field of more than 18 cm × 18 cm and a maximum SOBP size of 15 cm.

More than 300 patients have already been treated with the 3D scanning in the new treatment research facility since May 2011. In FY 2013, respiratory-gated irradiation with the pencil-beam 3D scanning is scheduled to be performed for the moving-tumor treatment. The rotating gantry will be installed in the third treatment room in the new treatment research facility.

3.3 New carbon-ion RT facility projects in Japan

Following the pilot facility at GHMC, two additional projects for carbon-ion RT have been proposed in Japan: the Saga-HIMAT (Saga Heavy Ion Medical Accelerator in Tosu) project and the Kanagawa Prefectural project.

The Saga-HIMAT project [17] entailed the construction of a carbon-ion RT facility, which began in February 2010, based on the design of the GHMC facility. This facility has successfully carried out treatments since August 2013. Although this facility has three treatment rooms, only two of them have been opened so far, but these rooms have both the single beam-wobbling and spiral beam-wobbling methods. One is equipped with both the horizontal and vertical beam delivery systems, while the other has both horizontal and 45-degree beam delivery systems. As the next step, the third room will be opened, using both the horizontal and vertical beam delivery systems with the fast 3D rescanning method developed by the NIRS. The bird's-eye view of this project is shown in Fig. 3.

Fig. 3. The bird's-eye view of the Saga-HIMAT.

The Kanagawa Prefectural Government has promoted the i-ROCK (Ion-beam Radiation Oncology Center in Kanagawa) project as part of the Kanagawa Prefectural Cancer Center. Although the accelerator system was designed based on the GHMC facility, the beam-delivery system will employ the NIRS scanning design, as described in the next section. The installation of devices will be started in February 2014, and the first treatment is scheduled for 2015.

4. Summary

On the basis of the HIMAC treatment experience, NIRS developed a standard-type carbon-ion RT facility, which is a downsized version of the HIMAC facility, in order to boost the use of carbon-ion RT in Japan. The pilot facility was constructed and has been successfully operated since 2010 by GHMC. The Saga-HIMAT project started cancer treatments in August 2013, based on the beam-wobbling method. The i-ROCK project, on the other hand, promoted by the Kanagawa prefectural cancer center, is being constructed on the basis of the fast 3D rescanning technology, because this technology was verified to be effective by clinical studies performed by the NIRS. The i-ROCK will open in 2015. At present, the NIRS is developing a compact heavy-ion rotating gantry using superconducting technology for more accurate heavy-ion RT. Such sophisticated technologies will boost the use of carbon-ion RT throughout the world.

References

[1] Y. Hirao et al., Nucl. Phys. A **538**, 541c–550c (1992).
[2] K. Noda *et al*., J. Radiat. Res., **48** (2007) A43-A54.
[3] K. Noda *et al*., Nucl. Instrum. Meth. **B 266** (2008) 2182-2185.
[4] T. Furukawa *et al*., Med. Phys. **34** (3), 1085-1097 (2007).
[5] S. Minohaya *et al*., Int. J. Radiat. Oncol. Bio. Phys. **47**(4) 1097.
[6] T. Kanai *et al*., Med. Phys. **33**, 2989 (2006).
[7] Y. Iwata *et al*., Phys. Rev. ST Accel. Beams **15**, 044701 (2012).
[8] K. Noda *et al*., Nucl. Instr. Meth. A **374** (1996) 269.
[9] K. Noda *et al*., Nucl. Instr. Meth. A **374** (1996) 269.
[10] T. Furukawa *et al*., Nucl. Instr. Meth. A **522** (2004) 196.
[11] S. Sato *et al*., Nucl. Instr. Meth. A **574** (2007) 226.
[12] K. Mizushima *et al*., Nucl. Instr. Meth. B **269** (2011) 2915.
[13] Y. Iwata *et al*., Nucl. Instr. Meth. A **624** (2010) 33.
[14] T. Inaniwa *et al*., Med. Phys. **39**, 2820 (2012).
[15] M. Komori *et al*., Jpn J. Appl. Phys. **43** (2004) 6463.
[16] M. Muramatsu *et al*., Rev. Sci. Instr. **75**(2004) 1925.
[17] Y. Iwata *et al*., Nucl. Instrum. Meth. A **572** (2007) 1007.
[18] M. Kanazawa *et al*., Proc. 8th Annual Meeting of Particle Accelerator Society of Japan, p.161-164.

Research Activity in Medical Physics at the New Carbon Ion Radiotherapy Facility

Toshiyuki Shirai

Research Center for Charged Particle Therapy, National Institute of Radiological Sciences, Chiba, Japan
e-mail address:t_shirai@nirs.go.jp

Abstract

We have developed a new treatment system at the New Particle Therapy Research Facility in the National Institute of Radiological Sciences (NIRS). The facility is equipped with a fast 3D scanning irradiation system for moving targets, a treatment planning system for fast scanning, and a patient handling system with robotic arms and 2D/3D auto-registration software. The treatment was started from May 2011 for fixed target. We are preparing moving target irradiation using a phase-controlled rescanning method. Systematic simulation studies and beam measurements have been carried out. A markerless tumor tracking system using fluoroscopic images has also been developed as a precise gating device.

Introduction

Particle therapy using carbon beams is a desirable treatment modality for cancer due to the high dose localization and the high biological effect around the Bragg peak. Since 1994, carbon beam treatment has been performed at the Heavy Ion Medical Accelerator in Chiba (HIMAC) [1]. Based on more than ten years of experience, we have constructed a new treatment system at the New Particle Therapy Research Facility at the National Institute of Radiological Sciences (NIRS). The aim of the new facility is to establish adaptive charged particle therapy and a compact rotating gantry for carbon ion radiotherapy [2]. The project design was started in 2006 and the facility building was completed in May 2010. A clinical trial for the therapeutic irradiation of patients was started in May 2011 and finished in November 2011. The number of patients was 11 in the clinical trial, and their target tumors were located in the pelvic and head and neck regions [3].

The size and shape of tumors varies during the treatment period. Adaptive therapy is a method that can respond to these changes of the targets. The scanning irradiation method has many good features; for example, it eliminates the need for compensating filters and collimators, and it is suitable for adaptive therapy. On the other hand, it has disadvantages, such as a long irradiation time and the difficulties associated with moving target irradiation. The most important feature of the NIRS scanning system is its speed; this shortens the irradiation time for patients and allows for the rescanning irradiation for the moving target within a reasonable time [4]. We have achieved speeds 100 times faster than in past systems by making improvements to the scanning system, the treatment planning system and the synchrotron control system.

Figure 1 shows a schematic view of the new facility and the HIMAC facility. There are three treatment rooms in the new facility. Two of them are equipped with fixed beam delivery systems in both the horizontal and vertical directions (Rooms E & F), and the other, now under construction, will be equipped with a superconducting rotating gantry (Room G). The carbon beam is provided from the HIMAC synchrotron. Table 1 shows the major parameters of the scanning beam delivery system. The maximum ion energy is designed to be ^{12}C, 430 MeV/n, in order to obtain a residual range of 30 cm.

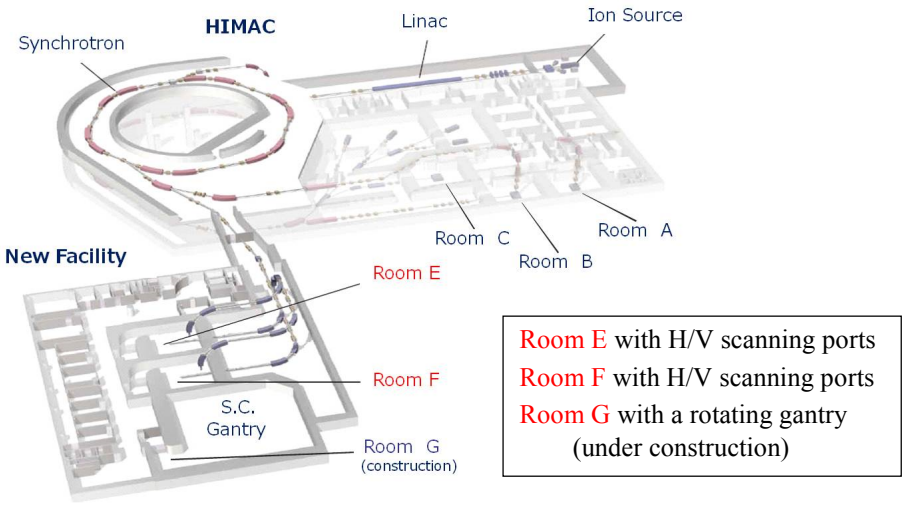

Fig. 1. A schematic view of the new facility (New Particle Therapy Research Facility) and the HIMAC facility. When completed, there will be three treatment rooms (E-G) in the new facility.

Table 1: Parameters of the beam delivery system

Ion species	^{12}C
Irradiation method	3D scanning
Beam energy	430 MeV/n (max.)
Maximum range	30cm in water
Maximum field	22×22 cm
Beam intensity	2 x 10^8 pps (typ.)

Table 2: A brief history of the new facility

2006 /4	New facility project was started.
2009/2	Building construction was started.
2010/3	Building construction was completed.
2011/5	Treatment at Room E was started.
2011/11	Clinical trial was finished.
2012/9	Treatment at Room E/F was started.

Operational Status of the New Facility

The beam range was controlled by inserting PMMA plates with given thicknesses at the start. This technique provides the desired range shift within a few hundred milliseconds. However, the range shifter plates increase the multiple scattering. It is therefore preferable to change the beam energy directly from the synchrotron; however, beam energies of more than 200 energies are necessary if a range shifter is not being used, which leads to long commissioning periods. We introduced a hybrid depth scanning method, where coarse tuning of the range (11 energies) was provided by an energy change of the synchrotron, while the fine tuning was provided by thin range shifter plates [5]. The dose conformity was improved with hybrid depth scanning.

The treatment room occupation time is also a key point for the clinical operation. Most of the room occupation time is spent for the patient positioning using the imaging system. These techniques involving patients are called the patient handling system (PTH). The PTH covers a wide range of functions, including X-ray/CT imaging, geometrical/position accuracy including motion management (immobilization, robotic arm treatment bed), software program and other factors [6]. Figure 2 shows treatment Room E, which has a SCARA-type (selective compliance assembly robot arm-type) robotic arm with a treatment table. Linear movements of 2400 mm, 600 mm and ± 300 mm are possible in the longitudinal, vertical and lateral directions, respectively. Rotational movements are −15° to 195° of rotation (isocentric rotation), ± 20° of roll, and ± 5° of pitch. The absolute and relative position accuracies are within the range of spheres of 0.5 mm and 0.3 mm in diameter, respectively. The

PTH also includes several custom software applications to facilitate treatment workflow, such as a patient position verification application. It has functions of landmark-based manual registration and GPU-based 2D/3D auto-registration.

In the clinical operation during FY2011, the treatment room occupation time averaged over all patients was 20 min. Of the total, 3 min were spent for preparation of the patient (including immobilization), 12 min for patient positioning, 2 min for irradiation (including preparation) and 3 min for exiting. The residual errors in translation and rotation averaged over all patients were 0.4 mm/0.2° at the end of the clinical trial [3]. In the clinical operation in FY 2012, the number of patients was 121 for the half-year period. The treatment room occupation time dropped to 13 min on average, as shown in Table 3. The patient positioning time was decreased to 7 min, while other times were almost the same. The PTH therefore plays an important role in improving the efficiency and precision of the treatment.

The average irradiation time was 1.2 min, with a PTV volume of 180 cc. The longest irradiation time was 3.5 min, with a maximum target volume of 1500 cc (Table 4). The irradiation time is comparable with that of the passive beam irradiation at the HIMAC. For the patient specific QA, all the planed beams are recalculated on a water phantom with the treatment planning system. Accordion type water phantom was developed to easily change the measurement depth by a remote control and the water equivalent depth can be changed from 30 to 300 mm, as shown in Fig. 3 [7]. The recalculated dose distributions are compared with the measured distributions by a commercial 2D ionization chamber array (OCTAVIUS Detector 729 XDR, PTW) at several depths, and are evaluated using a gamma index analysis with 3% and 3 mm criteria and 90% as a pass rate.

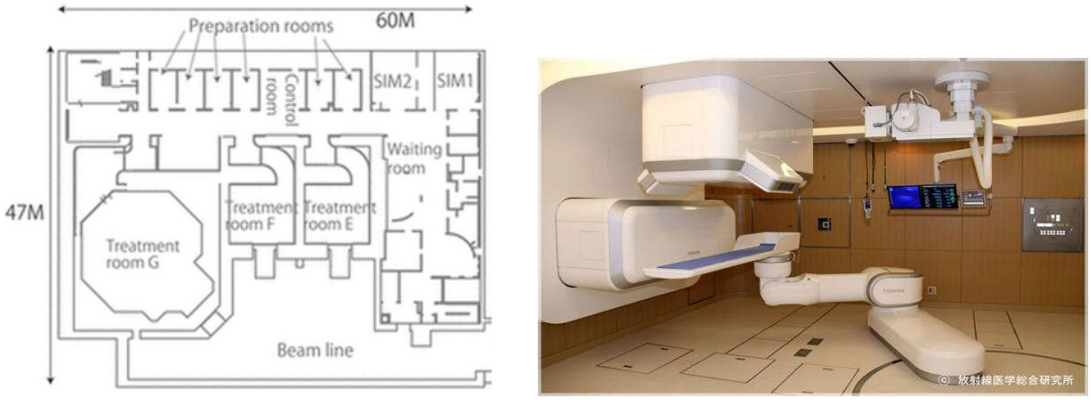

Fig. 2. Layout of the treatment floor in the new facility (left) and the treatment Room E, with two fixed beam ports and a SCARA-type robotic arm (right).

Table 3. The operational statics in FY2012

Number of patients	121
Target	Pelvis, uterus, head and neck
Days of operation	106 days (27 weeks) (Sept 2012 ~ Mar 2013)
Irradiation time	1~3.5 min
Treatment room occupation time	13 min (avg.) 9.5 min (prep. & positioning) 2.5 min (irradiation) 1.0 min (exit)

Table 4. The irradiation parameters in FY2012

	Average	Maximum
Irradiation time	1.2 min	3.8 min
PTV volume	180 cc	1,300cc
Number of spots	35,200	167,000
Number of slices	49	145
Number of particles	3.2×10^9	1.7×10^{10}

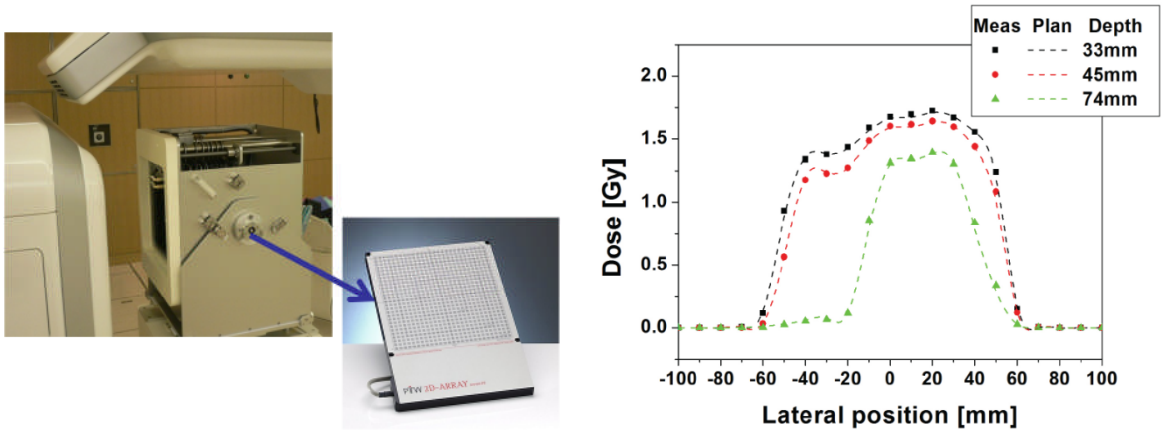

Fig. 3. The patient-specific QA setup (left) and typical results of the patient-specific QA for three different measurement depths (one-dimensional comparison) (right) [7].

Moving Target Irradiation

We are now preparing for moving target irradiation using the 3D scanning system. The degradation of dose conformation with tumor motion in particle therapy is a well-known problem due to interplay effects. Several approaches have been proposed to resolve this problem, such as beam tracking [8], gating and rescanning [9]. The gating method aims to reduce the residual respiratory motion, and is routinely used for passive beam irradiation at the HIMAC. Rescanning is based on the idea of averaging the positional errors of intrafractional motion and thereby smoothing the associated dose errors. We adopted the rescanning method with a gating technique. We also introduced the correlation of rescanning to respiratory motion, which is called phase-controlled rescanning (PCR) [10]. The time for the rescanning irradiation of each slice is matched to the gating duration in the PCR method, shown in Fig. 4. The dose rate from the beam delivery system is controlled to satisfy this PCR condition.

The treatment planning system (TPS) and the gating system have also been improved for the moving target irradiation, such as adoption of a field-specific target volume on TPS [11] and a tumor tracking system using fluoroscopic images as a precise gating device.

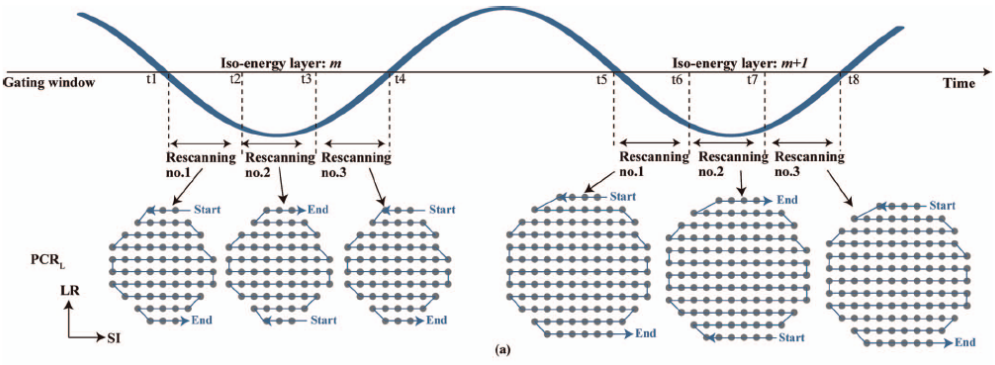

Fig. 4. Time chart of the phase-controlled rescanning (PCR). It shows an example of three times rescanning [12].

1. Field-specific target volume (FTV)

Target definitions for the PTV or ITV are not useful for particle therapy in some cases, because it is "geometrically" rather than "radiological path length" oriented. We defined a beam field-specific target volume

(FTV) for the moving target irradiation. First, the water equivalent path length (WEPL) was calculated at the proximal and distal edges of the target at respective phases on 4D-CT images, as shown in Figs. 5(a)–(c) [12]. Second, maximum and minimum WEPL were selected at the distal and proximal sides, respectively. For example, the WEPL were on the same ray line at respective phases in Fig. 5(d). Since WEPL 3 and WEPL 8 were the minimum and maximum values, respectively, the FTV was designed by selecting WEPL 3 and WEPL 8 on the ray line.

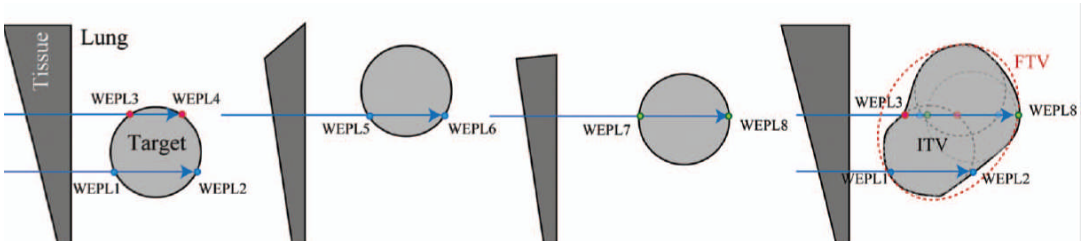

(a) Time: T_{ref} (b) Time: T1 (c) Time: T2 (d) Time: T3

Fig. 5. The target position at the reference time (a: T_{ref}), T1 (b), T2 (c), and the definition of FTV and ITV (d) [12].

2. The respiration gating system

LED sensors are routinely used as a gating device for passive beam irradiation at the HIMAC. Additionally, a tumor tracking system is available in the new facility. The orthogonal FPDs and X-ray tubes are used for patient positioning, and the oblique dynamic FPDs (DFPDs) are used for the tumor tracking in Fig. 6. The role of the tracking is to provide real-time monitoring of the tumor position for the gated irradiation. We adopted a markerless tracking method, which is a minimally invasive procedure. It tracks the tumor itself, or organs near the tumor, using fluoroscopic images. We apply a multiple template matching method to assess the tumor position during the irradiation [13]. This method can find the tumor position highly accurately and in real time by using templates at individual respiratory phases.

We evaluated the reliability of the markerless tumor tracking system using numerical human phantoms generated by the XCAT phantom and the movable lung phantom (CIRS Model008A), as shown in Fig. 7. Figure 8 shows representative results of the tracking for the lung phantom. The average tracking error was 0.4 mm, and the maximum error was 1.1 mm.

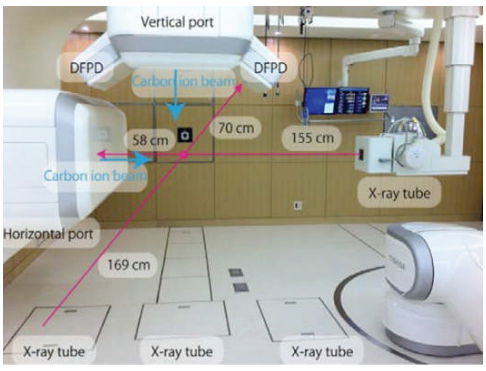

Fig. 6. A view of the imaging devices around the isocenter. The oblique DFPDs are used for markerless tracking.

Fig. 7. The commissioning of the tumor tracking system using a lung phantom.

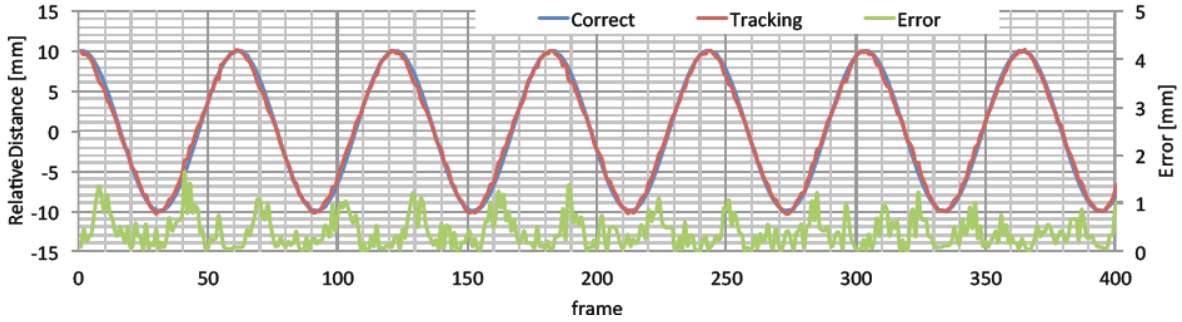

Fig. 8. The target motion (blue line), the tracking results (red line) and the difference (green line). The sweep direction was parallel to the direction of motion, with a 20 mm SI motion and 4.3 sec respiratory cycle.

3. The Fast 3D Scanning System

The 3D scanning system must be as fast as possible to treat the moving target with rescanning. The system was designed so as to provide a modulated dose delivery with beam-scanning velocities of 100 and 50 mm/msec at the isocenter in the horizontal and vertical directions, respectively. These scanning velocities enable us to achieve a short irradiation time of around 40 msec for an example uniform 2D field having a 100 x 100 mm size with spot spacing of 3 mm. To fulfill these requirements, we developed the fast scanning magnet and its power supply, the high-speed control system using FPGA circuits, as well as the fast beam monitoring system [4]. In the treatment planning, we also developed a novel optimization technique for the fast scanning, in which the exposure during transition from one spot to the next is taken into account [14]. This method enables us to reduce the irradiation time to approximately 1/5, as compared to that of the conventional one.

The layout of the fast scanning system is shown in Fig. 9. The distances from scanning magnets, SMX and SMY to the isocenter were designed to be 8.4 and 7.6 m, respectively. The vacuum window was made of 0.1 mm thick Kapton and is located 1.3 m upstream from the isocenter. The mini ridge filter is used to create Gaussian shaped mini peaks with 1 or 3 mm width at 1-sigma. The range shifters shift the mini peaks at a step size of 2 mm or 3 mm for the flat spread for the Bragg peak, in combination with 11 distinct synchrotron energies (430MeV/n - 140MeV/n). The maximal range shifter thickness is about 30 mm to minimize the multiple scattering of the carbon beam.

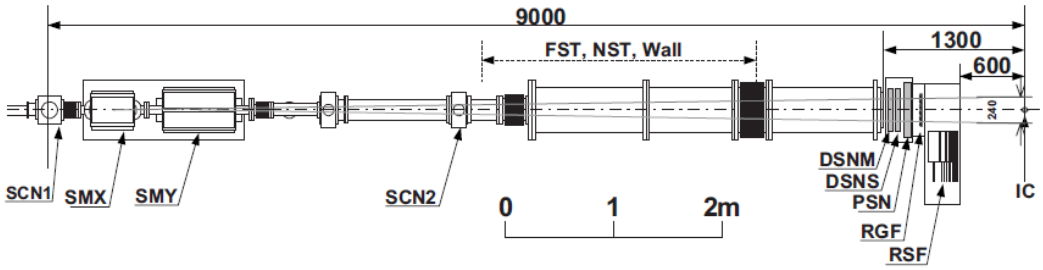

Fig. 9. The layout of the scanning-irradiation system. SMX, horizontal scanning magnet; SMY, vertical scanning magnet; SCN1 and SCN2, screen monitors; DSNM and DSNS, main and sub flux monitors; RGF, bar ridge filter; PSN, beam position monitor; RSF, range shifter [4].

Simulations and Measurements

1. Phantom study, simulations

The PCR method was evaluated using uniform density numeric phantoms [12]. A spherical tumor of 60 mm diameter was placed at a 150 mm depth in lung tissue. The target motion is a 12 mm SI motion with a 4.0 sec respiratory cycle. Figure 10(a) shows accumulated dose distributions without gating for one time phase-controlled scanning (1×PCR_L), four times phase-controlled rescannings (4×PCR_L) and eight times phase-controlled rescannings (8×PCR_L). It shows the considerably improved dose conformity. Figures 10(b) shows the dose for greater than 95% of the volume irradiation (D95) within the CTV at peak exhalation. The D95 increased with increasing numbers of rescannings. Figures 10(b) also shows the comparison between the phase-controlled rescanning (PCR_L) and other methods; the simple rescanning (LR), the simple volumetric rescanning (VR) and the phase-controlled volumetric rescanning (PCR_V). The phase-controlled rescanning method resulted in the small variation of the D95.

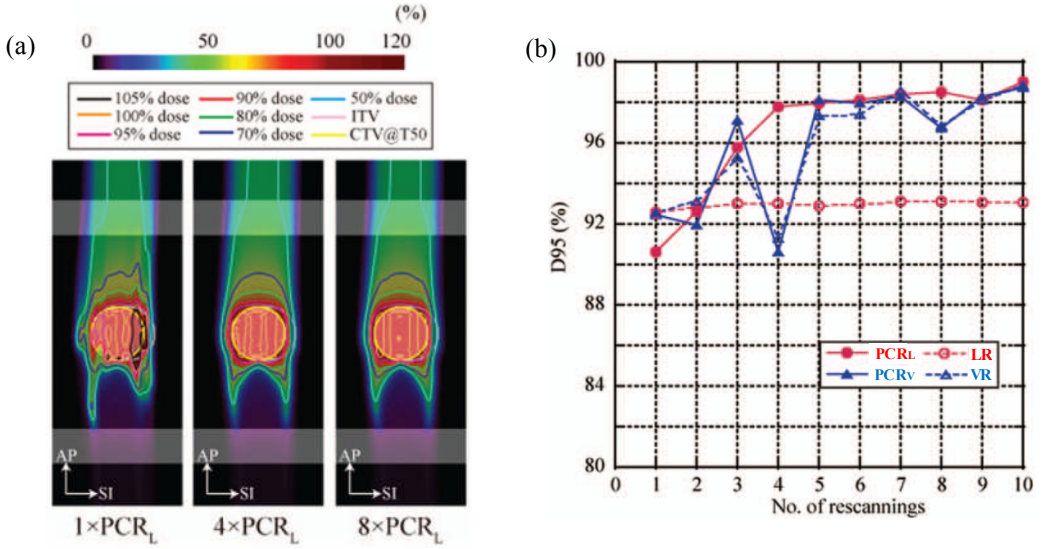

Fig. 10. The dose distribution by the PCR method (a). The target motion is 12 mm of SI motion with a 4.0 sec respiratory cycle and the prescribed dose was 3.0 GyE. The dose assessment metrics for the D95 (b). It compares the phase-controlled rescanning (PCR_L) to other methods; the simple rescanning (LR), the simple volumetric rescanning (VR) and the phase-controlled volumetric rescanning (PCR_V) [12].

2. Phantom study, experiments

The PCR method was verified by the 3D beam delivery system with gating [10]. The measurement setup is shown in Fig. 11(a). 24ch pinpoint chambers in the PMMA block (PTW31015, PTW) were used as the moving phantom. A spherical target of 60 mm in diameter was designed and optimized to deliver the uniform physical dose of 1 Gy. The phantom motion was sinusoidal with 4.0 s respiratory cycle. The amplitudes of the motion was 10 mm for x and y directions and 7 mm for depth direction. The duty factor of the gating was 37%. Figure 11(b) shows an example of the results. It is a rescanning number dependence of the dose uniformity for pinpoint chambers (ICs) 1 to 20 for the irradiation with and without the PCR method. The standard deviation was derived by using the percentage difference of the measured dose between the moving target and the static target for ICs 1 to 20. The error bar shows 1-sigma of the standard deviation for five different measurements. The deviation decreased with increasing numbers of rescannings and the PCR method resulted in smaller error bars. Consequently, the validity of the simulation study was confirmed experimentally.

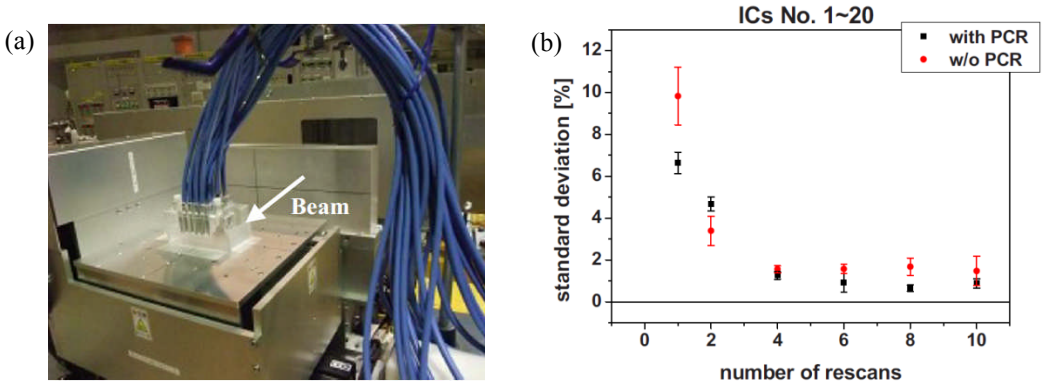

Fig. 11. The experimental setup for the moving target irradiation (a). 24ch pinpoint chambers in the PMMA block were used as a moving phantom and the amplitude of the motion was 10 mm for x and y directions and 7 mm for depth direction. A comparison of the dose distribution uniformities with and without the PCR method as a function of the rescanning number (b) [10].

3. Clinical example

The PCR method was also verified by the dose calculation on patient plans [12]. One example is shown in Fig. 12. The tumor in this patient was situated close to the diaphragm and showed a displacement of 13 mm during a single respiratory cycle. The radiological path length therefore varied significantly due to the high density differences. The dose conformation was improved by increasing the number of rescanning (Fig. 12(a)), and the CTV was successfully larger than 95% of the prescribed dose for four times phase-controlled rescanning ($4\times PCR_L$). Figures 12(b) shows the dose assessment metrics for the CTV in the D95 with the phase-controlled rescanning (PCR_L) and the phase-controlled volumetric rescanning (PCR_V). The phase-controlled rescanning method resulted in the small variation of the D95 and the dose conformity on the patient plan becomes acceptable by more than six times phase-controlled rescanning ($6xPCR_L$). It takes 213 sec for the six times rescanning irradiation in our system.

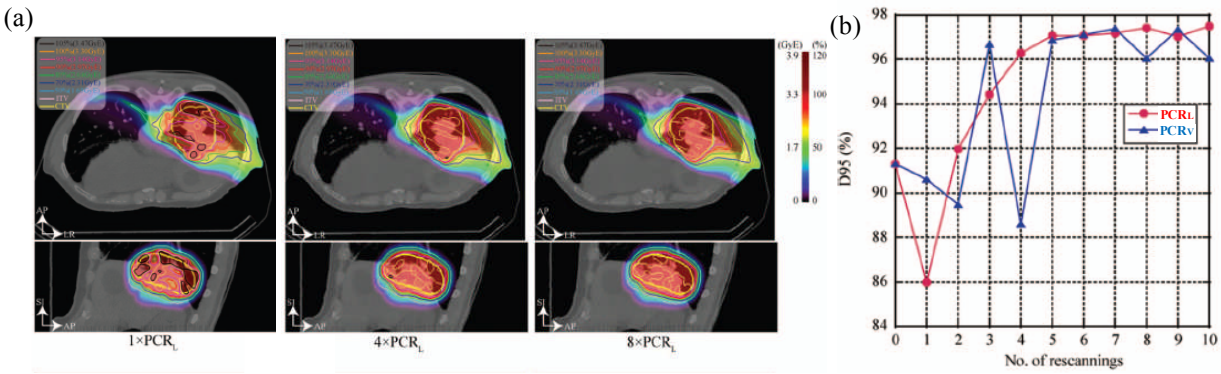

Fig. 12. The accumulated carbon-ion beam distribution with PCR_L (a). The beam angle was 110 degrees. The light pink and yellow lines are the CTV and ITV at peak exhalation. The dose assessment metrics for the CTV in the D95 (b), as a function of the number of rescannings [12].

Conclusion

The treatment with 3D scanning system was started at the new facility in May 2011. The irradiation targets are fixed ones in the pelvic, head and neck regions. The number of the patients is 132 until March 2013. We now continue the commissioning of the moving target irradiation and prepare the phase-controlled rescanning system and the tumor tracking gating system.

References

［1］ Hirao Y et al. Heavy ion synchrotron for medical use —HIMAC project at NIRS-Japan. Nucl. Phys. A 1992:538:541-550.

［2］ Noda K et al. NEW HEAVY-ION CANCER TREAT-MENT FACILITY AT HIMAC. Proceedings of EPAC08, Genoa, Italy 2008:1818-1820.

［3］ Mori S, et al. First clinical experience in carbon-ion scanning beam therapy: retrospective analysis of patient positional accuracy. Journal of Radiation Research 2012: 53:760-768.

［4］ Furukawa T, et al. Performance of the NIRS fast scanning system for heavy-ion radiotherapy. Medical Physics 2010:37:5672-82.

［5］ Inaniwa T, et al. Evaluation of hybrid depth scanning for carbon-ion radiotherapy. Medical Physics 2012:39:2820-2825.

［6］ Mori S, et al. Patient Handling System for Carbon-ion Beam Scanning Therapy. Journal of Applied Clinical Medical Physics 2012:13:3926.

［7］ Furukawa T, et al. Patient-specific QA and delivery verification of scanned ion beam at NIRS-HIMAC. Medical Physics to be published.

［8］ Grozinger SO, et al. Motion compensation with a scanned ion beam: A technical feasibility study. Radiat. Oncol. 2008: 3:34.

［9］ Phillips MH, et al. Effects of respiratory motion on dose uniformity with a charged particle scanning method. Phys. Med. Biol. 1992:37:223–234.

［10］ Furukawa T, et al. Moving target irradiation with fast rescanning and gating in particle therapy. Medical Physics 2010:37:4874-79.

［11］ Graeff C, et al. Motion mitigation in intensity modulated particle therapy by internal target volumes covering range changes. Medical Physics 2012:39:6004.

［12］ Mori S, et al. Systematic evaluation of four-dimensional hybrid depth scanning for carbon-ion lung therapy. Medical Physics 2013:40:031720-1-18.

［13］ Amano S, Ohnishi T, Mori S, Haneishi H. Automatic error detection in tumor tracking in respiratory gated radiotherapy. Proceedings of JAMIT2013, Tokyo, Japan 2013 (in Japanese).

［14］ Inaniwa T, et al. Optimization for fast-scanning irradiation in particle therapy. Medical Physics 2007:34:3302-11.

R & D of a Superconducting Rotating Gantry for Carbon Ion Radiotherapy

Yoshiyuki Iwata

Department of Accelerator and Medical Physics, Research Center for Charged Particle Therapy,
National Institute of Radiological Sciences (NIRS), Chiba, Japan
e-mail address:y_iwata@nirs.go.jp

Abstract

The new developments at the HIMAC include a super-conducting carbon gantry, a new therapy area with three new treatment rooms and substantial enhancements to the synchrotron extraction system to enable energy variation through multiple flattops within a synchrotron cycle to match the characteristics of the gantry and three-dimensional raster scanning. The carbon gantry consists of ten combined-function superconducting magnets, allowing a very compact geometry. The length and the radius of the gantry are approximately 13 and 5.5 m, respectively, comparable to the dimensions of existing proton gantries. Furthermore, these superconducting magnets are designed for fast slewing of the magnetic field to follow the multiple flattop operation of the synchrotron. In this paper, the recent research and development of a superconducting rotating-gantry for carbon-ion therapy is presented.

Introduction

The applications of particle accelerators cover a number of research areas, including both medical and industrial applications. In recent years, ion accelerators have been increasingly used for medical applications, including cancer therapy using energetic ions provided by such particle accelerators. Success has been achieved worldwide using such ions. At the National Institute of Radiological Sciences (NIRS), cancer treatments using energetic carbon beams, provided by the Heavy-Ion Medical Accelerator in Chiba (HIMAC), have been performed. The success of these cancer treatments has prompted us to design and construct a new treatment facility [1]. A major challenge associated with designing an irradiation system for the new facility is the ability to deliver a precise dose distribution using three-dimensional raster-scanning irradiation with a pencil beam [2], as well as to develop a compact rotating gantry.

A rotating gantry is an attractive tool to use during ion radiotherapy, because treatment beams can be directed to a target from any medically desirable direction, while the patient is kept in the best position. This flexibility of beam delivery for this type of gantry, an “isocentric rotating gantry,” is advantageous for treating tumors with a wide range of sites and sizes. Although these isocentric rotating gantries are commonly used for proton cancer therapy, it was thought to be very difficult to construct a rotating gantry for heavy-ion therapy, because the magnetic rigidity of the treatment beams for carbon therapy is roughly three times higher than that for proton therapy, and hence the size and weight of the gantry structure would need to be considerably higher.

We therefore designed a compact superconducting rotating-gantry for carbon ion radiotherapy [3]. This rotating gantry was designed to transport carbon ions having 430 MeV/*u* to an isocenter with irradiation angles of over ±180 degrees, and is further capable of performing the fast raster-scanning irradiation. The combined-function superconducting magnets will be employed for the rotating gantry. The use of the superconducting magnets with optimized beam optics allows for a more compact gantry design with a large scan size at the isocenter; the length and the radius of the gantry will be approximately 13 and 5.5 m, respectively, which are comparable to those of the existing proton gantries. This rotating gantry is currently under construction, and will be installed in room G of the new treatment facility. The recent research and development of the superconducting rotating-gantry are presented in this paper.

Layout

A three-dimensional image of the isocentric rotating gantry designed for the new treatment facility is presented in Fig. 1. This rotating gantry has a cylindrical structure with two large rings at both ends. The end rings support the total weight of the entire structure, and are placed on turning rollers so that the beam line can be rotated on the rotating gantry along the central axis over ±180 degrees. Carbon beams, provided by the HIMAC, are transported with ten sector-bending magnets, mounted on the gantry structure through each of their supporting structures; they are directed to a target located at the isocenter. In the treatment room, the patient's tumor is precisely positioned so that the isocenter is precisely targeted using a robotic couch.

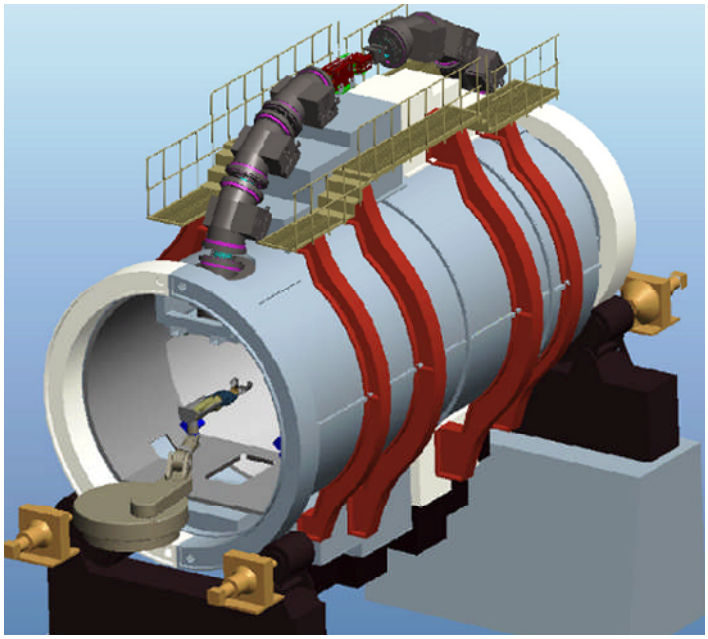

Figure 1: A three-dimensional image of the superconducting rotating gantry to be used for carbon therapy.

A layout of the beam-transport line for the compact rotating gantry is presented in Fig. 2. The rotating gantry has ten superconducting magnets (BM01-10), a pair of scanning magnets (SCM-X and SCM-Y) and two pairs of beam profile-monitor and steering magnets (ST01-02 and PRN01-02). The total length and radius of the rotating gantry is 13 m and 5.45 m, respectively. All of these devices are installed and mounted on the cylindrical structure. Since beam focusing can be done using only the combined-function superconducting magnets, no quadrupole magnets are needed in the rotating gantry, and thus, we could design the compact rotating gantry. The details of the beam optics for the beam-transport line are provided in Ref. [3].

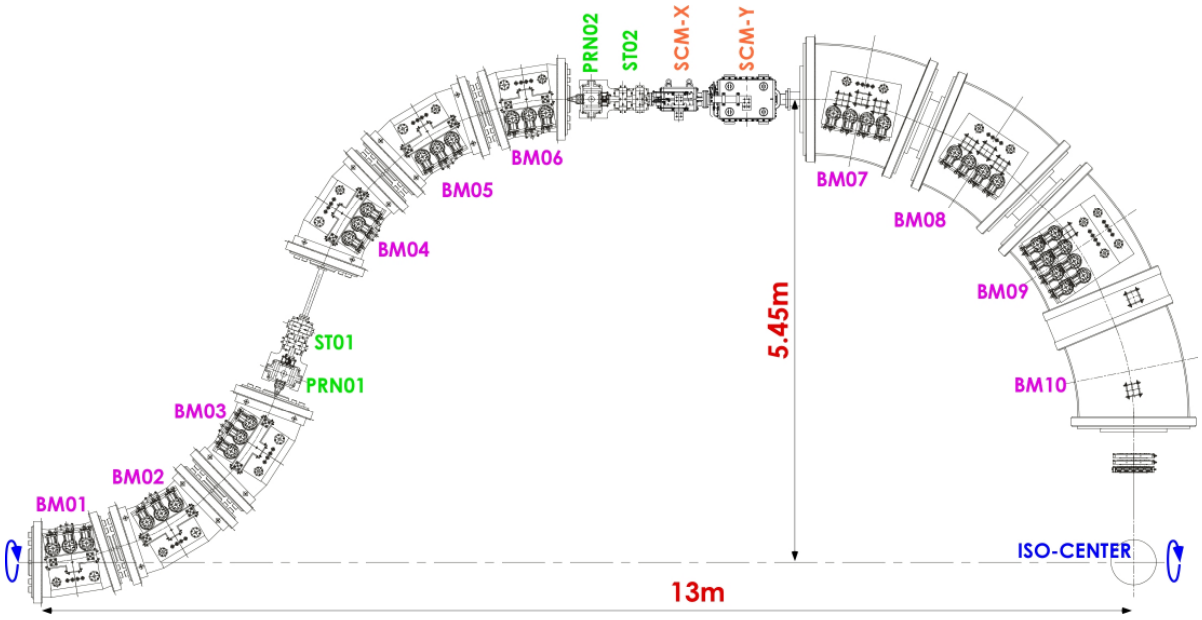

Figure 2: The layout of the superconducting rotating gantry. The gantry consists of ten combined-function superconducting magnets (BM01-10), a pair of scanning magnets (SCM-X and SCM-Y), and two pairs of beam profile-monitor and steering magnets (ST01-02 and PRN01-02).

TABLE I: SUMMARY OF THE PARAMETERS FOR THE SUPERCONDUCTING MAGNETS

Parameter	BM01,BM06	BM02-BM05	BM07	BM08	BM09, BM10	Units
Bending angle	18	26	22.5	←	←	degrees
Bending radius	2.3	←	2.8	←	←	m
Aperture diameter	60	←	170	240	290	mm
Reference radius or effective area	20	20	120×120	160×160	200×200	mm or mm^2
- Dipole coil -						
Maximum field	2.88	←	2.37	←	←	T
Coil current	136	←	227	225	231	amperes
Number of turns	3426	←	2458	3194	3702	turns/pole
Amperes per turn	465.9	←	558.0	718.7	855.9	kAT/pole
Stored energy	83.9	57.0	133	225	319	kJ
Inductance	9.07	6.16	5.18	8.90	11.9	H
- Quadrupole coil -						
Maximum field gradient	9.1	←	N/A	N/A	1.3	T/m
Coil current	130	←	N/A	N/A	200	amperes
Number of turns	400	←	N/A	N/A	232	turns/pole
Amperes per turn	52.0	←	N/A	N/A	46.4	kAT/pole
Stored energy	1.61	1.15	N/A	N/A	1.58	kJ
Inductance	0.190	0.136	N/A	N/A	0.0792	H

Design of the superconducting magnets

Based on the design of the beam optics, the specifications of the superconducting magnets were determined. According to their apertures, the magnets are categorized into five types, as summarized in Table I. All of the magnets have the curved shape, as presented in Fig. 3, and have a surface-winding coil structure. The magnetic field distributions of the magnets were calculated by using a 3D electro-magnetic field-solver, the Opera-3d code [4]. In the code, the curved superconducting coils, having typically a few thousand turns per pole, as well as the cold yoke and vacuum chamber, were precisely modeled, and a three-dimensional magnetic field was calculated. Representative results of the calculations are shown in Fig. 4. After having optimized the conductor position, we obtained the required uniformity of the calculated magnetic field.

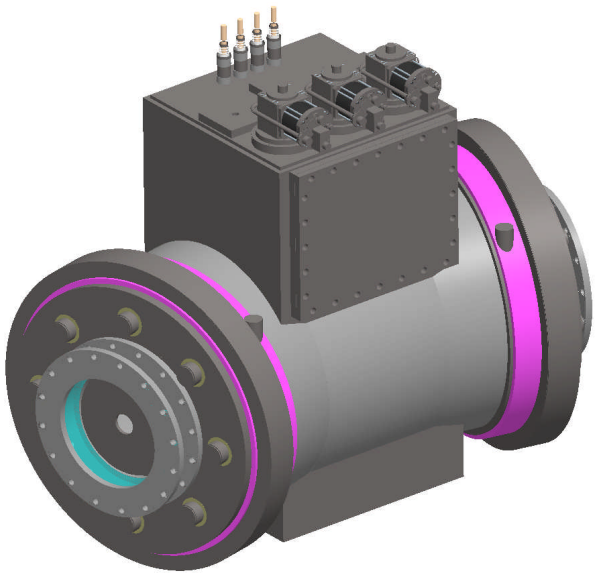

Figure 3: A three-dimensional image of the curved combined-function superconducting magnet used for BM02-BM05.

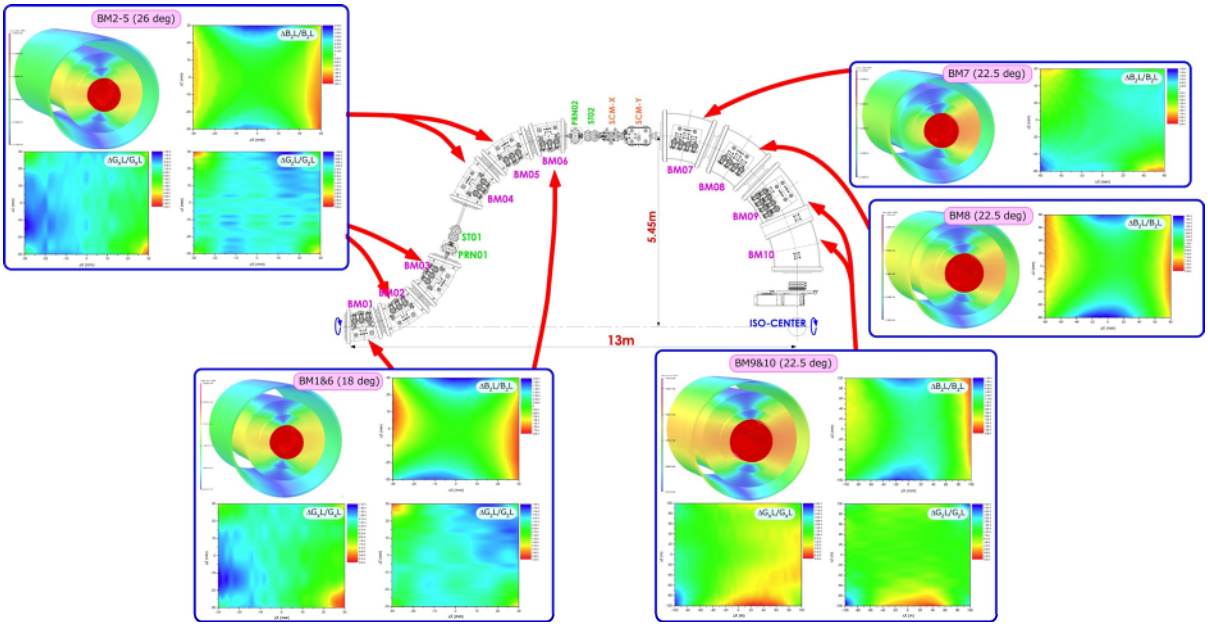

Figure 4: Representative results of the 3D magnetic field calculations for the five types of superconducting magnets.

To evaluate the field quality, and to concurrently confirm the design of the superconducting magnets, beam-tracking simulations were performed. Since the quality of scanned beams is important for treatments using the scanning irradiation method, tracking simulations were made downstream of the scanning magnets; the tracking of beam particles was initiated in the middle of SCM-Y, and the beam trajectories were calculated through BM07-BM10, before reaching the isocenter. In the simulation code, a relativistic equation of motion was numerically integrated using the fourth order Runge-Kutta method to calculate the trajectory of each beam particle. To determine the magnetic flux density, at which a particle is located, three-dimensional maps on the magnetic fields over a region of interest were initially extracted from the Opera-3d code for each of BM07-BM10, and then the magnetic flux density at a specific particle was calculated by interpolating from the proximal data provided by a field map. The basic methods used for the simulations were the same as those described in Ref. [3].

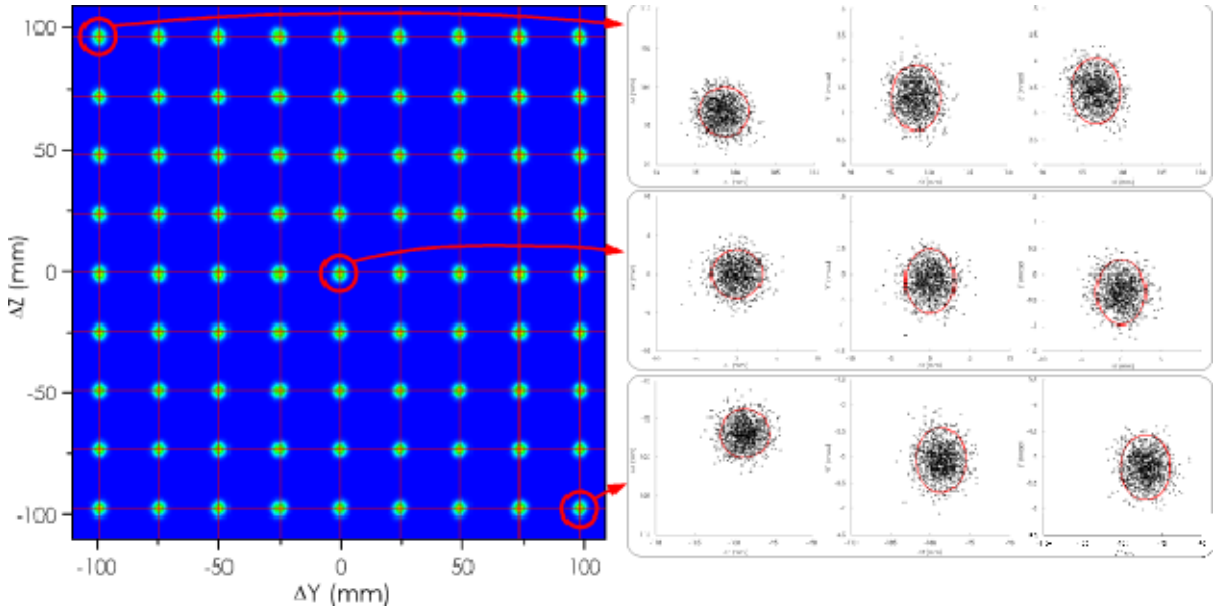

Figure 5: The calculated beam profile at the isocenter (left). The calculated phase-space distributions for the three beam sports (right). For comparison, the results of linear-optics calculations are also plotted and are shown by the red ellipses.

A beam-profile at the isocenter was calculated where the kick angles of SCM-X and SCM-Y were varied to provide 81 beam spots. Although the initial results of the calculated beam spots have displacement in the spot position due to the uniformity of the magnetic field, the displacement can be corrected by finely adjusting the kick angles of the scanning magnets. The calculated beam profile at the isocenter for a beam energy of E=430 MeV/u after the correction is shown in Fig. 5. Furthermore, phase-space distributions for the three beam spots are provided in the right figure. For comparison, the results of linear beam-optics calculations are also plotted, and are shown by the red ellipses. As can be seen in the figures, the results of the two independent calculations agreed with each other, proving the validity of the final design for the superconducting magnets.

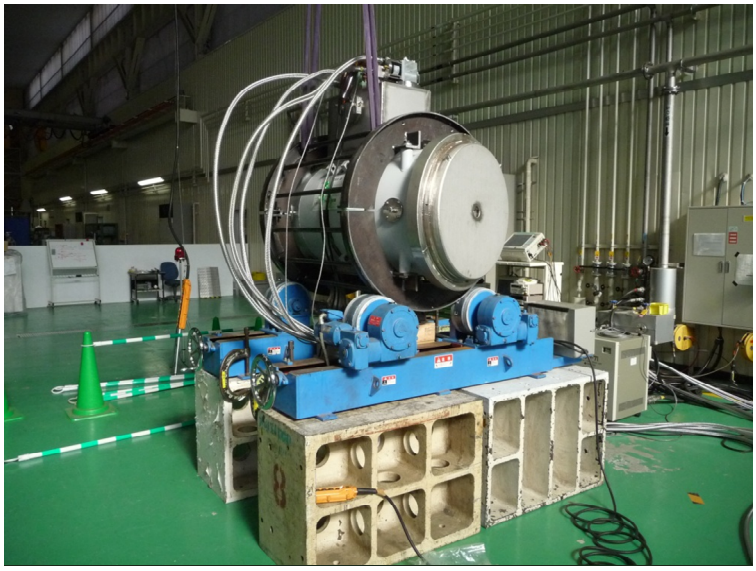

Figure 6: A photograph of the test bench during rotation tests of the model superconducting magnet.

Rotation tests

Since the superconducting magnets on the rotating gantry are to be rotated over ±180 degrees during treatments, an unexpected quenching of the superconducting magnets, as caused by rotations, is a concern. To verify whether this would be an issue, a model superconducting magnet was developed and tested by Toshiba Corporation. This model magnet had a similar structure to that of BM01-BM06, although this model magnet had only a dipole coil. Figure 6 shows a photograph of a test bench during rotation tests. Prior to the tests, the coil of the model magnet was cooled down to below 4K by cryocoolers, which were installed on the magnet. While exciting the superconducting coil with the maximum current, the model magnet was rotated by ±180 degrees, and the coil temperatures in the magnets were monitored. No unexpected temperature increase, which may cause quenching issues, was observed.

Magnetic field measurements

The five superconducting magnets of BM01-BM04 and BM10 (Fig. 7) were constructed, and the other five

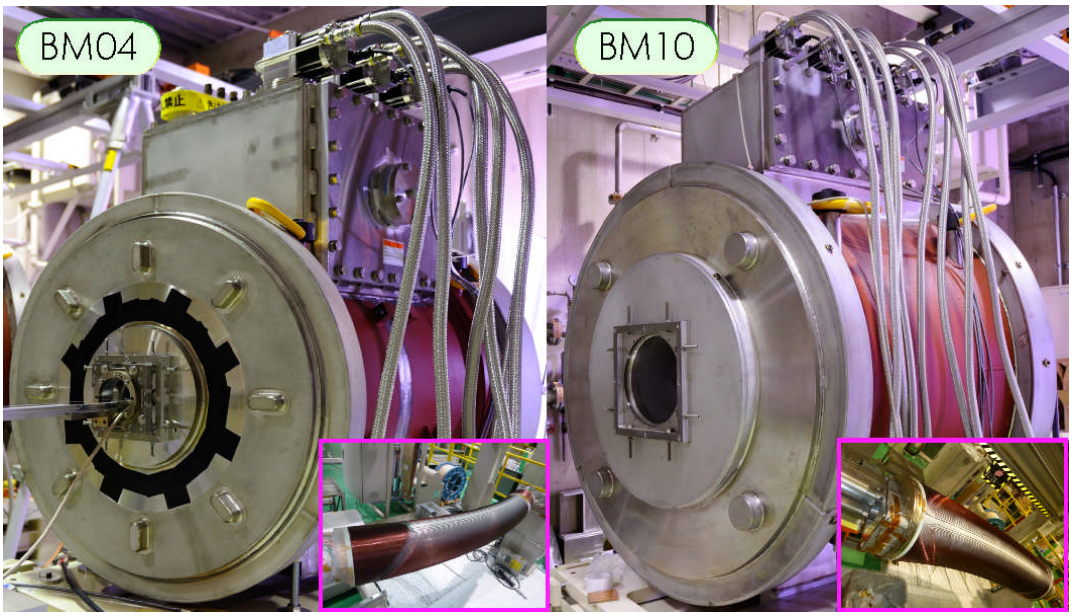

Figure 7: Photographs of the superconducting magnets for BM04 and BM10 being tested.

magnets will be constructed within a year. We first measured the central magnetic field using an NMR probe. The NMR probe was installed in the middle of the magnet, and a current between I=10-240 A was applied. The measured magnetic field, B, and the magnetic field divided by the coil current, B/I, for BM10, are shown by the solid and dashed curves in Fig. 8, respectively. For comparison, the calculated results of B and B/I using the Opera-3d code are also plotted by the filled and open dots in Fig. 8, respectively. We found that the measured and calculated magnetic fields were in agreement, although the measured B/I curve at the maximum current slightly differed from the calculated curve. This discrepancy might be attributable to differences in the estimates of a packing factor for the laminated cold yoke.

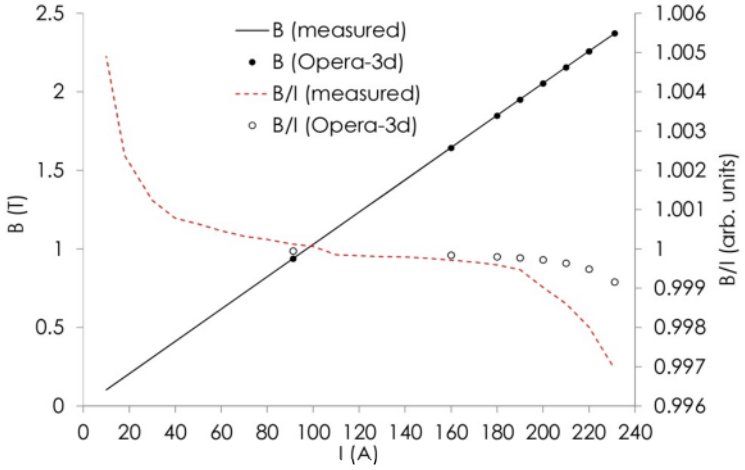

Figure 8: The measured magnetic field, B, and magnetic field divided by the coil current, B/I, as a function of the coil current, I, for BM10. For comparison, the calculated magnetic field is shown by the filled and open dots.

Measurements of the magnetic field distributions along beam trajectories were also performed. The measured magnetic field distributions along the central beam trajectory were integrated over the beam trajectories to determine a BL product and an effective length. The same analysis was performed for the calculated distribution with the Opera-3d code.

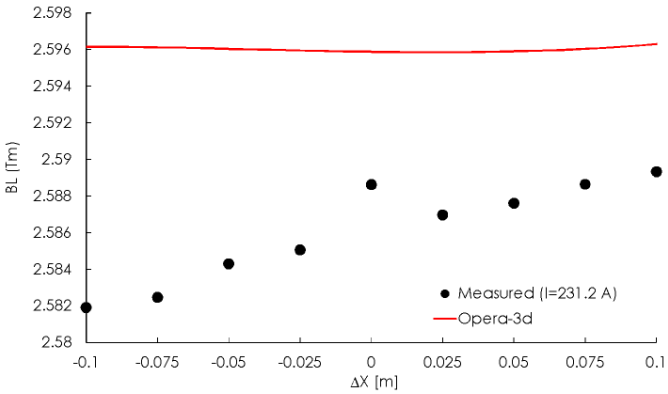

Figure 9: The measured BL products as a function of ΔX. The current for the dipole coil is I=231.2A. The solid curve shows the results calculated with the Opera-3d code.

Fig. 9 shows the BL products of various beam trajectories, as shifted horizontally by ΔX, for the dipole current of I=231.2A. Here, the values of the BL products are normalized, so as to have the same effective length of $L=\rho\theta$=2.8m×22.5° for all the trajectories. Corresponding results, as calculated by the Opera-3d code, are also shown by the solid curves in the figures. The absolute values of the measured BL agreed with the calculated values within an accuracy of a few times 10^{-3}; however the quadrupole component of approximately GL~3.8×10^{-2} T for the measured field can be clearly seen in Fig. 9. We presume that this unexpected quadrupole component might be attributable to an alignment error between the superconducting coil and cold yoke. However, since this magnet has a quadrupole coil, this quadrupole component can be corrected by adding or reducing the current for the quadrupole coil by approximately ΔI=5 A from the applied quadrupole current of I~200 A.

Fast slewing tests

To simulate the multiple flattop operation [5], fast slewing tests were performed. In the tests, the currents of both the dipole and quadrupole coils were maximized to initialize the magnet, and then were decreased by 201 steps. In each step, the coil currents were kept for 0.3 s, where carbon beams would be extracted from accelerators and transported through a beam-transport line including the rotating gantry during this

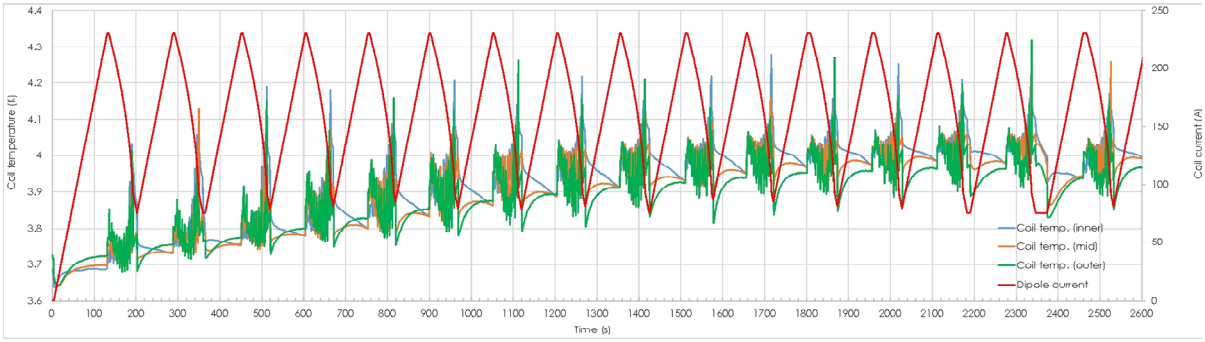

Figure 10: The results of the fast slewing tests for BM10. The average coil temperatures converged below 4K.

constant-current region. Further, the coil temperatures were measured with resistance temperature sensors, which were installed in the inner, middle and outer sides of the coil. A representative result for BM10 is provided in Fig. 10. Although the coil temperature gradually increased, we found that the average coil temperatures converged around 4 K, while the critical temperature is approximately 6.8 K.

Summary

A compact superconducting rotating gantry for heavy-ion therapy is being developed. This isocentric gantry can transport heavy-ion beams with a maximum kinetic energy of 430MeV/*u* to an isocenter over ±180 degrees. Having optimized the layout using the combined-function superconducting magnets, we could design a compact rotating gantry.

All of the superconducting magnets have been designed, and their magnetic fields were calculated using the Opera-3d code. Beam-tracking simulations were performing using the calculated magnetic fields. The simulation results agreed well with those of the linear beam-optics calculation, thus proving the validity of the final design for the superconducting magnets.

Five out of the ten superconducting magnets, as well as the model magnet, have already been manufactured. Rotation tests, magnetic field measurements and fast slewing tests were conducted using these magnets. We did not observe any significant temperature increase, which could cause a quenching problem, using these magnets. Further, the results of the magnetic field measurements roughly agreed with those calculated by the Opera-3d code.

The designed study, as well as major tests of the superconducting magnets, has been completed, and the construction of the superconducting rotating gantry is in progress. The construction of the superconducting rotating gantry will be completed at the end of FY2014, and be commissioned in FY2015.

References

[1] Noda K, Furukawa T, Fujimoto T, *et al.*, New treatment facility for heavy-ion cancer therapy at HIMAC, Nucl. Instrum. Meth. in Phys. Res. B 2010; 266: 2182.

[2] Furukawa T, Inaniwa T, Sato S, *et al.*, Performance of the NIRS fast scanning system for heavy-ion therapy, Med. Phys. 2010; 37: 5672.

[3] Iwata Y, Noda K, Shirai T, *et al.*, Design of a superconducting rotating-gantry for heavy-ion therapy, Phys, Rev. ST. Accel. Beams 2012; 15: 044701.

[4] Opera Version 16, http://www.cobham.com/.

[5] Iwata Y, Kadowaki T, Uchiyama H, *et al.*, Multiple-energy operation with extended flattops at HIMAC, Nucl. Instrum. Meth. in Phys. Res. A 2010; 624: 33.

Session 6: Potential Fields of Research

Heavy Ion Research Project at NIRS-HIMAC

Takeshi Murakami, Tsuyoshi Hamano, Akifumi Fukumura, Kiyomi Eguchi-Kasai[*a], Toshiaki Kokubo[*b], Takashi Shimokawa, Kyosan Yoshikawa, Shigeru Yamada

Research Center for Charged Particle Therapy, National Institute of Radiological Sciences, Chiba, Japan
e-mail address:muraka_t@nirs.go.jp
[*a] *Center for Human Resources Development, National Institute of Radiological Sciences, Chiba, Japan*
[*b] *Fundamental Technology Center, National Institute of Radiological Sciences, Chiba, Japan*

Abstract

HIMAC has been successfully carrying out cancer treatments using carbon beams since 1994. Although it is constructed for medical purposes, it supplies the beam time for research projects of a wide range of science. It is realized by operating the facility 24 hours a day and supplying the beams to basic-science programs during the night and on weekends, while the daytime is devoted to clinical use. Since the various beams are requested by the science projects, the accelerator condition must be changed twice a day. It allows an efficient use of the facility, and produces much outcome, although it requires the laborious and difficult operation of the facility. The present status of the facility and an outline of the basic-science programs are described.

Introduction

The Japanese government launched a campaign entitled the "Comprehensive 10 Year Strategy for Cancer Control" in 1983. Heavy Ion Medical Accelerator in Chiba (HIMAC), proposed by NIRS, was adopted as one of the major projects supported by this campaign. The purpose of HIMAC was to investigate both the effectiveness and extent of heavy-ion therapy for cancer treatment. The construction of HIMAC was completed in 1993 [1]. After half a year of accelerator conditioning and pre-clinical studies of the physical and biological properties of heavy ions, clinical studies began in June of 1994.

Accelerators that can deliver heavy-ion beams with energies of around a few hundred MeV/nucleon are very rare in the world. Supplying HIMAC beams to other fields without interfering with the daily clinical use was therefore strongly desired, although it was constructed for medical purposes. High-quality treatment technology also requires detailed knowledge concerning beam-material interaction processes. Basic-science programs involving researchers both inside and outside of the institute started in the fall of 1994.

Applying a large accelerator for clinical use was highly challenging subject. Obviously, the instruments of clinical use must be reliable and stable. Many people cast doubt on applying a large and complex accelerator, such as HIMAC, to a medical site. Furthermore, the dual-purpose use, i.e. clinical/research use, adds the other possible difficulty of coexisting clinical use and basic-science programs. Basic-science studies require a variety of ion beams, i.e. ion species, energies, intensities, and spot sizes, while clinical studies employ the same beam under definite conditions. Thus, all accelerator conditions must be changed from one purpose to another.

The research activities at HIMAC include radiology, nuclear physics, atomic and molecular physics, radiation chemistry, engineering, and biology, in addition to medical applications. For nearly 20 years, HIMAC has continued to provide the beams for these two purposes successfully. Furthermore, the cooperation between the different disciplines has been proven to be very productive and innovative.

Accelerator and irradiation rooms

1. Accelerator structure

Figure 1 gives a cut-away view of the HIMAC facility. HIMAC comprises ion sources, an injector, two synchrotron rings, a beam-transport system, three treatment rooms, and four experiment rooms. The major parts of the accelerator were constructed 20 m deep underground, because the facility is located in a densely populated area, and thus the outside appearance is important.

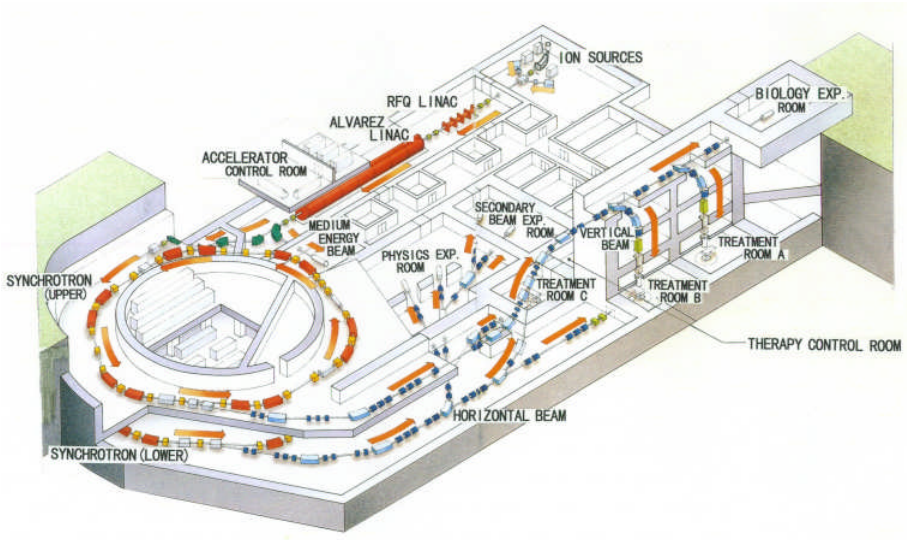

Fig. 1. Cut-away view of the HIMAC facility

A brief outline of the accelerator is given in Table 1. The development and improvement of ion sources and accelerators, including supplying new ion species, sophisticating the beam-transport system as pulse operation, and constructing a new beam course, continued after the official inauguration of the facility. Now, ion species available for basic-science studies range from the proton to Xe, including some unstable nuclei.

Table 1. Outline of the accelerator parameters

Ion source	PIG, 10GHz-ECR, and 18GHz-ECR	8 keV/nucleon
		Ion species: p to Xe
Injector	RFQ linac (0.6 m ϕ x 7.3 m long)	800 keV/ nucleon
	Alvarez linac (2.2 m ϕ x 24 m long)	6 MeV/ nucleon
Main accelerator	Synchrotron (42 m ϕ)	100 - 800 MeV / nucleon
		repetition rate: 3.3 seconds
Irradiation rooms	3 treatment rooms	
	4 experiment rooms	

It is a distinctive feature of HIMAC that the synchrotron has two “identical” rings (upper and lower rings). Three ion sources are in operation, and all of magnets of the injector section are pulse-operated ones. The beams from the injector are deflected from pulse to pulse in three directions, i.e. direct use of the injector beams and injection into the two rings. Thus, three user groups can share the beam time. The versatility of the facility is very high, because three user groups can request different ion species, and the beam energies of the two rings are independent.

2. Experiment rooms

There are four experiment rooms: the general-physics experiment room, the secondary beam experiment room, the biology experiment room, and the medium-energy experiment room.

2.1. General-physics experiment room

The highest and most intensive beams are available in the general-physics experiment room. Two beam courses, PH1 and PH2, are introduced into this room under vacuum all the way. In many cases, the targets and detectors are placed under atmospheric pressure, because the beams have a long residual range in air. Some groups prepare an irradiation chamber of their own style, directly connected to the beam line in order to avoid any slight change in the energy or scattering of the ions or electrons.

2.2. Secondary beam experiment room

Secondary beams produced by projectile fragmentation processes are introduced into the secondary beam experiment room, as shown in Fig.2. Beams ranging from Li through Mn isotopes, as well as ^{11}C, have been used in various experiments. There are two beam courses. One is equipped with a pair of large scintillation detectors, and is mainly used for medical-related experiments. A scanning system was also installed for this beam course. In the other course, beams are transported under vacuum, and can be extracted through a thin window, similar to PH1 or PH2. Users prepare the entire measuring system when using this course.

Fig 2. Secondary beam experiment room

2.3. Biology experiment room

The biology experiment room is equipped with a beam-delivery system similar to those in the treatment rooms. It delivers a uniform field with a diameter of typically 10 cm for various ion species. The residual range can be varied by an energy degrader made of acrylic resin. Small animals, such as mice and rats, as well as cultured cells, can be irradiated in the biology experiment room. In order to reduce the extra time necessary for sample changing, a “sample changer”, which is a remote controlled sliding bed that holds irradiation sample holders, was installed, as shown in Fig. 3. Combining the dose-monitoring system and the sample changer, several sample holders can be set and be irradiated in a predetermined sequence. Some of the instruments necessary for biology experiments, including incubators, clean benches, a flow cytometer,

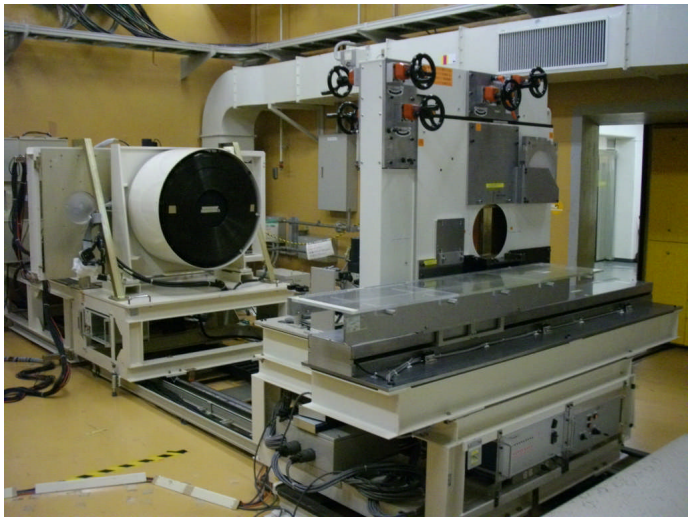

Fig 3. Biology experiment room

and microscopes, are available in a working room next to the irradiation room. These instruments and equipment are indispensable, especially for outside users.

Recently, non-biology researchers, such as in the fields of chemistry or physics, began to use a uniform large field available in the biology experiment room. These groups are called PIB, i.e. acronym of Physics In Biology. For example, some chemistry experiments collect data determining the relation between LET, or dose, and the quantity of some reaction products. Apparatus in the biology experiment room easily realize these measurements. Similarly, experiments related to space science, studying cosmic-ray effects on radiation detectors, etc. also often use the equipment in the biology experiment room.

2.4. Medium-energy experiment room

The beams from the injector, 6 MeV/nucleon, are directly transported to the medium-energy experiment room. Various ion species with the same velocity, i.e. the 6 MeV/nucleon, can be obtained.

Schedule and statistics concerning the basic-science programs at HIMAC

1. Operation schedule

HIMAC is operated Monday through Saturday. In the daytime, from 9:00 through 19:00, from Tuesday through Friday, it is devoted to clinical use or related work. Monday is mainly used for the maintenance and conditioning of new beams, etc. Experiments on basic science are carried out during the night and on weekends.

One year is divided into two periods: the 1st term is roughly from April through July, and the 2nd term is from September through the following February. August and March are reserved for large-scale maintenance. Remodeling of the accelerator or target rooms and installing new apparatus are carried out during these maintenance periods. The period depends on the fiscal year system in Japan.

2. Summary of operation

The operation of the HIMAC accelerator in FY2012, from April 2012 through February 2013, is summarized in Fig. 4. The accelerator was operated for about 6,080 hours. The "supply" of synchrotron rings indicates the time during which HIMAC supplied beams for therapy, basic science or device conditioning. The injector supplies beams to the synchrotron or the medium-energy experiment room: "direct use". It should be noted that the unscheduled downtime, denoted as "trouble", was less than 1% of the time. In FY2012, the beam time supplied for clinical use was roughly 2,000 hours for each of the upper and lower ring, the remaining hours were dedicated to basic science.

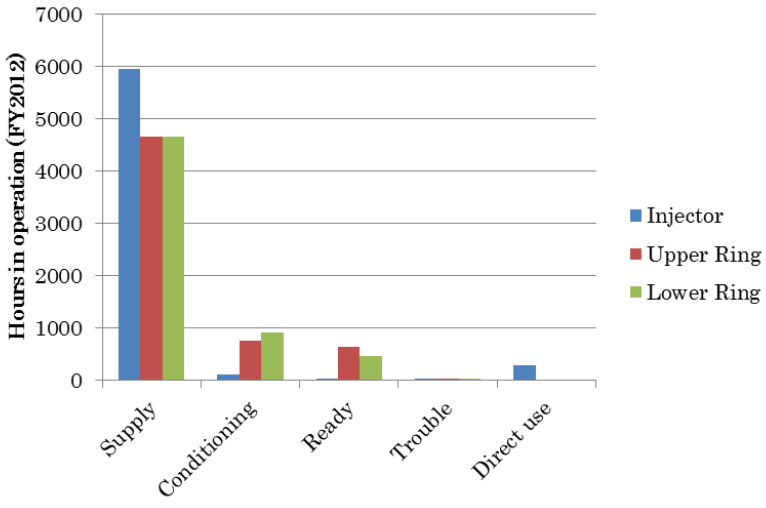

Fig 4. Hours in operation in FY2012

Concerning the basic-science programs, a summary of the beam time becomes more complex. A maximum of three user groups can share the beam time, each group with its own beams. The starting and ending time of each experiment is not the same. Thus, it seems straightforward to sum up the beam time "independently", because each group seems to occupy the whole accelerator. The summary of the beam times from 1994 through 2012 are shown in Fig. 5, categorized as Physics or Biology. The biology time was used for experiments employing cells and small animals. The times of other experiments are categorized as the physics time. More than 5,000 hours were supplied in total. This beam time can be compared to other accelerator facilities dedicated to basic science.

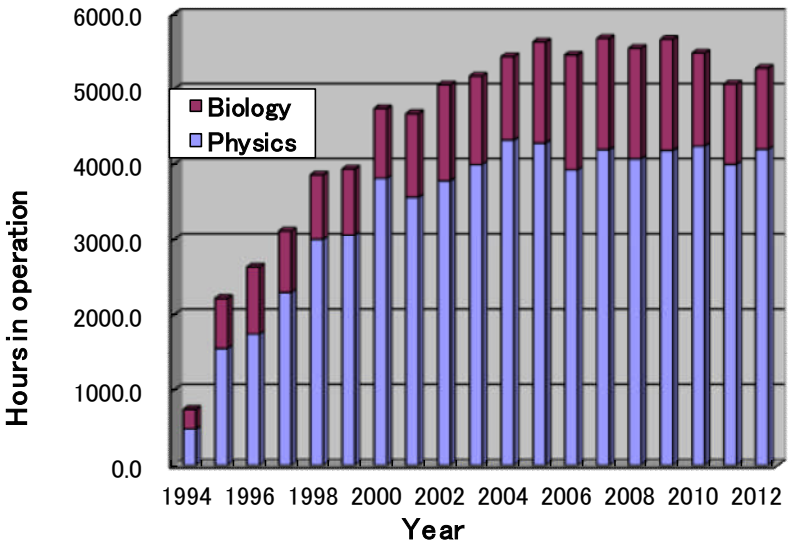

Fig 5. Beam time for Physics and Biology

The reasons why Biology uses the beam for a shorter time than Physics in spite of two ring structures include the following: First, several groups are scheduled in one night for biology experiments, since the irradiation time used for biology experiments is typically 1 or 2 hours each. As a result, un-assigned beam time is not negligible. The other reason is the fact that the groups categorized as PIB are included in the physics time.

3. Evaluation of the proposals and number of participants

Calls for proposals are posted twice a year. NIRS accepts proposals on an equal footing, from inside or outside NIRS, and from Japanese and foreign investigators. All proposals are evaluated by PAC. Virtually all PAC members are researchers outside NIRS, mainly nominated by scientific societies or science institutes. The number of accepted proposals per year has been around 120 in recent years, and roughly half of these involve

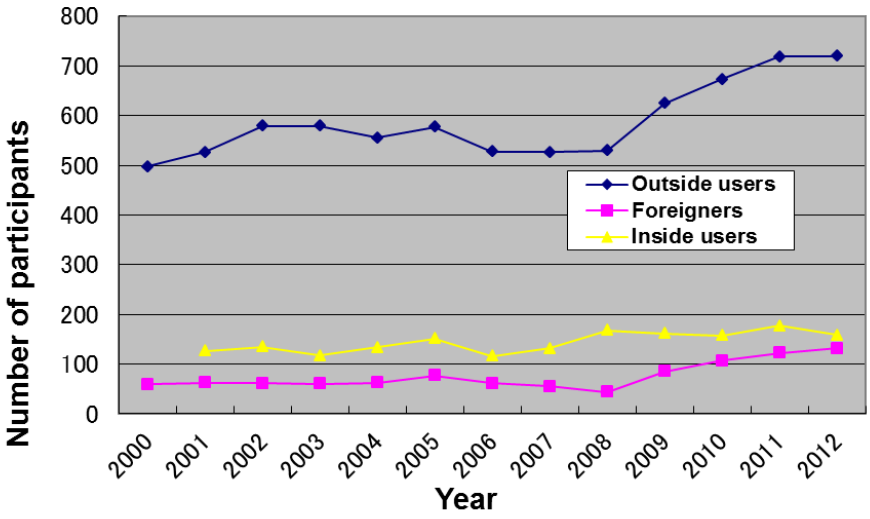

Fig 6. Number of participants in the basic

biology.

The number of participants is shown in Fig. 6. Exceeding 700 users outside of NIRS and 160 users from NIRS joined the basic-science programs last year. About 20% of the participants were non-Japanese.

4. Support system

Due to the broadness of the disciplines of the participants, users who are not accustomed to conducting ion-beam experiments are involved. Therefore, a support system, except for accelerator operation, is very important not only for clinical use but also for basic-science programs. Furthermore, it is essential that the experiment rooms and preparation rooms are kept clean and everything is properly arranged in order to carry out all experiments effectively, since many outside users are involved. The jobs for supporting researchers include: (1) assistance in operating the instruments in the biology experiment room, (2) assistance in necessary measures to carry out animal experiments, (3) maintenance of instruments installed in the experiment rooms, (4) detailed scheduling of the experiment rooms and preparation rooms, (5) consultation for arrangements of the measurement system, (6) consultation concerning the beam characteristics and the method of beam tuning, etc. These jobs are carried out by supporting staff dispatched from a contracted company.

5. Advantages and drawbacks to the dual-purpose use of the accelerator facilities

As stated above, HIMAC is used for the dual-purpose, i.e. clinical/research use, every day. Thus, the accelerator condition must be changed twice every day. This is a heavy burden on the accelerator staff, and it is the major drawbacks of the dual use.

However, it has been found that there are also advantages to the dual-purpose use. First, it provides opportunities for the operators to practice setting up the different conditions, which is especially useful for recruits. The operator's skill and knowledge tend to increase as they continue observing and changing the settings. Second, since reducing the conditioning time is highly important, it provides motivation for improving the operation processes. Third, experiments for basic science require accelerator operation under extreme conditions, such as the highest or lowest energies, most or least-intense beams, extraordinarily stable beam extraction, etc., while relatively fixed conditions are employed in clinical use. Operation under extreme conditions leads to improving the tuning processes as well as upgrading the hardware. Those improvements result in a more stable operation and higher-quality beams for clinical use. Furthermore, dormant problems tend to become known in an early stage.

Research activities

Some of the experiments are briefly described here. Readers should refer to the annual report [2] for more information.

1. Basic data compilation and R&D for medical physics

Basic data, such as LET or secondary particle production rates after passing through beam shaping devices are desired in various disciplines. Thus those measurements have been continued using various tools and by various groups inside and outside NIRS.

Neutron production cross section is also a concern for a lot of researchers. Main areas of those data are (1) evaluation of late effect accompanying particle therapy, and (2) design and evaluation of shielding of an accelerator facility. The systematic data for the design of the building of high energy heavy ion accelerators are compiled at HIMAC.

2. Radiobiology experiments

A large biology group, including both inside and outside users, is organized at HIMAC. Concerning basic data, such as RBE values determined using cultured cells, different tumor cells show different responses to radiation. It is therefore easily imaginable that a sizable effort must be paid to obtain systematic data.

Mice are the most common animals used in biology experiments at HIMAC. About 4,000 mice were utilized last year. Cages for mice or rats are prepared for temporary use before and after irradiation. Necessary processes for animal experiments, including scientific and ethical evaluation of planned experiments and the prevention of contamination, are strictly applied.

2.1. Visualization of track structure

Heavy particle irradiation produces complex DNA double strand breaks (DSBs) [3]. Those breaks arise from primary ionization events along the particle trajectory, and from ionization by secondary electrons which can create low linear energy transfer (LET) damage within but also distant from the track, i.e. so called truck structure. Using imaging with deconvolution, it was shown that at 8 hours after exposure to Fe (200 keV/mm) ions, γH2AX foci forming at DSBs within the particle track are large and encompass multiple smaller and closely localised foci, which we designate as clustered γH2AX foci. These foci are repaired with slow kinetics by DNA non-homologous end-joining (NHEJ) in G1 phase with the magnitude of complexity diminishing with time. These clustered foci (containing 10 or more individual foci) represent a signature of DSBs caused by high LET heavy particle radiation. We also identified simple γH2AX foci distant from the track, which resemble those arising after x-ray exposure, which can be attributed to low LET delta-electron induced DSBs. They are rapidly repaired by NHEJ. Clustered γH2AX foci induced by heavy particle radiation cause prolonged checkpoint arrest compared to simple γH2AX foci following x-ray irradiation. However, mitotic entry was observed when, 10 clustered foci remain.

3. Application of high-quality beams

A project of atomic physics has shown the excellent quality of the high-energy heavy-ion beams from HIMAC, including the observation of a phenomenon so-called “channeling”. The beams must be parallel with an angular divergence of less than 1 mrad and have a small momentum width, and the beams must be very stable for an order of 100 hours to observe this phenomenon. Furthermore, they employed ions with one or two electrons remaining, such as Ar^{17+} or Fe^{25+} ions, for observing resonance phenomena. It is a challenging theme to accelerate such ions to high energies.

3.1. Resonant coherent excitation

Combination of periodic structure of crystal and precise high-energy ion beams can play a role of x-ray lasers. Selective production of the doubly excited state in 464 MeV/u He-like Ar^{16+} ions was accomplished using three-dimensional resonant coherent excitation in a thin foil of silicon crystal [4]. Through a coherent interaction with the periodic crystal field, the Ar^{16+} ions were resonantly excited sequentially from the ground state to the $1s2p$ (^{1}P) state and then $2p^2$ (^{1}D) state in a way analogous to two-color x-ray laser excitation. The periodic crystal fields of 10^{11} V/m in the projectile’s frame are equivalent to the fields generated by x-ray lasers with photon energies of 3139.55 and 3286.95 eV and an energy flux of 10^{16} W/cm^2. The doubly excited state formation was confirmed through observation of the subsequent collisional ionization, Auger ionization, and radiative de-excitation.

4. Industrial application

Industrial application of heavy ion beams has just begun in recent years. The graded energy deposition of heavy ion beam irradiation to polymeric materials was utilized to synthesize a novel proton exchange

membrane (PEM) with the graded density of sulfonic acid groups toward the thickness direction [5]. Stacked Poly(tetrafluoroethylene-co-hexafluoropropylene) (FEP) films were irradiated by Xe^{54+} ion beam with the energy of 6 MeV/u under a vacuum condition. The induced trapped radicals by the irradiation were measured by electron spin resonance (ESR) spectroscopy. Irradiated films were grafted with styrene monomer and then sulfonated. The membrane electrode assembly (MEA) fabricated by the function-graded PEM showed improved fuel cell performance in terms of voltage stability.

5. Nuclear physics

Several experiments related to the nuclear physics, including the use of radioactive nuclear beams, are currently ongoing. They include: (1) measurements of the cross section of a projectile and target fragmentation, (2) measurements of nuclear properties, such as magnetic and quadrupole moments, of unstable nuclei, (3) testing of instruments used in unstable nuclear beam experiments at RIKEN.

6. Simulation of cosmic rays

High-energy heavy-ion beams are good simulators of cosmic rays. Thus, many groups from foreign countries, as well as from all over Japan, have conducted experiments to test the effects of cosmic rays. These include: (1) the calibration of many types of detectors used by astronauts, (2) the response of detectors installed in man-made satellites, (3) determination of the response of semiconductor devices to cosmic rays, (4) evaluation of the response of biological samples to cosmic rays, and (5) basic data for predicting the response of satellite walls, etc. to cosmic rays.

Summary

HIMAC, the first medical accelerator in the world, has been satisfactorily carrying out clinical studies since 1994. It also has been delivering heavy-ion beams for research programs in a broad range of basic science areas. The interest in and applications of HIMAC are due to the high quality of beams, the excellent operation of the facility, and the good support system.

References

［1］ Sato K, Yamada S, Ogawa H, et al. Performance of HIMAC. Nucl Phys. 1995;A588: 229c-234c.

［2］ 2012 Annual Report of the Research Project with Heavy Ions at NIRS-HIMAC. NIRS-M-260, HIMAC-140. 2012.

［3］ Izumi-Nakajima N, Brunton B, Watanabe R, et al. Visualisation of γH2AX foci caused by heavy ion particle traversal; distinction between core track versus non-track damage. PLOS ONE, 2013;8: e70107.

［4］ Nakano Y, Suda S, Hatakeyama A, et al. Selective production of the doubly excited 2 p^2 (^{1}D) state in He-like Ar^{16+} ions by resonant coherent excitation. Phys. Rev. 2012; A85: 020701.

［5］ Shiraki F, Yoshikawa T, Oshima A, et al. Development of function-graded proton exchange membrane for PEFC using heavy ion beam irradiation. Nucl. Instr. Meth. B. 2011;269: 1777-81.

The open-radART ion (ORAion) Software Suite

Philipp Steininger, Markus Mehrwald, Markus Neuner, Daniel Kellner, Michael Memelink, Martin Pinzger, Andreas Böhler, Bernhard Mitterlechner, Peter Keuschnigg, Harald Weichenberger, Michaela Mooslechner, Stefan Huber, Elvis Ruznic, Horst Schödl, Jakob Deutschmann, Christoph Gaisberger, Otto Diesenbacher, Andrea Zechner, Robert Meier, Peter Kopp, Felix Ginzinger, Jennifer Ematinger, Evelyn Guttmann-Döttl, Hans-Jürgen Gmeilbauer, Michael Hubauer, Christina Mittendorfer, Felix Sedlmayer, Heinz Deutschmann

Institute for Research And Development on Advanced Radiation Technologies (radART), Salzburg, Austria
University Clinic for Radiotherapy and Radio-Oncology, Salzburg, Austria
medPhoton GmbH, Salzburg, Austria
EBG MedAustron GmbH, Wr. Neustadt, Austria
e-mail address: philipp.steininger@pmu.ac.at

Abstract

This paper outlines the development history of the radiotherapy software open-radART (ORA) over the last ten years. Starting with modules for image acquisition, image processing and spatial registration, the software has gradually grown into a next generation RadioTherapy Software System (RTS²) integrating LINear ACcelerator (LINAC) control and software tooling for adaptive, image-guided treatment protocols. In 2012 the initiating scientific cooperation between the Institute for Research And Development on Advanced Radiation Technologies (radART) and the EGB MedAustron GmbH spawned open-radART ion (ORAion). This term describes the conglomerate of existing and newly developed ORA software modules for clinical operation of the carbon ion facility MedAustron. Furthermore, it denotes the collaborative efforts of both involved parties to translate their radiotherapy experience into the new particle therapy facility's workflows.

In this manuscript the scope and functionality of ORAion, which will be provided to MedAustron to treat the first patient in 2015, is explained. We describe the basic architectural characteristics behind ORA, not least to encourage the community to participate in future developments and research in the form of open source contributions. The ORAion installation at MedAustron will cover the aspects of an Oncology Information System (OIS), treatment beam delivery, patient alignment, image acquisition, image-guided position verification and image reconstruction. In order to give an overview, selected recently developed ORAion software modules such as the software plugins for collision-free operation of the Patient Alignment Imaging Ring (PAIR) system (medPhoton GmbH, Austria) are described in more detail.

1 Introduction and Scope of ORAion

As one of the leading photon centers in Austria with a strong focus on radiotherapy software development, the Institute for Research and Development on Advanced Radiation Technologies (**radART**) of the Paracelsus Medical University (**PMU**) Salzburg entered a scientific collaboration with EBG MedAustron – the provider of Austria's first heavy ion therapy facility **MedAustron** – in January 2012.

1.1 Development History

More than ten years ago from now, the founders of the radART institute have started to work on the software platform **open-radART (ORA)** in close cooperation with the University Clinic for Radiotherapy and Radio-Oncology Salzburg which has simultaneously been the clinical reference site for the software from the very beginning. First developments were made in the field of acquisition, correction as well as spatial registration of radiotherapy simulator x-ray images. From this point in time, driven by the obvious needs of clinical routine,

ORA developments started to grow towards a leading patient administration, clinical document and image management software system.

The establishment of 3D Treatment Planning Systems (TPS) as well as their interfaces in accordance with the Digital Imaging and COmmunications in Medicine (DICOM) standard and its emerging "RT" extensions (RT plan, RT structure sets, RT dose etc.) for radiotherapy encouraged the integration of ORA DICOM connectivity services for DICOM RT object receipt / dispatch and conversion to and from the proprietary format of ORA. On the one hand these central extensions turned the ORA database subsequently into a multimedia Picture Archiving and Communication System (PACS), and on the other hand it promoted integration of more and more TPS features within ORA. The latter developments have entailed capabilities such as holistically configurable physical and geometrical treatment machine models, contouring and optimized block modeling, safety margin tooling, means for volumetric image registration and last but not least scripting features inherent in open-radART's proprietary file format. The scripting mechanisms have enabled automated treatment plan setup (forward planning) based on the very fundamental input data consisting of the planning Computed Tomography (CT), delineations of Organs At Risk (OARs) and target volumes, and entity-related constraints packed into the templates themselves. The support of treatment templates degraded the essential TPS from ORA's point of view continuously into a pure dose calculation and optimization engine in the pre-interventional phase and simultaneously paved ORA's way for adaptive treatment protocols in the intra-interventional phase.

The radART institute's imaging-related research and developments headed gradually to image quality improvements in flat panel imaging [1] which has been a fundamental technological key factor for intra-interventional planar and volumetric imaging in radiotherapy. The integration of resultant image acquisition, calibration and correction algorithms with ORA, along with the implementation of bi-directional online interfaces for controlling and monitoring the LINear ACcelerator (LINAC) machine parameters made ORA an image-focused Record and Verify System (RVS). Integrating and clinically validating the aforementioned tools and pipelines which enable adaptive treatment protocols grew ORA into a next generation RadioTherapy Software System (RTS²) covering much more aspects than the traditional delivery of static treatment plans and accumulation of the dose record. One example reinforcing our software integration approach has been the early clinical release of an online, adaptive, aperture-based image-guided strategy to treat prostate cancer [2]. Making use of the tightly integrated imaging modules including online localization and spatial registration of the anatomy on the one hand, and correcting for the detected inter- and intra-fractional variations by automatically adapting the treatment segments utilizing open-radART's template-based scripting integration on the other hand, enabled the realization of this treatment approach.

While continuously researching and developing in the field of image-guided, adaptive radiotherapy the radART institute's roadmap was significantly influenced in 2011. In this year intensive discussions and negotiations between the radART institute and the EBG MedAustron were initiated. Austria's cutting-edge cancer treatment project, the first national particle therapy facility MedAustron, searched for an experienced partner in developing and implementing an integrated radiotherapy software solution. The major goal of the comprehensive collaboration between EGB MedAustron and the radART institute has been to adapt and to extend the ORA software platform such that it enables safe clinical patient treatment at MedAustron. The term **open-radART ion (ORAion)** describes the conglomerate of implied medical software packages on the one side, but simultaneously the collaborative efforts of both parties to translate the radART institute's specialized radiotherapy experience into the particle therapy facility's workflows. In addition to this, it has been an agreed principle to make the gained scientific knowledge available to the public involving open source software distribution and dissemination of research findings.

The cooperation has implicated close interaction of the radART institute on a technical as well as organizational level with international players in the MedAustron project: the European Organization for Nuclear Research (CERN, Switzerland / France) who have cooperated in establishing the particle facility, Cosylab (Slovenia) who deliver accelerator control system components, Centro Nazionale di Adroterapia Oncologica (CNAO, Italy) and Sky Technologies (Italy) who provide the Dose Delivery System (DDS) to MedAustron, and Raysearch Laboratories (Sweden) who provide the carbon ion TPS to name but a few. The radART institute

interacts especially tight with the academic spin-off **medPhoton GmbH** (Austria) who holds the intellectual property of the Patient Alignment Imaging Ring (PAIR) solution which is delivered to all irradiation rooms of MedAustron in cooperation with Buck Engineering and Consulting (BEC, Germany).

1.2 Overview of the open-radART ion Software Suite

The ORAion suite's set of tightly integrated software modules constitutes along with further medical third-party devices and software a complete radiotherapy facility system. As such, the scope and provided functionality of ORAion is easiest comprehensible by illuminating a specific, complete radiotherapy facility installation. When inspecting Figure 1, which schematically shows the planned system setup at the proton and carbon ion treatment center MedAustron, the first obvious finding is that multiple **sites** – a clinical and a non-clinical for research only – are involved. An open-radART site is a closed ORA installation with its own **database (ORA DB)** corresponding to an organizational or logical (business) unit. Typically a radiotherapy facility may get by with a single ORAion installation. However, in order to delimit clinical patient data sets and associated configuration from research data, it may make sense to introduce multiple ORA sites at a facility. The degree of separation can vary from completely independent ORA installations to setups where individual ORA DBs but shared ORA software modules and configurations such as LINAC machine or beamline data are involved. Data sets from a specified ORA site can be accessed and copied to another site if a network connection and proper uni- or bi-directional permissions are configured. If sites are extramurally spread, the **ORA collaboration portal** can be used to exchange data utilizing web services and safe encryption technologies. Additionally, this technology enables non-ORA organizations to share data such as medical findings and DICOM images with ORA facilities for, e.g., consultation purposes.

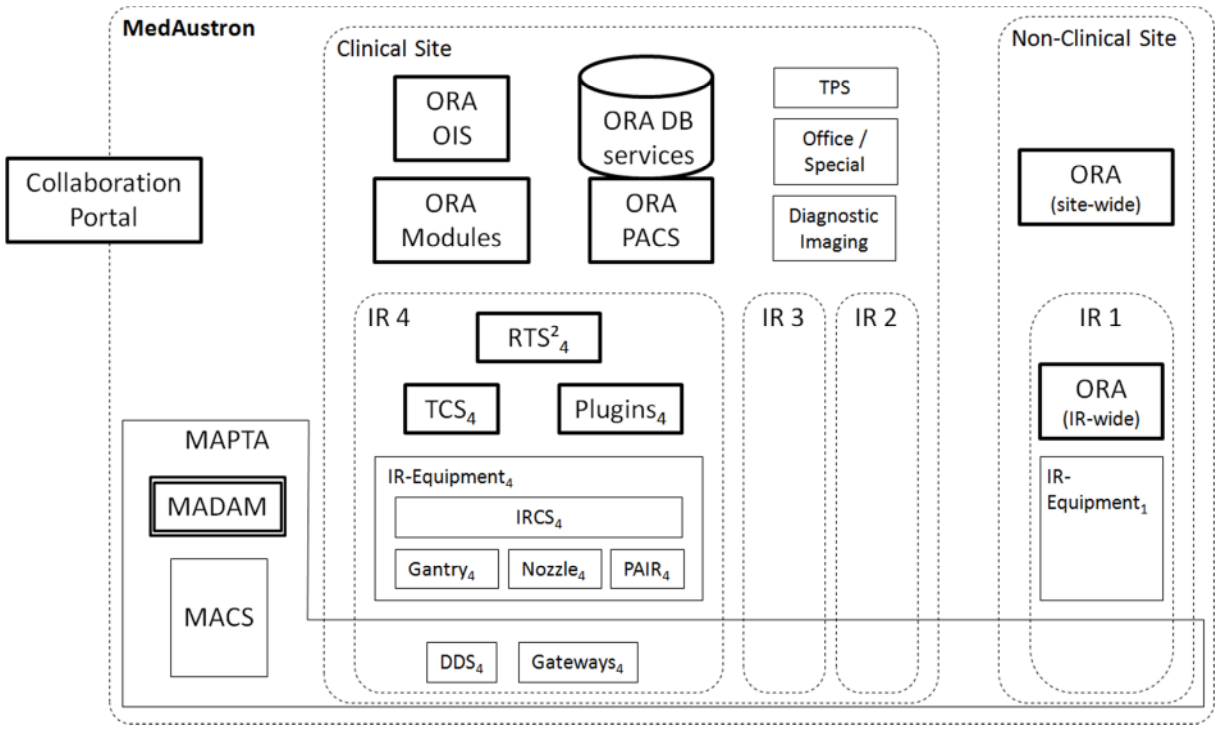

Figure 1: A schematic system overview of the MedAustron particle therapy facility in Wr. Neustadt which outlines the scope and provided functionality by ORAion. Dashed boxes show logical units: irradiation rooms (IR), sites and the MedAustron facility. Boxes with thinner lines group software and/or equipment provided by third parties. Boxes with thicker lines group software functionality covered by ORAion. The medical software frontend of the MedAustron Particle Therapy Accelerator (MAPTA), namely the MedAustron Delivery and Allocation Manager (MADAM), shown with surrounding double bars is not part of ORAion, however, the radART institute provides the software solution to EBG MedAustron. The accompanying text comprises a more detailed description of this overview graphics.

ORAion is grouped into software which is accessible from basically all places of work of the overall site on the one hand, and software which is exclusively available at a specified Irradiation Room (IR) and its associated areas (e.g. the local control room) on the other hand (schematically shown IR 1 of Figure 1).

Referring to the latter category, the central component is the ORA **Treatment Control System (TCS)** which offers a common and coordinated data sink and communication channel for similarly IR-related software. The belonging of software and equipment in Figure 1 is indicated by a subscript index of the respective IR; e.g. TCS_4 is the TCS instance associated with the proton gantry IR (IR 4) at MedAustron. A piece of software connecting to a TCS is referred to as ORA **PlugIn (PI)**. A PI is by definition a software module with an optional Graphical User Interface (GUI) per instance. It groups specific functionalities that are used during treatment or are associated with and wrap the functionality of a specific hardware type, e.g. a proton gantry, a flat panel detector or the multi-leaf collimator of a LINAC. For example, at MedAustron's IR 4 (see Figure 1) there are specified plugins for the gantry, the nozzle and the PAIR system which interface the equipment through a low-level Irradiation Room Control System (IRCS). Other plugins such as the Flat Panel PlugIn (FPPI) interface the underlying hardware directly through direct pathways for establishing fast feedback loops. A special plugin, the MedAustron PlugIn (MAPI) bidirectionally interfaces the medical software frontend of the MedAustron Particle Therapy Accelerator (MAPTA) and makes, thereby, the active scanning capability of MedAustron's core accessible for ORAion. A further important high level PI of the ORAion complex is the **RTS²**. It interfaces and controls underlying lower level PIs and, thereby, coordinates the treatment workflow including in-room barcode-based patient and equipment identification, imaging device movement, x-ray image acquisition, spatial patient setup verification, couch movement in six degrees of freedom, beam delivery based on active scanning (particle therapy) and/or LINAC control (photons, electrons), dose recording and more.

The **ORA DB** and its associated services are one of the most central components which are accessible for all parts of ORAion. On the one hand the database enables direct structured data access via network shares. On the other hand the ORA DB provides more general data access via a generic tree-based query language enabling to define and evaluate complex clinical as well as research questions based on the overall site data including machine configurations. In combination with the aforementioned ORA collaboration portal technology the extended querying mechanisms allow for easily realizing multicentric trials. The PACS services of the ORA DB provide a bidirectional interface based on DICOM to other software systems and equipment, e.g., TPS or diagnostic imaging modalities such as CT workstations. The **ORA Oncology Information System (OIS)** complex, which is similarly accessible from all places of work of the overall site, comprises a variety of modules: patient administration, clinical and study document management, patient and resource scheduling, imaging review, verification imaging review, contouring review, treatment record view, interfaces to external billing systems, spatial registration tooling and more. A subset of the software modules accessible from the OIS is denoted as **ORA Modules** in Figure 1. These modules are partially shared with or integrated into the IR-specific plugins. For example, a 2D/3D registration module for registration of the planning reference CT with intra-interventional planar x-ray images is available in the OIS for review of past setup corrections, and simultaneously in the RTS² for computation of the actual patient misalignment before patient setup correction and beam delivery.

The **MedAustron Delivery and Allocation Manager (MADAM)** – the medical software frontend of MAPTA – is not an integral part of ORAion. However, it has been designed and developed by the radART institute and EBG MedAustron to provide a simple, but flexible and safe bidirectional interface for clinical high level software. This enables the ORAion RTS² to efficiently control treatment delivery while abstracting from the comprehensive micro-workflows involving the virtual accelerator allocator of the MedAustron Control System (MACS), timing and interlock gateways as well as the beamlines' Dose Delivery Systems (DDS).

2 Fundamental Architectural Software Concepts

This section summarizes fundamental concepts and methods which have shaped the architecture and technical software landscape of ORAion.

2.1 Distributed Software Component Communication

ORA Distributed Inter-Process Communication (DIPC) provides a basic bidirectional point-to-point communication infrastructure for ORA system component processes on top of the Internet Protocol suite's Transmission Control Protocol (TCP/IP). It supports communication across process borders; i.e. distributed remote connections. DIPC does not make any implications on the higher level communication protocol; it rather provides a lightweight transport layer for realizing them efficiently.

One of the principles of DIPC-based higher level protocols is reflected by the **ORA command infrastructure**. This library enables fast realization of simple, but also comprehensive and type-safe object-oriented protocols. Instead of implementing protocol commands on a low level, commands can be derived from base classes of this library and customized as required. The transformation of custom commands into low level byte streams (serialization) and back-transformation into objects of the right type (deserialization) is inherent to the infrastructure and guarantees simultaneously type-safety. This type of interfacing protocol makes it feasible to harmonize communication within ORA, and to provide well-defined open interfaces to third parties and research institutions.

The so-called **ORA Distributed Dynamic Slot Invocation (DDSI)** technique utilizes the command infrastructure. This interface type allows for easily developing modules and plugins which have **separate core and GUI processes**. The separation enables outsourcing of computationally expensive processes and/or cores which have rigorous response requirements to dedicated higher performance computers and/or servers while the typically lightweight GUI process can remain at lower performance client machines. This enables flexible system setups depending on the computer equipment of a facility. The DDSI technology is used for forwarding events (signals) along with arbitrary data to their dedicated destination (slot). Using this technique, user-induced events perceived by the GUI are automatically forwarded to the core process (and vice versa) regardless whether the processes are running on the same computer or not.

2.2 Plugin Interaction trough the Treatment Control System

One aspect of the open-radART **TCS** is that it is an "online property database" that manages available concurrent plugins in and/or logically related to a specific IR. Plugins notify the TCS about their properties (e.g. states, device parameters) by registering (publishing) them via DIPC-based connections. Other plugins can manually or automatically receive notifications from the TCS which informs them about property value (e.g. state) changes of one or more specific plugins. The value (state) of a specified property can only be changed by the plugin that registered the property at the TCS; all other plugins have solely read-access. Furthermore, the TCS coordinates messaging between plugins by providing managed communication channels. Using the functionalities offered by the TCS, complex facility installations consisting of many plugins are manageable.

2.3 Centralized Logging

The open-radART **Central Logging System (CLS)** realizes a centralized, synchronized log message sink for all ORA software components of a facility. ORA modules and plugins can log state, access and relevant operational information via a DIPC-based connection to the CLS. Logged records are accessible for both developers and authorized users via a web-based frontend. This approach unburdens tracking and software troubleshooting across a facility.

2.4 RTCore

RTCore is a radiotherapy-specific library that enables object-oriented access to patient- and site-related data of the ORA DB. ORA software modules integrating this library are, for example, able to import and export treatment data in various data formats (e.g. DICOM RT, ORA inf). The data model builds on the powerful Qt property system which makes the library functionality per se accessible from scripting languages. Additionally, a basic set of capabilities is provided by each RTCore class, e.g. bidirectional traversal, copy constructors and

serialization. Object-specific methods round up the range of functions and allow developers to smoothly build applications on top of the data model.

3 Exemplary ORAion Modules and Plugins

Hereinafter selected recent software components of ORAion (see section 1.2), which have been developed based on the principles outlined in the previous section, are briefly described.

3.1 Path Checking Module (PC-M)

For safe collision-free operation of all in-room moving parts all planned trajectories have to be checked for collisions. The **Path Checking Module (PC-M)** is aware of all objects in the IR and represents them in the form of surface models (see Figure 2 left). These models are called static objects because they are always in the IR and do not change during checking. Additionally, there can be dynamic objects. These objects can appear and disappear during the path check. They can also change their appearance (e.g. acquired online patient surface scans). The connections between objects and associated kinematics are realized with joints. Joints can be none, rotational, or translational. The none-joints just change the frame of the consecutive joint. The other two types can change their own tip frame which leads to a movement of the corresponding objects. Joints have their specific maximum acceleration and maximum velocity configured along with further parameters such as identifier and name.

The check of the trajectory is based on so called **Room Control Points (RCP)** which are combined to a RCP sequence (RCPS). The sequence must contain at least two RCPs where the first is always the starting position and all further RCPs give the planned positions of the addressed axis (joints). It is ensured that all axes which are moving stop at the same time. For RCPSs with more than two RCPs all axes reach their position at the same time. The movement between the RCPs is linearly interpolated.

The essential collision avoidance takes the objects at their position and checks whether one object collides with another object in the room. To avoid unnecessary checks for objects which cannot collide, there is an additional parameter for the objects, the so-called ignore list. For example, two consecutive robot axes can never collide because they are already mounted together. The collision check uses partitioning algorithms to be as fast as possible. If the outer bounding box is not colliding it is clear that the object itself is not colliding. In case the outer bounding box is colliding, the object is subdivided into smaller parts which are checked again. This is done until the lowest level, i. e. the actual triangles of the objects, is reached. This makes the collision check both fast and accurate. However, the accuracy is defined by the resolution of the object and is, therefore, independent of the algorithm itself. The calculation of one pair check takes about 5 µs on a single standard CPU. This is sufficiently fast to perform checks also during in-room movements.

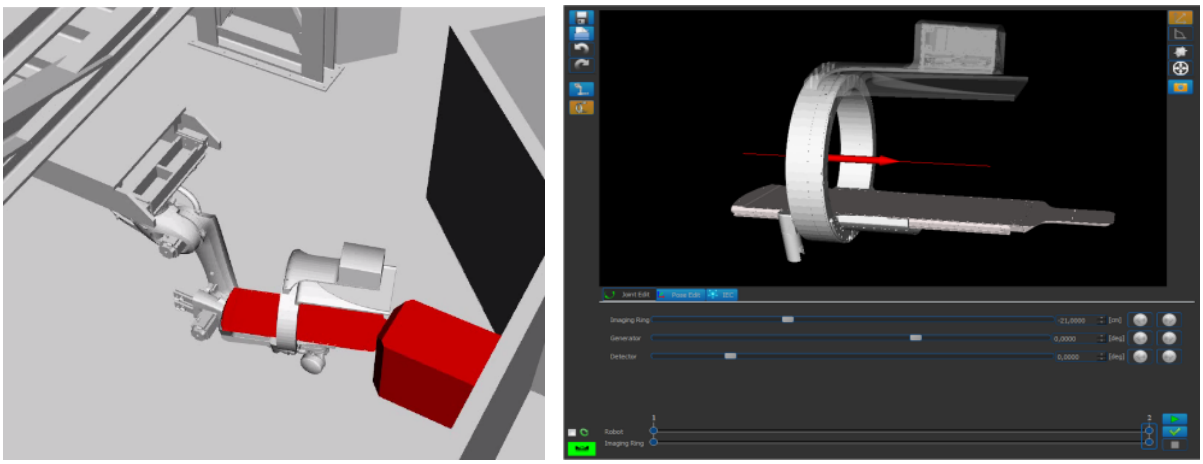

Figure 2: Left: screenshot of a collision check showing a collision between the PAIR table top and a fixed beamline nozzle. Right: Screenshot of the IRPI GUI showing the translational 3D actor moving the PAIR ring.

3.2 Robotic Couch PlugIn (RCPI)

The **Robotic Couch PlugIn (RCPI)** is responsible for communication with the PAIR control system (IRCS at MedAustron) concerning the movement of the patient couch (Patient Alignment of the PAIR system) in six degrees of freedom. Using the RCPI's GUI one is able to plan a trajectory for the robot. Nevertheless, the so planned trajectory is checked for collisions including the whole IR by interfacing the PC-M. There are various intuitive ways to control the position of the table mounted on the robot's tool tip. First, every single axis of the robot can be controlled independently. Second, the couch can be positioned by interactively specifying the parameters according to International Electrotechnical Commision (IEC) standard 61217. A third possibility is the so-called pose mode where a special GUI control allows picking the couch in the 3D room visualization (see Figure 3), and moving and rotating its components. The generated trajectory can be stored and used with other trajectories of different assemblies. If there is no collision detected by the connected PC-M, the trajectory can be sent to the PAIR control system for essential execution. Via the ORA command infrastructure the RCPI can be externally controlled enabling, for example, RTS² to integrate PAIR-based patient alignment.

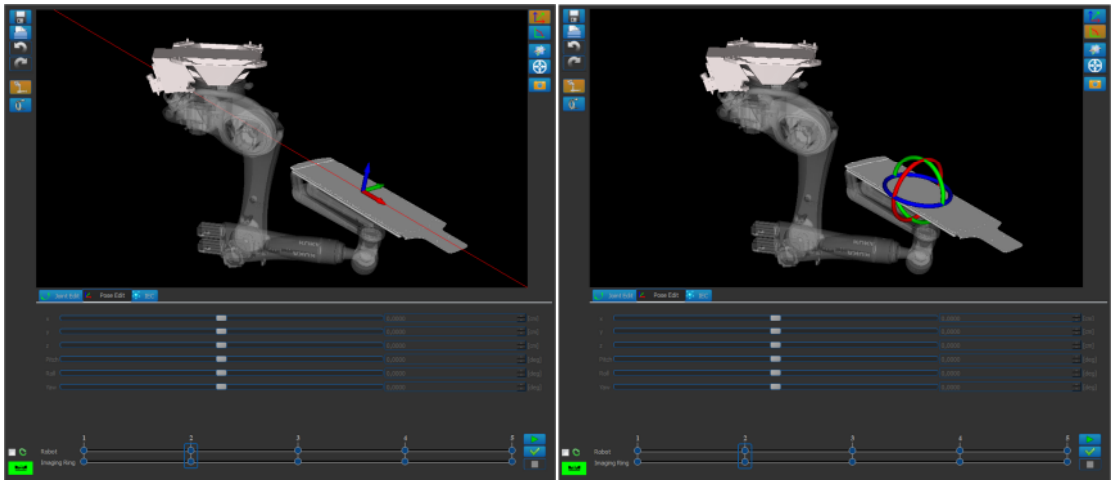

Figure 3: The 3D controls of the RCPI for translation and rotation of the patient couch.

3.3 Imaging Ring PlugIn (IRPI)

The **Imaging Ring PlugIn (IRPI)** is responsible for the communication with the PAIR control system (IRCS at MedAustron) concerning the planning of trajectories of the Imaging Ring of the PAIR system. In the planning mode the PAIR Imaging Ring can be controlled collision-free by using visual sliders to change the position, numerical input to simply enter the desired position and 3D controls to interact with the Imaging Ring directly in the 3D room visualization (see Figure 2 right). The IRPI provides an interface via the ORA command infrastructure to be externally controlled which, for example, enables the RTS² to integrate PAIR-based imaging.

3.4 X-Ray PlugIn (XRPI)

The open-radART **X-Ray PlugIn (XRPI)** is responsible for communicating directly with the x-ray generator. Its main responsibility is setting up the connected generator for coordinating the x-ray emission process. In case of a PAIR installation, the XRPI additionally controls the mechanical components which logically relate to the x-ray unit: the two-dimensional collimation shutters and the filter carousel utilized for exchanging the filter material for dual-energy x-ray imaging. Furthermore, the XRPI distributes feedback from the generator to the TCS in order to allow higher level PIs such as the RTS² to control the imaging workflow. The definition and management of presets and sequences of presets allows physicists to thoroughly test and evaluate the generator system when running the XRPI in medical physics mode (see Figure 4 left).

3.5 Flat Panel PlugIn (FPPI)

The **Flat Panel PlugIn (FPPI)** is a low level plugin to provide image acquisition management by directly interfacing to a flat panel detector. Images can be requested by a higher level application (e.g. CBCT-M or

RTS²) or captured manually via the flat panel plugin's GUI (medical physics mode, see Figure 4 right). The FPPI's main purpose is providing meaningful images of highest quality, ideally displaying absolute dose per pixel. This is achieved by applying various panel-specific corrections to the collected raw data frames before providing them in the form of a projection stream or an averaged, integrated image. The FPPI knows from the TCS at which geometrical position (corrected for flex-induced uncertainties) a frame was captured. Moreover, the FPPI is aware of the radiation-on status per frame and which energy and pulse repetition frequency (PRF) was in use. This enables the FPPI to perform proper corrections, to add proper meta-information to the frames, and to keep track of the total dose a detector has received over lifetime. It also enables the FPPI to extract the actual ghosting artifacts (post glowing of scintillator) from frames, regardless whether there has been radiation on the detector or not. In the plugin's GUI a range of manual acquisition parameters can be changed and saved to a configuration file. The GUI supports manual calibration of the device and reviewing of calibration images (e.g. flood field, bad pixel map). The FPPI is generic enough to interface to panels of different vendors and types. Similarly, it supports different frame rates and resolutions, and also capsules different hardware species, e.g. amorphous silicon detectors as well as gas electron multipliers.

Figure 4: Left: Screenshot of the XRPI GUI in medical physics mode. Right: FPPI GUI in medical physics mode showing an aquired portal image.

3.6 2D/3D Registration (UNO-2-3-REG)

The **Universal N-way Open 2D/3D Registration (UNO-2-3-REG)** module [3] (see Figure 5) enables rigid registration of a 3D volumetric image (e.g. a CT) with an essentially arbitrary number of projective 2D images (e.g. x-rays) for in-room patient setup verification. The transformation parameters (three rotations, three translations) are iteratively optimized with respect to a cost function which assesses the similarity between the x-rays and on-the-fly Digitally Reconstructed Radiographs (DRRs) computed from the volume. In order to restrict similarity evaluation to a certain regions of interest (ROIs) in the x-rays, a so-called auto-masking feature is available. Based on RT structure sets which are typically generated in the pre-planning stage, an entity-specific heuristic produces binary mask images that constrain the cost function evaluation. For example, in the case of pelvis registration, this mechanism enables automatic determination of ROIs that exclude the femora which are prone to move relatively over the treatment course.

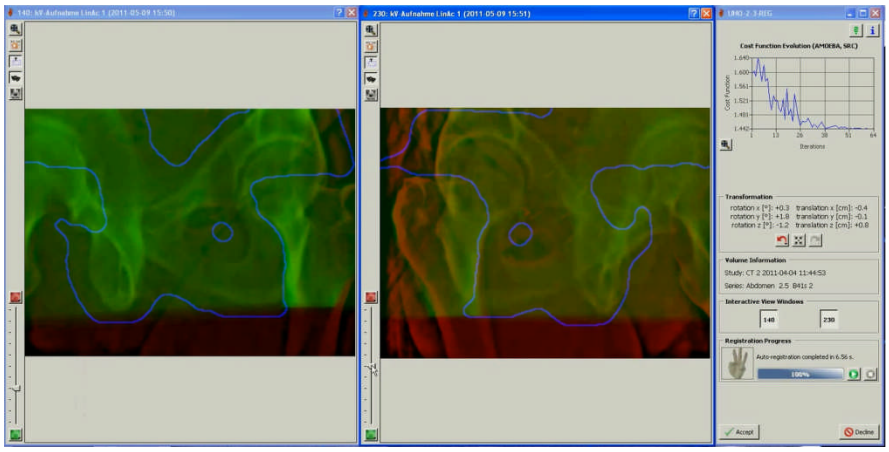

Figure 5:GUI of the UNO-2-3-REG module while computing the patient setup error before treatment delivery based on two orthogonal x-ray images and the planning CT.

3.7 Cone-Beam Computed Tomography Module (CBCT-M)

The Cone-Beam CT Module (CBCT-M) performs volumetric reconstruction from a set of acquired x-ray projections. The module supports offset detector positions for a large Field Of View (FOV), isocentric short-scan reconstruction for acquisition trajectories covering less than 360 degrees, and non-isocentric acquisitions around custom centers of interest (see Figure 6). Reconstruction is performed inline involving the **Graphics Processing Unit (GPU)** in order to increase the overall computational speed. The module is integrated into the CBCT acquisition and patient setup verification workflow handled by the RTS². The CBCT-M retrieves its configuration either from a command line interface or via DIPC from the RTS². Similarly it retrieves the input projection images either from the file system or directly from the FPPI via the ORA command infrastructure during the acquisition.

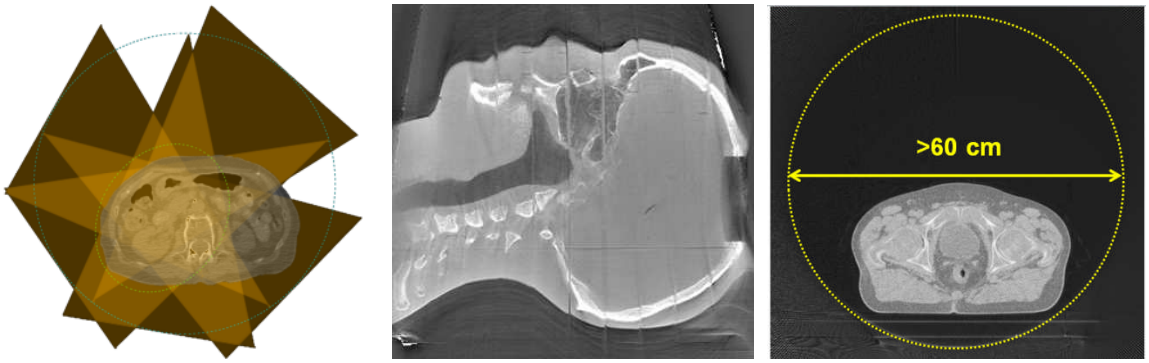

Figure 6: From left to right: Principle non-isocentric limited FOV CBCT, Sagittal short-scan CBCT and large FOV CBCT.

3.8 Portal Definition Module (PD-M)

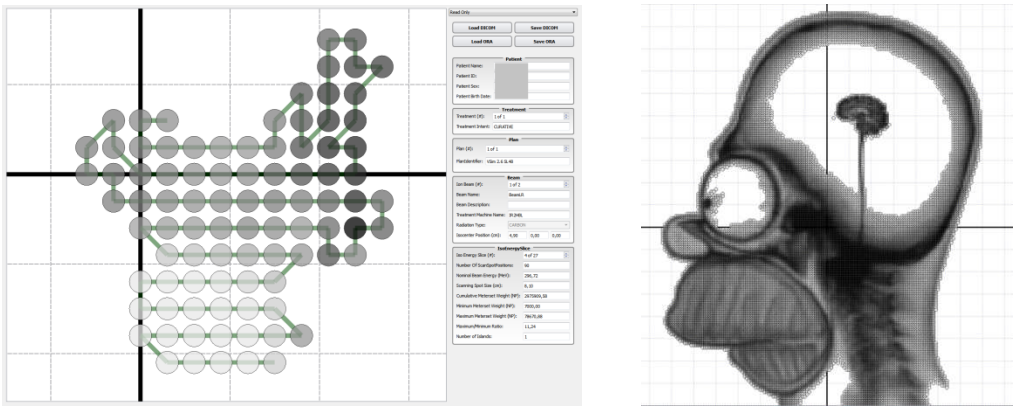

Figure 7:GUI of the PD-M enabling to set up and/or edit treatment plans in medical physics mode.

Due to the abundant degrees of freedom of pencil beam scanning applications, particle therapy treatment plans are typically inversely optimized, comparable with conventional intensity modulated radiotherapy approaches. In specific phases no volumetric input images are available which makes inverse planning impossible. This applies to commissioning processes, daily quality assurance to ensure proper scanning locations and pencil beam shapes, research in biology and physics (e.g. cell irradiations), as well as public relations in order to show the accuracy of the scanning beam with scanned portraits. In this case irradiations must be forwardly planned. The user is explicitly requested to set all relevant beam parameters (e.g. nominal beam energy, position and meter set weight for each scan spot position). The **Portal Definition Module (PD-M)** is a tool with a GUI (see Figure 7) allowing for generating active scanning plans from scratch or to modify existing plans that are not clinically used. In general, the plans may have multiple beams, multiple iso energy slices and, evidently, multiple scan spot positions. Scan spot positions are visualized on a per iso energy slice level or, alternatively, for the whole beam. The corresponding scanning path is equivalent to the order of scan spot positions and is initially set with a preferred scanning direction. Scan paths can also be set manually. Similarly, islands of scan spot positions can be defined. Islands are separately irradiated, i.e. the beam choppers forestall the beam until the scanning magnets have moved the beam to the intended position. All parameters can be set on the appropriate level, i.e. the targeted width of the scan spot positions is set for an iso energy slice whereas the meter set weight can be set separately for each scanning spot position. The image import does not only allow converting images into portrait plans, but can also be used as a starting point for generating plans.

Further PD-M framework functionalities are import and export of the treatment plans to different data formats, as for example DICOM RT Plan with an ion beams sequence. Plan modifications such as parameter editing and drag-and-drop-based GUI actions are directly incorporated in the data model which is also accessible from various scripting languages for research. Generated plans can be exported into the DICOM format or into a format which is compatible with the specific particle accelerator.

3.9 Treatment-To-Machine Conversion Module (T2M)

The **Treatment-To-Machine Conversion Module (T2M)** provides conversion of treatment plan data in DICOM RT or ORA inf format into applicable accelerator (MAPTA) machine files which depend besides the TPS plan on the irradiation room and associated beamline characteristics. The conversion is performed after treatment planning and before irradiation as an integral part of the workflow within RTS². It comprises an underlying reliable and deterministic conversion algorithm. Since the TPS is responsible for dose calculations, the T2M conversion does not modify any parameters that may have an impact on the resulting dose.

3.10 Collaboration Portal

The **open-radART Collaboration Portal** is a web-based platform to safely exchange specified patient centric data from the web into local ORA OIS installations. It is connected to a secure communication platform (ORA RT.net) specialized for interoperable data exchange of radiotherapy-specific data. Based on a flexible architecture it is easy to extend the portal with various use-case-specific input fields and frames (see Figure 8). These can act as standalone portlets, but can also be interconnected through defined interfaces to other portlets. The collaboration portal supports a complex user management system suited for handling organizations and users based on a modern and easy-to-administrate role-based access control system.

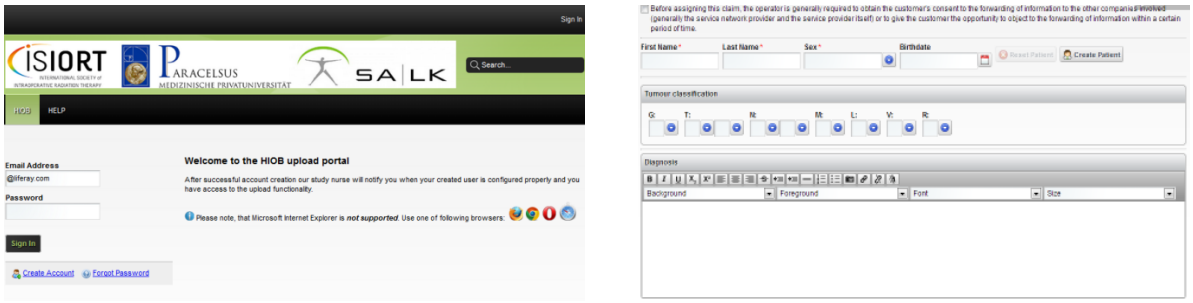

Figure 8: The log-on screen of the HIOB portal. This is a specific ORA collaboration portal installation in Salzburg dedicated to the multicentric international HIOB study (Hypofractionated Whole-Breast Irradiation).

4 Roadmap

The current open-radART ion roadmap is focusing on integrating connecting subsystems and implementing ORAion at MedAustron in order to support the treatment of the first patient at the Austrian carbon ion facility in 2015. In 2014 the first ORAion packages as well as MADAM will be installed at MedAustron for medical commissioning. At the beginning of 2014 a central core library of ORAion will be made open source (www.open-radART.org) which initiates the process of opening the software to the community for research.

5 References

[1] Deutschmann H et al. First clinical release of an online, adaptive, aperture-based image-guided radiotherapy strategy in intensity-modulated radiotherapy to correct for inter- and intrafractional rotations of the prostate. Int J Radiat Oncol Biol Phys. 2012;83(5): 1624-32.

[2] Mooslechner M et al. Analysis of a free-running synchronization artifact correction for MV-imaging with aSi:H flat panels. Med Phys. 2013;40(3): 031906.

[3] Steininger P et al. Auto-masked 2D/3D image registration and its validation with clinical cone-beam computed tomography. Phys Med Biol. 2012;57(13): 4277-92.

Combination of Carbon-ion Irradiation and Immunotherapy in Mouse Models

Takashi Shimokawa

Cancer Metastasis Research Team, Advanced Radiation Biology Research Program,
Research Center for Charged Particle Therapy, National Institute of Radiological Sciences, Chiba, Japan
e-mail address:takshi@nirs.go.jp

Abstract

Carbon-ion (C-ion) radiotherapy (RT) is an advanced radiotherapy effective against tumors that are resistant to conventional radiotherapy. C-ion RT can provide better results, especially local control, due to its biological properties and excellent dose distribution. However, metastasis control is an important issue that needs to be resolved to improve C-ion RT, similar to other types of cancer treatment. It is known that C-ion irradiation tends to prevent metastasis and metastasis-related behaviors, such as invasion and migration, in *in vitro* and *in vivo* assays. However, the underlying mechanisms are still not clearly understood.

Our goal is to identify an optimal combination therapy to use with C-ion RT to prevent distant metastasis. In this study, we evaluated a type of immunotherapy, dendritic cells (DCs) immunotherapy, in combination with C-ion RT. We established mouse metastasis models using three mouse cancer cell lines and two mouse strains. Under conditions where there were no significant effects on the growth of the primary implanted tumor by the treatments, the number of lung metastases was significantly decreased by the combined therapy, but not by C-ion irradiation or DC injection alone. Additionally, the combined therapy suppressed pre-metastatic changes in the lungs. These results clearly indicated that the combination therapy was effective for repressing metastasis.

Introduction

Heavy-ion beams are used for various types of tumor treatments as an advanced type of radiotherapy instead of X-rays or gamma-rays. The heavy-ion beams, such as carbon-ions (C-ion), are able to deliver precise dose localization to solid tumors because the beams form a Bragg peak, where all the energy is lost and abruptly stops [1,10]. Compared to conventional radiotherapy, heavy-ion radiotherapy is a promising method associated with stronger anti-tumor effects and less damage to normal tissues surrounding the tumor [9,21]. However, metastasis control, including micrometastasis, is one of the important issues that still needs to be resolved.

Recently, various immunotherapeutic approaches have been applied in the clinical setting. Dendritic cells (DCs) are involved in the innate immunity, and play important roles in initiating an immune response after receiving signals from pathogens, surrounding cells and their products. Immunotherapy using DCs has been applied as a novel therapeutic strategy for patients with various advanced malignancies. These immunotherapies have the potential to attack not only primary tumor cells, but also distant metastases. However, there still remain several issues, such as the selection of optimal cancer antigens, control of large primary tumors, and so on, associated with using DC-based immunotherapy.

In our laboratory, we have been investigating the effects of carbon ion irradiation on metastasis using clinical materials [6,12-14] and murine models of distant metastasis [16,19], and have also been investigating the adverse reactions [11,17]. We have previously reported that irradiation with a carbon ion beam upregulates more membrane-associated immunogenic molecules in murine tumors than gamma-ray irradiation [7] . We observed that surgical resection of the primary tumor after local tumor irradiation significantly decreased distant metastases, whereas surgical resection without irradiation showed no inhibitory effect on distant metastases (unpublished data). These results led us to hypothesize that local carbon ion irradiation induces a systemic response, and that C-ion radiotherapy (RT) has the potential to provide highly curative effects, even for distant metastases, when combined with systemic immunotherapy.

In this study, the efficacy of this combination therapy using the injection of immature DCs and C-ion RT was investigated in *in vivo* murine metastatic models.

Materials and methods

1. Mice and cancer cell lines

C3H/He and C57BL/6J female mice, aged seven to eight weeks old, were purchased from SLC Co., Ltd. (Shizuoka, Japan). Murine carcinoma cell lines, SCCVII (squamous cell carcinoma) and NR-S1 (squamous cell carcinoma), were grown in monolayers in Dulbecco's modified Eagle's medium (DMEM) supplemented with 10% fetal bovine serum and 1% penicillin/streptomycin (Invitrogen, Carlsbad, CA) at 37°C in a humidified atmosphere of 5% CO_2. The study protocol was reviewed and approved by the National Institute of Radiological Sciences Institutional Animal Care and Use Committee (protocol No. 18-2015).

2. Preparation of bone marrow-derived immature dendritic cells (DCs)

The preparation of DCs has been described previously [3,18]. In brief, bone marrow cells (2x 10^5/mL) obtained from C3H/He or C57BL/6J female mice were cultured with murine granulocyte-macrophage colony-stimulating factor (20 ng/mL; Wako Pure Chemical Industries, Osaka, Japan) for eight days, resulting in the generation of immature dendritic cells (iDCs), which were preserved by freezing in nitrogen liquid. The ability of the collected immature DCs (iDCs) to induce an immune response was confirmed by lipopolysaccharide (LPS) treatment.

3. Assessment of pulmonary metastasis in mouse models

Seven days before irradiation, mice were inoculated with 1 x 10^6 cancer cells subcutaneously into the right thigh. Growing tumors (7-8 mm in greatest dimension) were irradiated with C-ions using the Heavy Ion Medical Accelerator in Chiba (HIMAC) facility at the NIRS (Figure 1)[10]. Tumor xenografts and cultured cells were irradiated with 290 MeV/nucleon C-ion beams at the center of a spread-out Bragg peak (SOBP) (6

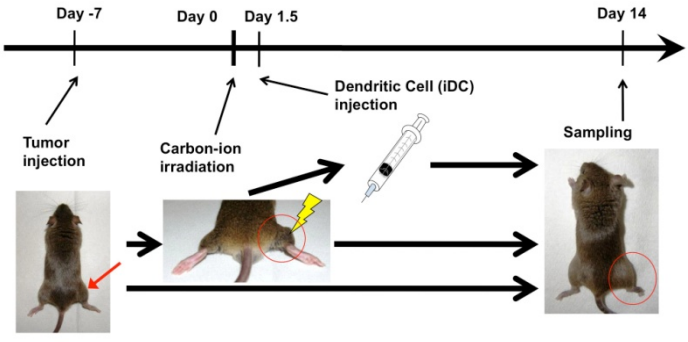

Figure 1. The experimental schema.

cm). The irradiation system and the biophysical characteristics of the beam have been described elsewhere [10]. Thirty-six hours after irradiation, iDCs were injected (1 x 10^6 cells/mouse). The control mice received only anesthesia and no irradiation.

4. Assessment of the tumor growth delay and lung metastasis

After irradiation with C-ions or γ-rays, the tumor size was measured three times per week for two weeks with calipers (n = 7 per group). The tumor volume was calculated according to the following formula: $(a \times b \times c \times \pi) / 6$, where a, b, and c represent the three orthogonal diameters of the tumor, as described previously [2]. The bilateral lungs were initially placed in Bouin solution. The metastatic nodules on the surfaces of all the pulmonary lobes were macroscopically counted (n = 7 per group).

5. Tissue isolation and histological analyses

At two weeks after irradiation, the mice were euthanized by intraperitoneal injection of pentobarbital sodium and subjected to pneumonectomy and tumor extraction. For the histologic analyses, primary tumors were fixed in 10% neutralized formalin, embedded in paraffin, sectioned at a mean thickness of 3 mm, and stained with hematoxylin–eosin. The bilateral lungs were initially placed in Bouin solution for the metastasis assay, and were then washed and fixed in 10% neutralized formalin before being prepared for histology.

The histological studies of the lung tissues were conducted in the same way as for the primary tumors (i.e., hematoxylin–eosin staining). The histologic imaging analyses were performed with a microscope (BX51 bright-field microscope; Olympus, Center Valley, PA) mounted with a camera (DP70; Olympus). The microscopic images were acquired by use of the image acquisition software provided by the manufacturer (DP BSW; Olympus).

Immunohistochemical studies were performed with the streptavidin–biotin immunoperoxidase technique [8] and the Discovery automated system (Ventana Medical Systems,Tucson, AZ).

6. Statistical analysis

The statistical significance of differences in the measured volumes of the primary tumors, numbers of lung metastatic nodules and measured surface areas of the lung metastases was tested by use of the Steel-Dwass test. We considered a value of $p < 0.05$ to be statistically significant.

Results

1. Prevention of tumor growth and lung metastasis by C-ion irradiation

Two mouse models were generated using radioresistant cell line, NR-S1, and a radiosensitive cell line, SCCVII. The studies in both of these models showed that C-ion irradiation could prevent tumor growth significantly better than gamma irradiation (Figure 2A) [15]. Additionally, local irradiation with C-ions dramatically inhibited the incidence of lung metastasis. Even low-dose irradiation (~10 Gy of C-ions), which did not inhibit the growth of the primary tumors, decreased the number of metastatic nodules by >50% (Figure 2B) [20].

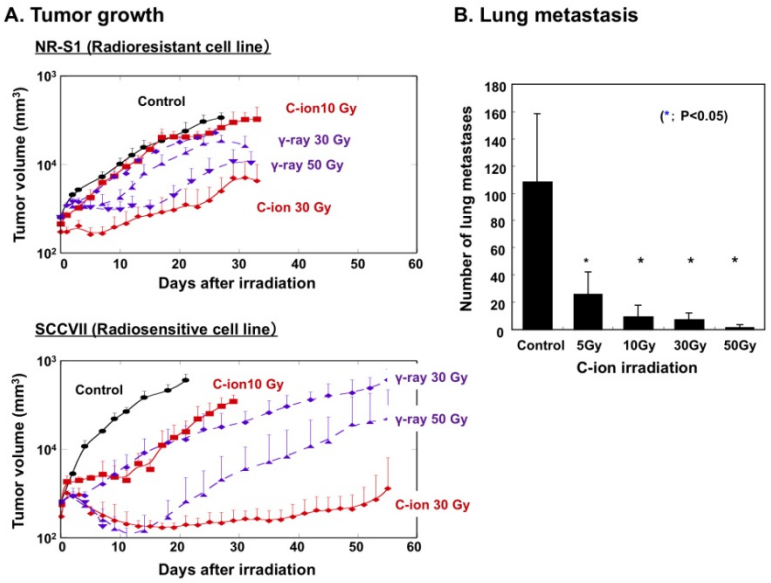

Figure 2. Local effects of C-ion irradiation.

These results clearly indicated that radiation treatment might be able to prevent distant metastasis, and this effect is independent from the inhibition of the growth of the irradiated primary tumor.

2. Evaluation of combined therapy using carbon ions and DCs

C-ion treatment dramatically reduced the distant metastasis, however, the underlying mechanism(s) was unclear. Since high dose irradiation inhibits tumor growth, it is difficult to evaluate the nature of C-ion induced metastasis inhibition. Namely, it is unclear whether such irradiation has a direct effect on the metastatic process, such as the invasive potential, or it is just a consequence of growth inhibition (Figure 3). To focus on the metastasis-related effects of C-ion irradiation, we chose lower radiation doses, which could not significantly repress the growth of the irradiated tumor.

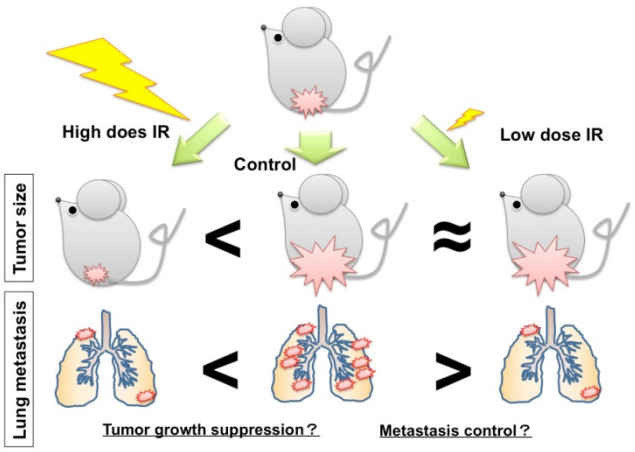

Figure 3. The possible mechanisms of action

Under these conditions, we investigated the effects of the combination of C-ion irradiation and immature DC injection in C3H/He mice bearing NR-S1 murine carcinoma cells.

The tumor growth (volume) increased progressively in the all groups (Figure 4A). The injection of immature DCs did not diminish the tumor volume for two weeks after irradiation. The combination of C-ion irradiation and immature DC injection also did not affect the primary tumor volume.

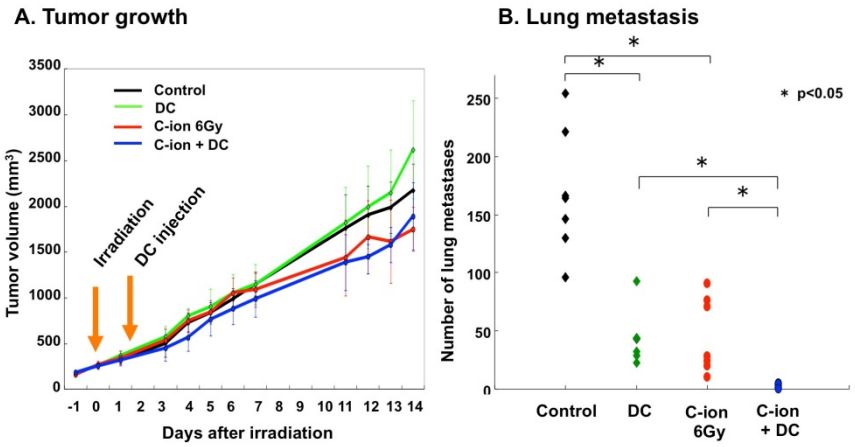

Figure 4. Effects of the combination therapy in the NRS1/C3H model.

The mice in the control group had more than 100 metastatic nodules at two weeks (Figures 4B and 5). When the primary tumors were treated with either immature DCs or C-ion irradiation, the numbers of metastatic nodules were reduced by approximately 75% after the treatment. When the combination of immature DCs and C-ion irradiation was used, the number of lung metastatic nodules was < 5. In addition, no lung metastases developed in one of the seven mice.

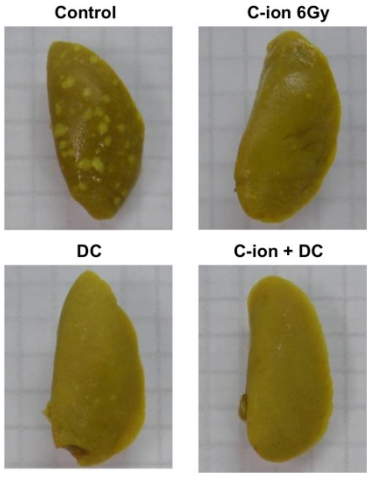

Figure 5. Microscopic images of lung metastasis.

3. Expansion in the range of application of the combination therapy

We showed that immature DCs injection combined with C-ion irradiation significantly suppressed pulmonary metastases in a mouse model using NR-S1 cancer cells and the C3H/He mouse strain. However, this finding was demonstrated in the limited model using only one cancer cell line and one mouse strain. Since the immune response might be different depending on the mouse host strains and tumor, it is necessary to evaluate whether this effect is also applicable to additional tumor and/or mouse strains.

To obtain evidence that the combination therapy using C-ion irradiation and DC-based immunotherapy is likely to be effective against a broad range of tumors/host strains, we established two more mouse metastasis models. Under the same condition where there was no significant primary tumor growth inhibition induced by the treatment, the number of lung metastases was significantly decreased by the combined therapy, but not by single treatment with either C-ion irradiation or immature DCs injection. This result indicated that the combination therapy were effective against these additional tumors and mouse strains.

4. Histochemical analysis

It was previously reported that primary tumors influence distal organs, resulting in later colonization of metastatic cells, and that inflammatory chemoattractants, such as S100A8 and S100A9, were induced by distant primary tumors [4]. The lung tissues of the NRS1-implanted mice exhibited increased expression of S100A8. The S100A8 protein and mRNA expression were not affected by either C-ion irradiation or iDCs treatment (Figure 6). In contrast, the lung tissues of the combination therapy group (C-ion irradiation plus iDCs) showed significant repression of S100A8 at seven days after C-ion irradiation.

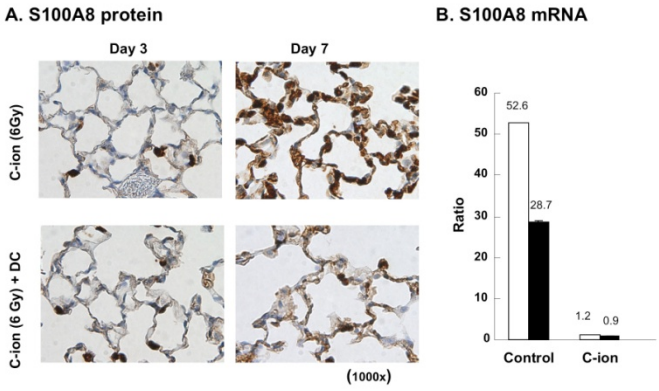

Figure 6. Repression of premetastatic changes by the combination therapy.

Discussion

In this study, we showed that combination therapy with carbon ion irradiation and immature DCs significantly reduced the incidence of lung metastases in mice compared with the respective monotherapies. Ionizing radiation exerts various immunomodulatory effects, in addition to its direct cytotoxicity on tumor cells. Degenerated tumor cells killed by radiation therapy might be a very good source of antigens for DCs.

We used 6 Gy or 2 Gy of carbon ion beams, which is a relatively low dose of irradiation in terms of the clinically used doses. Because high-dose carbon ion irradiation strongly suppressed lung metastases in the current experimental system, we selected the low dose so as to quantify the suppressive effects of each modality on the lung metastases [19] under conditions where the primary tumor was unaffected. In the present study, carbon ion irradiation used alone as a local therapy decreased the number of pulmonary metastases to the same extent as immature DCs alone. Our results raise the possibility that irradiation suppresses lung metastases by inducing immunomodulatory effects.

We previously showed that the S100 proteins were strongly expressed in metastatic tumor cells that originated from nonirradiated primary tumors, whereas their expression was suppressed in the tumor cells that originated from primary tumors subjected to carbon ion irradiation [19]. Calprotectin (S100A8 and S100A9) is a proinflammatory protein that was originally discovered as an immunogenic protein expressed and secreted by neutrophils. Recently, increased levels of S100A8 and S100A9 in distal organs were reported [4]. Several molecules, including tumor necrosis factor-alpha and transforming growth factor-beta, possibly secreted from the primary tumor, may induce the expression of S100A8 and S100A9 in pre-metastatic lungs, in agreement with the ‘‘seed-and-soil’’ hypothesis of metastasis [5]. S100A8 and S100A9, which are expressed in lung macrophages and endothelial cells, induce inflammation-like states that accelerate the migration of primary tumor cells to lung tissues. In this study, S100A8 was used as a marker of the lung pre-metastatic phase. The expression of S100A8 increased in the mice implanted with cancer cells. In contrast, S100A8 staining was not detected in the lungs of mice in the combination treatment group even seven days after irradiation. These

findings support the suppression of metastasis by the combination of carbon-ion radiotherapy and immature DCs.

It is important to obtain direct evidence that the suppression of distant metastasis by the combination therapy is immune-mediated. Additionally, it is also necessary to evaluate the efficiency of the different treatment strategies to induce the reduction of metastasis.

One of the features of carbon ion radiotherapy is that it is less invasive than conventional x-ray or gamma radiation, given the convergence of the dose distribution. An attractive strategy is to combine local therapy, which can produce effects on tumors while minimizing normal tissue damage, with less toxic systemic therapy. This study is the first to show the efficacy of combination therapy with carbon ion radiotherapy and the local injection of immature DCs.

Conclusion

The combination of carbon ion irradiation and the injection of immature DCs significantly inhibits pulmonary metastases. Our findings have clinical implications that may help to improve patient survival after carbon ion radiotherapy.

Acknowledgements

This research was supported in part by JSPS NAKENHI Grant Number 24591857 and by the Research Project Heavy Ions at National Institute of Radiological Sciences (NIRS) –Heavy Ion Medical Accelerator in Chiba (HIMAC).

We would like to thank Drs. K. Kakimi and A. Hosoi (Univ. Tokyo Hospital), Dr. K. Seino (Hokkaido Univ.) and H. Fujita, K. Ando, K. Sato, L. Ma, D. Irie, M. Nakawatari, E. Nakamura, H. Moritake, H. Otsuka, K. Suga, Dr. T. Imai and the FACS support team (NIRS) for kind discussions and technical support.

References

[1] Allen C, Borak TB, Tsujii H, et al. Heavy charged particle radiobiology: Using enhanced biological effectiveness and improved beam focusing to advance cancer therapy. *Mutat Res* 2011;711:150-157.

[2] Ando K, Koike S, Ohira C, et al. Accelerated reoxygenation of a murine fibrosarcoma after carbon-ion radiation. *Int J Radiat Biol* 1999;75:505-512.

[3] Fujita S, Seino K, Sato K, et al. Regulatory dendritic cells act as regulators of acute lethal systemic inflammatory response. *Blood* 2006;107:3656-3664.

[4] Hiratsuka S, Watanabe A, Aburatani H, et al. Tumour-mediated upregulation of chemoattractants and recruitment of myeloid cells predetermines lung metastasis. *Nature cell biology* 2006;8:1369-1375.

[5] Hiratsuka S, Watanabe A, Sakurai Y, et al. The s100a8-serum amyloid a3-tlr4 paracrine cascade establishes a pre-metastatic phase. *Nature cell biology* 2008;10:1349-1355.

[6] Imadome K, Iwakawa M, Nakawatari M, et al. Subtypes of cervical adenosquamous carcinomas classified by epcam expression related to radiosensitivity. *Cancer Biology & Therapy* 2010;10:1019-1026.

[7] Imadome K, Iwakawa M, Nojiri K, et al. Upregulation of stress-response genes with cell cycle arrest induced by carbon ion irradiation in multiple murine tumors models. *Cancer Biology & Therapy* 2008;7:208-217.

[8] Iwakawa M, Ohno T, Imadome K, et al. The radiation-induced cell-death signaling pathway is activated by concurrent use of cisplatin in sequential biopsy specimens from patients with cervical cancer. *Cancer Biol Ther* 2007;6:905-911.

[9] Jensen AD, Munter MW Debus J. Review of clinical experience with ion beam radiotherapy. *Br J Radiol* 2011;84 Spec No 1:S35-47.

[10] Kanai T, Endo M, Minohara S, et al. Biophysical characteristics of himac clinical irradiation system for heavy-ion radiation therapy. *International journal of radiation oncology, biology, physics* 1999;44:201-210.

[11] Moritake T, Fujita H, Yanagisawa M, et al. Strain-dependent damage in mouse lung after carbon ion irradiation. *International Journal of Radiation Oncology Biology Physics* 2012;84:E95-E102.

[12] Nakamura E, Iwakawa M, Furuta R, et al. Villin1, a novel diagnostic marker for cervical adenocarcinoma. *Cancer Biology & Therapy* 2009;8:1146-1153.

[13] Nakamura E, Satoh T, Iwakawa M, et al. Villin1, a diagnostic marker for endometrial adenocarcinoma with high grade nuclear atypia. *Cancer Biology & Therapy* 2011;12:181-190.

[14] Nakawatari M, Iwakawa M, Ohno T, et al. Change in fibroblast growth factor 2 expression as an early phase radiotherapy-responsive marker in sequential biopsy samples from patients with cervical cancer during fractionated radiotherapy. *Cancer* 2010;116:5082-5092.

[15] Nojiri K, Iwakawa M, Ichikawa Y, et al. The proangiogenic factor ephrin-a1 is up-regulated in radioresistant murine tumor by irradiation. *Experimental Biology and Medicine* 2009;234:112-122.

[16] Ohkubo Y, Iwakawa M, Seino KI, et al. Combining carbon ion radiotherapy and local injection of alpha-galactosylceramide-pulsed dendritic cells inhibits lung metastases in an in vivo murine model. *International Journal of Radiation Oncology Biology Physics* 2010;78:1524-1531.

[17] Saito-Fujita T, Iwakawa M, Nakamura E, et al. Attenuated lung fibrosis in interleukin 6 knock-out mice after c-ion irradiation to lung. *Journal of Radiation Research* 2011;52:270-277.

[18] Sato K, Yamashita N, Yamashita N, et al. Regulatory dendritic cells protect mice from murine acute graft-versus-host disease and leukemia relapse. *Immunity* 2003;18:367-379.

[19] Tamaki T, Iwakawa M, Ohno T, et al. Application of carbon-ion beams or gamma-rays on primary tumors does not change the expression profiles of metastatic tumors in an in vivo murine model. *International Journal of Radiation Oncology Biology Physics* 2009;74:210-218.

[20] Tamaki T, Ohno T, Yoshikawa K, et al. Accumulation of cu-62-atsm in tumors correlates with radioresistance in in vivo mouse model. *International Journal of Radiation Oncology Biology Physics* 2008;72:S684-S685.

[21] Tsujii H Kamada T. A review of update clinical results of carbon ion radiotherapy. *Jpn J Clin Oncol* 2012;42:670-685.

Ion Beam Therapy and the Christian Doppler Laboratory

Dietmar Georg[1, 2] and Barbara Knäusl[1, 2]

[1]*Department of Radiation Oncology, Division of Medical Physics, Medical University of Vienna/AKH Vienna*
[2]*Christian Doppler Laboratory for Medical Radiation Research for Radiation Oncology*
e-mail address: dietmar.georg@akhwien.at

Abstract

The recently established Christian Doppler Laboratory for Medical Radiation Research for Radiation Oncology, which started its activities in the beginning of 2012 at the Medical University of Vienna encompasses four workpackages "Multimodality Imaging", "Image guided adaptive radiation therapy", "Normal tissue and tumour radiobiology" and the "Ion beam" workpackage. Ion beam research in the framework of the Christian Doppler Laboratory comprises a widespread field of research topcis and works in close collaboration with all Christian Doppler Laboratory workpackages and MedAustron. The main ion beam research activities are focused on 1) biologically and image guided adaptive ion beam therapy, and 2) novel ion species besides protons and carbon ions. These topics include aspects of dose calculation and optimization, treatment plan comparison and studies on treatment plan robustness as well as conceptual work for treatment adaptations and multimodality treatments.

1. Introduction

The Department of Radiation Oncology, Medical University of Vienna, has as a long-standing research tradition in proton and ion beam therapy. With the clinical implementation of advanced treatment techniques in external beam therapy and brachytherapy during the last decade, such as intensity modulated radiotherapy (IMXT) or image guided MR based brachytherapy (IGBT), it was obvious to benchmark the most advanced treatment techniques with conventional beam qualities against proton beam therapy [1-7]. On the other hand, with the involvement in MedAustron from the very beginning ion beam therapy became gradually a major field of interdisciplinary research at the Medical University of Vienna. Starting with “ENLIGHT” (European Netowork of Light Ion Therapy) the Department of Radiation Oncology became partner in several EC funded ion-beam projects, such as “ULICE” (Union of Light Ion therapy Centers in Europe) or “ENVISION” (European Novel Imaging Systems for Ion therapy), and collaborated closely with MedAustron on other EC funded projects such as “PARTNER” (Particle Training Network for European Radiotherapy) or “RegIonCo” (Regional Ion Therapy Co-operation). Based on these fruitful collaborations in 2012 the Christian Doppler (CD) Laboratory for Medical Radiation Research for Radiation Oncology could be established, in which the Medical University of Vienna and MedAustron collaborate closely in the field of ion beam therapy. CD labs are funded by the Christian Doppler research association after a peer reviewed research application and a hearing with the objective to support collaborations between academia and enterprises/industry.

The overall vision of the CD Laboratory for “Medical Radiation Research for Radiation Oncology” is to perform interdisciplinary research for the optimization of the treatment outcome of radiation oncology. This vision is based on the fact that progress in radiation oncology has always been closely linked with innovations in medical radiation physics and computer sciences, morphological and molecular/biological imaging methodologies, and new insights into the radiobiology of both tumors and normal tissues. At present all disciplines involved in the diagnosis and management of malignant diseases, e.g. radiation and medical oncology, nuclear medicine and diagnostic radiology, as well as radiation biology and medical physics are in a process of very dynamic advancements. Therefore the following multi-disciplinary modules/work packages have been established within the framework of the CD Laboratory:

(1) Multimodality Imaging (MMI) for response assessment: identification of parameters predictive for the tumor response to the therapy or the risk for treatment complications.

(2) Image Guided Adaptive Radiation Therapy: technology development, clinical implementation and clinical validation of adaptive image guided treatment strategies for the optimization of dose conformation to the tumor and improved normal tissue sparing.
(3) Normal Tissue and Tumor Radiobiology: long term visions aim at the investigation and comparison of the mechanisms and biological consequences of irradiation with ion beams and photons, both at a clinical and pre-clinical level.
(4) Ion Beam Therapy: Exploration and expansion of the potential of ion beam therapy, especially with respect to novel ion species and image guided adaptive ion beam therapy.

In the following the achievements and future research directions of workpackage 4 on ion beam therapy are described in more detail.

2. Ion beam therapy - one of the main research foci in the Christian Doppler Laboratory

In brief, the ion beam research activities are focused on 1) biologically and image guided adaptive ion beam therapy, and 2) novel ion species besides protons and carbon ions. Besides these topics that include aspects of dose calculation and optimization, treatment plan comparison and studies on treatment plan robustness, conceptual work on treatment adaptations and multimodality treatment, the CD Laboratory activities are linked to other research groups at the Medical Radiation Physics section, Department of Radiation Oncology, that work on on-line verification of ion beam delivery (in-situ monitoring) [8] as well as basic and applied dosimetry [9]. All these topics are in line with the dedicated white book on "Research Opportunities for Medical Radiation Physics and Radiation Biology" [10], in which a more detailed description and motivation of these research topics can be found.

3. Helium Ion Beam Therapy

Ion beam centers focus mostly on proton and carbon ion therapy. However, there are other ion species like helium or oxygen with great potential for clinical applications. In the frame of the CD Laboratory a flexible pencil beam model has been developed for helium ions and the corresponding calculated dose distributions were validated using Monte Carlo (MC) methods [11,12]. The algorithm was based on the established theory of fluence weighted elemental pencil beam (PB) kernels. Using a new real-time splitting approach, a minimization routine selected the optimal shape for each sub-beam. Dose depositions along the beam path were determined using a look-up table (LUT), whereas data for LUT generation were derived from MC simulations in water using GATE 6.1. For materials other than water, dose depositions were calculated by the algorithm using water-equivalent depth scaling. Lateral beam spreading caused by multiple scattering has been accounted for by implementing a non-local scattering formula developed by Gottschalk. A new nuclear correction was modeled using a Voigt function and implemented by a LUT approach. Validation simulations have been performed using a phantom filled with homogeneous materials or heterogeneous slabs of up to 3 cm. In homogeneous phantoms, maximum range deviations between PB and MC of less than 1.1% and differences in the width of the distal energy falloff of the Bragg-Peak from 80% to 20% of less than 0.1 mm were found, as depicted in Figure 1. Heterogeneous phantoms using layered slabs satisfied a γ -index criterion of 2%/2mm of the local value except for some single voxels. In the framework of these activities existing PB algorithms for protons have been improved as well.

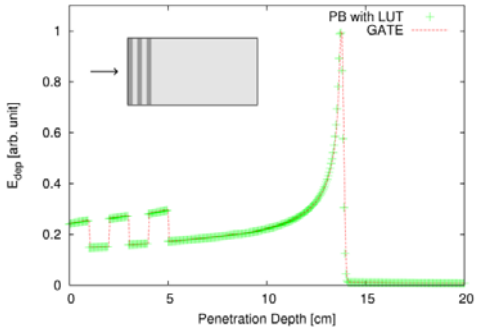

Figure 1: Comparison between GATE and PB calculations, of a Gaussian helium ion beam with σ = 2 mm at 150 MeV/A, hitting a water phantom with three 1 cm thick inserts. The dark grey area was filled with bone, the light grey area with water. longitudinal energy deposition (E_{dep}), lateral energy contributions up to 20 times of the initial sigma were taken into account in the PB calculation; modified from [12].

Furthermore the developed PB algorithm was expanded to allow biologically weighted dose optimization for protons and helium ions and it was integrated into the treatment planning systems (TPS) Hyperion. The relative biological

effectiveness (RBE) of ^{4}He was described using a 'zonal' model including data from literature and different LET regions enabling the TPS module to calculate biologically weighted doses for ^{4}He [13]. With respect to novel ion species the CD Laboratory works in close cooperation with ELEKTA as well.

First plan comparison showed that organs at risk (OAR) received systematically less dose by ^{4}He compared to protons, nevertheless the dosimetric improvements of ^{4}He motivate a more thorough investigation. Especially for pediatric patients which could profit the most from the dosimetric advantages of helium ions. Further investigations will go towards an experimental validation of the 'zonal' RBE model for helium ions and the extension of the PB algorithm for oxygen.

4. Comparative treatment planning and treatment plan robustness

In ion beam therapy organ motion and anatomic changes are especially important for particle beams since variations in the heterogeneity along the beam path have a significant impact on the particles range. Different research projects focused on the assessment of treatment plan robustness against these temporal variations [14,15]. In a recent treatment planning study employing intensity modulated proton therapy (IMPT) plan robustness was evaluated with respect to inter-fractional patient positioning for various beam arrangements (two opposing or individual fields and three/four individual beams) for skull base (SB) and paranasal sinus (PS) patients, as depicted in Figure 2.

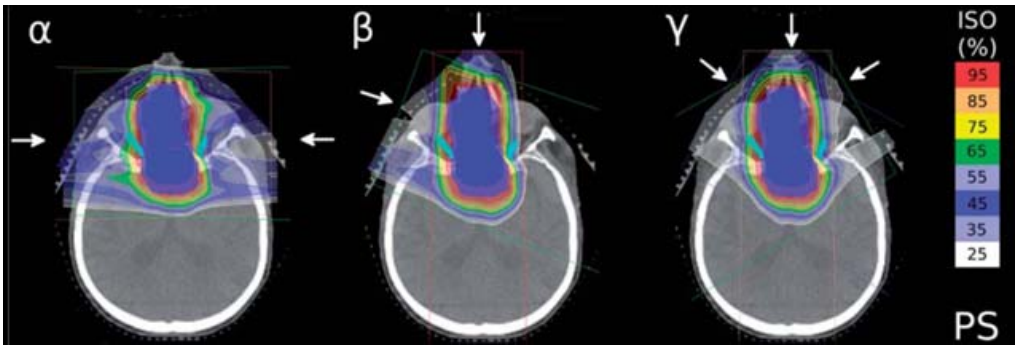

Figure 2: Representative layer of a PS case. The left column depicts beam arrangement α (two lateral opposed beam ports). The central column represents one representative setup of beam arrangement (individual OAR sparing two beam arrangement) while the right column shows the beam arrangement using three beam ports; modified from [15].

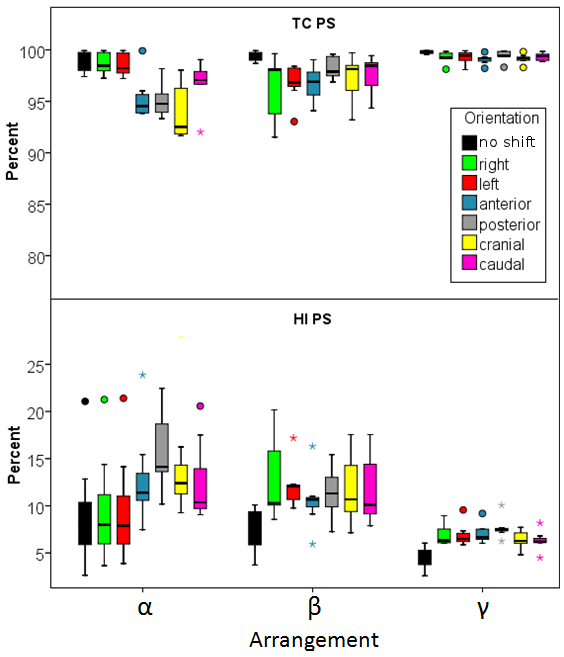

Figure 3: Boxplots representing target coverage (TC) as well as dose homogeneity (HI) for PS patients influenced by translational shifts of the patients for the three beam arrangements; modified from [15].

After optimizing the respective treatment plans dose distributions were recalculated subjected to virtual patient translations along the major anatomical axes. Dose distributions were distorted after introducing shifts. The beam arrangement employing three or four individual beams exhibited the least spread of data regarding target indices, like homogeneity (HI) and conformity (CI), and was consequently considered the most robust, as depicted in Figure 3. This study showed that for cranial IMPT, set-up uncertainties may lead to pronounced deterioration of dose distributions. According to our investigations, multi-beam arrangements were dosimetrically more robust and hence preferable over two beam arrangements.

Furthermore comparative treatment planning studies were performed, which have been the method of choice for comparing one treatment technique against another to evaluate the potential of a new approach against current standards [e.g. 16,17].

In a recently submitted work [17] various combinations of photons, protons and carbon ions were compared for treatment of skull base meningioma. Since anaplastic meningioma lesions are frequently showing an aggressive local growths and a high incidence of tumor recurrences after neurosurgical resection, the rapid dose falloff of particles and the increased RBE of heavy ions such as carbon ions could be of potential benefit leading to an increased local tumor control. In a comparative treatment planning study the advantages of protons and carbon ions over traditional photon therapy were investigated. Two planning target volumes ($PTV_{initial}$ and PTV_{boost}) were delineated for 10 patients (prescribed dose 50 Gy(RBE) and 10Gy(RBE) or higher). Plans for intensity modulated photon therapy (IMXT), proton therapy (IMPT) and carbon ion therapy (^{12}C) were generated assuming a non-gantry scenario for particle beam treatments, shown in Figure 4 for a representative patient.

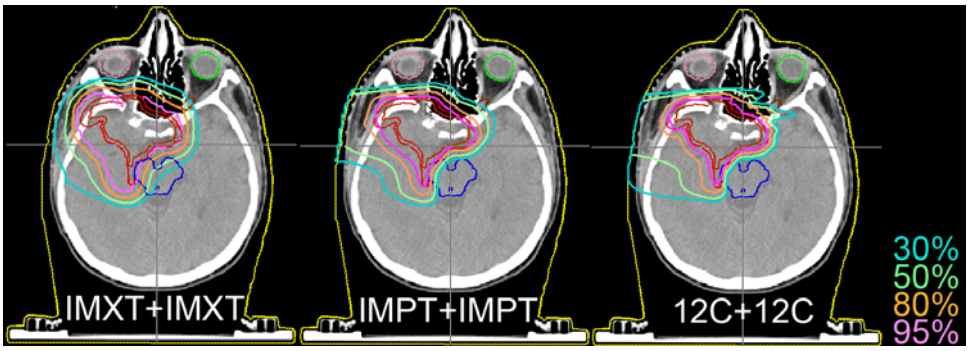

Figure 4: Typical isodose distributions of a representative patient in an axial slice that contains the most relevant OARs. For illustration purposes combined treatment plans for IMXT+IMXT, IMPT+IMPT and ^{12}C+^{12}C (60 Gy(RBE) prescribed dose) were depicted only;

In order to consider particle beam therapy not only as boost opportunity, the following combinations were compared: IMXT+IMXT/IMPT/^{12}C; IMPT+IMPT/^{12}C; and ^{12}C+^{12}C. Highly conformal IMPT and ^{12}C beam plans could be generated with a non-gantry scenario. Furthermore improved OAR sparing favors both sole ^{12}C and/or IMPT plans.

Not only for Meningioma patients, but also for many other indications suitable for ion beam therapy the treatment using fixed beam lines only has to be considered. Proton only treatment rooms are mostly equipped with a gantry, whereas almost all carbon ion centers, with the exception of the HIT center in Heidelberg, use fixed horizontal or vertical beam lines. Moreover, centers using both carbon ions and protons, like CNAO and MedAustron, do not have a gantry in every treatment room. Therefore identifying indications that do not necessarily require a proton gantry for an ideal treatment is essential to gain the full potential of centers which have to include treatments with fixed beam lines into their clinical workflow. In the framework of the "Ion Beam" workpackage of the CD Laboratory a study is initiated that aims to compare the quality and robustness of ion beam treatment plans for the gantry to fixed beam lines for different tumor sites and to evaluate which possible “losses” are associated with ion beam treatment based on fixed beam lines. For selected tumour indications two different approaches for both modalities are explored using protons and carbon ions: one plan is created with horizontal or horizontal plus vertical beams only and the other one with a rotating gantry. To get a widespread overview, the following tumor sites are included in the treatment plan data base: skull base and brain tumors, head and neck, prostate, bone and soft tissue sarcoma and for further investigations also liver, rectum, pancreas and lung cancer patients. Further investigations on the robustness and the feasibility will be initiated. Working in close cooperation with MedAustron this study aims to support the start-up phase of the MedAustron facility and to improve the clinical workflow.

5. Image guided and (biologically) adaptive ion beam therapy

Accounting for temporal variations (“4D-radiotherapy") of the anatomy during radiotherapy, both during (intra-fraction variations) and between fractions (inter-fraction variations), and taking into account temporal variations in tumor biology, is one of the research topics the CD Laboratory. Ongoing research activities in

workpackage 2 focus on ultrafast image registration [18,19] and deformable registration for intra-fraction motion management and adaptive radiotherapy, which can be transferred from photon beam therapy to ion beam therapy. Especially for improving lung cancer treatments image-guided advanced photon and particle beam treatments are promising options. Nevertheless extensive use of imaging increases the overall patient dose. In order to optimize imaging protocols a study was initiated in order to determine the imaging dose for different IGRT solutions used in photon and particle beam therapy [20]. Measurements were performed in an Alderson phantom with TLDs investigating the clinically applied protocols for orthogonal planar kV imaging, stereoscopic imaging, CT scout views, fluoroscopy, CT, 4D-CT and CBCT at five ion beam centers and one conventional radiotherapy department. The overall imaging dose was determined for a patient undergoing a lung tumor irradiation with institute specific protocols. OAR doses depended on imaging modality and OAR position, whereas the dose values were in the order of 1 mGy for planar and stereoscopic imaging and 10–50 mGy for volumetric imaging, except for one CBCT device leading to lower doses. The highest dose per exam (up to 150 mGy to the skin) was recorded for a 3-min fluoroscopy. Overall the study demonstrated that low-dose protocols and protocol optimization can reduce the imaging dose to the patient substantially and could help to include image guidance into clinical routine for particle beam therapy (Figure 5).

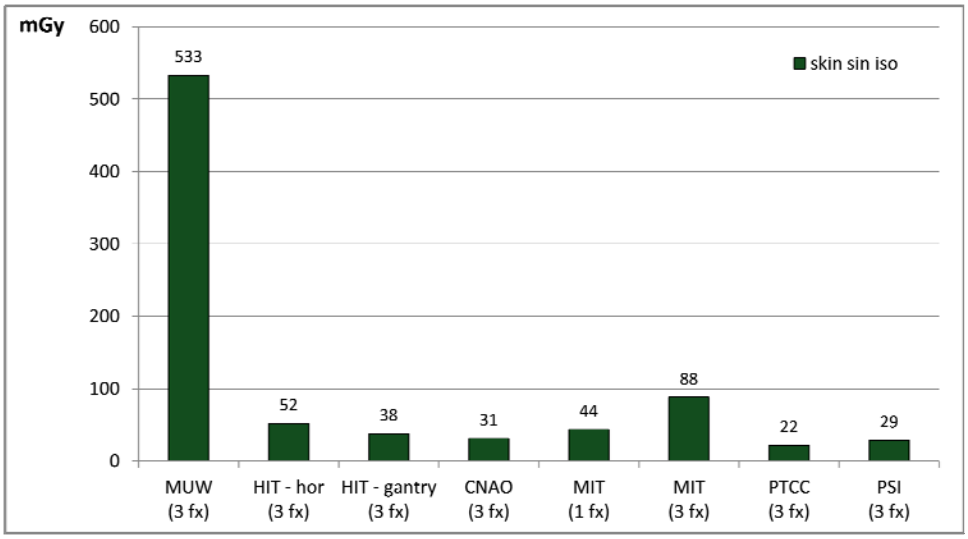

Figure 5: Comparison of the imaging dose for (hypothetical) treatment protocols at the participating centers; modified from [20].

The exploration of multimodality and multi-parametric functional imaging for dose painting with scanned ion beams is another upcoming research topic. In this context the quantification of PET [21] and MR imaging parameters was already investigated. In workpackage 1 of the CD Laboratory a clinical imaging dose response assessment study in prostate cancer patients is performed that is based on multiparametric (DCE, DWI, MRS, T2w) MR imaging data in combination with [11C]-Acetate PET/CT. Thirteen biopsy-confirmed prostate cancer cases were included in a dose painting study using VMAT, protons and HDR brachytherapy. The major aim is to deliver higher treatment doses to the dominant intraprostatic lesions (DIL). Studies on recurrence of prostate cancer after RT show, that local relapses most often occur at the location of the dominant intra-prostatic lesions [22] and therefore dose escalation could improve local control and reduce disease recurrences even proximity of bladder and rectum prevents arbitrary dose prescription. All imaging modalities were (visually) used for GTV delineation (see Figure 2). OARs, $PTV_{initial}$ and PTV_{boost} were defined on fused CT and MRT2w datasets by both an experienced radiation oncologist and a radiologist.

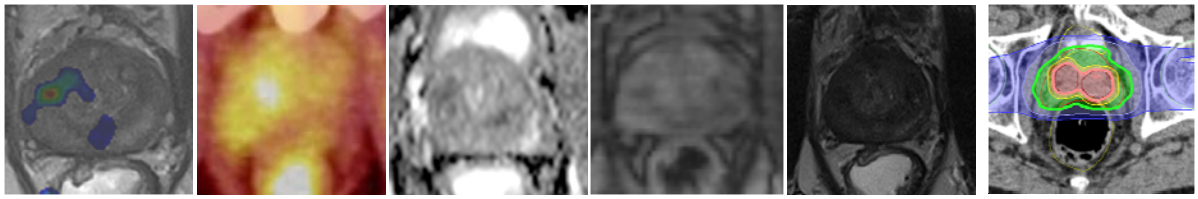

Figure 2: Different MR sequences and 11C PET for a respective prostate patient with two dominant intraprostatic lesions; from left to right: MRSI, 11C PET, DWI, DCE, T2w, isodose distribution from two opposing proton beams.

The prescribed doses to $PTV_{initial}$ and PTV_{boost} were 77Gy and 95Gy at maximum (delivered in 35 fractions), whereas the boost escalation dose was limited by the dose limits for rectum and bladder [23].

6. Summary and outlook

During the last years ion beam research was successfully initiated and conducted at the Department of Radiation Oncology of the Medical University of Vienna in close collaboration with MedAustron. This building up of multidisciplinary research expertise was conducted in parallel with the design and construction of the MedAustron facility. After passing successfully the first scientific evaluation after 2 years (covering the period 2012-2013) and the prolongation of the CD Laboratory until the end of 2016 the team of 10 PhD and Post-Doc researchers got the possibility to continue their research. In the coming years the experimental validation of the RBE model for helium ion beams as well as treatment planning studies will be pursued to reveal their clinical potential. Furthermore the development of dose calculation algorithms for high LET particles is envisaged. Dose painting strategies, improved image guidance for treating moving targets using novel image processing algorithms are others challenges to be tackled in the coming research period of the CD Laboratory. Once operational, MedAustron will offer outstanding research opportunities in the field of ion beam therapy.

Acknowledgements

The financial support by the Federal Ministry of Economy, Family and Youth and the National Foundation for Research, Technology and Development is gratefully acknowledged.

References

[1] Mock U, Bogner J, Georg D, Auberger T, Pötter R Treatment planning comparison of 3D conformal, intensity modulated radiotherapy and proton therapy for prostate carcinoma. Strahlenth. Onkol. 2005;181: 448-455.

[2] Mock U, Georg D, Bogner J, Auberger T, Pötter R Treatment planning comparison of conventional, 3D conformal, intensity modulated photon (IMRT) and proton therapy for paranasal sinus carcinoma. Int. J. Rad. Onc. Biol. Phys. 2004;58:147-154.

[3] Weber D, Bogner J, Verwey J et al Proton beam radiation therapy versus fractionated stereotactic radiotherapy for uveal melanomas: a comparative study. Int. J. Rad. Onc. Biol. Phys. 2005;63: 373-384.

[4] Hillbrand M, Georg D, Gadner H, Pötter R, Dieckmann K Potential role of intensity modulated proton therapy for infradiaphragmatic neuroblastoma during childhood. Radioth. Oncol. 2008; 89:141-149.

[5] Georg D, Hillbrand M, Stock M, Dieckmann K, Pötter R Can Protons improve SBRT for lung lesions? – dosimetric considerations. Radioth. Oncol. 2008; 88: 368-375.

[6] Georg D, Kirisits Ch, Hillbrand M, Dimopoulos, J, Pötter R Image-guided radiotherapy for cervix cancer: high-tech external beam therapy vs. High-tech brachytherapy Int. J. Rad. Onc. Biol. Phys. 2008;71:1272-1278.

[7] Hillbrand M and Georg D Assessing a set of optimal user interface parameters for intensity modulated proton therapy planning. J. Applied Clinical Med. Phys. 2010;11: 93-104.

[8] Kuess P, Birkfellner W, Enghardt W, Helmbrecht S, Fiedler F, Georg D Using statistical measures for automated comparison of in-beam PET data. 2012 Med.Phys;39:5874-5881

[9] Ableitinger A, Vatnitsky S, Herrmann R et al Dosimetry auditing procedure with alanine dosimeters for particle therapy: results of a pilot study. 2013 Radioth.Oncol;108:99-106

[10] Georg D and Schreiner T (editors) (2010), MedAustron - Research Opportunities for Medical Radiation Physics and Radiation Biology, ISBN 978-3-200-01792-4

[11] Ströbele J, Schreiner T, Fuchs H, Georg D Comparison of basic features of proton and helium ion pencil beams in water using GATE. Z. Med. Phys. 2012;22:170-178.

[12] Fuchs H, Ströbele J, Schreiner T, Hirtl A, Georg DA pencil beam algorithm for scanned helium ion beam dose calculation. Med. Phys. 2012;39:6726-6737.

[13] Fuchs H, Alber M, Schreiner T, Georg D A new helium ion beam treatment planning modality and possible advantages. 2013 ***Submitted*** to Strahlenth. Onkol.

[14] Góra J, Stock M, Lütgendorf-Caucig C, Georg D Is there an advantage in designing adapted, patient specific PTV margins in scanned proton therapy for prostate cancer? Int.J.Rad.Onc.Biol.Phys. 2013;85:881-888

[15] Hopfgartner J, Stock M, Georg D Proton treatment plan robustness in the cranial region as a function of beam arrangement. Do we really need a gantry? Acta Oncol. 2013;52:570-579

[16] Knäusl B, Lütgendorf-Caucig C, Hopfgartner J, Dieckmann K, Kurch L, Pelz T, Pötter R, Georg D. Can treatment of Paediatric Hodgkin's Disease be improved by PET imaging and proton therapy? 2013 Strahlenth.Onkol;189:54-61

[17] Mock U, Georg D, Sölkner L et al Assessment of improved organ at risk sparing for meningioma: Light ion beam therapy as boost versus sole treatment option. ***Submitted*** to Radioth.Oncol

[18] Gendrin C, Weber C, Blocha C, Figl M, Pawiroa SA, Bergmann H, Stock M, Georg D, Birkfellner W Monitoring tumor motion by real time 2D/3D registration during radiotherapy. 2012 Radioth.Oncol;102:274-280.

[19] Furtado H, Steiner E, Stock M, Georg D, Birkfellner W Real-time 2D/3D registration using kV-MV image pairs for tumor motion tracking in image guided radiotherapy. 2013Acta Oncol;52:1464-1471.

[20] Steiner E, Stock M, Kostresevic B et al Imaging dose assessment for IGRT in particle beam therapy 2013 ***In press*** Radiother.Oncol.

[21] Knäusl B, Rausch I, Bermann H, Dudczak R, Georg D Influence of PET reconstruction parameters on the TrueX algorithm - A combined phantom and patient study. 2012 Nuklearmedizin;52:28-35

[22] Cellini N, Morganti AG, Mattiucci GC et al Analysis of intraprostatic failures in patients treated with hormonal therapy and radiotherapy: implications for conformal therapy planning. 2002 Int.J.Radiat.Oncol.Biol. Phys;53: 595-599

[23] Lips IM, van der Heide UA, Hausertmans K et al Single blind randomized phase III trial to investigate the benefit of a focal lesion ablative microboost in prostate cancer (FLAME-trial): study protocol for a randomized controlled trial. 2011 Trials;12:255

NIRS & MedAustron Joint Symposium on Carbon Ion Therapy

・Date of Publishing: November 2013

・Research Promotion Section

Dept. of Planning and Management

National Institute of Radiological Sciences

Anagawa 4-9-1, Inage-ku, Chiba, 263-8555, Japan

Tel: +81-43-206-3025 Fax: +81-43-206-4061

E-mail: kokusai@nirs.go.jp Homepage: http://www.nirs.go.jp/ENG/index.html

NIRS-M-262 Printed in Japan